

NEW WAYS OF STRAPPING CALIX[4]PYRROLES

A Thesis Submitted for the Degree of

DOCTOR OF PHILOSOPHY



By
Ritwik Samanta

School of Chemistry
University of Hyderabad
Hyderabad-500 046
INDIA

September 2014

*Dedicated
to
my
Baba-Maa*

CONTENTS

Declaration	i
Certificate	ii
Preface	iii
Acknowledgement	iv
List of Abbreviations	vi
Chapter 1 Introduction	1-33
1.1 Anion: Role in Biology and Environment	3
1.2 Natural Anion Binding Receptors	6
1.3 Artificial Anion Binding Receptors	12
1.3.1 Receptor Design	12
1.3.2 Historical Evolution	14
1.3.3 Classification	16
1.3.3.1 Acyclic Anion Receptors	16
1.3.3.2 Cyclic Anion Receptors	20
1.5 References	25
 Chapter 2 Materials and Methods	 35-49
2.1 General Experimental	37
2.1.1 Solvents	37
2.1.1.1 Solvent for Reactions	37
2.1.1.2 NMR Solvents	37
2.1.1.3 Solvents for Analytical Studies	37
2.1.2 Reagents	37
2.2 Chromatography	38
2.3 Characterization and Analytical Instrumentation	38
2.4 Computational Details	39
2.5 Analytical Techniques	39
2.5.1 Introduction	39
2.5.2 Sample Preparation	41

2.5.3 Evaluation of Binding Constants	41
2.5.3.1 NMR Spectroscopy	41
2.5.3.2 Optical Methods	42
2.5.3.3 Isothermal Titration Calorimetry	43
2.5.4 Job Plot Analysis	44
2.6 Preparation of Starting Materials	45
2.6.1 Preparation of 1-methylcyclohexanol	45
2.6.2 Preparation of 7-bromo-2-heptanone	46
2.6.3 Preparation of 4,5-dibromobenzene-1,2-diol	46
2.6.4 Preparation of 1,2-isopropylidenedioxybenzene	46
2.6.5 Preparation of 2,2-dimethyl-5-nitro-1,3-benzodioxole	47
2.6.6 Preparation of 4-nitrobenzene-1,2-diol	47
2.6.7 Preparation of bromoacetone	47
2.7 References	48
 Chapter 3 Catechol Derived Strapped Calix[4]pyrrole	 51-80
3.1 Introduction	53
3.2 Calix[4]pyrrole: Synthesis	57
3.2.1 One-pot Condensation	57
3.2.1.1 Homo-condensation	58
3.2.1.2 Mixed Condensation	59
3.2.2 (2+2) Condensation	59
3.2.3 (3+1) Condensation	60
3.3 Modulating the Anion Binding Properties of Calix[4]pyrroles	60
3.3.1 C-rim Functionalization	61
3.3.2 <i>meso</i> Functionalization	62
3.4 Research Goal	65
3.5 Results and Discussion	66
3.5.1 Synthesis and Structural Characterization	66
3.5.2 Anion Binding Study	69
3.6 Conclusion	75

3.7 Experimental Details	75
3.7.1.1 Synthesis of 7-[2-(6-oxo-heptyloxy)phenoxy]-2-heptanone (R1)	75
3.7.1.2 Synthesis of 1,2-bis[6,6-di(pyrrol-2-yl)heptyloxy]benzene (R2)	76
3.7.1.3 Synthesis of strapped calix[4]pyrrole (R3)	76
3.7.2 Crystallographic Details	76
3.8 References	77
Chapter 4 Isomeric Naphthalene Derived Strapped Calix[4]pyrroles	81-114
4.1 Introduction	83
4.1.1. Design Principles of Chemosensors for Anion Sensing	83
4.1.1.1 Binding Site-Signaling Subunit Approach	84
4.1.1.2 Displacement Approach	85
4.2 Calix[4]pyrrole as Chemosensor	86
4.2.1 Binding Site-Signaling Subunit Approach	86
4.2.2 Displacement Approach	93
4.3 Research Goal	95
4.4 Results and Discussion	96
4.4.1 Synthesis and Characterization	96
4.4.2 Anion Binding Study	97
4.5 Conclusion	109
4.6 Experimental Details	109
4.6.1.1 Synthesis of R4	109
4.6.1.2 Synthesis of R5	109
4.6.1.3 Synthesis of R6	110
4.6.1.4 Synthesis of R7	110
4.6.1.5 Synthesis of R8	111
4.6.1.6 Synthesis of R9	111
4.7 References	112
Chapter 5 Calix[4]pyrroles with Shortest Possible Strap	115-143
5.1 Introduction	117

5.2 Size Modification of the Binding Domain of Calixpyrrole	120
5.2.1 Modification of Core	120
5.2.2 Modification of the Size of the Binding Domain	126
5.3 Research Goal	127
5.4 Results and Discussion	129
5.4.1 Synthesis and Characterization	129
5.4.2 Anion Binding Study	131
5.5 Conclusion	134
5.6 Experimental Details	135
5.6.1 Crystallographic Details	135
5.6.2.1 Synthesis of 1,2-bis(acetonyloxy)benzene (R10)	136
5.6.2.2 Synthesis of 1,1'-(naphthalene-2,3-diylbis(oxy))dipropan-2-one (R11)	136
5.6.2.3 Synthesis of 1,1'-(4,5-dibromo-1,2-phenylene)bis(oxy)dipropan-2-one (R12)	136
5.6.2.4 Synthesis of 1,1'-(4-nitro-1,2-phenylene)bis(oxy)dipropan-2-one (R13)	137
5.6.2.5 Synthesis of 1,2-bis(2,2-di(1H-pyrrol-2-yl)propoxy)benzene (R14)	137
5.6.2.6 Synthesis of 2,3-bis(2,2-di(1H-pyrrol-2-yl)propoxy)naphthalene (R15)	138
5.6.2.7 Synthesis of 1,2-bis(2,2-di(1H-pyrrol-2-yl)propoxy)-4,5dibromobenzene (R16)	138
5.6.1.8 Synthesis of 1,2-bis(2,2-di(1H-pyrrol-2-yl)propoxy)-4-nitrobenzene (R17)	138
5.6.1.9 Synthesis of R18	139
5.6.1.10 Synthesis of R19	139
5.6.1.11 Synthesis of R20	139
5.6.1.12 Synthesis of R21	140
5.7 References	140

Chapter 6 Strapping One Calix[4]pyrrole with Another: a Flexible Biscalix[4]pyrrole	145-161
6.1 Introduction	147
6.2 Calix[4]pyrrole Dimers and Anion Recognition	152
6.3 Research Goal	156
6.4 Synthesis and Structural Characterization	156
6.5 Conclusion	157
6.5 Experimental Details	158
6.6.1 Synthesis of 1,4-bis(acetonyloxy)benzene (R22)	158
6.6.2 Synthesis of 1,4-bis(2,2-di(1H-pyrrol-2-yl)propoxy)benzene (R23)	158
6.6.3 Synthesis of biscalix[4]pyrrole (R24)	158
6.7 References	159
Chapter 7 Summary	163-167
7.1 Summary	165
7.2 References	267
Appendix	169-218
Publications and Presentations	219

DECLARATION

I hereby declare that the matter embodied in the thesis entitled “*New ways of strapping Calix[4]pyrroles*” is the result of investigations carried out by me in the School of Chemistry, University of Hyderabad, Hyderabad, India under the supervision of **Dr. Pradeepta K. Panda** and it has not been submitted elsewhere for the award of any degree or diploma or membership, etc.

In keeping with the general practice of reporting scientific investigations, due acknowledgements have been made wherever the work described is based on the findings of other investigators. Any omission or error that might have crept in is sincerely regretted.

September, 2014

Ritwik Samanta

UNIVERSITY OF HYDERABAD
Central University (P.O.), Hyderabad-500046, INDIA

Dr. Pradeepta K Panda,
Associate Professor,
School of Chemistry



Tel: 91-40-23134818 (Office)
Fax: 91-40-23012460
e-mail: pkpsc@uohyd.ernet.in
pradeepta.panda@uohyd.ac.in
pradeepta.panda@gmail.com

CERTIFICATE

This is to certify that the work described in this thesis entitled “*New ways of strapping Calix[4]pyrroles*” has been carried out by Mr. Ritwik Samanta under my supervision and the same has not been submitted elsewhere for any degree.

Dean,
School of Chemistry,
University of Hyderabad,
Hyderabad-500 046, India.

Dr. Pradeepta K Panda
(Thesis supervisor)

PREFACE

The current thesis entitled “*New ways of strapping Calix[4]pyrroles*” has been divided into seven chapters. The thesis is principally deals with the synthesis and anion binding studies of some calix[4]pyrrole based anion receptors, which can recognize anions primarily on the basis of their H-bonding ability. **Chapter 1** provides a succinct introduction on the chemical, biochemical and environmental relevance of anions and an overview of various literature reported synthetic anion receptors. **Chapter 2** gives a short account of various solvents, chemicals used in the study and different instruments and computational methods employed for characterization in our investigation. Further, it presents an overview of the theory of the various methods used in calculating the binding constants and the synthetic procedures of the precursor materials employed in the subsequent investigations. **Chapter 3** describes the synthesis of catechol-derived strapped calix[4]pyrrole for the first time. The strap with 1,2-diether link is providing a relatively constrained geometry on its side of the calix[4]pyrrole moiety. **Chapter 4** describes the synthesis of two novel isomeric strapped calix[4]pyrroles using diether straps derived from naphthalene, which is employed as the fluorescent reporting unit. The receptor derived from 2,3-dihydroxynaphthalene shows apex sensitivity towards chloride ion, whereas that derived from 2,7-analogue shows peak sensitivity for fluoride ion. **Chapter 5** explores the synthesis of calix[4]pyrroles with shortest possible strap and its consequences upon their anion binding properties. Due to the small binding domain these receptors display exclusive selectivity towards fluoride ion. **Chapter 6** describes the first synthesis of a biscalix[4]pyrrole by using double (2+2) condensation path way. Here the calix[4]pyrrole moieties are bridged through flexible linkers. Finally, **Chapter 7** summarizes the findings of the present exploration along with the future scopes.

September, 2014

Ritwik Samanta

Acknowledgement

First and foremost I want to thank my supervisor, Dr. Pradeepta K Panda. He has taught me both consciously and un-consciously. I appreciate all his contributions of time, ideas, and funding to make my Ph.D. experience productive and stimulating. The joy and enthusiasm he has for his research was contagious and motivational for me, even during tough times in the Ph.D. pursuit.

I would like to thank the former and present Dean(s), School of Chemistry, for their constant inspiration and for allowing me to use the available facilities. I am extremely thankful individually to all the faculty members of the School for their kind help and cooperation at various stages of my stay in the campus.

I am grateful to CSIR and University of Hyderabad for providing financial support.

I would wish to thank Akkaladevi Narahari, Susanta Ghanta and Sauradip Chaudhuri for their contribution in some of our works.

The members of our group have contributed immensely to my personal and professional time at UOH. The group has been a source of friendships as well as good advice and collaboration. Thank you to Naren, Sanjeev, Tridib, Brijesh, Nandakishore, Anup, Sathish, Obaiiah, Vikranth, Prameela, Nagamaiah and Sandip.

My pleasurable association with some persons in UOH such as Dinu, Maityda, Paromita and Susrutda is unforgettable.

I would like to thank Arindamda, Prashantda, Utpalda, Taptada, Sandeepda, Ghantada, Ranjitda, Palash, Santanu, Raja, Satya, Sugata, Koushik, Suman Gosh, Navendu, and all others whose names are not mentioned due to limited space.

Finally, I would like to express my love and gratitude to my Baba-Maa, Dadu-Dida, Dadubhai-Didabhai, Dada-Boudi-SREE and Tuli for their unconditional love and blessings. They made me what I am today and I owe everything to them.

September, 2014

University of Hyderabad,
Hyderabad, 500 046,
India.

Ritwik Samanta

List of Abbreviations

Anhyds.	Anhydrous
AMP	Adenosine monophosphate
ADP	Adenosine diphosphate
ATP	Adenosine triphosphate
Bcl-2	B-cell lymphoma 2
BisDPM	Bisdipyrromethane
br	Broad
Calcd.	Calculated
CMP	Cytidine monophosphate
Conc.	Concentration
d	Doublet
DCM	Dichloromethane
DFT	Density functional theory
DMF	N,N-Dimethylformamide
Equiv.	Equivalent
HRMS	High resolution-mass spectrometry
ITC	Isothermal titration calorimetry
LCMS	Liquid chromatography mass spectrometry
L	Ligand and/or guest
m	Multiplet
m/z	Mass/charge
min	Minute (s)
NMR	Nuclear magnetic resonance
ORTEP	Oak Ridge thermal ellipsoid program
p	Para
PET	Positron Emission Tomography
s	Singlet

TBAF	Tetrabutylammonium fluoride
TBACl	Tetrabutylammonium chloride
TBABr	Tetrabutylammonium bromide
TBAI	Tetrabutylammonium iodide
TBACN	Tetrabutylammonium cyanide
TBA(CH ₃ COO)	Tetrabutylammonium acetate
TBAH ₂ PO ₄	Tetrabutylammonium phosphate
TFA	Trifluoroacetic acid
TLC	Thin layer chromatography
t	Triplet
TEA	Triethylamine
UMP	Uridine monophosphate
UV-Vis	Ultraviolet-Visible
XRD	X-Ray diffraction

CHAPTER 1

Introduction

1.1 Anion: Role in Biology and Environment

Anions are negatively charged chemical species that get attracted towards anode. The word ‘anion’ was coined in 1834 from the Greek word ‘ἄνοδος’ (anodos), by William Whewell, who had been consulted by Michael Faraday over some new names needed to complete a paper on the recently discovered process of electrolysis.¹ Anions are present almost everywhere in our day to day life e.g. fluoride in tooth paste, chloride in water, nitrate and sulfate in acid rain, carbonates in biomineralized materials, even ionosphere of the Earth contains carbonate, nitrate, nitrite and most importantly, more than two third of enzyme substrates and cofactors are anionic in nature.^{2,3} Because of this ubiquitous nature of anions, the selective recognition of anionic guest species of biochemical and environmental importance by abiotic receptor molecules is an area of ever increasing research activity encouraged by their applications in medical diagnostics, environmental and industrial monitoring, and nuclear waste remediation. The role of some of the anions in biology and environment is discussed below.

Fluoride ion is of great importance to researchers owing to its duplicitous nature. The disagreement on its allegedly benign health effect on humans, nowadays elicited by mounting evidence of its severe toxicity, makes it a controversial species. United States fluoridates over 70% of its water supplies by adding industrial grade fluoride chemicals to water for the purpose of preventing tooth decay since about 1950s.⁴ Fluoride ion has a benign effect up to 1 ppm concentration, whereas it seems to be toxic at higher doses.^{5a} Over the years, high concentration of the fluoride ion in the environment and in drinking water has been related to the occurrence of several types of pathologies in humans, such as osteoporosis, neurological and metabolic dysfunction, and more recently also cancer.⁵ Some studies have also been reported on the fluoride ion effect on the biochemistry of organisms. It seems DNA synthesis and the activity of some enzymes, as well as the metabolism of nutrients, can be severely influenced by the presence of fluoride ion.⁶ It also has importance in industrial applications and transformations, especially in steel making and aluminum refining, and is also a well-established reagent in organic synthesis.⁷ Novel applications of fluoride ion have also been found in the field of ion batteries, for enhancing the photocurrent in supramolecular solar cells and in ¹⁸F- PET (positron emission tomography) imaging, and, in the future, it might have a role in the construction of superconducting and hydrogen storage materials.⁸

Chloride ion is a predominant anion in blood, where it represents 70 % of the anions and together with sodium, potassium and bicarbonate serves as electrolyte in our body and helps in maintaining the blood's pH level.⁹ It is specially transported into the gastric lumen, in exchange for another negatively charged electrolyte (bicarbonate), in order to maintain electrical neutrality across the stomach membrane.¹⁰ The transmembrane transport of anions is also important, since defective anion transport has been linked to various diseases, for example, the malfunction of natural chloride channels has been associated with Bartter syndrome,¹¹ Dent's disease¹² and cystic fibrosis.¹³ Similarly, defects in proteins that facilitate transmembrane bicarbonate transport have been linked to diseases related to brain, heart and bones.¹⁴

Iodide ion is an essential trace element for life, the heaviest element commonly needed by humans and many other living bodies. At present, the only physiological role known for this ion in the human bodies is the synthesis of thyroid hormones by the thyroid gland.¹⁵ Deficiency of the iodide ion could lead to disorders in physiological functions. Hence its content in blood, urine and milk is often analyzed for nutritional, metabolic, and epidemiological studies of thyroid disorder.¹⁶ Along with elemental iodine, it is used for many areas of chemistry for synthesizing valuable molecules such as drugs and dyes.

Cyanide ion is commonly known as a poison and a chemical warfare agent. However, its industrial need in many chemical processes, such as mineral extraction, electroplating, and the fabrication of synthetic fibers,¹⁷ drives its production to over 1.1 million tons per year. Therefore, industrial use of mass quantities of cyanide, with its associated transportation through highly populated areas, drastically increases the risk of exposure. Cyanide exposure may also occur through diet, smoke inhalation (fire or cigarette smoke), or exposure from illicit use.¹⁸ Biological sources of cyanide include bacteria, fungi, and algae, which produce this ion as part of their nitrogen metabolic pathways. Vegetables containing cyanogenic glycosides are also sources of cyanide ingestion in humans and animals. Other potential sources of cyanide in humans and animals are sodium nitroprusside, succinonitrile and organic thiocyanates.¹⁹ It also acts as an inhibitor of metalloenzymes and of some non-metalloenzymes that function through the intermediacy of Schiff bases.²⁰ It can also affect many functions in the body, including the vascular, visual, central nervous, cardiac, endocrine, and metabolic systems. Perhaps the best known effect of cyanide is its inhibition of respiration, which is caused by the inhibition of the terminal oxidase (cytochrome oxidase) of the mitochondrial respiratory chain. Sub-lethal doses

of cyanide cause a decrease in the rate of glycolysis and inhibit the operation of the TCA (tricarboxylic acid) cycle.²¹

Oxoanions, as a group is characterized by high aqueous solubility, are formed by a large majority of the chemical elements. Phosphate is the most important among all oxoanions, as inorganic phosphate is an essential component of various biomolecules responsible for cellular structure and storage of cellular energy, and is thus indispensable for survival of all living organisms. Hence, it is crucial for living organisms to maintain proper phosphate homeostasis, as any imbalance (hyper- or hypophosphatemia) will impact cellular processes, viz. cell differentiation and proliferation, metabolic functions, and cytoskeletal organization.²² Abnormally elevated phosphate level in blood leads to hyperphosphatemia and the adverse effects of this, includes the development of hyperparathyroidism, soft tissue calcification, cardiovascular complications and increased morbidity and mortality.²³ Phosphate is a well-known contaminant of ground and surface water, due to massive use of phosphate based fertilizer and detergents, and it is one of the two substances that have been implicated in the frequent eutrophication of lakes and coastal waterways. Processes such as wind erosion, surface runoff and leaching are the main pathways for transport of phosphorus from terrestrial to aquatic ecosystems.^{23b} Recent research has shown that the perchlorate ion may be found at high concentrations >1000 ppm in surface waters and groundwater by disposal of waste water of solid propellant manufacturers.^{24a} Trace amount of perchlorate ion has shown thyreostatic activity by inhibiting iodine uptake and may, therefore, hinder the ability of humans to produce hormones and regulate their metabolism. It has been applied as growth promoters and as drug for hyperthyroidism.^{24b} Perchlorate ion is also used extensively as rocket fuel, fireworks, flares, and explosives. Oxoanions such as nitrate and aluminate also contributed to eutrophication of water bodies. Some radioactive nuclear waste products, particularly the pertechnetate ($^{99}\text{TcO}_4^-$) and metaperhenate ($^{188}\text{ReO}_4^-$), are mobile in the environment, making their control and monitoring important.²⁵ Sulfate ion in clinical medicine has been regarded as an end metabolite of cysteine and methionine, both sulfur-containing amino acids.^{26a} It is a prominent troublesome species in the nuclear wastes that can interfere in their treatment processes.^{26b} This anion is also responsible for the permanent hardness of water.^{26c}

Due to the above mentioned roles of anions played in various biological and environmental processes selective complexation of anion has emerged as an important area of research.

1.2 Protein: Natural Anion Binding Receptors

It is commonly understood that anions are highly important species in the living cycle of cell. Their influence on cellular biological processes is usually affected via macromolecular receptors, which are proteins by nature. Anion-protein complexes trigger a number of further biochemical transformations. In biological systems, the protein-anion interactions serve specific purposes, for example enzymatic transformations (where majority of enzymes bind anions as either substrates or cofactors), substance transportation, or signal transduction. They are usually non-covalent in nature. The high specificity of binding of anions to the respective proteins is due to a recognition site in which anion is completely desolvated and bound exclusively via hydrogen bonds. Furthermore, a so-called macrodipole effect, caused by orientation of amino terminus of the protein backbones towards the negative guests, contributes to the stability of the complex. Then the oppositely charged functional groups of the protein and the anion are paired, and lipophilic groups of the ligand display hydrophobic pockets formed by side chains of the hydrophobic amino acids. The known anion binding proteins differ in structure, biochemical functions, and mechanisms of complex formation. The structures of some of the natural anion binding receptors and their mode of interaction are discussed below.

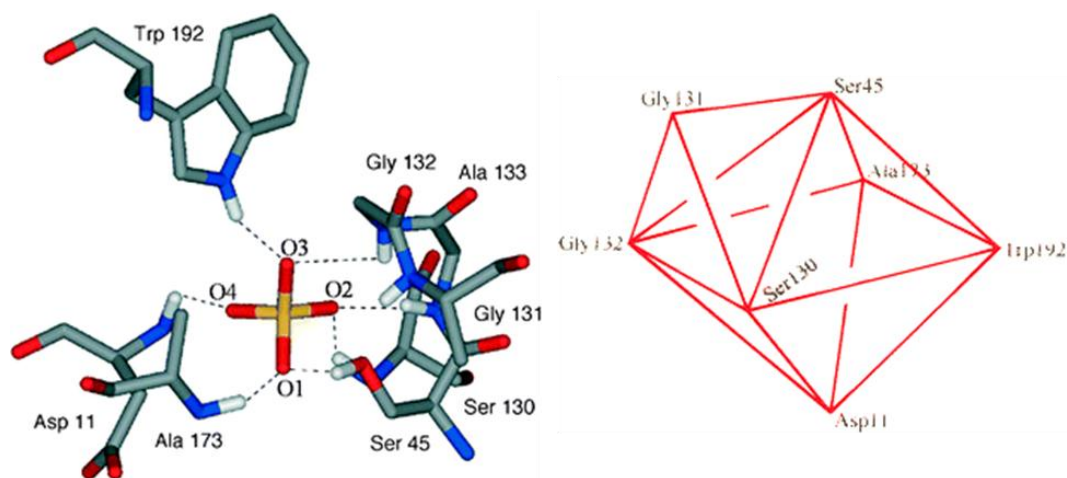


Figure 1.1 Left: The portion of single crystal X-ray structure of the active sulfate-binding site in the sulfate-binding protein (SBP). Right: The anion is bound to SBP by seven hydrogen bonds. Mono-capped distorted trigonal prismatic geometry of seven-coordinated sulfate in SBP (anion removed for clarity).^{26b,27}

The structure of sulfate binding proteins (SBP) was elucidated by Pflugrath and Quirocho in 1988.²⁷ The substrate is bound ~ 8 Å deep inside the cavity formed by the intersection of two protein globular domains which is inaccessible to solvents. Interestingly, the pocket does not

contain any positively charged residues, or cations or water molecules within the van der Waal's distance to the buried sulfate ion and hence the anion binding therefore relies primarily on hydrogen bond formation. The sulfate is held tightly in the pocket by seven hydrogen bonds with the protein: five of these hydrogen bonds are donated by the main chain peptide –NH groups, another by a serine –OH group and the last one by the indole –NH of the tryptophan side chain (Figure. 1.1). This protein is capable of highly selective binding of sulfate ion with an association constant approximately 10^6 M^{-1} in water (pH 5-8.1). Bowman-James have shown that the sulfate ion in SBP has an approximate geometry close to capped octahedron with Trp192, Ala173 and Asp11 and Gly132, Ser45 and Ser130 occupying the two trigonal planes whereas Gly131 provides the axial cap (Figure. 1.1 right).^{26b}

In 1992, Jordan and coworkers reported the crystal structure of porphobilinogen deaminase, a key enzyme in the biosynthesis of the linear tetrapyrrole, a precursor of protoporphyrin IX.²⁸ The structure shows that the pyrrolic NH protons of the dipyrromethane substrate is hydrogen bonded with the carboxylate side chain of Asp 84 (Figure 1.2). Further, the

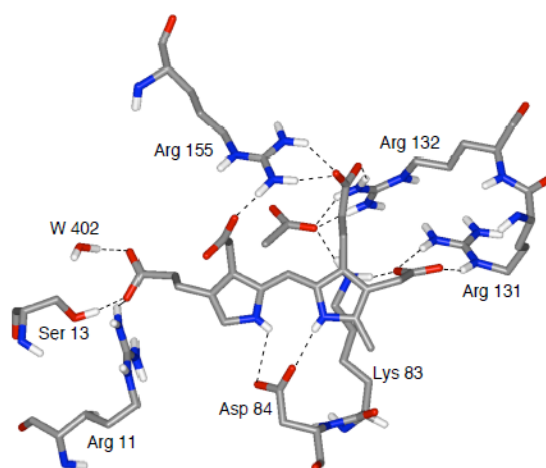


Figure 1.2 Partial view of the X-ray structure of the enzyme porphobilinogen deaminase showing the binding of a dipyrromethane cofactor.²⁸

four carboxyl groups at the β -pyrrolic positions are seen to interact with the positively charged enzyme residues of Arg 11, Arg 131, Arg 132, Arg 155, Lys 55 and Lys 83, and to be involved in hydrogen bond with Ser 13. The replacement of Asp 84 by Glu causes the enzyme to lose 99% of its activity and prevents the enzyme from catalyzing the formation of pre-europorphyrinogen. This result underscores the importance of the interactions between the two pyrrole units and the

Asp 84 carboxylate ion, thus providing a further incentive to design and study pyrrole based anion receptors. The X-ray crystal structure, of the DNA helicase RepA sulfate complex shows seven hydrogen bonding interactions between the sulfate ion and RepA protein scaffold. The anion is further hydrogen bonded to Asp 140 via an intervening water molecule (Figure 1.3).²⁹

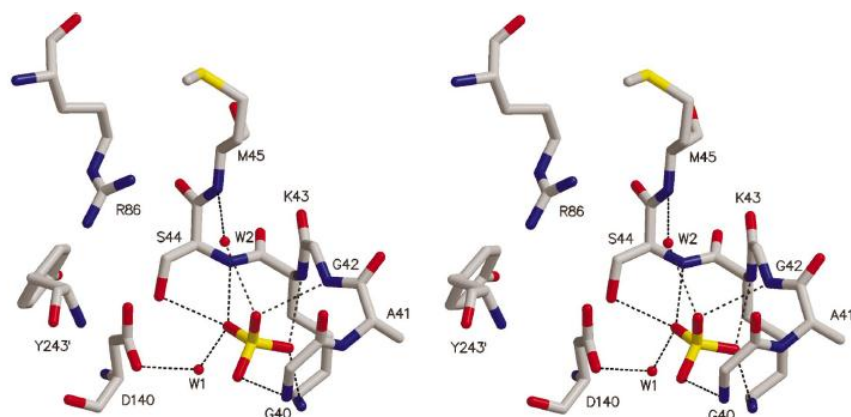


Figure 1.3 Stereo view of the ATPase active site showing the interaction of sulfate ion and P-loop residues.²⁹

The guanidinium group present in the side chain of arginine is ubiquitous in enzymes that bind anionic substrates and also involved in stabilization of protein tertiary structures via internal salt bridges with carboxylate functions. This motif is realized in phosphatases and phosphorylases, which selectively bind phosphate ion, as well as in decarboxylases,

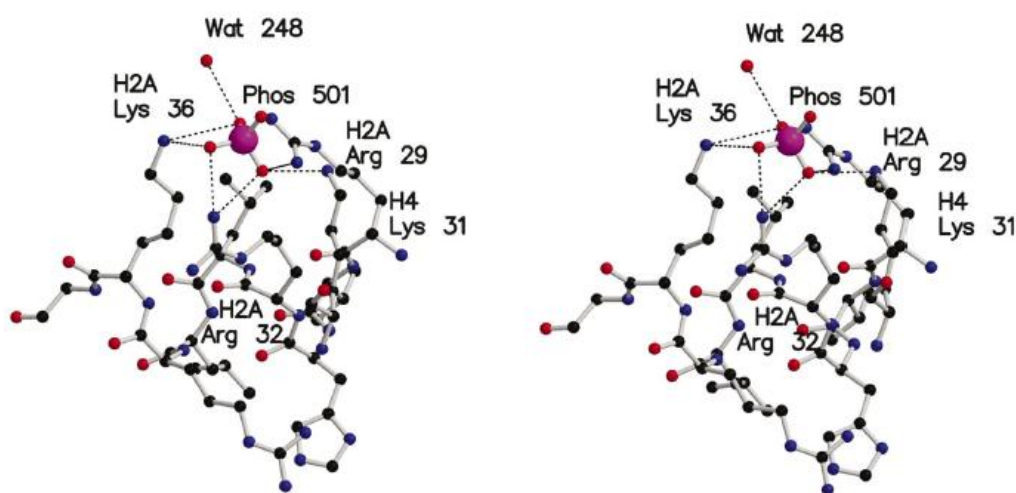


Figure 1.4 Stereo structures of amino-acid residues interacting with phosphate ion in histone octamer-phosphate complex.³⁰

dehydrogenases, isomerases, and in some proteases that bind carboxylates. The crystal structure of the histone octamer-phosphate complex, by Baldwin *et al.* shows how the phosphate ion is binding with several basic amino-acid residues (Figure 1.4).³⁰

Dutzler and MacKinnon combinedly reported the X-ray crystal structure of two prokaryotic ClC chloride channels (which catalyses the selective flow of Cl^- ions across cell membranes) in 2002, from *Salmonella enterica serovar typhimurium* and *Escherichia coli* at 3.0 and 3.5 Å Bragg spacing, respectively. Both structures reveal two identical pores, each pore being formed by a separate subunit contained within a homo-dimeric membrane protein (Figure 1.5). Individual subunits are composed of two repeated halves that span the membrane with opposite orientations.³¹ At the anion binding sites, the Cl^- ion is coordinated by main-chain

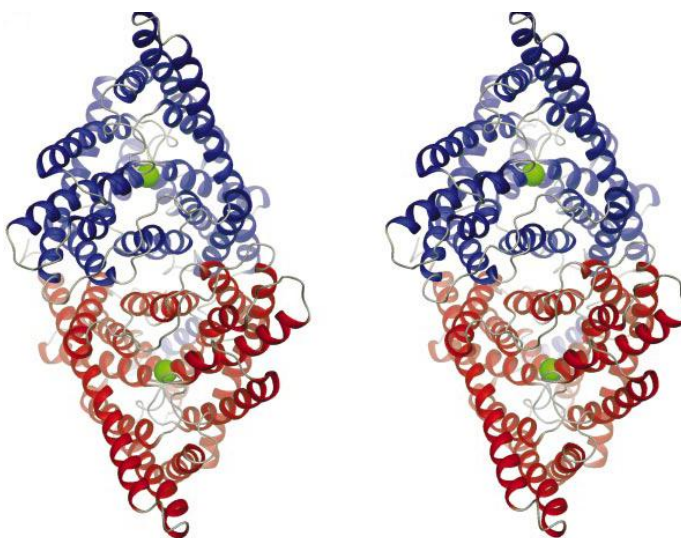


Figure 1.5 Structure of the ClC dimer: Stereo view of the ribbon representation of the ClC dimer from the extracellular side. The two subunits are in blue and red color. A Cl^- ion in the selectivity filter is represented as a green sphere.³¹

amide nitrogen atoms from amino acids Ile 356 and Phe 357 and by the side chain oxygen atoms from Ser 107 and Tyr 445 (Figure 1.6). The nitrogen atoms are not involved in hydrogen bonding with the protein, and are available for anion binding. The side chains of Ser 107 and Tyr 445 contact the Cl^- ion opposite the nitrogen cradle. In addition to the interactions with polar functional groups, the Cl^- ion is surrounded by a number of hydrophobic amino acid side chains (Figure 1.6). On the other hand, the structure does indicate the presence of negatively charged glutamate side chain just above the channel entrance. This residue is thought to act as an anion regulating gate. By swinging out to open the channel, it allows chloride ion to enter channel pore

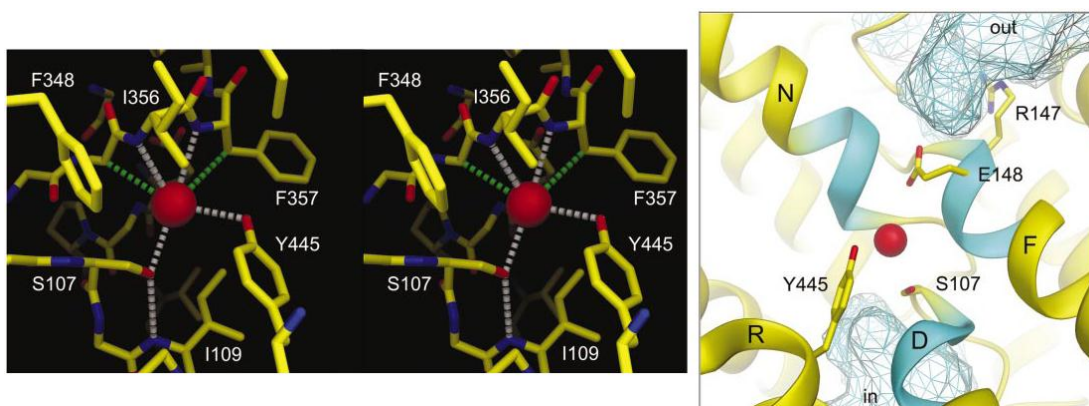


Figure 1.6 Left: Stereo view of the Cl^- ion binding site. Distances ($< 3.6 \text{ \AA}$) to the Cl^- ion (red sphere) are shown for polar (white dashed lines) and hydrophobic (green dashed lines) contacts. A hydrogen bond between Ser 107 and the amide nitrogen of Ile 109 is shown (white dashed line). Right: Ion conduction pathway. The ion binding site viewed from the dimer interface, along the pseudo two-fold axis, with foreground α -helices removed for clarity.³¹

from where they are pulled (presumably) towards the constricted neutral center of the channel by surface rich in positively polarized residues. In spite of these significant developments, still further work is needed to understand how anion transporters gate and how the gating processes are coupled towards ion conduction through the pore.

Smith and colleagues reported the crystal structures of the anion binding sites of the nitrate (NrtA) and bicarbonate (CmpA) transporters from cyanobacteria (Figure 1.7).³² The two

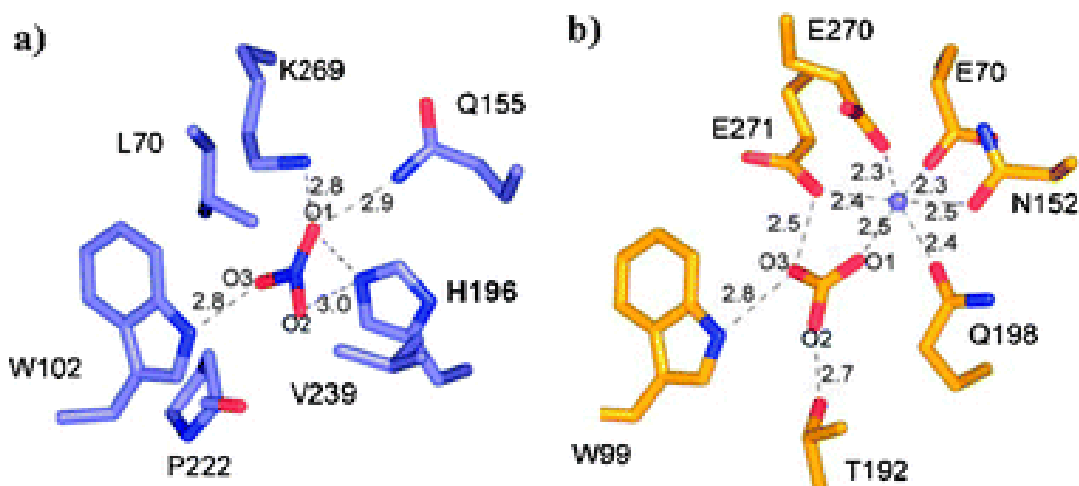


Figure 1.7 Depiction of the anion binding sites of nitrate binding protein NrtA (left), and bicarbonate binding protein CmpA (right), showing the electrostatic interactions between protein amino acid residues and anionic substrates NO_3^- and HCO_3^- respectively.³²

proteins are homologous, being 48 % identical in sequence. However, each protein is selective towards its own substrate. The difference in anion selectivity is attributed to changing a single amino acid from a hydrogen bond donor in NrtA to a hydrogen bond acceptor CmpA (Figure 1.7). In NrtA, nitrate is bound within a cleft by a combination of hydrogen bonds, and in CmpA, bicarbonate ion is bound by hydrogen bonds and electrostatic interactions provided by the Ca^{2+} ion (not by positively charged amino acid side chain).

In comparison to cation transporter across the lipid bilayer, there are only a few number of natural carriers to transport anions.³³ Due to the immense structural complexity of the biomolecules, it is important and convenient for synthetic chemists to design small molecules, which can mimic the role of biomolecules to study their selective anion binding and transport properties. Prodigiosins are a family of naturally occurring tripyrrolic red pigments that were first isolated in 1930s, from microorganism including *Serratia* and *Streptomyces* that are characterized by a pyrrolopyrromethene skeleton. These molecules, especially prodigiosin 25-C

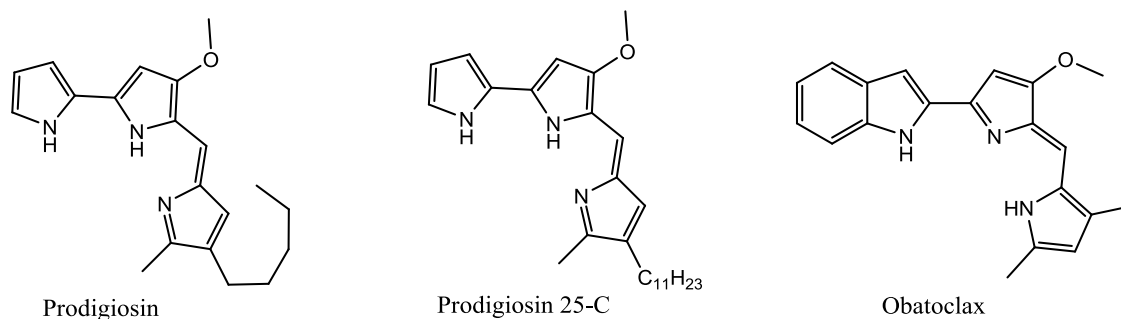


Figure 1.8 Some naturally occurring and artificial Prodigiosins.

have been studied extensively for their promising immunosuppressive and anticancer activity.^{2b} The cytotoxic and anticancer effects of prodigiosin are believed to arise from its ability to affect the transport of H^+ and Cl^- ions across membranes. As prodigiosin is basic in nature, hence readily gets protonated. Binding of chloride ion allows for charge neutralization and produces a species, prodigiosin-HCl, which is readily transported across membranes. Resulting ion transport events give rise to the reduction of intracellular pH, an effect that is known to trigger apoptosis.^{34,35} Obatoclax, an abiotic prodigiosin, which is an inhibitor of the Bcl-2 (B-cell lymphoma 2) family of proteins, is undergoing Phase II clinical trials for the treatment of lung cancer.³⁶ These properties are inspiring for the synthesis of pyrrole based drugs and anion carriers.

1.3 Artificial Anion Binding Receptors

Apart from nature, synthetic chemists have developed many small organic molecules that can bind to anions. In supramolecular chemistry they are known as ‘Host’ (for anion). In a definitive fashion we can say that ‘Host’ is a species which can interact with ‘Guest’ (anion) either by columbic interaction (if host is positively charged) or by non-columbic interaction (if host is neutral) with anion and as a result of these interactions, some other structurally defined entity is formed, called a ‘Host-Guest’ complex. The pertinent thermodynamic quantity characterizing these interactions is called the binding constant (K_a), comprises all direct mutual interactions between the binding partners as well as the changes in the environment (*e.g.* in the solvent). Both contributions are heavily dependent on the covalent structures of the binding partners.³⁷ This principle is the basis for the recognition of both cation and anion, however, anion recognition chemistry showed a slow growth rate as compared to cation recognition chemistry. This is attributed to the associated difficulties involved in the design of receptors capable of anion binding.

1.3.1 Receptor Design







Anions are larger than isoelectronic cations (table 1.1) and therefore have a lower charge to radius ratio. This means that electrostatic binding interactions are less effective than they would be for the isoelectronic cation, on the other hand a larger host cavity is needed to accommodate them. Further, anions are sensitive to pH (becoming protonated at low pH and so losing their negative charge), thus receptors must function within the pH window of their targeted anion. Moreover, anionic species possess a wide range of geometries (table 1.2) and

Table 1.1 Ionic sizes, experimental enthalpies and Gibb’s enthalpies of hydration for selected isoelectronic ions.^{37,38}

Cation	r [Å]	ΔH_{hyd} [kJ.mol ⁻¹]	ΔG_{hyd} [kJ.mol ⁻¹]	Anion	r [Å]	ΔH_{hyd} [kJ.mol ⁻¹]	ΔG_{hyd} [kJ.mol ⁻¹]
Na ⁺	1.16	-416	-365	F ⁻	1.19	-510	-465
K ⁺	1.52	-334	-295	Cl ⁻	1.67	-367	-340
Rb ⁺	1.66	-296	-275	Br ⁻	1.82	-336	-315
Cs ⁺	1.81	-283	-250	I ⁻	2.06	-291	-275

therefore, a higher degree of design may be required to make receptors complementary to their corresponding anionic guest. Solvent also play a crucial role in controlling anion binding strength and selectivity. Electrostatic interactions generally dominate in anion solvation, and hydroxylic solvents in particular can form strong hydrogen bond with anions. A potential anion receptor must therefore effectively compete with the solvent environment in which the anion-recognition event takes place. For example, a neutral receptor binds with anions solely through ion-dipole interactions, whereas a charged receptor although binds strongly with the anion, however has to compensate for a large desolvation energies of both the host and the guest.

Table 1.2 Structural diversities of anions.³⁹

Geometry	 spherical	 linear	 trigonal planar	 tetrahedral	 octahedral	 complex
Anions	F ⁻ , Cl ⁻ , Br ⁻ , I ⁻	N ₃ ⁻ , CN ⁻ , SCN ⁻ , OH ⁻	CO ₃ ²⁻ , NO ₃ ⁻	PO ₄ ³⁻ , VO ₄ ³⁻ , SO ₄ ²⁻ , MoO ₄ ²⁻ , SeO ₄ ²⁻ , MnO ₄ ⁻	[Fe(CN) ₆] ⁴⁻ , [Co(CN) ₆] ³⁻	DNA double helix

Hydrophobicity can also influence the selectivity of a receptor. The Hofmeister series⁴⁰ (Figure 1.9), which was first established through studies on the effect of salts on the solubility of proteins, orders anions by their hydrophobicity (and therefore degree of aqueous solvation). This series is more pronounced for anions than for cations. The species to the left of Cl⁻ are called

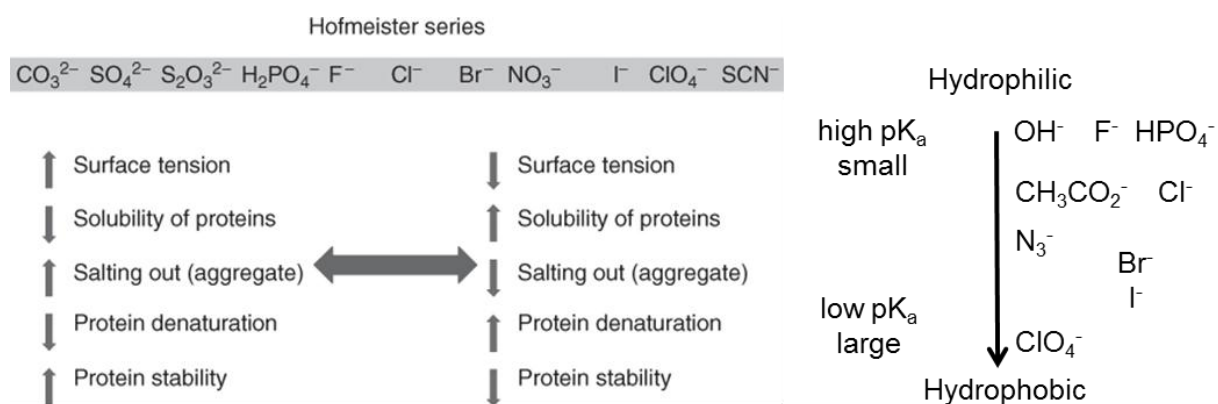


Figure 1.9 Representation of the Hofmeister series and hydrophilic/hydrophobic series of anions.

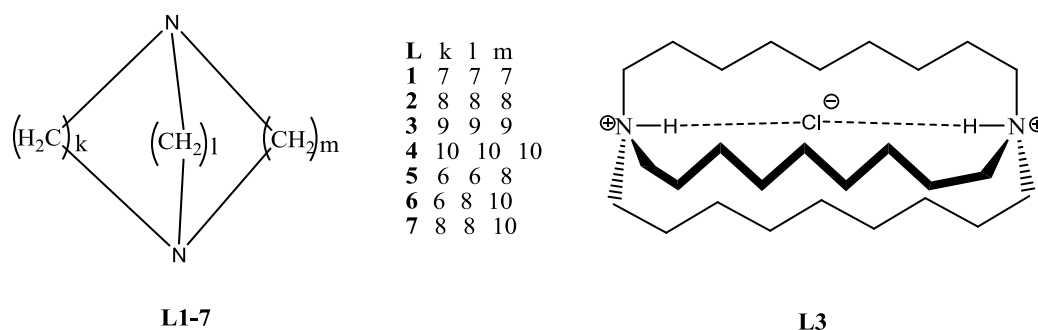
kosmotropes, “water structure makers,” and those to the right of chloride are termed *chaotropes*, “water structure breakers.” While the kosmotropes are strongly hydrated and have stabilizing and salting-out effects on proteins and macromolecules, the chaotropes destabilize folded proteins and have a salting-in behavior. Hydrophobic anions are generally bound more strongly in hydrophobic binding sites.

1.3.2 Historical Evolution

Ability of a receptor depends on two basic aspects of supramolecular chemistry: complementarity and preorganisation. Complementarity in simple terms refers to host and guest complimenting each other. The shape and size of the cavity of the host must match that of guest. The electronic interactions between host and guest must be attractive. Of all possible interactions between host and guest including ion-ion, ion-dipole, dipole-dipole, hydrogen bonds, π - π and van der Waals interactions, the more complementarity between the host and guest, the stronger will be the binding. Cram described it as, “to complex, host must have binding sites which can simultaneously contact and attract the binding sites of guest without generating internal strain or stronger non bonded repulsion”.⁴¹ If a receptor molecule does not undergo a significant conformational change upon guest binding, it is said to be preorganised. Host preorganisation is a key concept because it represents a major enhancement to the overall free energy of guest complexation. The corollary of preorganisation is in the binding kinetics. Rigidly preorganised receptors may have significant difficulty in passing through a complexation transition state and so tend to exhibit slow guest binding kinetics. Conformationally flexible receptors could able to adjust rapidly to changing conditions and hence, both complexation and decomplexation are rapid. Solvation enhances the effect of preorganisation since the solvation stabilisation of the unbound receptor is often greater than the case when it is wrapped around the guest, effectively presenting less surface area to the sounding medium.⁴²

The field of synthetic anion receptor chemistry traces its origins back to the 1968 communication by Simmons and Park from du Pont Central Research in Delaware (USA).⁴³ In this seminal work, the halide ion binding properties of several macrobicyclic receptors (**L1-7**), consisting of two ammonium bridge-head centers spanned by three alkyl linkers, were reported. The authors noted that the proton on the ammonium group could either point out of or into the cavity of the receptor, and it was found that the different conformations could be observed by ¹H

NMR spectroscopy. From the various compounds studied, with differently sized linkers, varying from 6 to 10 methylene groups in length, compound **L3** was found to have affinity for chloride ($K_a = 4 \text{ M}^{-1}$ in 50% TFA solution) and bromide ($K_a = 1 \text{ M}^{-1}$ in 50% TFA solution). Although, **L3** shows a higher affinity towards chloride ion over bromide ion, **L4** does not show selectivity among chloride, bromide and iodide ions ($K_a > 10 \text{ M}^{-1}$ in 50% TFA solution). These results showed that three dimensional cavity-size plays an important role on selectivity of the receptors. Under these conditions the only conformer observed, in the presence of the chloride ion, had both ammonium hydrogens pointed toward the center of the cavity, leading to the suggestion that the anion was bound within the confines of this cavity. This discovery showed the importance of complementarity and preorganization in supramolecular chemistry. The crystal structure of this complex reported by Marsh and co-workers in 1975, confirmed that the chloride ion was indeed bound within the central cavity of the positively charged receptor in the solid state.⁴⁴ However,



fourteen years earlier (i.e., in 1954), Tanford inferred through changes in the effective pKa values the formation of a complex between the anionic conjugate base of acetic acid and guanidinium moieties.⁴⁵ Following Simmons and Park's report, the next step forward came in the mid-1970s, when Lehn and co-workers described the anion binding properties of a variety of macrobicyclic and macrotricyclic ammonium based receptors. This research clearly demonstrated how optimizing the fit of an anion for a given charged cavity can lead to strong binding (discussed later in this chapter). Since these pioneering discoveries, the field of anion recognition drew increasing attention from the scientific community.² As a result, a variety of anion receptor motifs such as polyamines,⁴⁶ amides,^{26b,47} ureas and thioureas,⁴⁸ guanidiums,⁴⁹ steroids,⁵⁰ metal-based systems⁵¹ and heterocycles were developed subsequently. Among heterocycles, pyrroles,⁵² indoles,⁵³ and imidazoles⁵⁴ are quite popular anion binding motifs, which interacts via N-H...anion hydrogen bonding. Flood and coworkers reported triazole-based heterocyclic anion binding motif, which uses preorganised C-H moiety as the hydrogen bond

donor.⁵⁵ Besides, receptors with capability of recognition of anion through anion- π interactions have also been reported.⁵⁶

1.3.3 Classification

In general anion receptors are classified on the basis of the anion binding functional group present in the receptor (e.g. ammonium, amide, urea etc.). In another approach they may be classified on the structural nature of the molecule, whether they are acyclic or cyclic in nature and spatial arrangement of these acyclic and cyclic molecules (Figure 1.11).

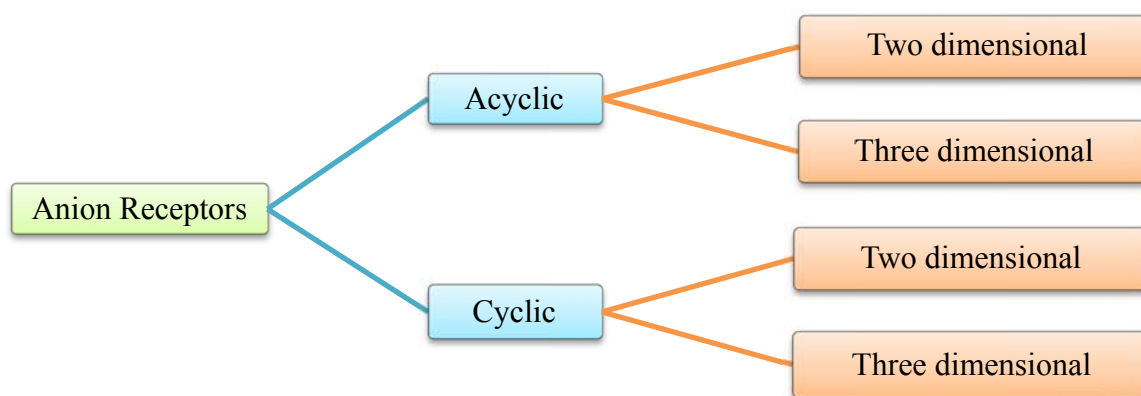
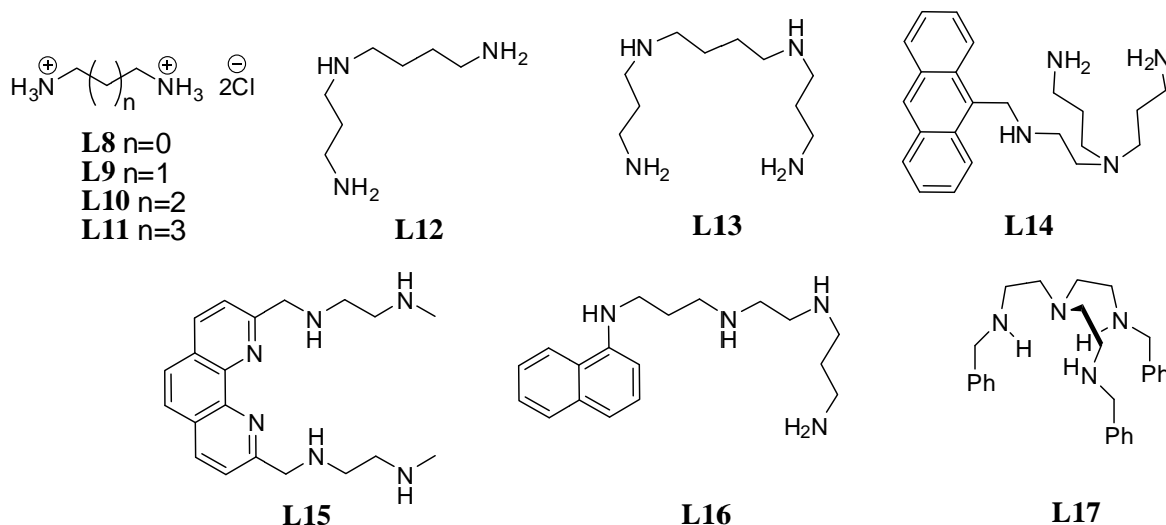


Figure 1.11 Classification of anion receptors.

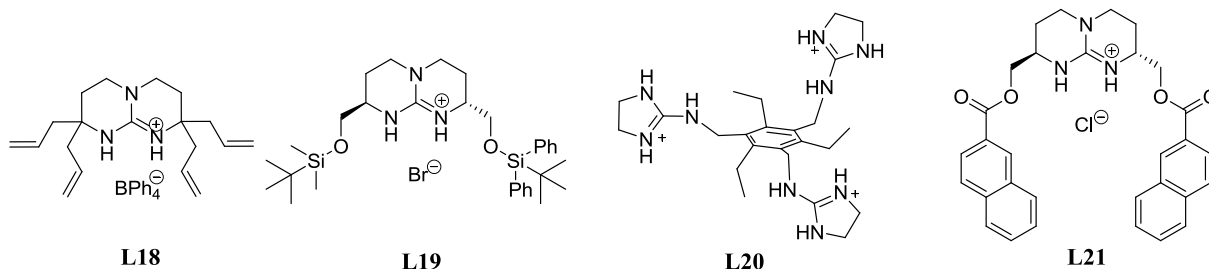
1.3.3.1 Acyclic Anion Receptors

Although, anion receptor chemistry had begun with complex cyclic molecules as stated above, but due to the difficulty of synthesis and complex anion binding modes of them, chemists gradually shifted to small acyclic molecules. First report came when Glusker and coworker in 1977 showed that simple ethylenediammonium cation (**L8**) are capable of anion



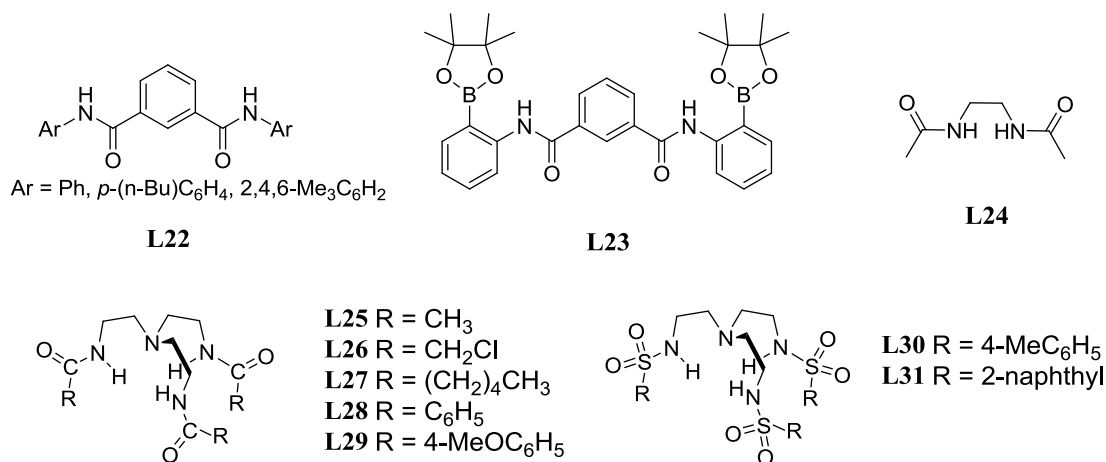
binding at least in the solid state.⁵⁷ After the seminal work of Glusker, Nakai and Glinsmann showed that putrescine **L10** can bind to AMP, ADP and ATP with association constants 82, 200 and 290 M^{-1} , respectively at 303 K at pH 7.5. Spermidine **L12** and spermine **L13**, naturally occurring polyamines, which stay in their protonated form in biological pH, are reported to bind to phosphates in aqueous solution.⁵⁹ Later many groups separately shown (**L14-16**) that attaching fluorophoric unit to these linear polyamine moieties transform them to efficient luminescent chemosensor for ATP in acidic aqueous medium.⁶⁰ Bowman-James and coworkers reported that **L17** display selectivity towards tetrahedral oxoanions (dihydrogenphosphate and bisulphate).⁶¹

Nature frequently uses guanidinium moieties to coordinate different anionic groups. Mimicking this attribute, several linear guanidinium based receptors have been reported. These receptors mainly recognize oxo-anions (phosphate, acetate, carboxylate, benzoate etc.). Schmidtchen and coworkers first reported in 1988 that **L18** can bind tetrabutylammonium-*p*-nitrobenzoate ($K_a = 7 \times 10^6 \text{ M}^{-1}$).⁶² The crystal structure of an acetate salt confirmed the

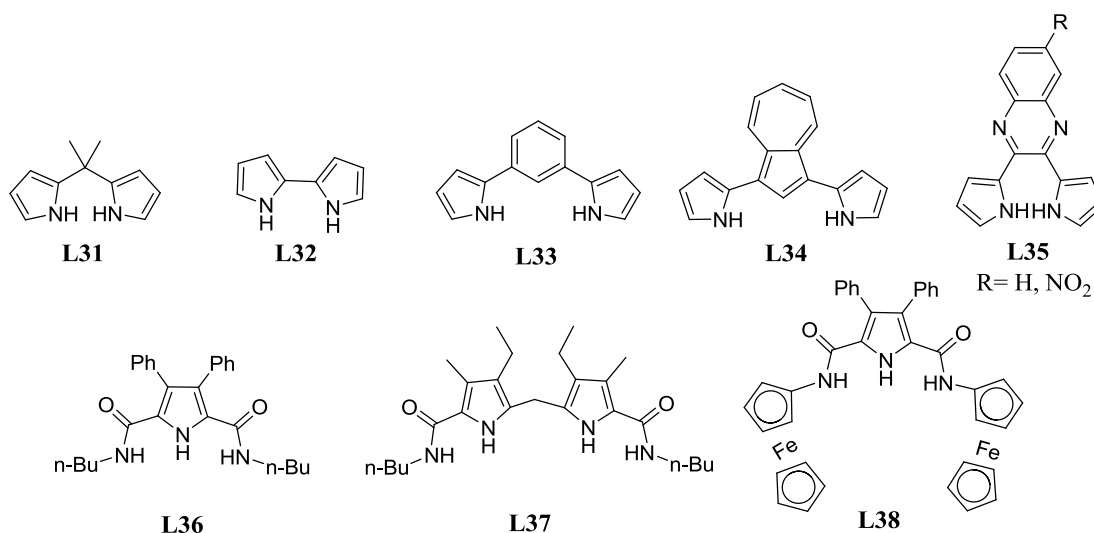


formation of two strong symmetric hydrogen bonds between the host and the guest. Later they had also shown guanidinium–carboxylate interactions by isothermal titration calorimetry (ITC). The binding isotherm between **L19** and tetraethylammonium acetate in acetonitrile ($K_a = 2.0 \times 10^5 \text{ M}^{-1}$) revealed that the process was both entropically and enthalpically favorable for a 1:1 complex.⁶³ Anslyn and co-workers developed receptor **L20**, with preorganized tripod platform, showing selective binding towards citrate ion in pure water ($K_a = 6.9 \times 10^3 \text{ M}^{-1}$).⁶⁴ The first example of chiral recognition of a carboxylate ion by a guanidinium-based receptor was reported by de Mendoza and coworker, showing **L21** can extract enantiomeric salts of N-protected amino acids, such as tryptophan, with modest selectivity (up to 17% excess of N-Ac-L-Trp or N-Boc-L-Trp were extracted by (S,S)-**L21** from water to chloroform).⁶⁵

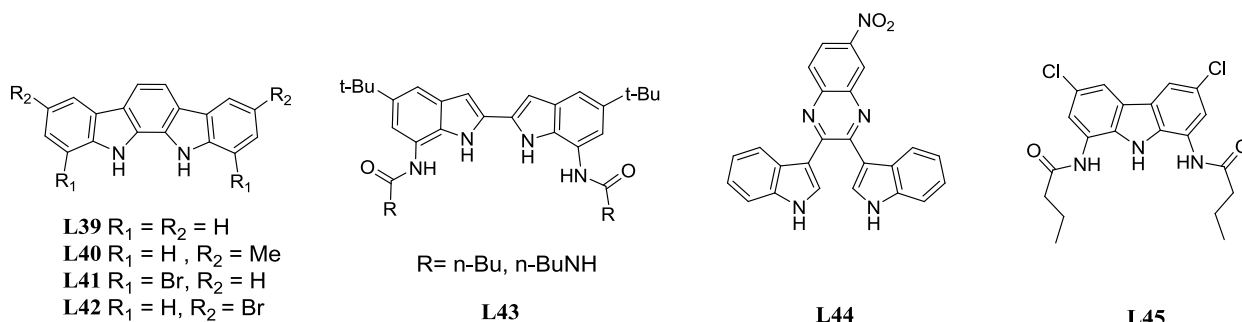
Amide functional group is quite popular in designing the anion receptors, as formation of this functional group is very easy. Simple acyclic, non-preorganized diamide receptors **L22** were designed by Crabtree and coworkers. These receptors showed strong and non-selective anion binding, due in part to their flexibility. This flexibility allowed for adjustments in the size of the cavity, as well as for the formation of almost linear hydrogen-bonds.⁶⁶ Smith and coworkers studied the binding of carboxylates with **L23**, containing a Lewis acidic boronate



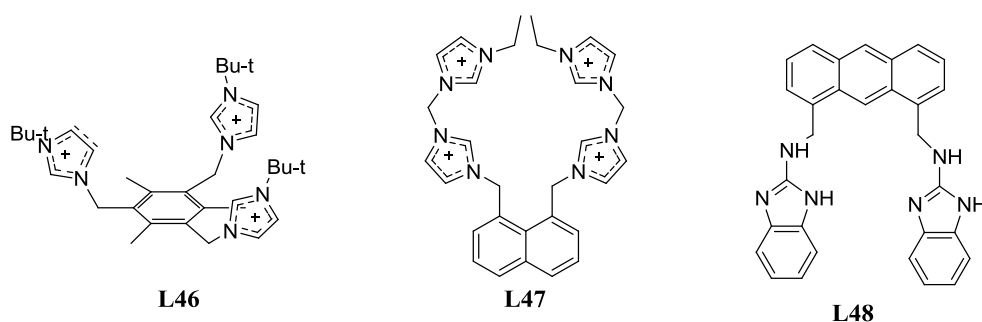
group showed ten times higher affinity ($K_a = 2.1 \times 10^3 \text{ M}^{-1}$) toward acetate compared to receptor not containing boronate group. Introduction of more number of amide groups in the receptor have mixed effect on selectivity as seen in case of **L24** and **L25**.⁶⁷ Reinhoudt and coworkers reported a series of tris-amides and tris-sulphonamides based upon tren skeleton and these receptors (**L26-31**) show selectivity towards phosphate ion in acetonitrile.^{68a} Various kinds of tripodal amide based receptors have been reported in the literature.^{68b-d}



Although anion binding affinities of cyclic pyrrole based receptors have been extensively studied, acyclic pyrrole based receptors got a little attention due to the perception that they would show low affinity for anions. Belying this misconception linear pyrrole systems **L31-35**, showed quite higher selectivity towards fluoride ion.⁶⁹ As described earlier in this chapter, various artificial prodigiosins were also capable of binding anions.³⁵ Pyrrole units with amide, urea functionalities (**L36-38**) can bind with benzoate and fluoride ions.⁷⁰



Beer and coworkers, and Jurczak and coworkers independently reported carbazoles (**L39-42**), as anion receptor.⁷¹ Jeong and co-workers have also synthesised bis-amido and bis-urea biindole derivatives **L43** having a higher affinity towards phosphate and pyrophosphate ions in DMSO.⁷² Sessler group reported diindolylquinoxalines **L44**, which showed selectivity towards dihydrogenphosphate ion, whereas previously reported pyrrole conjugate (**L35**) showed greater affinity for fluoride ion.⁷³ Jurczak and coworkers in 2004 showed that carbazole derivative **L45** could also act as anion receptor, in particular towards dihydrogenphosphate ion.⁷⁴

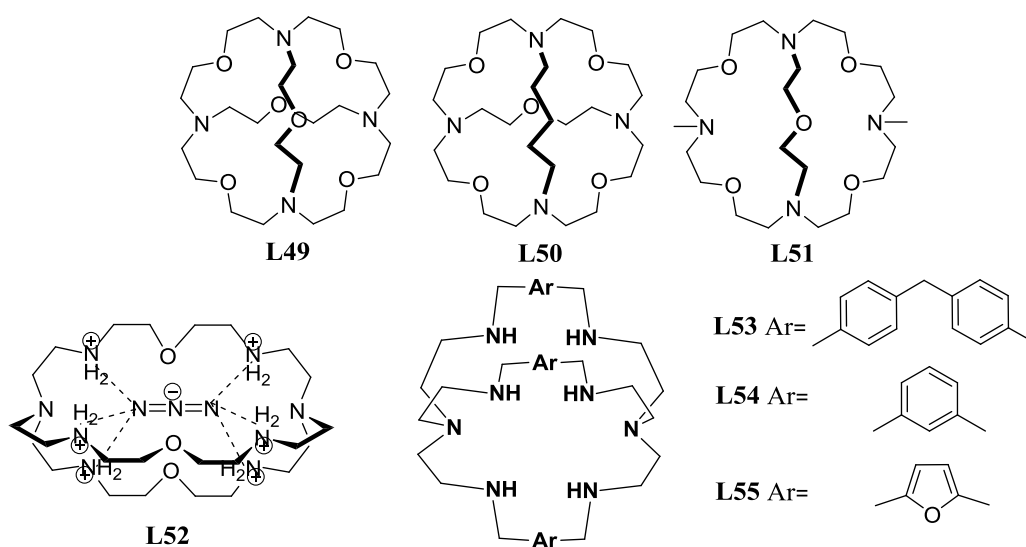


Sato and coworkers in 1999 reported that **L46** can serve as halide ion receptor.⁷⁵ Kang and coworkers reported a naphthalene derivative **L47**, which contained two methylene bridged bis-imidazolium rings showing selective affinity for iodide ion.⁷⁶ Jang and coworkers reported that benzimidazole moiety could also act as anion receptor (**L48**).⁷⁷

Acyclic molecules are easy to synthesize compared to cyclic ones, but due to their structural flexibility selectivity is less obvious in many cases.

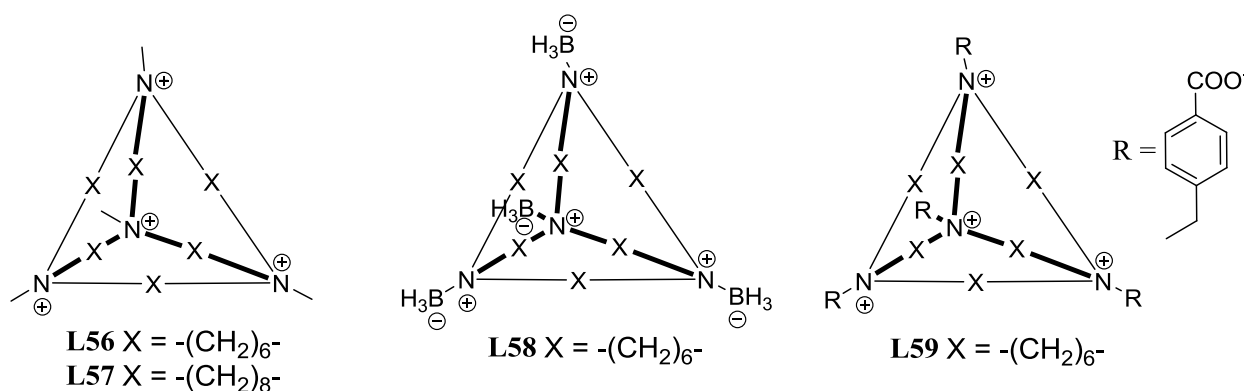
1.3.3.2 Cyclic Anion Receptors

From early days of anion receptor chemistry it was found that cyclic receptors possessed greater superiority over the acyclic ones in terms of their selectivity towards anions. After the seminal work of Simmons and Park, Lehn and co-workers in the mid-1970s described the anion binding properties of a variety of ammonium based receptors. Which clearly demonstrated, how optimizing the fit of an anion, for a given charged cavity can lead to strong binding. As shown in their report, **L49** and **L50** in their tetraprotonated forms were found to bind chloride ions

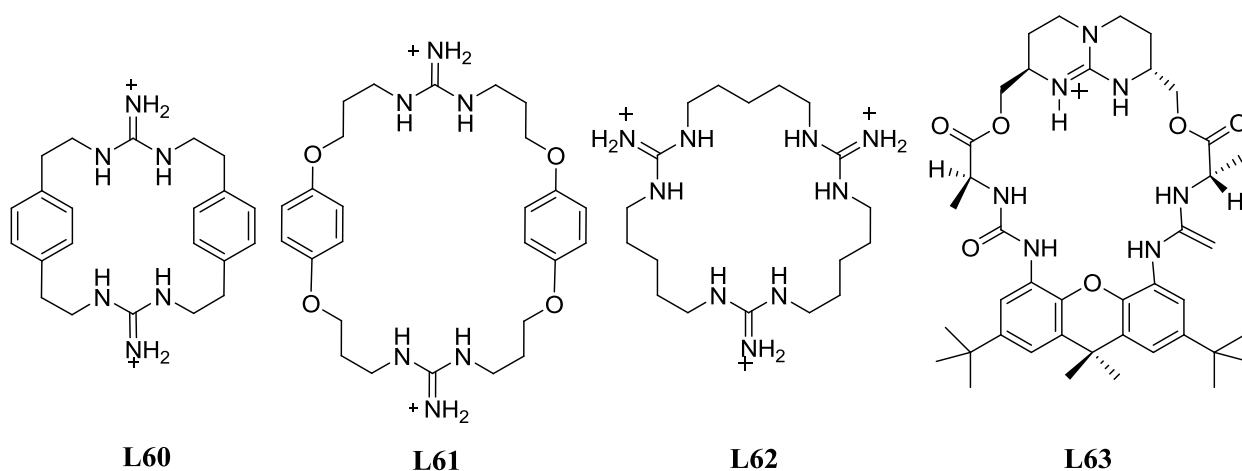


selectively with an association constant ($\log K_a$) of greater than 4 in aqueous solution.⁷⁸ Iodide is too large to fit into the cavity and is therefore bound considerably less strongly. The model compound **L51** was also studied and displayed a much lower affinity for anions than the cryptand systems. The crystal structure of the chloride complex of **L49** was reported by Weiss and coworkers in 1976 and revealed its presence in the center of the cryptand.⁷⁹ On the other hand, **L52** an ellipsoidal cryptand, was found to be selective for linear anions such as azide ($\log K_a = 4.6$ in water) and showed much lesser interaction with spherical anions (chloride and iodide).⁸⁰ Azide ion is more complementary to the shape of the cavity than chloride.⁸¹ **L53-55** emerged as good receptors for dicarboxylate ions, whereas **L54**, in particular can bind to perrhenate^{82a,b} and later Ghosh and coworker have showed that it could also bind to halide ions also^{82c} After these findings, various reports appeared with cyclic amines as anion receptors.^{2b} Soon after Lehn's work, Schmidtchen produced a series of receptors possessing quaternary

ammonium groups arranged in a tetrahedral manner. By altering the length of the alkyl chains between the ammonium centers, it was possible to “tune” the selectivity of the receptors for particular anions. For example, **L56** is selective towards iodide and **L57** is selective towards larger *p*-nitrophenolate ion.⁸³ As they are charged, therefore are associated with counter anions that may compete for the anion-binding site. To overcome this limitation, subsequently Schmidtchen prepared zwitterionic receptors such as **L58** and **L59** that are neutral and **L59** forms much stronger complex with halide ions than **L56**.⁸⁴

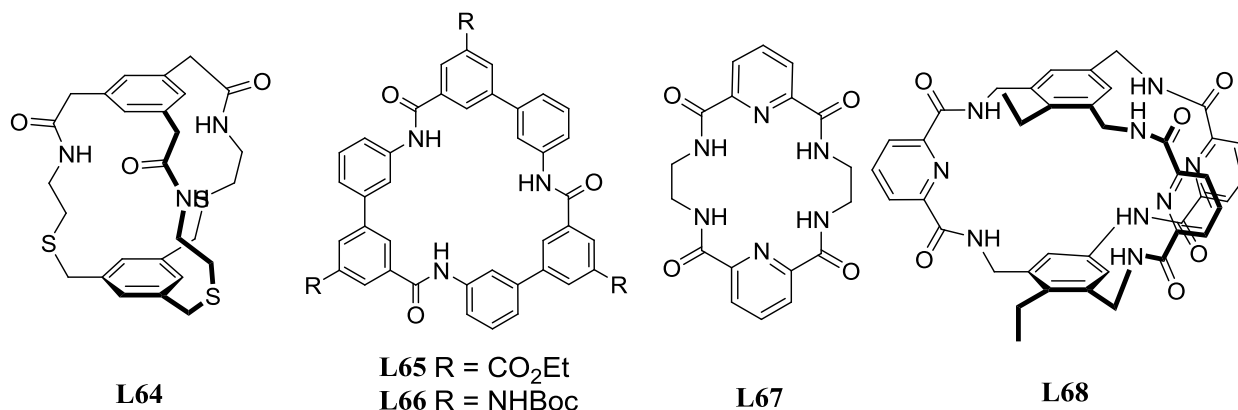


Cyclic guanidinium based molecules also emerged as good anion receptors. Major contributions came from Lehn and coworkers; they have reported **L60-62**, which can bind to phosphate ions.⁸⁵ Later, de Mendoza and coworkers have reported a hybrid type receptor **L63**, which can bind to tetrahedral oxoanions.⁸⁶

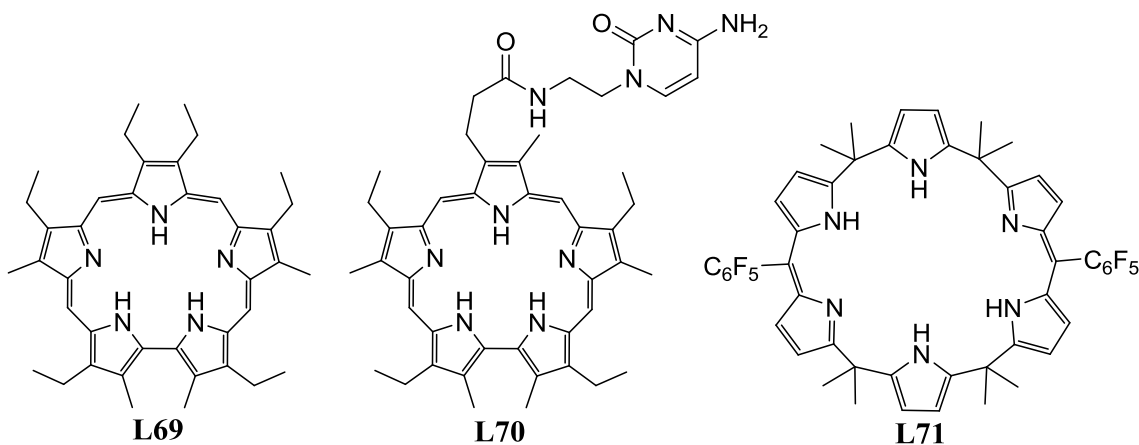


First synthetic anion receptor to utilize amide NH^{\cdots} anion interactions was reported by Pascal and co-workers in 1986, a cryptand like tris-amide **L64**, which displayed interaction with fluoride ion in DMSO-d_6 .⁸⁷ Rigid amide based receptors **L65** and **L66** reported by Hamilton and

coworkers can effectively bind tetrahedral anions.⁸⁸ Jurczak in 2004 showed that **L67** can bind fluoride and chloride ions in solid state, whereas solution phase study revealed highest binding affinities for acetate ion in DMSO.⁸⁹ Anslyn and coworkers demonstrated that **L68**, a **L64** type molecule can selectively bind to nitrate ion.⁹⁰

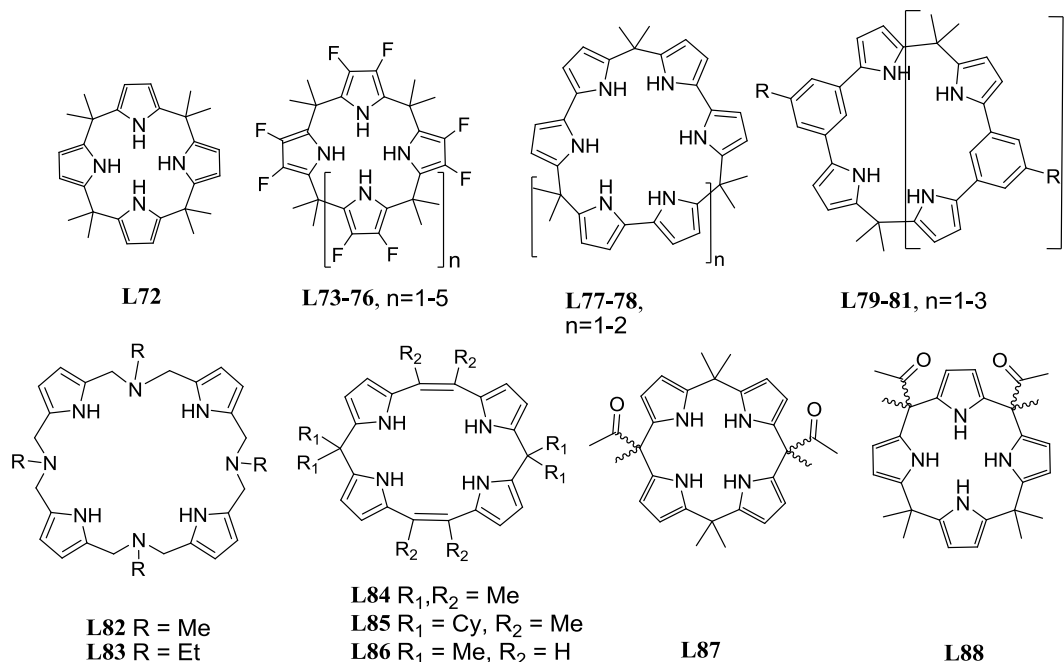


In 1990, Sessler and coworkers reported sapphyrin **L69** having one fluoride ion, bound inside its diprotonated core, which was extracted by the receptor from the external medium used.⁹¹ Sapphyrin **L70** could selectively transport 5'-GMP over 5'-CMP and 5'-AMP.⁹² Calix[6]pyrrole **L71** displayed strongly binding towards iodide and bisulphate ions in high concentration of fuming sulfuric acid ($K_a = 2.55 \times 10^4 \text{ M}^{-1}$ and $3.5 \times 10^3 \text{ M}^{-1}$ respectively).⁹³

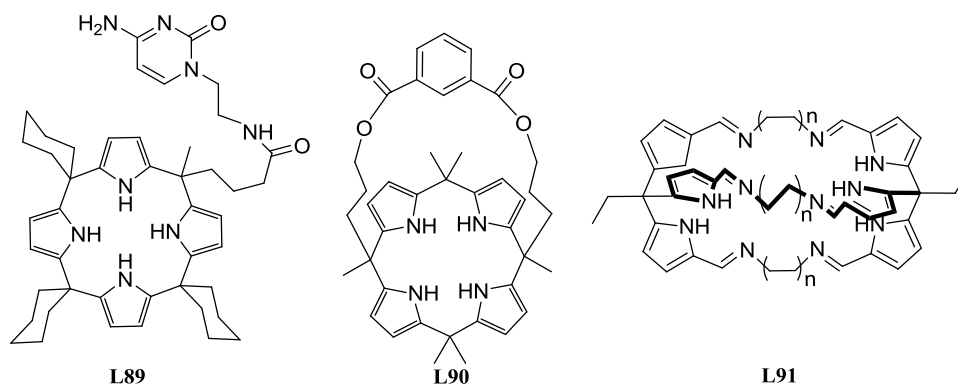


Along with the protonated pyrrole based receptors there are many neutral pyrrolic receptors reported in the literature. In the year 1996, Sessler and coworkers first reported calix[4]pyrrole, a porphyrinogen, which binds to halides and small neutral molecules.⁹⁴ Subsequently, several core expanded calix[n]pyrroles were reported. In this regard, octafluoro-derivative **L73** and **L78** displayed a higher chloride selectivity over their other homologs.⁹⁵ **L79**-

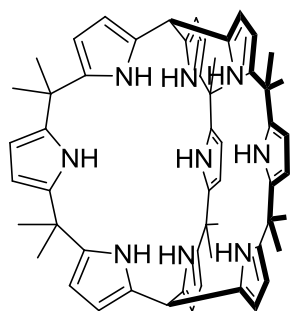
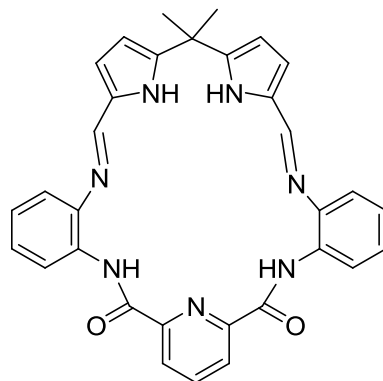
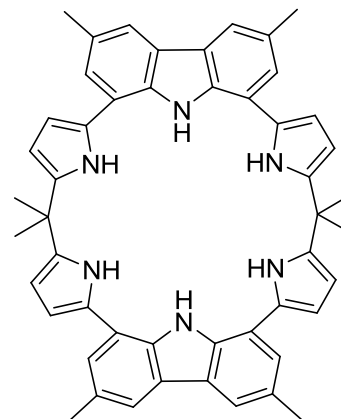
81 type receptors could bind to halide, bisulphate and nitrate ions without much selectivity.⁹⁶ Mani and coworkers have reported that azatetrapyrrolic receptors **L82-83** can bind to halides.⁹⁷ Expanded calix[4]pyrrole type receptors, **L84-85** are effective halide receptors and in particular **L86** displayed colorimetric sensing of fluoride ion.⁹⁸ Meso-substituted calix[4]pyrrole **L87**



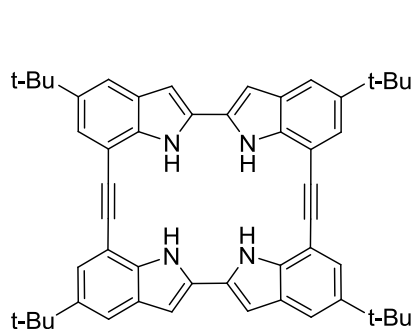
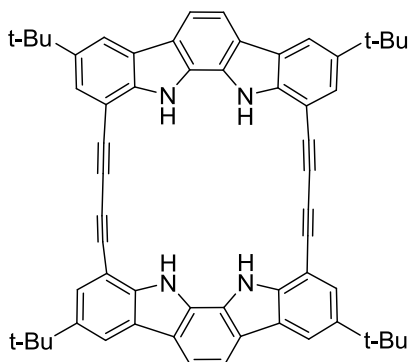
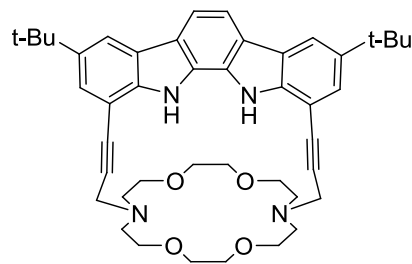
possesses higher affinity for dihydrogenphosphate ion, whereas **L88** can bind to various halide ions along with dihydrogenphosphate.⁹⁹ Towards modification of this class of receptors, many meso-substituted calixpyrroles came into picture.¹⁰⁰ **L89** reported by Sessler and coworkers shows higher capability of transporting 5'-GMP than the sapphyrin analog **L70**.^{2b,101} In 2002, Lee and coworkers demonstrated through single side strapping of calix[4]pyrrole (**L90**) a new path for making efficient anion receptors.¹⁰² First cryptand like pyrrole derivative **L91** reported by Beer and coworkers in 2001 could only bind to neutral molecules (e.g. diamine and diols).¹⁰³



Nearly contemporaneous with this report, Sessler and coworkers reported **L92** having interesting binding ability towards various anions.¹⁰⁴ Various kinds of hybrid pyrrolic macrocycles (e.g. **L93-94**) are also reported in the literature which can interact with various halide, pseudohalide,

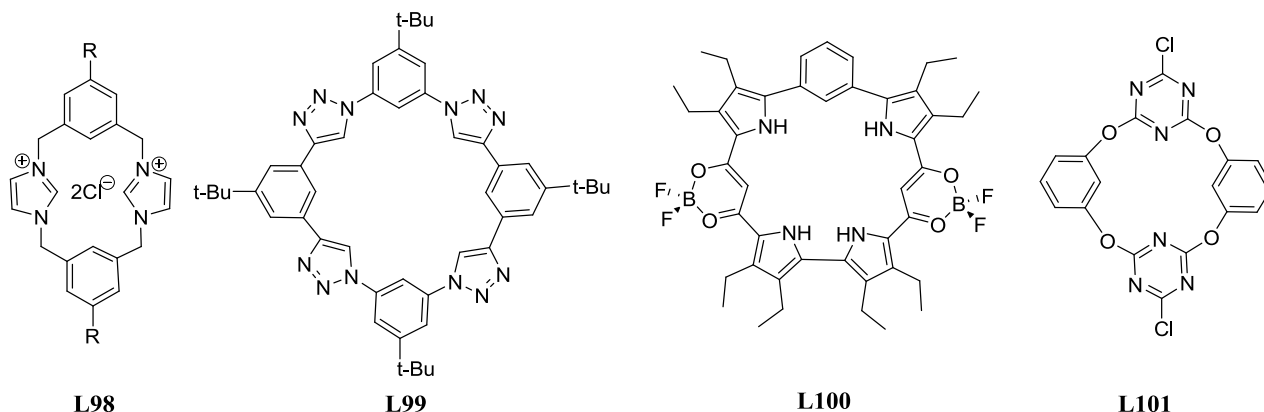
**L92****L93****L94**

oxoanions and anions derived from various carboxylic acids.^{100c-f,105} Besides, many kinds of pyrrole based receptors are reported in recent years, which show selective and compelling binding behavior towards anions and neutral molecules.¹⁰⁶

**L95****L96****L97**

In parallel with pyrrole many indole, carbazole and indolocarbazole based cyclic anion receptors have also been synthesized. For example, **L95** showed good affinity toward chloride ion ($K_a = 2 \times 10^8 \text{ M}^{-1}$), while indolocarbazole based **L96** displayed strong affinity toward iodide and azide ions.¹⁰⁷ Receptor **L97**, by Jeong has proved to be an excellent ion pair receptor for sodium chloride.¹⁰⁸ Alcalde and coworkers have reported an imidazole based cyclic receptor **L98**,⁵⁴ capable of binding anions, and subsequently, few other imidazole based receptors were also reported in the literature.¹⁰⁹ Very recently macrocycles with interactive C-H bonds came into picture as anion receptors. Flood and coworkers reported triazole-based anion receptors (**L99**)

which uses preorganized C-H moiety as the hydrogen bond donor.⁵⁵ Haketa and Maeda showed that **L100** display 200 times stronger affinity for chloride ion than its linear oligomer (K_a for **L100** $>10^{10} \text{ M}^{-1}$ in CH_2Cl_2).¹¹⁰ Another class of macrocyclic receptors, derived from *s*-triazine i.e. **L101** emerged recently, which uses π -electron deficient motifs for anion binding.^{56h,111}



Above discussed classification and examples provide a brief glimpse about the large number of ever increasing anion receptors.

1.5 References

1. Ross, S. *Notes Rec. R. Soc.* **1961**, *16*, 187.
2. (a) In *Supramolecular Chemistry of anions* Eds. Bianchi, A.; Garcia-Epsána, E.; Bowman-James, K. Wiley-VCH, New York, 1997. (b) *Anion Receptor Chemistry* Sessler, J. L.; Gale, P. A.; Cho, W. S. RSC Publishing, Cambridge, UK, 2006. (c) Gale, P. A. *Chem. Commun.* **2011**, 82. (d) Bratthall, D.; Hansel-Petersson, G.; Sundberg, H. *Eur. J. Oral Sci.* **1996**, *104*, 416. (f) Haider, S. A.; Abdu, M. A.; Batista, I. S.; Sobral, J. H.; Luan, X.; Kallio, E.; Maguire, W. C.; Verigin, M. I.; Singh, V. *J. Geophys. Res.* **2009**, *114*, A03311.
3. (a) Wright, E. M.; Diamond, J. M. *Physiol. Rev.* **1977**, *57*, 109. (b) Bauduin, P.; Renoncourt, A.; Touraud, D.; Kunz, W.; Ninham, B. W. *Curr. Opin. Colloid Interface Sci.* **2004**, *9*, 43.
4. (a) Connet, P. *Fluoride* **2007**, *40*, 155. (b) Foulkes, R. G. *Fluoride* **2007**, *40*, 229. (c) Carton, R. J. *Fluoride* **2006**, *39*, 163.
5. (a) Gazzano, E.; Bergandi, L.; Riganti, C.; Aldieri, E.; Doublier, S.; Costamagna, C.; Bosia, A.; Ghigo, D. *Curr. Med. Chem.* **2010**, *17*, 2431. (b) Spittle, B. *Fluoride*, **2011**, *44*, 117. (c) Barbier, O.; Arreola-Mendoza, L.; Del Razo, L. M. *Chem.-Biol. Interact.*

- 2010**, 188, 319. (e) Sandhu, R.; Lal, H.; Kundu, Z. S.; Kharb, S. *Bio. Trace Elem. Res.* **2011**, 144, 1. (f) Yu, Y.; Yang, W.; Dong, Z.; Wan, C.; Zhang, J.; Liu, J.; Xiao, K.; Huang, Y.; Lu, B. *Fluoride* **2008**, 41, 134.
6. (a) Zhang, M.; Wang, A. G.; Xia, T.; He, P. *Toxicol. Lett.* **2008**, 179, 1; (b) Wurtz, T.; Houari, S.; Mauro, N.; MacDougall, M.; Peters, H.; Berdal, A. *Toxicology* **2008**, 249, 26.
 7. Clark, J. H. *Chem. Rev.* **1980**, 80, 4292.
 8. Cametti, M.; Rissanen, K. *Chem. Soc. Rev.* **2013**, 42, 2016.
 9. Jentsch, T. J.; Stein, V.; Weinreich, F.; Zdebik, A. A. *Physiol. Rev.* **2002**, 82, 503.
 10. Malnic, G.; Aires, M. M. *Am. J. Physiol.* **1970**, 218, 27.
 11. Simon, D. B.; Bindra, R. S.; Mansfield, T. A.; Nelson-Williams, C.; Mendonca, E.; Stone, R.; Schurman, S.; Nayir, A.; Alpay, H.; Bakkaloglu, A.; Rodriguez-Soriano, J.; Morales, J. M.; Sanjad, S. A.; Taylor, C. M.; Pilz, D.; Brem, A.; Trachtman, H.; Griswold, W.; Richard, G. A.; John, E.; Lifton, R. P. *Nature Genet.* **1997**, 17, 171.
 12. Devuyst, O.; Christie, P. T.; Courtoy, P. J.; Beauwens, R.; Thakker, R. V. *Human Molec. Genetics* **1999**, 8, 247.
 13. (a) Anderson, M. P.; Rich, D. R.; Gregory, R. J.; Smith, A. E.; Welsh, M. J. *Science* **1991**, 251, 679. (b) Riordan, J.; Bear, C.; Rommens, J.; Reyes, E.; Ackerly, C.; Sun, S.; Nalmsmith, A.; Jensen, T.; Hanraha, J.; Kartner, N. *Cell* **1991**, 64, 681. (c) Welsh, M.; Smith, A.; Manavalan, P.; Gregory, R.; Anderson, M.; Rich, D. *Science* **1991**, 253, 205.
 14. (a) Choi, J. Y.; Muallem, D.; Kiselyov, K.; Lee, M. G.; Thomas, P. J.; Muallem, S. *Nature* **2001**, 410, 94. (b) Bok, D.; Galbraith, G.; Lopez, I.; Woodruff, M.; Nusinowitz, S.; Beltrandel-Rio, H.; Huang, W.; Zhao, S.; Geske, R.; Montgomery, C.; Van Sligtenhorst, I.; Friddle, C.; Platt, K.; Sparks, M. J.; Pushkin, A.; Abuladze, N.; Ishiyama, A.; Dukkupati, R.; Liu, W.; Kurtz, I. *Nat. Genet.* **2003**, 34, 313. (c) Rousselle, A. V.; Heymann, D. *Bone* **2002**, 30, 533. (d) Vaughan-Jones, R. D.; Spitzer, K. W.; Swietach, P. *J. Mol. Cell. Cardiol.* **2009**, 46, 318.
 15. World Health Organization, *Vitamin and mineral requirements in human nutrition*, 2004, ISBN: 9241546123.
 16. Brownstein, D., *Iodine: Why You Need It, Why You Can't Live Without It*, Medical Alternatives Press, 2009.

17. Logue, B. A.; Hinkens, D. M.; Baskin, S. I.; Rockwood, G. A. *Crit. Rev. Anal. Chem.* **2010**, *40*, 122.
18. Jackson, R.; Oda, R. P.; Bhandari, R. K.; Mahon, S. B.; Brenner, M.; Rockwood, G. A.; Logue, B. A. *Anal. Chem.* **2014**, *86*, 1845.
19. World Health Organization, *Guidelines for Drinking Water Quality*, Geneva, 1996.
20. Kulig, K. W. *Cyanide Toxicity*, U.S. Department of Health and Human Services, Atlanta, GA, 1991.
21. Xu, Z.; Chen, X.; Kim, H. N.; Yoon, J. *Chem. Soc. Rev.* **2010**, *39*, 127.
22. Dick, C. F.; Dos-Santos, A. L. D.; Meyer-Fernandes, J. R. *Enzyme Res.* **2011**, 103980.
23. (a) Hargrove, A. E.; Nieto, S.; Zhang, T.; Sessler, J. L.; Anslyn, E. V. *Chem. Rev.* **2011**, *111*, 660. (b) Lawal, A. T.; Adeloju S. B. *Talanta* **2013**, *114*, 191.
24. (a) Logan, B. E. *Biorem. J.* **1998**, *2*, 69. (b) Batjoens, P.; D-Brabander, H. F.; T'Kindt, L. *Anal. Chim. Acta.* **1993**, *275*, 335.
25. McKee, V.; Nelson, J.; Town, R. M. *Chem. Soc. Rev.* **2003**, *32*, 309.
26. (a) Markovich, D. *Physiol Rev.* **2001**, *81*, 1499. (b) Katayev, E. A.; Ustynyuk, Y. A.; Sessler, J. L. *Coord. Chem. Rev.* **2006**, *250*, 3004. (c) Ravikumar, I.; Ghosh, P. *Chem. Soc. Rev.* **2012**, *41*, 3077.
27. Pflugrath, J. W.; Quiocho, F. A. *J. Mol. Biol.* **1988**, *200*, 163.
28. Louie, G. V.; Brownlie, P. D.; Lambert, R.; Cooper, J. B.; Blundell, T. L.; Wood, S. P.; Warren, M. J.; Woodcock, S. C.; Jordan, P. M. *Nature* **1992**, *359*, 33.
29. Xu, H.; Straeter, N.; Schroeder, W.; Boettcher, C.; Ludwig, K.; Saenger, W. *Acta Cryst. D* **2003**, *59*, 815.
30. Chantalat, L.; Nicholson, J. M.; Lambert, S. J.; Reid, A. J.; Donovan, M. J.; Reynolds, C. D.; Wood, C. M.; Baldwin, J. P. *Acta Cryst. D* **2003**, *59*, 1395.
31. Dutzler, R.; Campbell, E. B.; MacKinnon, R. *Nature* **2002**, *415*, 287.
32. (a) Koropatkin, N. M.; Pakrasi, H. B.; Smith, T. J. *Proc. Natl. Acad. Sci. U. S. A.* **2006**, *103*, 9820. (b) Koropatkin, N. M.; Koppelaar, D. W.; Pakrasi, H. B.; Smith, T. J. *J. Biol. Chem.* **2006**, *282*, 2606.
33. (a) Sheth, T. R.; Henderson, R. M.; Hladky, S. B.; Cuthbert, A. W. *Biochim. Biophys. Acta, Biomembr.* **1992**, *179*, 1107. (b) Jeong, E. J.; Kang, E. J.; Sung, L. T.; Hong, S. K.; Lee, E. *J. Am. Chem. Soc.* **2002**, *124*, 14655. (c) Tanigaki, K.; Sato, T.; Tanaka, Y.;

- Ochi, T.; Nishikawa, A.; Nagai, K.; Kawashima, H.; Ohkuma, S. *FEBS Lett.* **2002**, *37*, 524.
34. (a) Sato, T.; Konno, H.; Tanaka, Y.; Kataoka, T.; Nagai, K.; Wasserman, H. H.; Ohkuma, S. *J. Biol. Chem.* **1998**, *273*, 21455. (b) Seganish, J. L.; Davis, J. T. *Chem. Commun.* **2005**, 5781.
35. Sessler, J. L.; Eller, L. R.; Cho, W.S.; Nicolaou, S.; Aguilar, A.; Lee, J. T.; Lynch, V. M.; Magda, D. J. *Angew. Chem. Int. Ed.* **2005**, *44*, 5989.
36. Yamamoto, D.; Kiyozuka, Y.; Uemura, Y.; Yamamoto, C.; Takemoto, H.; Hirata, H.; Tanaka, K.; Hioki, K.; Tsubura, A. *J. Cancer Res. Clin. Oncol.* **2000**, *126*, 191.
37. Schmidtchen, F. P.; Berger, M. *Chem. Rev.* **1997**, *97*, 1609.
38. Marcus, Y. *J. Chem. Soc. Faraday Trans.* **1991**, *87*, 2995.
39. Beer, P. D.; Gale, P. A. *Angew. Chem. Int. Ed.* **2001**, *40*, 486.
40. Hofmeister, F. *Arch. Exp. Pathol. Pharmacol.* **1888**, *24*, 247.
41. *Encyclopedia of Supramolecular Chemistry*, Vol. 2, edited by Atwood, J. L.; Steed, J. W. CRC Press, 2004.
42. *Supramolecular Chemistry*, Steed, J. W.; Atwood, J. L., John Wiley & Sons, Ltd., 2000.
43. (a) Simmons, H. E.; Park, C. H. *J. Am. Chem. Soc.* **1968**, *90*, 2428. (b) Park, C. H.; Simmons, H. E. *J. Am. Chem. Soc.* **1968**, *90*, 2429. (c) Park, C. H.; Simmons, H. E. *J. Am. Chem. Soc.* **1968**, *90*, 2431.
44. Bell, R. A.; Christoph, G. G.; Fronczek, F. R.; Marsh, R. E. *Science* **1975**, *190*, 151.
45. Tanford, C. *J. Am. Chem. Soc.* **1954**, *76*, 945.
46. (a) Garcia-España, E.; Díaz, P.; Llinares, J. M.; Bianchi, A. *Coord. Chem. Rev.* **2006**, *250*, 2952. (b) Wichmann, K.; Antonioli, B.; Söhnle, T.; Wenzel, M.; Gloe, K.; Price, J. R.; Lindoy, L. F.; Blake, A. J.; Schröder, M. *Coord. Chem. Rev.* **2006**, *250*, 2987.
47. (a) Bondy, C. R.; Loeb, S. J. *Coord. Chem. Rev.* **2003**, *240*, 157. (b) Kang, S. O.; Hossain, Md. A.; Bowman-James, K. *Coord. Chem. Rev.* **2006**, *250*, 3038.
48. Li, A. -F.; Wang, J. -H.; Wang, F.; Jiang, Y. -B. *Chem. Soc. Rev.* **2010**, *39*, 3729.
49. (a) Best, M. D.; Tobey, S. L.; Anslyn, E. V. *Coord. Chem. Rev.* **2003**, *240*, 3. (b) Schmuck, C. *Coord. Chem. Rev.* **2006**, *250*, 3053.
50. (a) Davis, A. P.; Joos, J. -B. *Coord. Chem. Rev.* **2003**, *240*, 3. (b) Davis, A. P. *Coord. Chem. Rev.* **2006**, *250*, 2939.

51. (a) Beer, P. D.; Hays, E. J. *Coord. Chem. Rev.* **2003**, *240*, 167. (b) O'Neil, E. J.; Smith, B. D. *Coord. Chem. Rev.* **2006**, *250*, 3068. (c) Rice, C. R. *Coord. Chem. Rev.* **2006**, *250*, 3190.
52. (a) Sessler, J. L.; Camiolo, S.; Gale, P. A. *Coord. Chem. Rev.* **2003**, *240*, 17. (b) Sessler, J. L.; Davis, J. M. *Acc. Chem. Res.* **2001**, *34*, 989. (b) Sessler, J. L.; Cho, W. S.; Lynch, V.; Kral, V. *Chem. Eur. J.* **2002**, *8*, 1134. (c) Cafeo, G.; Kohnke, F. H.; White, A. J. P.; Garozzo, D.; Messina, A. *Chem. Eur. J.* **2007**, *13*, 649. (d) Sessler, J. L.; Barkey, N. M.; Pantos, G. D.; Lynch, V. *New J. Chem.* **2007**, *31*, 646.
53. Gale, P. A. *Chem. Commun.* **2008**, 4525.
54. Yoon, J.; Kim, S. K.; Singh, N. J.; Kim, K. S. *Chem. Soc. Rev.* **2006**, *35*, 355.
55. McDonald, K. P.; Hua, Y.; Lee, S.; Flood, A. H. *Chem. Commun.* **2012**, 5065.
56. (a) Gamez, P.; Mooibroek, T. J.; Teat, S. J.; Reedijk, J. *Acc. Chem. Res.* **2007**, *40*, 435. (b) Schottel, B. L.; Chifotides, H. T.; Dunbar, K. R. *Chem. Soc. Rev.* **2008**, *37*, 68. (c) Hay, B. P.; Bryantsev, V. S. *Chem. Commun.* **2008**, 2417. (d) Berryman, O. B.; Johnson, D. W. *Chem. Commun.* **2009**, 3143. (e) Frontera, A.; Gamez, P.; Mascal, M.; Mooibroek, T. J.; Reedijk, J. *Angew. Chem. Int. Ed.* **2011**, *50*, 9564. (f) Wang, D. -X.; Wang, M. -X. *Chimia* **2011**, *65*, 939. (g) Ballester, P. *Acc. Chem. Res.* **2012**, *46*, 874. (h) Wang, D. X.; Wang, M. X. *J. Am. Chem. Soc.* **2013**, *135*, 892.
57. Gavrushenko, N.; Carrel, H. L.; Stallings, W. C.; Gulsker, J. P., *Acta Cryst B.* **1977**, *33*, 3936.
58. Nakai, C.; Glinsmann, W. *Biochemist* **1977**, *16*, 5636.
59. (a) Zuber, G.; Sirlin, C.; Behr, J. P. *J. Am. Chem. Soc.* **1993**, *115*, 4939. (b) D'Agostino, L.; Luccia, A. D. *Eur. J. Biochem.* **2002**, *269*, 4317.
60. (a) Albelda, M. T.; Bernardo, M. A.; España, E. G.; Godino Salido, M. L. G.; Luis, S. V.; Melo, M. J.; Pina, F.; Soriano, C. *J. Chem. Soc. Perkin Trans. 2* **1999**, 2545. (b) Bazzicalupi, C.; Bencini, A.; Berni, E.; Bianchi, A.; Fornasari, P.; Giorgi, C.; Masotti, A.; Paoletti, P.; Valtancoli, B. *J. Phys. Org. Chem.* **2001**, *14*, 432. (c) Huston, M. E.; Akkaya, E. U.; Czarnik, A. W. *J. Am. Chem. Soc.* **1989**, *111*, 8735.
61. Hossai, M. A.; Liljegren, J. A.; Powell, D.; James, K. B. *Inorg. Chem.* **2004**, *43*, 3751.
62. Müller, G.; Reide, J.; Schmidtchen, F. P. *Angew. Chem. Int. Ed. Engl.* **1988**, *27*, 1516.
63. Berger, M.; Schmidtchen, F. P. *J. Am. Chem. Soc.* **1999**, *121*, 9986.

64. Metzger, A.; Lynch, V. M.; Anslyn, E. V. *Angew. Chem. Int. Ed. Engl.* **1997**, *36*, 862.
65. Echavarren, A.; Galán, A.; Lehn, J. M.; de-Mendoza, J. *J. Am. Chem. Soc.* **1989**, *111*, 4994.
66. Kavallieratos, K.; Bertao, C. M.; Crabtree, R. H. *J. Org. Chem.* **1999**, *64*, 1675.
67. Werner, F.; Schneider, H. *Helv. Chim. Acta* **2000**, *83*, 465.
68. (a) Valiyaveetil, S.; Engbersen, J. F. J.; Verboom, W.; Reinhoudt, D. *Angew. Chem. Int. Ed. Engl.* **1993**, *32*, 900. (b) Dey, S. K.; Das, G. *Chem. Commun.* **2011**, *47*, 4983 (c) Bose, P.; Ravikumar, I.; Akhuli, B.; Ghosh, P. *Chem. Asian J.* **2012**, *7*, 2373. (d) Basu, A.; Das, G. *Chem. Commun.* **2013**, *49*, 3997.
69. (a) Sessler, J. L.; An, D.; Cho, W. -S.; Lynch, V.; Marquez, M. *Chem. Eur. J.* **2005**, *11*, 2001. (b) Cureil, D.; Cowley, A.; Beer, P. D. *Chem. Commun.* **2005**, 236. (c) Salman, H.; Abraham, Y.; Tal, S.; Meltzman, S.; Kapon, M.; Tessler, N.; Speiser, S.; Eichen, Y. *Eur. J. Org. Chem.* **2005**, *11*, 2207.
70. Dydio, P.; Lichosyt, D.; Jurczak, J. *Chem. Soc. Rev.* **2011**, *40*, 2971.
71. (a) Chmielewski, M. J.; Charon, M.; Jurczak, J. *Org. Lett.* **2004**, *6*, 3501. (b) Cureil, D.; Cowley, A.; Beer, P. D. *Chem. Commun.* **2005**, 236.
72. Lee, J. Y.; Lee, M. H.; Jeong, K. S. *Supramol. Chem.* **2007**, *19*, 257.
73. Sessler, J. L.; Cho, D. G.; Lynch, V. *J. Am. Chem. Soc.* **2006**, *128*, 16518.
74. Chmielewski, M. J.; Charon, M.; Jurczak, J. *Org. Lett.* **2004**, *6*, 3501.
75. Sato, K.; Arai, S.; Yamagishi, T. *Tetrahedron Lett.* **1999**, *40*, 5219.
76. Kim, H.; Kang, J. *Tetrahedron Lett.* **2005**, *46*, 5443.
77. Kang, G.; Kim, H. S.; Jang, D. O. *Tetrahedron Lett.* **2005**, *46*, 6079.
78. (a) Graf, E.; Lehn, J. M. *J. Am. Chem. Soc.* **1976**, *98*, 6403; (b) Graf, E.; Lehn, J. M. *J. Am. Chem. Soc.* **1975**, *97*, 5022.
79. Metz, B.; Rosalky, J. M.; Weiss, R. *J. Chem. Soc. Chem. Commun.* **1976**, 533.
80. (a) Lehn, J. M.; Sonveaux, E.; Willard, A. K. *J. Am. Chem. Soc.* **1978**, *100*, 4914. (b) Kintzinger, J. P.; Lehn, J. M.; Kauffmann, E.; Dye, J. L.; Popov, A. I. *J. Am. Chem. Soc.* **1983**, *105*, 7549.
81. Dietrich, B.; Guilhem, J.; Lehn, J. M.; Pascard, C.; Sonveaux, E. *Helv. Chim. Acta* **1984**, *67*, 91.

82. (a) Jazwinski, J.; Lehn, J. M.; Lilienbaum, D.; Ziessel, R.; Guilhem, J.; Pascard, C. *J. Chem. Soc. Chem. Commun.* **1987**, 1691. (b) Menif, R.; Rebenspies, J.; Martell, A. E. *Inorg. Chem.* **1991**, *30*, 3446. (c) Ravikumar, I.; Lakshminarayanan, P. S.; Suresh, E.; Ghosh, P. *Inorg. Chem.* **2008**, *47*, 7992.
83. (a) Schmidtchen, F. P. *Angew. Chem. Int. Ed. Engl.* **1977**, *16*, 720. (b) Schmidtchen, F. P. *Chem. Ber.* **1980**, *113*, 864. (c) Schmidtchen, F. P. *Chem. Ber.* **1981**, *114*, 597. (d) Schmidtchen, F. P.; Muller, G. *J. Chem. Soc. Chem. Commun.* **1984**, 1115.
84. Worm, K.; Schmidtchen, F. P.; Schier, A.; Schafer, A.; Hesse, M. *Angew. Chem. Int. Ed. Engl.* **1994**, *33*, 327; Worm, K.; Schmidtchen, F. P. *Angew. Chem. Int. Ed. Engl.* **1995**, *34*, 65.
85. Dietrich, B.; Fyles, T. M.; Lehn, J. M.; Pease, L. G.; Fyles, D. *J. Chem. Soc., Chem. Commun.* **1978**, 934.
86. Alcázar, V.; Segura, M.; Prados, P.; de Mendoza, J. *Tetrahedron Lett.* **1998**, *39*, 1033.
87. Pascal, R. A.; Spergel, J.; Van Engen, D. *Tetrahedron Lett.* **1986**, *27*, 4099.
88. Choi, K.; Hamilton, A. D. *J. Am. Chem. Soc.* **2003**, *125*, 10241.
89. Szumna, A.; Jurczak, J. *Eur. J. Org. Chem.* **2001**, 4031.
90. (a) Bisson, A. P.; Lynch, V. M.; Monahan, M. K. C; Anslyn, E. V. *Angew. Chem. Int. Ed. Engl.* **1997**, *36*, 2340. (b) Niikura, K.; Bisson, A. P.; Anslyn, E. V. *J. Chem. Soc., Perkin Trans. 2* **1999**, 1111.
91. (a) Sessler, J. L.; Cyr, M. J.; Lynch, V.; McGhee, E.; Ibers, J. A. *J. Am. Chem. Soc.* **1990**, *112*, 2810. (b) Shionoya, M.; Furuta, H.; Lynch, V.; Harriman, A.; Sessler, J. L. *J. Am. Chem. Soc.* **1992**, *114*, 5714.
92. Kral, V.; Sessler, J. L.; Furuta, F. *J. Am. Chem. Soc.* **1992**, *114*, 8704.
93. Bucher, C.; Zimmerman, R. S.; Lynch, V.; Král, V.; Sessler, J. L. *J. Am. Chem. Soc.* **1992**, *123*, 2099.
94. (a) Gale, P. A.; Sessler, J. L.; Král, V.; Lynch, V. *J. Am. Chem. Soc.* **1996**, *118*, 5140. (b) Allen, W. E.; Gale, P. A.; Brown, C. T.; Lynch, V.; Sessler, J. L. *J. Am. Chem. Soc.* **1996**, *118*, 12471.
95. (a) Sessler, J. L.; Anzenbacher, Jr., P.; Shriver, J. A.; Jursíková, K.; Lynch, V. M.; Marquez, M. *J. Am. Chem. Soc.* **2000**, *122*, 12061. (b) Anzenbacher Jr., P.; Try, A. C.; Miyaji, H.; Juriskova, K.; Lynch, V. M.; Marquez, M.; Sessler, J. L. *J. Am. Chem. Soc.*

- 2000**, 122, 10268. (c) Sessler, J. L.; An, D.; Cho, W. -S.; Lynch, V. *Angew. Chem. Int. Ed.* **2003**, 42, 2278.
96. Sessler, J. L.; An, D.; Cho, W. S.; Lynch, V.; Marquez, M. *Chem. Eur. J.* **2005**, 11, 2001.
97. Mani, G.; Jana, D.; Kumar, R.; Ghorai, D. *Org. Lett.* **2010**, 12, 3212.
98. Mahanta, S. P.; Kumar, B. S.; Sambath, B.; Sivasankar, C.; Panda, P. K. *Org. Lett.* **2012**, 14, 548.
99. (a) Mahanta, S. P.; Kumar, B. S.; Panda, P. K. *Chem. Commun.* **2011**, 47, 4496. (b) Mahanta, S. P.; Panda, P. K. *Org. Biomol. Chem.* **2014**, 12, 278.
100. (a) Scherer, M.; Sessler, J. L.; Gebauer, A.; Lynch, V. *Chem. Commun.* **1998**, 1. (b) Gale, P. A.; Anzenbacher Jr., Sessler, J. L. *Coord. Chem. Rev.* **2006**, 250, 3004. (c) Gale, P. A. *Chem. Soc. Rev.* **2010**, 39, 3746. (d) Lee, C. H. *Bull. Korean Chem. Soc.* **2011**, 32, 768. (e) Sharma, A.; Oubai, A.; Kumar, A. *J. Chem. Bio. Phy. Sci. Sec. A* **2013**, 3, 91. (f) Wenzel, M.; Hiscock, J. R.; Gale, P. A. *Chem. Soc. Rev.* **2012**, 41, 480. (g) Gale, P. A.; Busschaert, N.; Haynes, C. A. J.; Karagiannidis, A. E.; Kirby, I. L. *Chem. Soc. Rev.* **2014**, 43, 205. (h) Kim, S. K.; Sessler, J. L. *Acc. Chem. Res.* **2014**, 47, 2525. (i) Kim, D. S.; Sessler, J. L. Calix[4]pyrroles: versatile molecular containers with ion transport, recognition, and molecular switching functions, *Chem. Soc. Rev.* [Advance Article]. Published online 01 Jul 01 2014 DOI: 10.1039/C4CS00157E. <http://pubs.rsc.org/en/content/articlehtml/2014/cs/c4cs00157e> (accessed Jul 02, 2014).
101. Sessler, J. L.; Král, V.; Shishkanova, T. V.; Gale, P. A. *Proc. Natl. Acad. Sci. U.S.A.* **2002**, 99, 4848.
102. Yoon, D. W.; Hwang, H.; Lee, C. H. *Angew. Chem. Int. Ed.* **2002**, 41, 1757.
103. Fox, O. D.; Rolls, T. D.; Drew, M. G. B.; Beer, P. D. *Chem Commun.* **2001**, 1632.
104. Bucher, C.; Zimmerman, R. S.; Lynch, V.; Sessler, J. L. *J. Am. Chem. Soc.* **2001**, 123, 9716.
105. (a) Lee, C. H.; Miyaji, H.; Yoon, D. W.; Sessler, J. L. *Chem Commun.* **2008**, 24. (b) Král, V.; Gale, P. A.; Anzenbacher Jr., P.; Jursíková, K.; Lynch, V.; Sessler, J. L. *Chem. Commun.* **1998**, 9. (c) Sessler, J. L.; An, D.; Cho, W. S.; Lynch, V. *J. Am. Chem. Soc.* **2003**, 125, 13646. (d) Sessler, J. L.; An, D.; Cho, W. S.; Lynch, V.; Yoon, D. W.; Hong,

- S. J.; Lee, C. H. *J. Org. Chem.* **2005**, *70*, 1511. (e) Katayev, E. A.; Sessler, J. L.; Khrustalev, V. N.; Ustynyuk Y. A. *J. Org. Chem.* **2007**, *72*, 7244.
106. (a) Chang, K. C.; Minami, T.; Koutnik, P.; Savechenkov, P. Y.; Liu, Y.; Anzenbacher, Jr., P. *J. Am. Chem. Soc.* **2014**, *136*, 1520. (b) Louis, A.; Guzman; G. R.; David, F. A. Q.; Eduardo, C. E. D.; Ballester, P. *J. Am. Chem. Soc.* **2014**, *136*, 3208. (d) Albano, G.; Eduardo, C. E. D.; Antonio, F; Ballester, P. *J. Org. Chem.* **2014**, *79*, 5545.
107. (a) Chang, K. J.; Moon, D.; Lah, M. S.; Jeong, K. S. *Angew. Chem. Int. Ed.* **2005**, *44*, 7926. (b) Kim, N. K.; Chang, K. J.; Moon, D.; Lah, M. S.; Jeong, K. S. *Chem. Commun.* **2007**, 3401.
108. Chae, M. K.; Lee, J. I.; Kim, N. K.; Jeong, K. S. *Tetrahedron Lett.* **2007**, *48*, 6624.
109. (a) Alcalde, E.; Alvarez-Rúa, C.; García-Granda, A.; Graci'a-Rodriguez, E.; Mesquida, N.; Pérez-García, L. *Chem. Commun.* **1999**, 295. (b) Molina, P.; Tárraga, A.; Otón, F. *Org. Biomol. Chem.* **2012**, *10*, 1711.
110. Haketa, Y; Maeda, H. *Chem. Eur. J.* **2011**, *17*, 1485.
111. Gamez, P. *Inorg. Chem. Front.* **2014**, *1*, 35.

CHAPTER 2

Materials and Methods

This chapter provides a brief idea about the analytical techniques used for the measurement of association constant and also synthetic procedure for literature reported compounds employed during our investigation. Purification procedures adopted for the reagents and the solvents used are also described.

2.1 General Experimental

2.1.1 Solvents

2.1.1.1 Solvent for Reactions

Chloroform, dichloromethane and 1,2-dichloroethane were dried by distillation over calcium hydride. Diethylether was dried by passage through columns of activated alumina followed by refluxing with sodium metal in presence of benzophenone. Acetone was dried by refluxing with potassium carbonate. Pyrrole was dried with calcium hydride and redistilled immediately before use.¹

2.1.1.2 NMR Solvents

Chloroform-*d*, acetonitrile-*d*₃ and DMSO-*d*₆ were purchased from Sigma-Aldrich and Cambridge isotope Inc. and used as such.

2.1.1.3 Solvents for Analytical Studies

Acetonitrile (HPLC grade) was purchased from Sigma-Aldrich® and Hi-Pure fine chem industries and used as such for UV-Vis and fluorescence titrations, and isothermal titration calorimetry (ITC) study.

2.1.2 Reagents

Anions for binding studies were used in the form of their tetrabutylammonium salts (fluoride as its trihydrate). The salts were purchased from Sigma-Aldrich® and used as such in the titration experiments. Pyrrole was purchased from Sisco research laboratories and Spectrochem. Cyclohexanone, BF₃-OEt₂ and TFA were purchased from Sigma-Aldrich® and used as such. Acetone, acetonitrile, diethylether and other reagent grade solvents were purchased from Finar chemicals, S D Fine-Chemicals and Merck. Magnesium turning was purchased from SRL. Catechol, resorcinol, 1,4-hydroquinone, 2,3-Dihydroxynaphthalene, 2,7-Dihydroxynaphthalene and α,α' -Dibromo-*o*-xylene were purchased from Sigma-Aldrich®. All the inorganic salts and solvents used for the routine laboratory work were purchased from Merck and standard reagents respectively.

2.2 Chromatography

Thin layer chromatography was performed using TLC Silica gel 60 F₂₅₄ purchased from Merck. Column chromatography was carried out on silica gel (100-200 mesh size) purchased from various local companies (Acme Synthetic Chemicals, Sisco Research Laboratories, Desicca Chemicals etc.).

2.3 Characterization and Analytical Instrumentation

Melting points were determined by open capillary tubes on a BIO-TECH, India apparatus and on MR-Vis⁺ visual melting point range apparatus from LABINDIA instruments private limited.

Infrared spectra were recorded on a JASCO 5300 and NICOLET 5700 FT-IR spectrometers. Elemental analyses were obtained through Thermo Finnigan Flash EA 1112 analyzer.

Nuclear magnetic resonance (NMR) spectra were recorded on Bruker 400 and 500 MHz FT-NMR spectrometer operating at ambient temperature. TMS was used as internal standard for ¹H NMR spectra. LCMS were carried out by Shimadzu-LCMS-2010 mass spectrometer and HRMS data were recorded with Bruker Maxis spectrometer.

Some of the crystallographic data were collected on BRUKER SMART-APEX CCD diffractometer. Mo-K α ($\lambda = 0.71073 \text{ \AA}$) radiation was used to collect X-ray reflections on the single crystal. Data reduction was performed using Bruker SAINT² software. Intensities for absorption were corrected using SADABS³ and refined using SHELXL-97⁴ with anisotropic displacement parameters for non-H atoms. Hydrogen atoms on O and N were experimentally located in difference electron density maps. All C-H atoms were fixed geometrically using HFIX command in SHELX-TL. A check of the final CIF file using PLATON⁵ did not show any missed symmetry. Some of the crystallographic data were also collected on Oxford Gemini A Ultra diffractometer with dual sources. Mo-K α ($\lambda = 0.71073 \text{ \AA}$) radiation was used to collect the X-ray reflections of the crystal. Data reduction was performed using CrysAlis^{Pro} 171.33.55 software.⁶ Structures were solved and refined using Olex2-1.0, with anisotropic displacement parameters for non-H atoms. Hydrogen atoms on N were located from the Fourier map in all of the crystal structures. All C-H atoms were fixed geometrically. Empirical absorption correction was done using spherical harmonics, implemented in SCALE3 ABSPACK scaling algorithm. A check of the final CIF file using PLATON⁵ did not show any missed symmetry. UV-Vis spectra

were recorded on Perkin Elmer Lambda 35 UV-Vis spectrophotometer. Fluorescence spectra were recorded on Horiba Zoin Yovan Fluoromax-4 instrument. The titration data were fitted to a 1:1 binding profile in Origin 8 software to evaluate the association constant (K_a). Microcalorimetric titrations were performed using isothermal titration calorimeter (ITC), purchased from Microcal Inc., MA. The Origin software provided by Microcal Inc. was used to calculate the binding constant (K_a) and the enthalpy change (ΔH).⁷

2.4 Computational Details

The quantum mechanical DFT calculations were performed with the Gaussian 03 program package.⁸ The Becke three-parameter hybrid (B3) functional was used along with Lee-Yang-Parr (LYP) correction.^{9,10} The 6-311+G (d, p) basis set is employed in all calculations reported. Solvation is accounted with the help of PCM model.¹¹

2.5 Analytical Techniques

2.5.1 Introduction

The interaction of anions with artificial receptor systems can be monitored and quantified using several methods, the choice of which has been largely dependent on the nature of the receptor in question. These are carried out by using different analytical techniques, including ¹H NMR spectroscopy, UV-Vis and fluorescence spectroscopy, mass spectrometry (especially ESI-MS), reaction kinetics, potentiometry, solubility measurement, liquid-liquid partitioning, dialysis, chromatography, calorimetry, refractometry, polarimetry etc.¹² Each of the techniques depends on the understanding of the intermolecular forces responsible for the complexation from a chemical point of view. For instance, NMR spectroscopic titration monitors changes in the chemical shift of one or more resonances, present in the spectrum of the interacting partners. On the contrary, optical spectroscopy records changes in optical properties of the receptor such as molar absorptivity or emissivity as a consequence of complex formation. On the other hand, calorimetry provides information about the heat change of the system as a whole.¹³

In host-guest interaction, association constants are also often expressed as stability, binding, and equilibrium constants depending on the expertise of the researcher and the systems involved.

In terms of the underlying chemical equilibrium,



It is generally considered that when the rates of the forward (K_a) and reverse (K_d) reactions are equal (i.e., equilibrium is attained), the concentration of the host, guest, and host-guest complex will remain constant with time. Under these conditions, the equilibrium expression can be written and the corresponding association constant (K_a) can be calculated. For the simple equilibrium the general expression of K_a is:

$$K_a = \frac{[HG]}{[H][G]} = \frac{k_1}{k_2} = \frac{1}{K_d} \dots\dots\dots 2.2$$

where [H], [G] and [HG] are the concentrations of the free host, free guest, and the host-guest complex respectively, k_1 and k_2 are the rate constants for the forward and the backward reactions respectively, and K_d is the dissociation constant.

To measure quantitatively K_a values, titrations are often performed. These are carried out by using an appropriate spectroscopic or calorimetric tools, including NMR spectroscopy, UV-vis absorption spectroscopy, fluorescence emission spectroscopy, or isothermal titration calorimetry (ITC). Each of these techniques looks at a different part of the binding process and/or overall equilibrium. For instance, titrations involving ^1H NMR spectroscopy that involved monitoring the proton shifts in, e.g., NH proton of amide- or pyrrole-type receptors, provide insights into the direct interaction of the anion with the hydrogen bond donor subunits of the receptor. By contrast, UV/vis and fluorescence spectroscopy reflect changes in the optical properties of the light absorbing/emitting portions of the receptor (including any appended chromophore), whereas ITC provides information about the change in the energetics of the system as a whole. These techniques often operate over different concentration ranges, typically 10^{-3} M for NMR spectroscopy, 10^{-4} M for ITC, and 10^{-5} M or lower for UV/vis and fluorescence spectroscopy, hence the latter being most sensitive.

The evaluation of binding constants is often made in solvents of different polarity, which has a direct effect on the binding affinities. In general, the affinities are considerably higher in less competitive aprotic organic solvents. In such solvents, studies involving tetrabutylammonium anion salts are common. This is due to the high solubility of these salts in organic solvents. However, these salts are difficult to keep dry, being in some cases extremely hygroscopic. In addition to concerns involving salt purity, assumptions are made about ion pairing in solution that may not be valid. For example, tetrabutylammonium is generally regarded as an ‘innocent’ counter cation with little tendency to form ion pairs in this media. This

assumption is incorrect and, in fact, it has been suggested that 1 mM solutions of tetrabutylammonium chloride in dichloromethane are less than 20% dissociated at 22 °C.¹⁴ Therefore, going from one solvent to another can change not only the strength of the interaction between the anion and receptor, but also the degree of ion pairing in solution between the anion and its counter cation. Therefore, while comparing data sets of binding constants across a range of receptors, it is essential that the binding studies be conducted under identical conditions (e.g., temperature, solvent, concentration, and even measurement method). Otherwise, any conclusions drawn may well be highly erroneous.

2.5.2 Sample Preparation

To achieve accurate association constants, it is very important to choose an appropriate concentration range for the sample, being subject to analysis. In the case of standard ¹H NMR spectroscopic titrations, wherein the change in the chemical shift of one or more proton signals are monitored as a function of anion (actually salt of the anion) concentration (*vide infra*), Wilcox proposed that the most reliable titration curves can be obtained when the concentration range of the sample is chosen in a numeric range of 1 to 10 times the dissociation constant K_d ; units of M. In other word, $K_a \times [S] = 1$ to 10, where K_a is the association constant and $[S]$ is the molar concentration of the sample.¹⁵ However, a concentration range given by $K_a \times [S] = 10$ to 50 has been suggested as being the best for ITC-based studies.⁷ To allow for a correct comparison of results obtained from these two methods, it is clear that choosing a proper (*i.e.*, overlapping) sample concentration from the outset of the study will be helpful.

2.5.3 Evaluation of Binding Constant

2.5.3.1 NMR Spectroscopy

NMR spectroscopic titrations constitute one of the most widely used techniques to determine the association constants (K_a) for host-guest interactions. This method is particularly useful when there is an involvement of hydrogen bonding interaction and can be used to gain both structural and thermodynamic information. ¹H NMR spectroscopic titration, generally monitor the effect of an added substrate *i.e.* guest has on the chemical shift of one or more proton signals of the receptor *i.e.* host when subjected to titration. Under conditions of fast exchange and for a simple 1:1 binding equilibrium, the chemical shift of the signal in question is the average of the chemical shifts of the nucleus in the free and in the complexed form. Thus, by

monitoring the chemical shift as a function of added substrate, it is possible to construct binding profiles, from which apparent K_a values may be derived.¹⁵ The advantage of NMR compared to other spectroscopies (i.e., UV-Vis and fluorescence) is that more extensive structural information is potentially forthcoming with regard to, e.g., the nature of the host-guest interaction. On the other hand, its low detection limit deters reliable measurement of strong host-guest interaction cases (i.e., $K_a > 10^5 \text{ M}^{-1}$). Often, the concentration for NMR titration (i.e., $\sim 10^{-3} \text{ M}$) is too high to make the proper host or guest solution. Historically, the first experiment designed to determine a K_a value using NMR spectroscopy was performed by Huggins, Pimentel, and Shoolery in 1955. Using equation:

$$v_{\text{HG}} = v_{\text{H}} + \frac{1}{K_a}(v_{\text{H}} - v_{\text{G}}) \dots\dots\dots 2.3$$

where, K_a values between chloroform and acetone (triethylamine) were obtained as 1.8 (3.0) and 4.0 (12.0) M^{-1} at 28 and -23°C , respectively.¹⁶

2.5.3.2 Optical Methods

Optical techniques require comparatively much lower concentration of receptor than the NMR method and hence, relatively are more sensitive than the latter and optical methods possess broad detection limit over 10^7 M^{-1} , and are easy and quick process to measure association constants. In these methods, the main requirement is that there should be some binding/complexation induced changes in the absorption or emission properties of the receptor. Therefore, the system must have a combination of a substrate recognition functionality (receptor) and optical signaling (absorption or emission) reporter, which, may be either directly linked or appropriately associated in a non-covalent manner. However, it is recommended checking many background experiments as much as we can. There are many facts, which can change colour/optical response of host or guest solution (i.e., pH, aggregation of host or guest, and so on). Particularly, some of the anions (e.g. fluoride and acetate etc.) are basic and most of the neutral anion receptors have acidic protons. Therefore, small acid-base interactions cannot be ignored owing to their effect towards optical change during the titration. In these methods host or guest must have chromophore or fluorophore. In case of chromophore, the change in the absorption spectrum, generally originates from the anion induced change in HOMO-LUMO gap or anion induced modulation in key charge transfer bands. Changes can occur due to photo-induced electron transfer (PET), electronic energy transfer, metal-to-ligand charge transfer

(MLCT), excimer/ exciplex formation, internal charge transfer (ICT), and excited state proton transfer (ESPT) to respond to the complexation and/or recognition event. Between UV-Vis and fluorescence spectroscopy, the latter one offers an enhancement in sensitivity by a factor of roughly 100-1000. Ideally, the Lambert-Beer-Bouguer law ($A = \epsilon bc$, where A : absorbance, ϵ : absorption coefficient, and c : concentration of species)¹⁷ is fully applicable to an understanding of fluorescence titrations. This is because the fluorescence intensity (F) is directly related to the concentration of sample (c) of fluorescent molecules in solution, at least at low concentrations ($F = 2.3 \times I_0 \times \Phi \times \epsilon \times l \times c$; where I_0 is the intensity of the excitation source, ϵ is the molar absorption at the excitation wavelength, l is the path length of solution, and Φ is the fluorescence quantum yield).

Like UV-Vis titration methods, the use of fluorescence quenching to determine K_a values has been extensively studied. However, among the equations used for the treatment of fluorescence quenching based titration data, the one introduced by Connors is more popular,¹⁸ where the constant “ k ” represents proportionality constant connecting the intensity and concentration of the species and F_0 is the initial fluorescence intensity.

$$F = \frac{1 + \left(\frac{k_{HG}}{k_H}\right) K_a [G]_t F_0}{1 + K_a [G]_t} \dots\dots\dots 2.4$$

2.5.3.3 Isothermal Titration Calorimetry (ITC)

ITC analysis provides a measure of the overall heat change, during the complexation process. Thus, it provide ready access to the energetics (*i.e.* ΔH , ΔS and ΔG) of the recognition event without retreating into a structural probe (*e.g.*, a NMR signal), which may or may not reflect the entirety of the associative process. Therefore, calorimetry accounts for the individual contributions of all simultaneous processes, in solution. Since the output is an ensemble of all these processes, the analysis of ITC data in terms of an interpretable binding model is not so easy and hence is a major challenge. In ITC, only ΔH is obtained directly, whereas ΔG and K_a are computed from the modeling of the experimental data to a binding profile, a process that permits the calculation of $T\Delta S$. Thus, the choice of curve fitting methods and models, for the proposed equilibrium events underlying the experimental observations is absolutely critical.⁷ Once the

For a single identical sites, binding constant,

$$K_a = \frac{\theta}{(1-\theta)[L]} \dots\dots\dots 2.5$$

Where θ = fraction of sites occupied by guest L.

$$[L]_t = [L] + n\theta[S]_t \dots\dots\dots 2.6$$

Combining equation 2.5 and 2.6,

$$\theta^2 - \theta \left[1 + \frac{[L]_t}{n[S]_t} + \frac{1}{nK_a[S]_t} \right] + \frac{[L]_t}{n[S]_t} = 0 \dots\dots\dots 2.7$$

$$Q = n\theta[S]_t \Delta H V_o \dots\dots\dots 2.8$$

Where, n = number of sites; V_o = active cell volume; and $[S]$, $[L]$, $[S]_t$, $[L]_t$ are the free and bulk concentration of S and L respectively.

$$Q = \frac{n[S]_t \Delta H V_o}{2} \times \left[1 + \frac{[L]_t}{n[S]_t} + \frac{1}{nK_a[S]_t} - \sqrt{\left(1 + \frac{[L]_t}{n[S]_t} + \frac{1}{nK_a[S]_t} \right)^2 - \frac{4[L]_t}{n[S]_t}} \right] \dots\dots\dots 2.9$$

Where, Q is the total heat content of the solution contained in V_o and H is the molar heat of binding.

$$\Delta Q(i) = Q(i) + \frac{\Delta V_i}{V_o} \left[\frac{Q(i) + Q(i-1)}{2} \right] - Q(i-1) \dots\dots\dots 2.10$$

Where, ΔV_i is the injection volume and $\Delta Q(i)$ is the heat content from the i^{th} injection.

experimental data are in hand, four steps are required to complete the analysis. The first involves putting initial guesses for the values of K_a and ΔH into equation 2.9; the second, is the calculation of $\Delta Q(i)$ for each injection and comparison of these values with the observed heats (equation 2.10); the third step involves putting improved values of K_a and ΔH to equation 2.9 and the fourth step needs repeating these first three steps iteratively, until no further significant change in the value of the parameters is observed. This iteration was performed with the Origin[®] software provided by the manufacturer.

2.5.3.4 Job's Plots

Job's method¹⁹, also called the method of continuous variation, is a simple and effective approach towards the determination of chemical reaction stoichiometry of predominant complex. The classical procedure calls for mixing aliquots of equimolar solutions of H and G. Generally, the Job plot graphs are made showing complex concentration (Y axis) vs. mole fraction (X axis). A maximum value of complex concentration is reached at the composition corresponding to the

stoichiometry of the predominant complex. The maximum at a mole fraction of 0.3, 0.5, and 0.6 indicates formation of a 1:2, 1:1, and 2:1 host:guest complexes respectively (Figure 2.1).

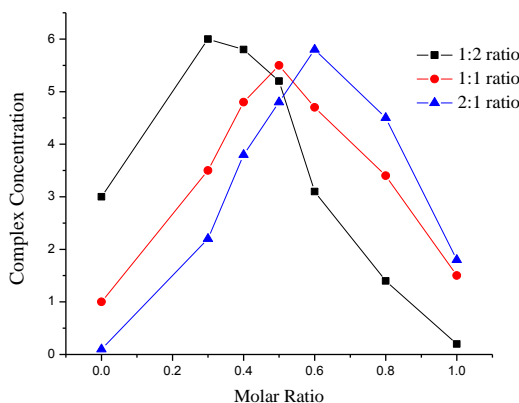
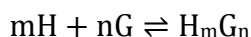


Figure 2.1 Examples of continuous variation curve plots.

In the context of generic reaction,

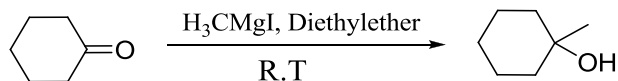


where m and n designate the number of mole of host and guest required to form a host guest complex (H_mG_n).

2.6 Preparation of Starting Materials

The following compounds were prepared by using literature methods, in order to utilize them as the starting material for our work. Their identification was further confirmed, by matching the analytical data with that reported in the literature.

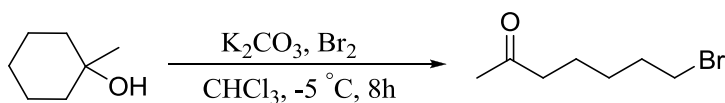
2.6.1 Preparation of 1-methylcyclohexanol²⁰



In a 2L three-necked round-bottomed flask, magnesium turnings (18 g, 0.74 mol) and catalytic amount of iodine were taken, to which dry diethyl ether (200 mL) was added, while keeping the system at 0 °C. Methyl iodide (46 mL, 0.74 mol) in dry diethylether (200 mL) was added slowly to the flask, keeping the reaction temperature around 0 °C. After completion of addition, the reaction mixture was stirred at r. t. for 2 h. Then cyclohexanone (60 mL, 0.67 mol) in dry diethylether (200 mL) was added, keeping the reaction at 0 °C and after complete addition, stirring was continued for another 4 h at r. t. The reaction was quenched by slow addition of

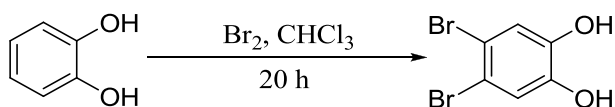
water (200 mL). The organic layer was decanted and passed through anhydrous Na_2SO_4 and concentrated under vacuum. The crude product was vacuum distilled to obtain pure 1-methylcyclohexanol (38 g, 50 %; lit. 82 %).

2.6.2 Preparation of 7-bromo-2-heptanone²¹



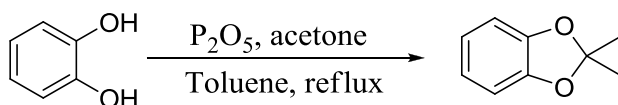
A solution of 1-methylcyclohexanol (20 mL, 175 mmol) and finely powdered K_2CO_3 (144.9 g, 1.05 mol) in distilled CHCl_3 (0.66 L) was stirred well for 1 h at -5°C . To the reaction mixture, bromine (45 mL, 875 mmol) was added and the mixture is left to stir for 8 h at the same temperature. Excess bromine was neutralized by dropwise addition of saturated solution of aq. $\text{Na}_2\text{S}_2\text{O}_3$ till the colour is discharged. The resulting solution was then extracted with CHCl_3 , dried over anhydrous Na_2SO_4 , and concentrated under vacuum. The crude liquid was distilled under reduced pressure to obtain the pure 7-bromo-2-heptanone (35 g, 80 %; lit. 95 %).

2.6.3 Preparation of 4,5-dibromobenzene-1,2-diol²²



A solution of Br_2 (13.9 mL, 272 mmol) in CHCl_3 (20 mL) was added dropwise over 1 h to a suspension of catechol (15.0 g, 136 mmol) in CHCl_3 (150 mL) at 0°C . After stirring at r. t. for 20 h, the desired product 4,5-dibromobenzene-1,2-diol (30 g, 82 %; lit. 85 %) was isolated by filtration as an off-white solid.

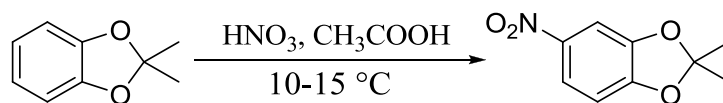
2.6.4 Preparation of 1,2-isopropylidenedioxybenzene²³



A mixture of catechol (11 g, 0.1 mol) and phosphorus pentoxide (3 g, 20 mmol) in toluene (50 mL) was heated at 75°C . To this suspension acetone (15 mL, 0.1 mol) was added dropwise. During the addition, four portions of phosphorus pentoxide (3 g, 20 mmol) were added to the reaction mixture at 10 min intervals. The reaction mixture was stirred at 75°C for another 1 h, cooled to r. t. and 25% NaOH (20 mL) was added. Organic layer was separated,

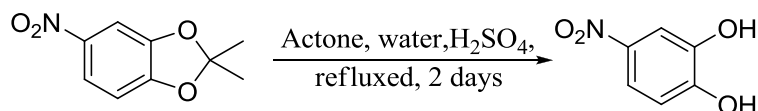
washed with water dried over anhyds. Na_2SO_4 , and concentrated under reduced pressure to an oil, which upon vacuum distillation at 60-70 °C yielded 1,2-isopropylidenedioxybenzene (10 g, 67 %, lit. 70 %) as a colourless liquid.

2.6.5 Preparation of 2,2-dimethyl-5-nitro-1,3-benzodioxole²⁴



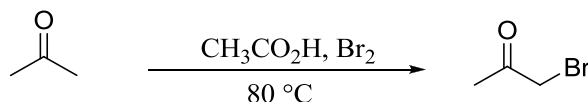
To a solution of conc. nitric acid (20 mL) and glacial acetic acid (10 mL) cooled below 15 °C, 1,2-isopropylidenedioxybenzene (5 g, 33.3 mmol) was added dropwise maintaining the internal temperature at 15-20 °C. Stirring was continued for another 15 min after addition, and then the brown slurry was diluted with water (100 mL). The solid was filtered and washed with water, taken up in dichloromethane, dried with anhyds. Na_2SO_4 and evaporated to obtain pure 2,2-dimethyl-5-nitro-1,3-benzodioxole (5.40 g, 83 %; lit. 83 %) as yellow solid.

2.6.6 Preparation of 4-nitrobenzene-1,2-diol²⁵



In a two-necked, round-bottomed flask water (30 mL) containing conc. sulphuric acid (1 mL) and acetone (20 mL) were mixed, followed by addition of 2,2-dimethyl-5-nitro-1,3-benzodioxole (1 g, 5 mmol). The reaction mixture was heated at 80 °C for 2 days. After cooling, the dark red colour mixture was extracted with ethyl acetate (5 × 100 mL). Combined organic layer was dried with anhyds. Na_2SO_4 and evaporated to dryness. Crude solid was purified by column chromatography over silica gel (eluent: 50% ethyl acetate in hexane) to yield the pure 4-nitrobenzene-1,2-diol (600 mg, 76 %; lit. 84 %).

2.6.7 Preparation of bromoacetone²⁶



In 1-l, three-necked, round-bottomed flask water (30 mL), acetone (10 mL, 140 mmol), and glacial acetic acid (7.5 mL, 130 mmol) were taken and heated to 80 °C. Then bromine (7.2 mL, 145 mmol) was added through pressure equalising funnel, very slowly to prevent the

accumulation of unreacted bromine. After complete addition of the molecular bromine, the reaction mixture was stirred for another twenty min, by which time colour of the bromine got decolourised. The reaction mixture was diluted with cold water (20 mL), cooled to 10 °C, made neutral by addition of solid sodium carbonate. The biphasic mixture was extracted with dichloromethane and organic layer was dried over anhyds. calcium chloride. After evaporation of the solvent, residue was vacuum distilled at 40–50 °C to obtain pure bromoacetone as colourless liquid (7.5 g, 48 %; lit. 51 %).

Note: bromoacetone is a highly lachrymatory agent, so all the procedures are performed under well ventilated fume hood.

2.7 References

1. Armarego, W. L. F.; Chai, C. In *Purification of laboratory chemicals*; sixth edition, Elsevier, Burkington, 2003.
2. SAINT, version 6.45 /8/6/03, Bruker AXS, 2003.
3. Sheldrick, G. M.; *SADABS, Program for Empirical Absorption Correction of Area Detector Data*, University of Göttingen, Germany, 1997.
4. Sheldrick, G. M.; *SHELXS-97 and SHELXL-97, Programs for the Solution and Refinement of Crystal Structures*, University of Göttingen, Germany, 1997.
5. (a) Spek, A. L.; *PLATON, A Multipurpose Crystallographic Tool*, Utrecht University, Utrecht, The Netherlands, 2002. (b) Spek, A. L. *J. Appl. Cryst.* **2003**, 36, 7.
6. Oxford Diffraction. CrysAlis CCD and CrysAlis RED. Versions 1.171.33.55. Oxford Diffraction Ltd, Yarnton, Oxfordshire, England, 2008.
7. ITC Data Analysis in Origin-Tutorial Guide; MicroCal, LLC, Northampton, Version 7.0, 2004.
8. Frisch, M. J. *Gaussian 03, Revision B.05*, Gaussian, Inc., Pittsburgh PA. 2003.
9. Becke, A. D. *J. Chem. Phys.* **1993**, 98, 5648.
10. Lee, C.; Yang, W.; Parr, R. G. *Phys. Rev. B.* **1988**, 37, 785.
11. (a) Tomasi, J.; Mennucci, B.; Cammi, R. *Chem. Rev.* **2005**, 105, 2999. (b) Cossi, M.; Rega, N.; Scalmani, G.; Barone, V. *J. Comput. Chem.* **2003**, 24, 669.
12. (a) Schalley, C.; Hirose, K. In *Analytical Methods in Supramolecular Chemistry*; Wiley-VCH, 2007. (b) Hirose, K. *J. Incl. Phenom. Macrocycl. Chem.* **2001**, 39, 193.

13. Wadso, I.; Goldberg, R. N. *Pure Appl. Chem.* **2001**, 73, 1625.
14. Alunni, S.; Pero, A.; Reichenback, G. *J. Chem. Soc. Perkin Trans. 2*, **1998**, 1747.
15. Wilcox, C. S., In *Frontiers in Supramolecular Organic Chemistry and Photochemistry*, Schneider, H. J., Eds. VCH: Weinheim, 1991, 123.
16. Huggins, C. M.; Pimentel, G. C.; Shoolery, J. N. *J. Chem. Phys.* **1955**, 23, 1244.
17. Kortüm, *Kolorimetrie, Photometrie und Spektrometrie*; Springer Verlag: Berlin, 1962.
18. Connors, K. A. *Binding Constant Determination*; Wiley, New York, 1987.
19. Job, P. *Ann. Chim. Appl.* **1928**, 9, 113.
20. Johnstone, R. A. W.; Liu, J. Y.; Whittaker, D. J. *Mol. Catal. A: Chem.* **2001**, 174, 159.
21. Zhang, W. C.; Li, C. J. *J. Org. Chem.* **2000**, 65, 583.
22. Fleming, M. J.; McManus, H. A.; Rudolph, A.; Chan, W. H.; Ruiz, J.; Dockendorff, C.; Lautens, M. *Chem. Eur. J.* **2008**, 14, 2112.
23. Iwagami, H.; Yatagai, M.; Nakazawa, M.; Orita, H.; Honda, Y.; Ohnuki, T.; Yukawa, T. *Bull. Chem. Soc. Jpn.* **1991**, 64, 175.
24. Ermann, P. H.; Straub, H. *Heterocyclic hydrazide derivatives of monocyclic beta-lactam antibiotics. U.S. Patent* 5, 318, 963, June, 7, **1994**.
25. Neiland, Y. O.; Kraupsha, I. L.; Gudele, I. Y. *Chem. Heterocycl. Compd.* **1993**, 29, 1428.
26. Levene, P. A. *Org. Synth.* **1930**, 10, 12.

CHAPTER 3

Catechol Derived Strapped Calix[4]pyrrole

3.1 Introduction

Calix[4]pyrrole **L72**, formally known as *meso*-octamethylporphyrinogen, is a macrocycle composed of four pyrrole units linked via four sp^3 -hybridized *meso*-carbons at their α -positions. Unlike *meso*-free porphyrinogens (**L102**), calix[4]pyrroles are not readily oxidized to form porphyrin-like structures (**L103**) (Figure 3.1). Moreover, these molecules are conformationally flexible and nonplanar in nature, lacking any macrocyclic conjugation among the constituent pyrrolic entities. In 1886, Baeyer first synthesized a white crystalline material by condensing

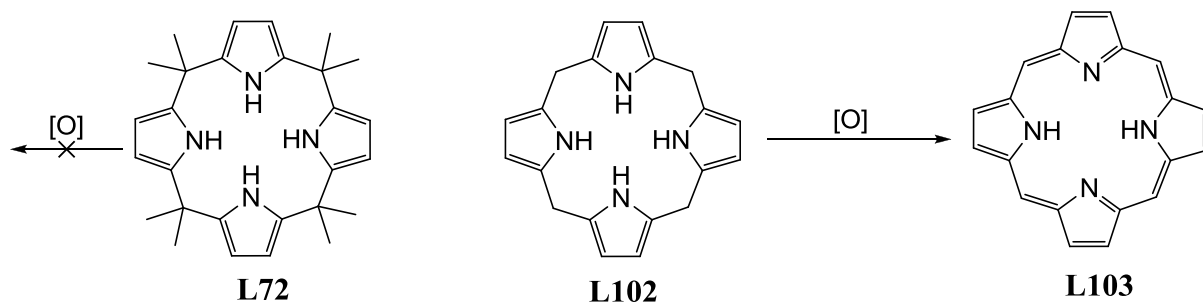


Figure 3.1 Schematic representations showing the different behavior of porphyrinogens **L72** and **L102** with respect to oxidation.

pyrrole with acetone in the presence of hydrochloric acid.¹ Thirty years later, Chelintzev and Tronov repeated this reaction and proposed a cyclic tetrametric porphyrinogen structure for the product, which later proved to be correct.² In 1955, Rothemund and Gage further improved its synthesis by using methanesulfonic acid as the catalyst.³ Other than these important findings, this class of compounds (e.g., **L72**) were only studied sporadically in the next 100 years following their discovery, most of which merely focused on the refined syntheses of these macrocycles and their *meso*-substituted derivatives but not their applications.⁴ However, in the early 1990s, Floriani and coworkers started exploring their metal coordination chemistry extensively, thus reviving interest in these venerable macrocycles after a long dormant period.⁵ In 1996, Sessler and coworkers first reported that this kind of macrocycle could bind anions and small neutral molecules in organic media, thus demonstrating their applications in novel areas, viz. anion recognition, transport etc.⁶ Since this seminal report, many new calixpyrrole-based anion receptors have been synthesized and studied worldwide. This activity has served to establish firmly this branch of anion coordination chemistry. The development of calixpyrrole-based anion coordination chemistry is reflected in the number of publications appearing each year since 1996

(Figure 3.2, based on a search using SciFinder[®] Scholar on September 12, 2014). The graph shows that the popularity of this class of molecules has grown with researchers over the last two decades.

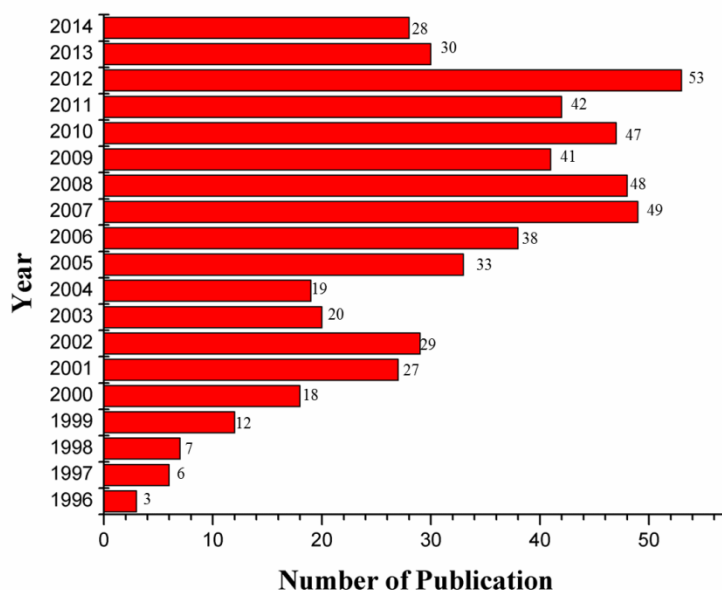


Figure 3.2 Number of publications involving calix[4]pyrrole-based anion coordination chemistry appearing each year during the period of 1996-2014. This graphic is based on the results of a search made using SciFinder[®] on September 12, 2014

The term calix[4]pyrroles was first introduced by Sessler and coworkers to highlight the fact that these macrocycles display conformational behavior, similar to that of the calix[4]arenes.⁶ They studied **L72** as a neutral anion coordinating host, using both solution-phase and solid-phase measurements.^{6a} ¹H NMR spectroscopic titration analyses in CD₂Cl₂ revealed

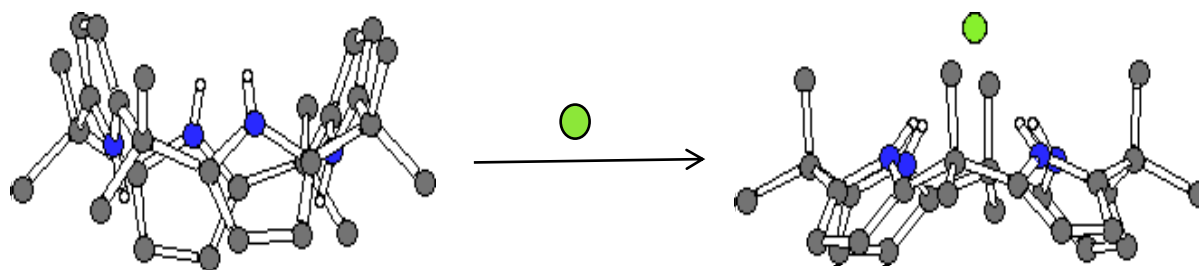


Figure 3.3 X-ray crystal structures of **L72** in the absence and presence of chloride ion.

Table 3.1 Summary of anion binding constants for calix[4]pyrrole **L72** as determined by ^1H NMR studies carried out in CD_2Cl_2 . The counter cation was tetrabutylammonium in all cases.^{6a}

Anion	F^-	Cl^-	Br^-	I^-	H_2PO_4^-	HSO_4^-
$K_a (\text{M}^{-1})$	17170	350	10	< 10	97	< 10

that it is not only an effective 1:1 anion-binding agent in solution, but also displayed a marked preference for fluoride ion compared to other anions. For example, **L72** binds fluoride ion with a much higher affinity (table 3.1). X-ray crystal structure analysis revealed that without anion, **L72** adopts a 1,3-alternate conformation, wherein adjacent rings are oriented in opposite directions. However, in the presence of chloride ion, the molecule adopts a cone-like conformation, where all the four NH protons can hydrogen bond to anion (Figure 3.3). When theoretical calculation (DFT) was performed on the molecule, it was found that calix[4]pyrrole can adopt four limiting conformations: 1,3-alternate, 1,2-alternate, partial cone, and cone as noticed in case of calix[4]arenes (Figure 3.4). Both gas phase and solution phase (CH_2Cl_2) studies revealed a stability sequence for the various conformers as 1,3-alternate > partial cone > 1,2-alternate > cone.⁷ The nature of the fluoride binding behavior was further explained by the studies of Orozco and coworkers.⁸ They showed that the inherent binding preference of **L72** for fluoride ion

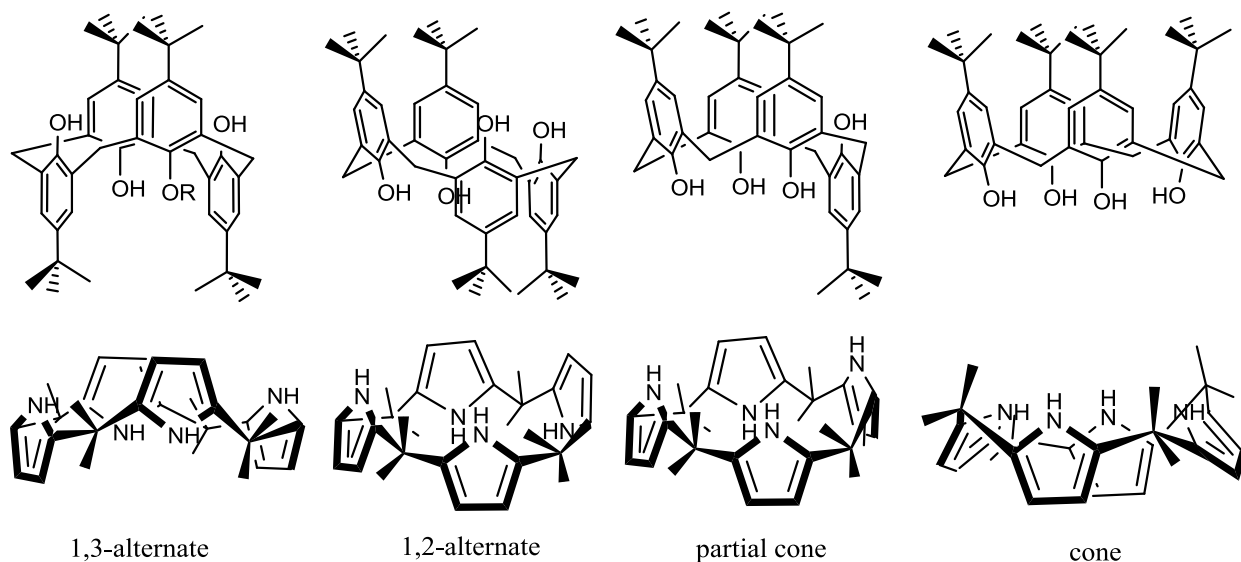


Figure 3.4 Four limiting conformations of representative calix[4]arenes (upper) and calix[4]pyrroles (lower).

Table 3.2 Association constants, K_a (M^{-1}) of different anions with **L72** in different solvents determined by 1H NMR titration.

Anion	DCM- d_2	Acetonitrile- d_3 + 0.5% v/v D_2O	Acetonitrile- d_3 + $CDCl_3$ (1:9 v/v)	DMSO- d_6
F^-	17 170	>10 000	23 800	1060
Cl^-	350	5 000	6 800	1025
Br^-	10	N.D.	270	17
I^-	< 10	17	N.D.	N.D.
$H_2PO_4^-$	97	1300	N.D.	N.D.

N.D. = not determined.

calculated in the gas phase or observed by experiment in pure aprotic solvents, such as dichloromethane, can change dramatically in protic solvents or in the presence of the hydrated cation as co-solute of the anion.⁸ Their theoretical studies also served to underscore the importance of considering all relevant factors, including solvent, hydration, counter cation, concentration, binding stoichiometry, and so forth when comparing different experimental results. Various groups have experimentally proved the solvent dependent binding of anions (table 3.2).⁹ In 2002, Schmidtchen first time using isothermal titration calorimetry (ITC)

Table 3.3 Association constant measured in dry acetonitrile (<10 ppm H_2O) at 298 K as determined by ITC.¹⁰

Anion	Mode	F [−]	Cl [−]	H ₂ PO ₄ [−]		Br [−]	
Cation		R	R	NEt ₄ ⁺	R	NBu ₄ ⁺	NBu ₄ ⁺
K _a (M ^{−1})	A	153,000	185,000	95,400	16,800	15,100	2,770
	B	129,000	111,000	66,700	N.T.	N.T.	N.T.

R = $[K.(2.2.2\text{-cryptand})]^+$; ^a A = titration of guest into host solution; B = titration of host into guest solution; N.T. = not tested.

measured association constant (K_a). In the same report he clearly pointed out the effect of counter cation on K_a (table 3.3).¹⁰ This report also demonstrated how to use ITC as an useful method for determining the various thermodynamic parameters, in an easy and reproducible way.

The results of NMR and ITC analyses are generally concordant, even though these two methods probe different aspects of the binding interaction (magnetic effect on selected proton signals and changes in overall system energetics, respectively).^{11a} Further information about the solvent effect and effect of counter cation can be found in literature, tabulated in table 3.4.¹¹

Table 3.4 Association constants, K_a (M^{-1}) measured in different solvents at 298 K by ITC and NMR spectroscopy.^{11c}

Solvent	Guest	K_a (ITC) (M^{-1})	K_a (NMR) (M^{-1})
DMSO	a	1.2×10^3	2.3×10^3
	b	1.1×10^3	2.2×10^3
Nitromethane	a	2.0×10^4	1.9×10^4
	b	1.6×10^4	2.4×10^4
Dichloroethane	a	7.5×10^4	4.2×10^4
	b	2.8×10^4	1.5×10^4
Dichloromethane	a	3.2×10^4	3.7×10^4
	b	N.D.	4.3×10^2
Acetonitrile	a	1.9×10^5	2.2×10^5
	b	2.2×10^5	2.5×10^5

a = tetraethylammonium Chloride (TEACl), b = tetrabutylammonium chloride (TBACl), N.D. = no reliable fit to a 1:1 binding isotherm possible.

3.2 Calix[4]pyrrole: Synthesis

There are three general methods for the synthesis of calix[4]pyrroles: a one-pot (1+1+1+1) condensation, (2+2) condensation and (3+1) condensation, where the numbers in the bracket refer to the number of pyrrolic subunits in the precursors involved. Among these, the one-pot approach is the most popular for preparing simple calix[4]pyrroles.

3.2.1 One-pot Condensation

As commonly practiced, the one-pot synthesis of calix[4]pyrroles involves the condensation of pyrrole(s) and ketone(s) in a 1:1 ratio (total) in the presence of an acid catalyst. Commonly used catalysts include methanesulfonic acid, trifluoroacetic acid, and borontrifluoride diethyletherate. Favored solvents include methanol, ethanol, acetonitrile, and dichloromethane. In some cases the reactant ketone can be used in large excess as the solvent. Depending on how many types of pyrroles or ketones are used in the reaction, one-pot condensation can be categorized into homo-condensation and mixed condensation.

3.2.1.1 Homo-condensation

The term homo-condensation is meant to define the reaction of a specific pyrrole with a specific ketone. According to the symmetry of the pyrrole or ketone components, these homo-condensations can be further categorized as symmetric homo-condensations and asymmetric homo-condensations.

A symmetric homo-condensation represents a reaction employing a symmetric pyrrole and a symmetric ketone. Generally such reaction produces one easy-to-separate major product in good yield. One typical example of symmetric homo-condensation is the synthesis of **L72** via the condensation of pyrrole with acetone in a 1:1 ratio in methanol using methanesulfonic acid as the acid catalyst.¹²

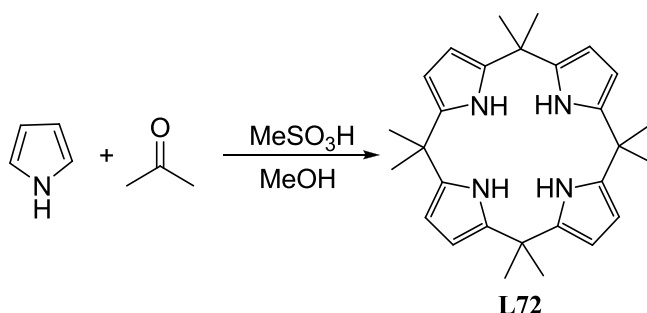


Figure 3.5 A prototypical symmetric homo-condensation as illustrated via the synthesis of **L72**.

An asymmetric homo-condensation normally involves the reaction of a pyrrole with an asymmetric ketone. For example, condensation of pyrrole with *p*-hydroxyacetophenone in methanol in the presence of methanesulfonic acid afforded the desired calix[4]pyrrole **L104** in

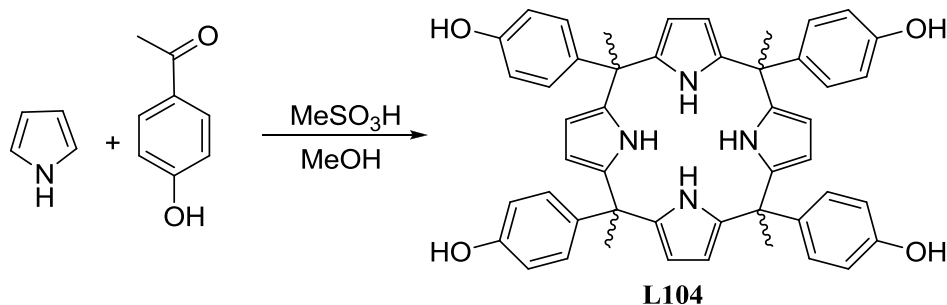


Figure 3.5 A typical asymmetric homo-condensation showing the synthesis of the tetraphenolic **L104**. As explained in the text, this product is obtained as a mixture of configurational isomers.¹³

62% yield (Figure 3.5).¹³ Since each of the four *meso* bridges formed under the conditions contains both a methyl and aryl substituent, the product, actually, consists of a mixture

containing four different configurational isomers; these isomers can be difficult to separate and may require tedious separation procedures including careful repeated column chromatography or HPLC techniques.

3.2.1.2 Mixed Condensation

Mixed condensation involves the condensation of more than one kind of pyrrole with a specific ketone or more than one kind of ketone with a specific pyrrole. Mixed condensations have low yields of individual products due to the fact that a mixture of products is formed. As a result, the reactants ratio must be carefully controlled so as to optimize the yield of the desired products. However, once separated, the various calix[4]pyrroles can often find application in a

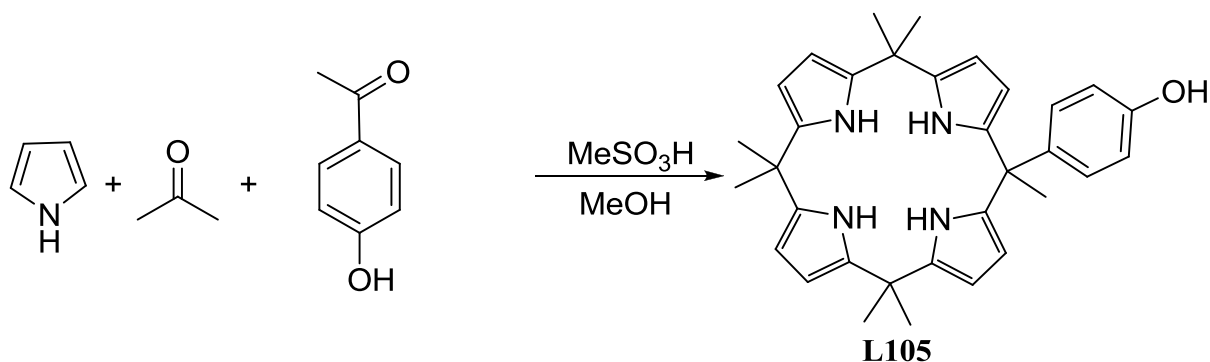


Figure 3.6 Mixed condensation reaction leading to functionalized calix[4]pyrrole.

variety of areas, in part because mixed condensations provide a good entry into functionalized systems. For instance, the monophenolic-calix[4]pyrrole **L105** was synthesized by stirring pyrrole, acetone, and *p*-hydroxyacetophenone in a 2:1:1 ratio under the same reaction conditions as used to prepare **L72**.¹⁴ Column chromatography (silica gel; dichloromethane, eluent) afforded **L105** in 17 % yield (Figure 3.6).

3.2.2 (2+2) Condensation

(2+2) Condensations refer to acid catalyzed condensations of two dipyrromethane units, generally synthesized in a predicative step from pyrrole and a ketone, with two ketone units (normally different from those used in the syntheses of the dipyrromethanes). This (2+2) approach represents an important means of constructing a variety of calix[4]pyrrole macrocycles, particularly less symmetric ones, that may not be obtained under the less well-controlled one-pot reaction conditions and if explored, needs very tedious chromatographic isolation process. Using

a (2+2) approach two isomers of **L108** were successfully synthesized by our group. These particular products were synthesized from the dipyrromethane precursor **L106** (Figure 3.7).¹⁵ Precursor **L106** was prepared from the condensation of pyrrole with 2,3-butanedione using trifluoroacetic acid (TFA) as the catalyst. Once in hand, the dipyrromethane was condensed with acetone using $\text{BF}_3 \cdot \text{OEt}_2$ as a catalyst in dichloromethane solvent at room temperature, which resulted in the cyclic products **L108** in decent yields.

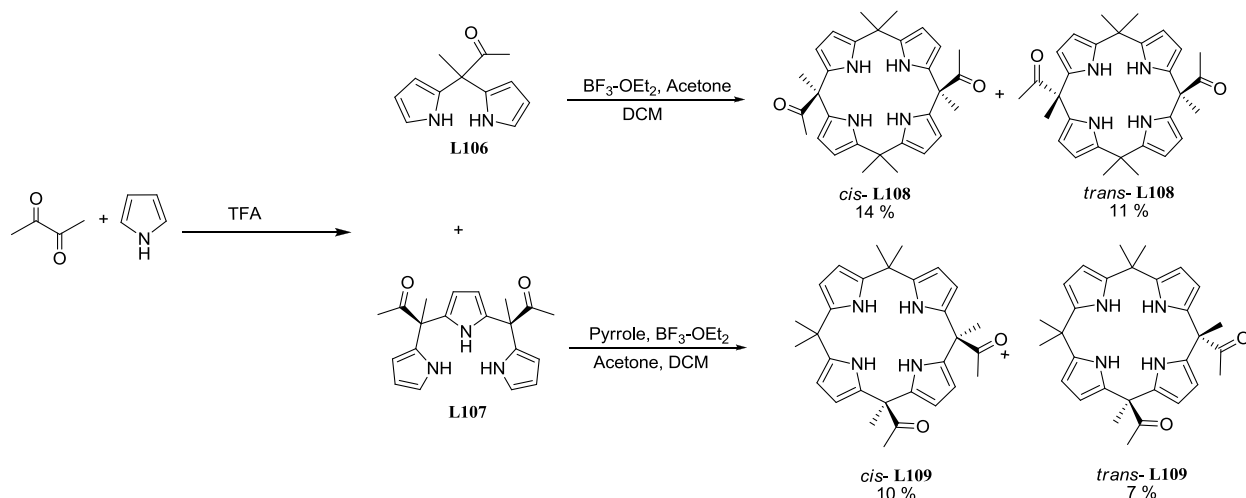


Figure 3.7 Examples of (2+2) and (3+1) condensation

3.2.3 (3+1) Condensation

(3+1) Condensations involve the reaction of a tripyrrane or tripyrrane derivative with a pyrrole or pyrrole derivative in the presence of an acid catalyst. This method is less popular due to the poor stability of most tripyrranes in the presence of acid and more importantly due to lack of many examples of tripyrranes derived from ketones and difficulty associated in their synthesis. Recently our group condensed the tripyrrane **L107** with pyrrole and acetone using $\text{BF}_3 \cdot \text{OEt}_2$ as a catalyst in dichloromethane solvent at room temperature, to obtain the two isomers of **L109**. Although the tripyrrane precursor was pure *cis* in nature, *trans*-**L109** could be formed due to acidolysis of **L107** in the reaction medium.¹⁶

3.3 Modulating the Anion Binding Properties of Calix[4]pyrrole

Calix[4]pyrrole has been modified using a variety of methods in an effort to modify their inherent anion binding properties. The known modification methods include C-rim substitution and *meso*-modification. Such reshaping not only affect the anion binding properties of

calix[4]pyrroles, but also help produce materials useful for the syntheses of calix[4]pyrrole-based anion sensors, transporting agents, or as solid support for anion separation.

3.3.1 C-rim Functionalization

Functionalization at β -pyrrolic positions of calix[4]pyrrole, called C-rim functionalization, has been extensively explored. The most popular C-rim functionalizations are β -octa-functionalizations and β -mono-functionalizations since they produce only one dominant product. β -Functionalization procedures intermediate between these two extremes have not been extensively explored due to the production of multiple products, poor reaction control, and

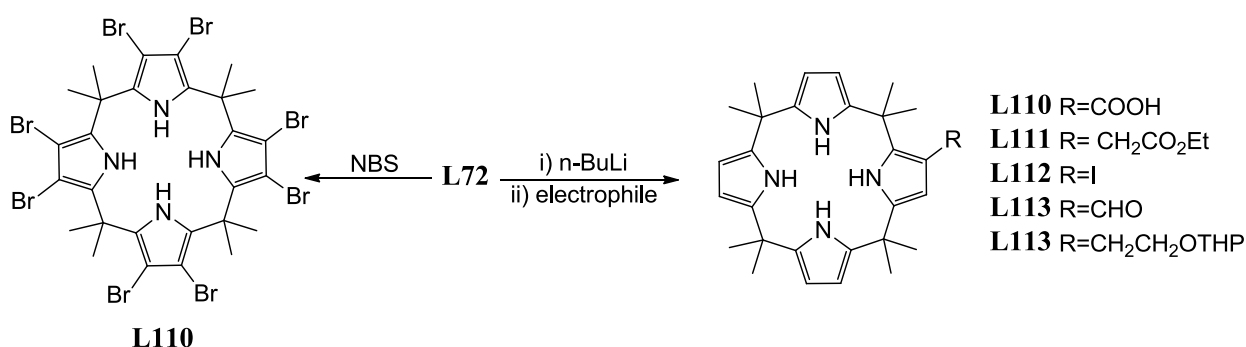


Figure 3.6 Various C-rim functionalized calix[4]pyrrole.

difficulties in achieving product separation. β -Octabromocalix[4]pyrrole (**L110**) was synthesized in 90% yield by heating **L72** with eight equivalents of NBS in THF at reflux for five hours (Figure 3.6).¹⁷ β -Monosubstituted calix[4]pyrroles were also synthesized and studied (Figure 3.6). However, their synthesis proved somewhat unusual and serves to illustrate an interesting feature of calix[4]pyrrole chemistry. In particular, it was found that lithiation of **L72** with four equivalents of n-butyllithium in THF at -78°C produced a polyanion intermediate, which upon

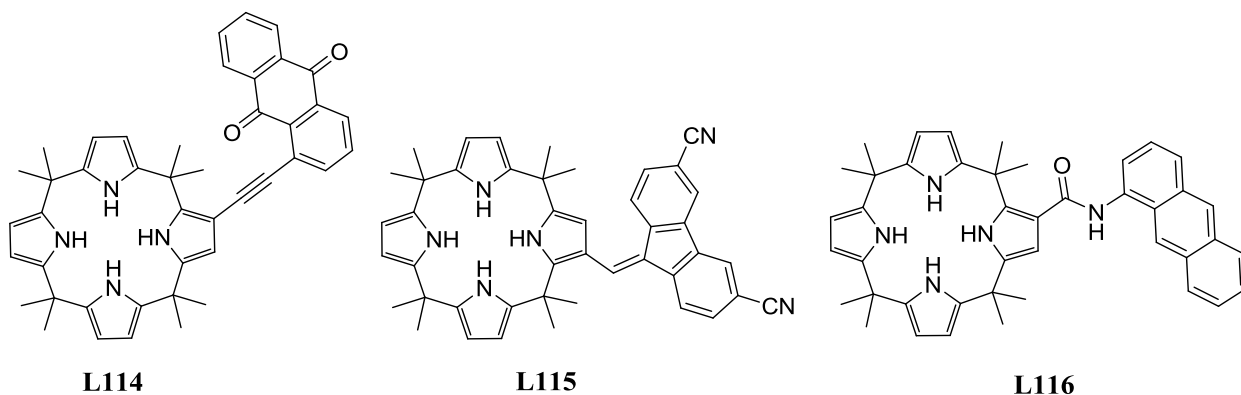


Figure 3.7 Various photochemically active C-rim functionalized calix[4]pyrroles.

treatment with a suitable electrophile followed by quenching with water, gave the β -mono-substituted calix[4]pyrroles **L110-113** and some β -di-substituted calix[4]pyrroles.¹⁸ This method provided a variety of elaborated calix[4]pyrroles, among which few could be utilized as building blocks for subsequent modification (Figure 3.7).¹⁹

3.3.2 *meso* Functionalization

Introduction of appropriate groups into the *meso*-like positions of calix[4]pyrroles could serve not only to change the intrinsic anion selectivity of the calix[4]pyrrole skeleton, but also create a cavity. Due this cavity, isolation of the binding domain from the solvent matrix imparts a number of advantages in terms of substrate recognition; i) such isolation can enhance the affinity for a specific guest by minimizing the guest–solvent and guest–counter cation interactions, ii) the modifications may produce binding domains of controlled size and shape that in turn, generally give rise to greater inherent selectivity, and iii) particularly in case of the calixpyrroles, these structural variations can be used to lock the conformation of the receptor into the so-called cone form, a conformation that is known to favor anion binding. In this regard, *meso*-functionalization of calix[4]pyrrole has undergone a vast amount of metamorphosis in last two decades, which is summarized in figure 3.8. This schematic representation shows a series of sequential modifications. The simplest modification involves generation of a functionalized calix[4]pyrrole

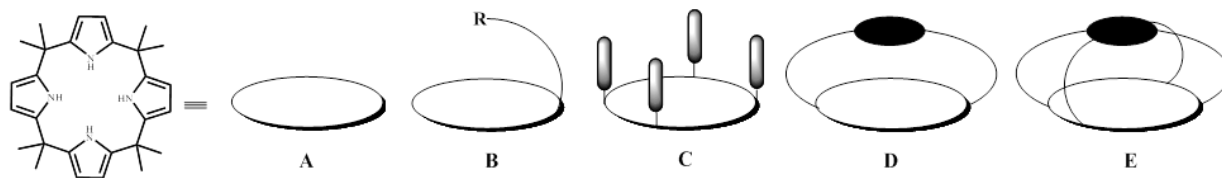


Figure 3.8 Schematic representation showing various possible *meso*-modifications to the basic calix[4]pyrrole core.

(**B**) bearing one (or more) “arms”. The second one, illustrated by generalized structure **C**, contains bulky *meso*-substituents, also known as calix[4]pyrroles with deep cavity. The third modification is the single side strapping of the calix[4]pyrrole systems through its two opposite *meso*-positions, which are represented by structure **D**. Final level of complexity involves capped models, generalized as system **E**. Since the degree of preorganization is increasing along the progression from **A** to **E**, it might be expected that both the inherent anion selectivity and the thermodynamics of binding for appropriately sized anionic substrates would increase in a

corresponding fashion. Mixed condensation protocol for synthesizing type **B** calix[4]pyrroles are quite popular in literature.²⁰ Though examples of type **C** are few in number, reported mainly by

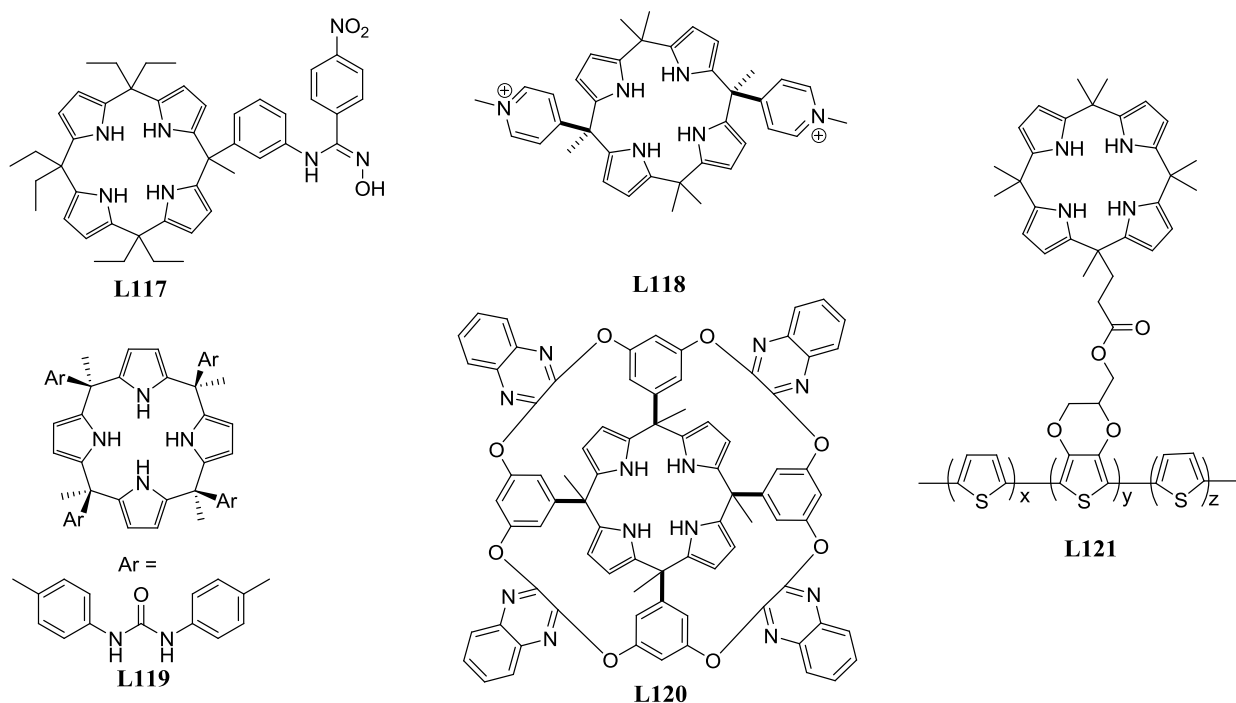


Figure 3.9 Few recently reported type **B** and **C** calix[4]pyrroles

Sessler et. al. and Ballester et. al., but they show many interesting nature in their binding behavior.^{13,21} Some of the very recently reported type **B** and **C** calix[4]pyrroles are shown in figure 3.9.²² Type **D** are called strapped calix[4]pyrroles, and a schematic retrosynthetic analysis gives us two approaches one divergent (**M**) other one is convergent (**N**) in nature. In route **M**, one **F** type calix[4]pyrrole core has to be synthesized bearing two functionalized *meso* positions then coupling with a linker will give rise to desired type **D** derivative. However, the synthesis of

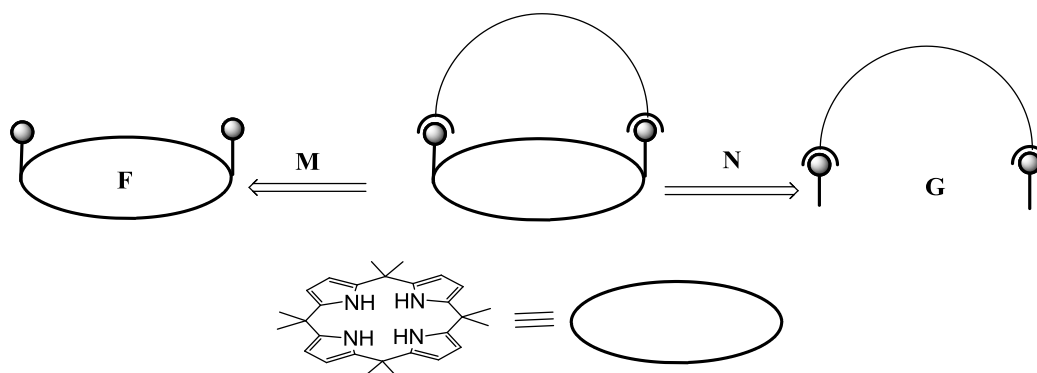


Figure 3.10 Retrosynthetic analysis showing generalized route for type **D**.

precursors **F** is difficult, since it incorporates tedious separation of isomeric mixtures regardless of the specific synthetic route chosen. Route **N** involves creation of a linked precursor **G** with incipient strap, followed by intramolecular cyclization to form calix[4]pyrrole ring. In 2002, Lee and co-workers, following route **N** reported the first strapped calix[4]pyrrole **L124**. The synthesis of **L124** was performed in three steps (Figure 3.11). The condensation of 5-hydroxy-2-

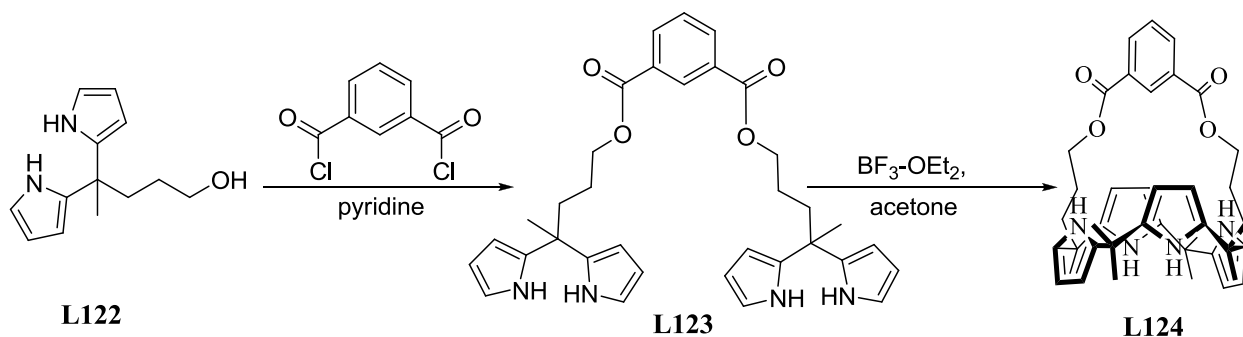


Figure 3.11 Synthesis of the ester strapped calix[4]pyrrole **L124**

pentanone with pyrrole in the presence of an acid catalyst afforded the corresponding dipyrrromethane (**L122**) and the reaction of isophthaloyl dichloride with two equivalents of **L122** in the presence of pyridine yielded the bisdipyrrromethane **L122**. Subjecting the acyclic precursor to Lewis acid-catalyzed condensation with acetone then afforded the product **L124**. A crystallographic analysis of **L124** revealed that the calix[4]pyrrole core exists in a twisted, 1,3-alternate conformation in the solid state.²³ Association constant measurements reveal that this molecule bind strongly with fluoride ion than chloride ion in DMSO. Quantitative binding constant measured from ITC for TBACl was 1.01×10^6 which is 84 times higher than **L72**

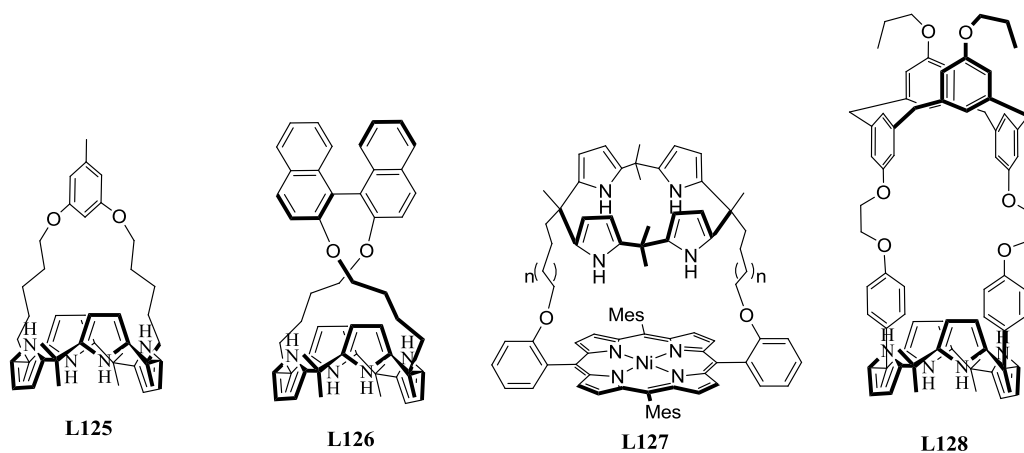


Figure 3.11 Some of the literature reported strapped calix[4]pyrrole.

measured in same solvent (table 3.3). This seminal work showed that single side strapping is a unique way to enhance binding affinity of this class of receptors. Subsequently, many strapped calix[4]pyrroles have been synthesized bearing various kind of straps which transformed this class of molecule to a better anion receptors.²⁴ Introduction of the strap to calix[4]pyrrole provides chemist a new path by which various kinds of functional groups can be introduced at its periphery, as a result of which these molecules can respond to a variety of measuring tools e.g. photo active. Type **E**, are fully capped calix[4]pyrroles and are yet to be realized synthetically. Recently Lee and coworkers reported two isomeric doubly strapped calix[4]pyrroles **L129** capable of binding small halides (i.e. fluoride and chloride ion), while trying to synthesize **E** type of systems.²⁵ Another interesting fully capped calixpyrrole system has been reported by Sessler

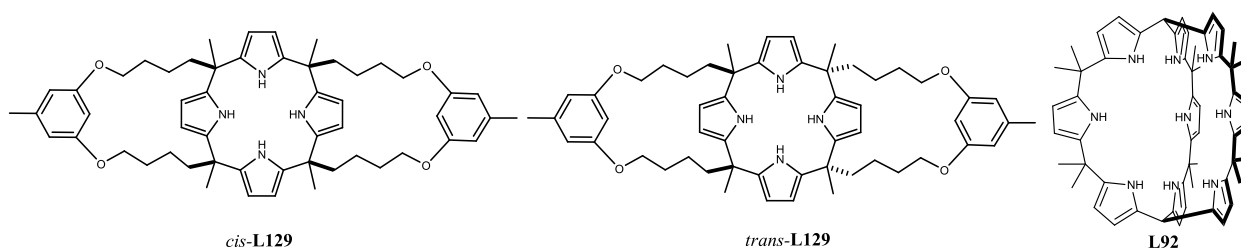


Figure 3.12 Example of fully capped calixpyrrole

and coworkers in 2001.²⁶ This receptor does not incorporate fluoride ion into its cavity, may be due to the higher rigidity or lesser cavity size. In case of chloride ion, two **L92** molecules bind to a single chloride ion.

3.4 Research Goal

From the above discussion, it could be noticed that strapped calix[4]pyrrole systems demonstrate enhanced anion affinities and improved selectivity relative to analogous compounds with a lower level of preorganization. However, a closer inspection of this class of molecules led us to find that the strapped calix[4]pyrrole molecules possess a larger binding domain under the strap, with the smallest one (generally employed) bearing aromatic functional groups in their 1,3-position (Figure 3.13).²⁷ This may be owing to the fact that in the very first report regarding strapped calix[4]pyrrole, Lee and coworkers mentioned about the strong interaction of inner aromatic CH hydrogen with the anion, leading to very high affinity constant. Subsequently, it seems to be customary to introduce this kind of aromatic moieties in the strap to introduce an extra hydrogen bonding site in the receptor for higher affinity towards anions. Therefore, we

presumed it would be quite interesting to check the anion binding in the absence of this aromatic-CH entity. To achieve it, the easiest method is to prepare a strapped calix[4]pyrrole, where it is connected to an aromatic group via its 1,2-positions. In this context, we have contemplated to synthesize **R3**, a 1,2-diether linked strapped calix[4]pyrrole.

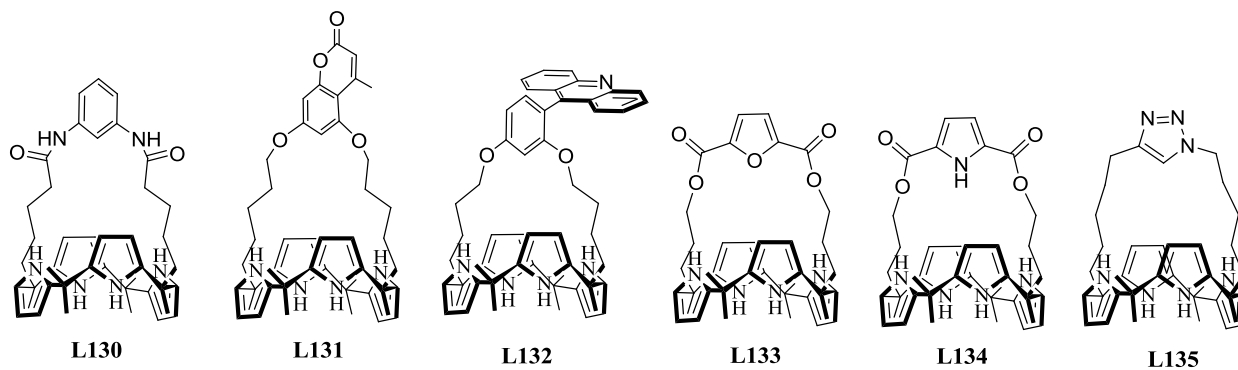


Figure 3.13 Literature reported calix[4]pyrroles bearing 1,3-functional aromatic groups.

3.5 Results and Discussion

3.5.1 Synthesis and Structural Characterization

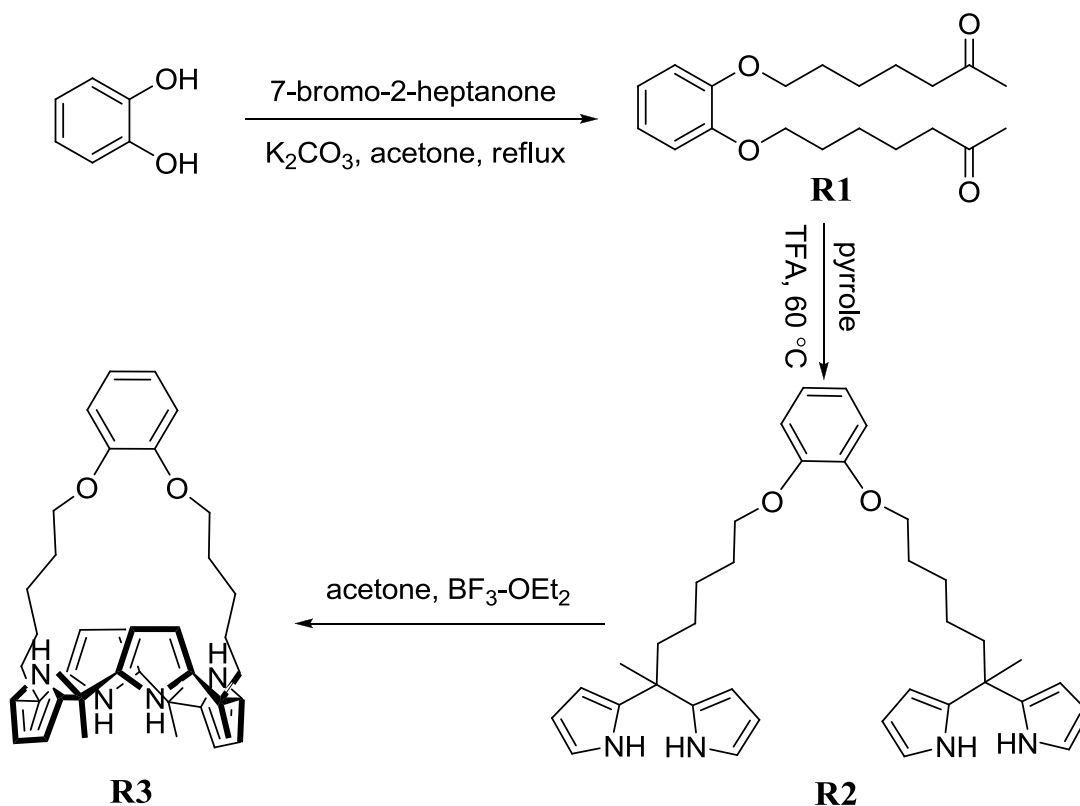


Figure 3.14 Synthetic route for **R3**.

The desired strapped calix[4]pyrrole **R3** was synthesized in three steps from catechol i.e. 1,2-dihydroxybenzene (Figure 3.14). First, 1,2-dihydroxybenzene was alkylated using 7-bromo-2-heptanone in presence of anhydrous potassium carbonate. When we used literature reported protocol for alkylation of 1,2-dihydroxybenzene in DMF,²³ we found that yield of desired product **R1** is very less. When the reaction mixture was heated at higher temperature to accelerate the rate of alkylation, decomposition of excess 7-bromo-2-heptanone was observed (which could be reused otherwise). Change in solvent, from DMF to acetone gave us targeted dialkylated product **R1** with moderate yield (70 %). However, in acetone also reaction was very sluggish, needed very long time to undergo completion. Reaction time was found to dependent on the scale of the reaction performed, therefore, completion of the reaction was always monitored by TLC. From the crude, excess 7-bromo-2-heptanone and desired **R1** were separated by column chromatography. Synthesis of bisdipyrromethane **R2** from **R1** was performed following conventional procedure; treating diketone **R1** with excess freshly distilled pyrrole in presence of trifluoroacetic acid at 60 °C and subsequent purification, provided **R2** in 65 % yield. Condensation of bisdipyrromethane **R2** with acetone resulted in the desired macrocycle **R3** in 8 % yield, in 10 min. Longer reaction time not only reduced the yield but also, led to coloration of

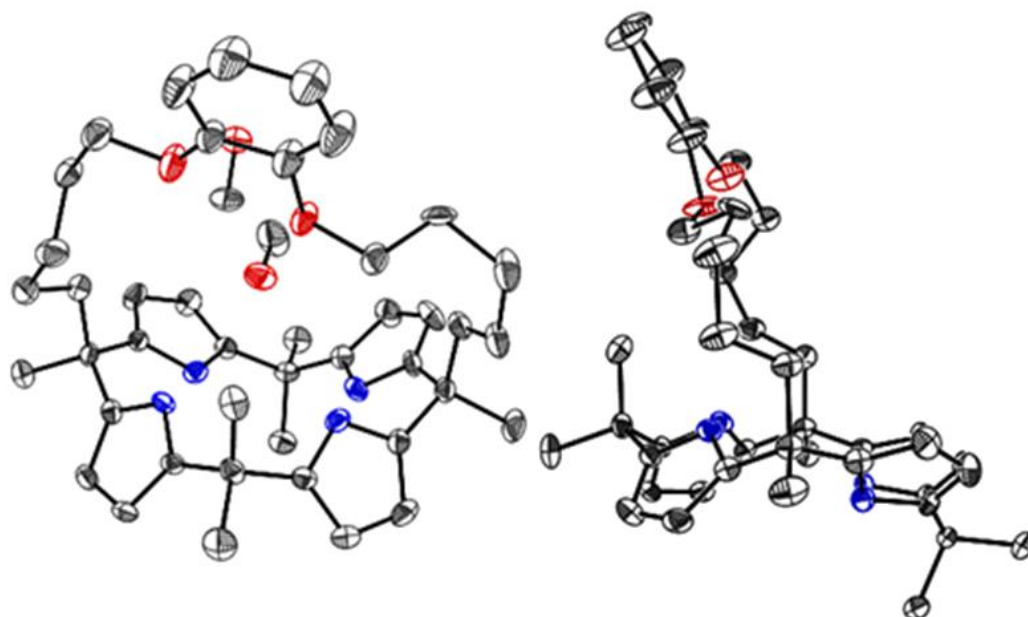


Figure 3.15 View of **R3** showing 1,2-alternate conformation of pyrrole units and the two bound methanol molecules (left) and orientation of the strap with respect to the calix[4]pyrrole moiety (right). Hydrogen atoms, disorders and methanol molecules (for right only) have been omitted for clarity.

the product which could not be removed by methanol washing. All the compounds including the desired strapped calix[4]pyrrole **R3** were characterized by ^1H , and ^{13}C NMR spectroscopy and mass analysis. ^1H NMR of **R3** shows that NH-protons are resonating at 7.42 ppm which is slightly downfield shifted compared to **L125** (7.32 ppm). Same trend was also observed for β -pyrrolic protons.²³ Single crystals were obtained by slow evaporation of **R3** from dichloromethane and methanol mixture. Significant disorder was found in two methylene carbon and one of the ether oxygen of the strap. Each of these was resolved over two positions by fractional independent refinement. X-ray diffraction analysis of the crystals showed that calix[4]pyrrole core stays in a 1,2-alternate conformation and two methanol molecules were

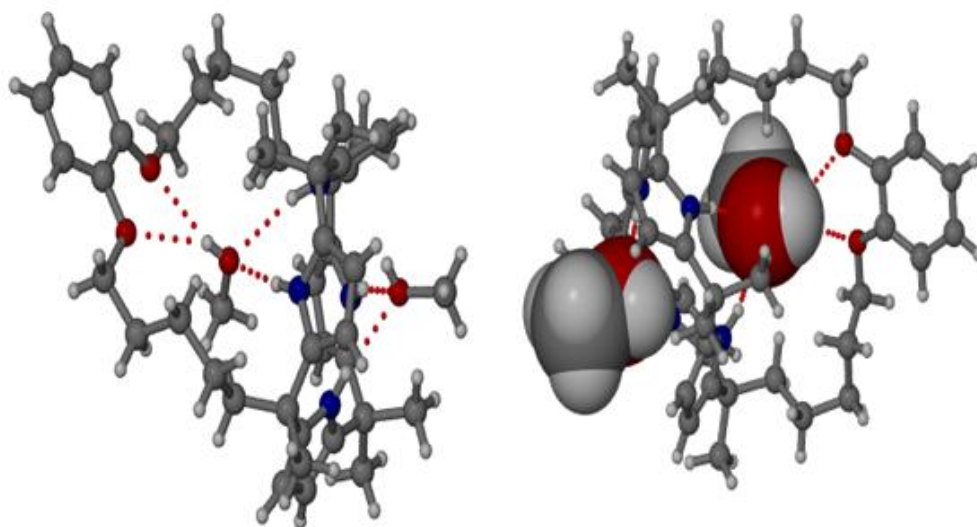


Figure 3.16 Hydrogen bonding pattern of **R3**.(**MeOH**)₂. Here one atom of each pair of disordered moiety was removed for clarity. Thermal ellipsoids are scaled to the 35 % probability level.

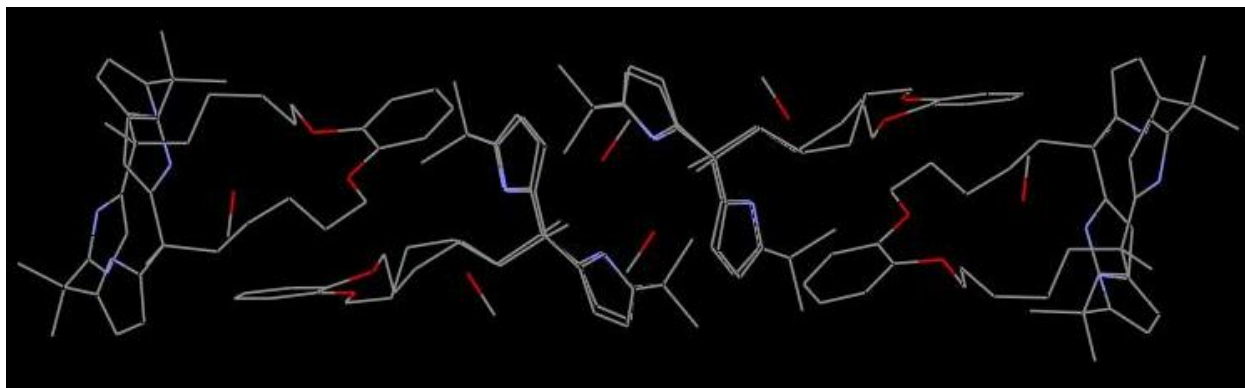


Figure 3.17 Packing diagram of **R3**.(**MeOH**)₂. (hydrogens and disordered atoms are removed for clarity).

incorporated in the structure (Figure 3.15), where one methanol was bound to the NHs of calix[4]pyrrole moiety by hydrogen bonding and the other methanol H-bonded to the remaining two pyrrolic NHs directed towards the strap and one of the oxygen of the 1,2-dihydroxybenzene derivative (Figure 3.16). The strap is slightly tilted (49.85°) towards one side of the calix[4]pyrrole core, where two adjacent pyrrolic NHs are pointing in the direction of strap. Crystal packing diagram of **R3**.(MeOH)₂ shows a nice packing for the molecules where two of the **R3** molecule facing each other from the opposite direction (Figure 3.17).

3.5.2 Anion Binding Study

Preliminary solution phase anion binding behavior of **R3** was carried out by ^1H NMR titration studies in CD_3CN with various anions viz. F^- , Cl^- , Br^- , as their tetrabutylammonium (TBA) salts. Gradual addition of TBAF in CD_3CN to a solution of **R3** in CD_3CN showed

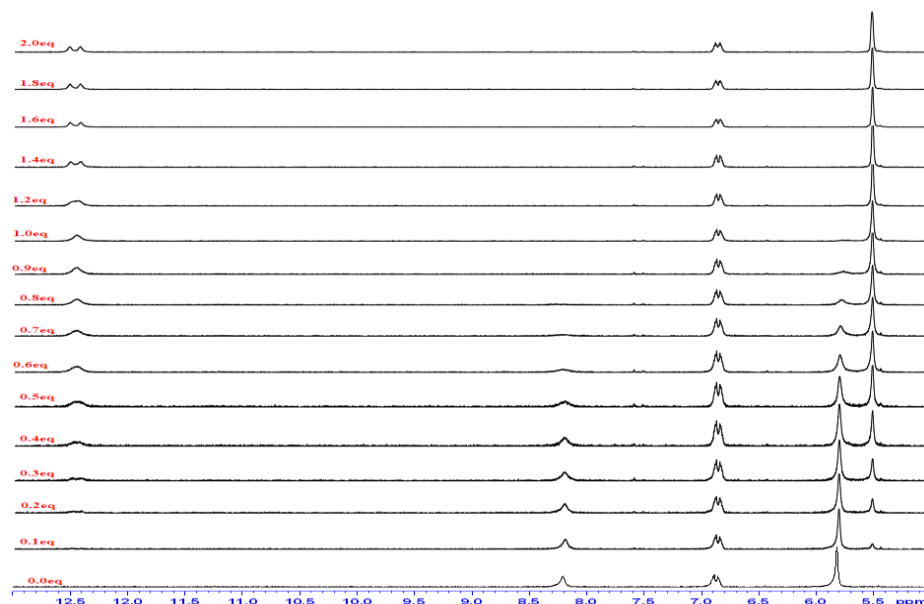


Figure 3.19 ^1H NMR titration of **R3** with TBAF. $3\text{H}_2\text{O}$ in CD_3CN .

appearance of a new signal at 12.5 ppm, indicating the occurrence of pyrrole-NH \cdots fluoride hydrogen bonding, while upfield shift was observed for the pyrrole β -CH resonances (from 5.8 to 5.5 ppm) indicating the increase in the electron density in the pyrrole rings owing to the NH \cdots fluoride interaction. This titration also revealed that addition of ~ 1 equivalent of anion was sufficient to shift the equilibrium towards complete bounded form (**R3.F**⁻). After addition of higher amount of fluoride ion (1.4 equivalent) NH-F coupling could be noticed (Figure 3.19). Stepwise addition of TBACl (in CD_3CN) to a solution of **R3** in CD_3CN showed similar kind of

shift for pyrrolic-NH and β -CH signals (Figure 3.20), which confirmed hydrogen bonding interaction for chloride also. But relatively lesser shift for the pyrrole-NH signal (from 8.2 to 11.2 ppm) suggested that the strength of hydrogen bonding involved in case of chloride binding was lesser than that with the fluoride ion. When larger bromide ion was subjected to same kind

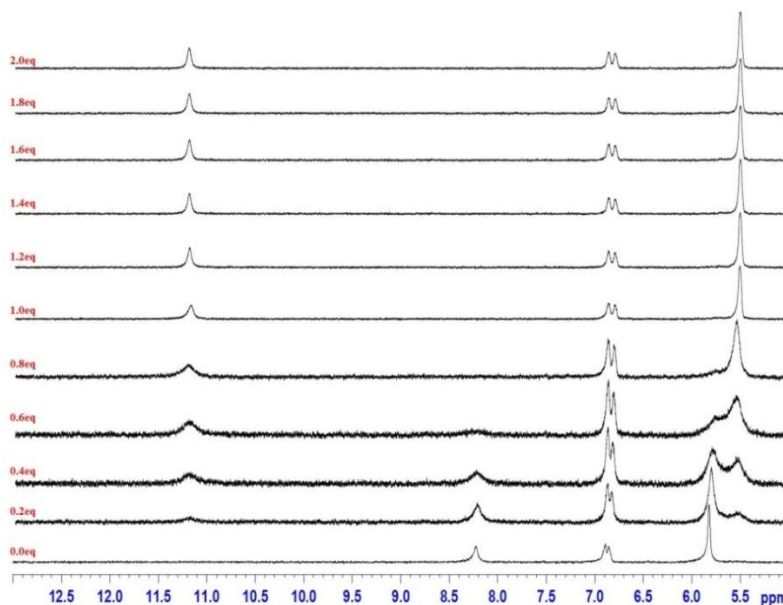


Figure 3.20 ^1H NMR titration of **R3** with TBACl in CD_3CN .

of titration experiment (Figure 3.21), it was found that hydrogen bond interaction is quite similar to that of TBACl. Whereas, TBAI did not show any interaction with **R3**, probably due to its large size and very low charge to radius ratio.

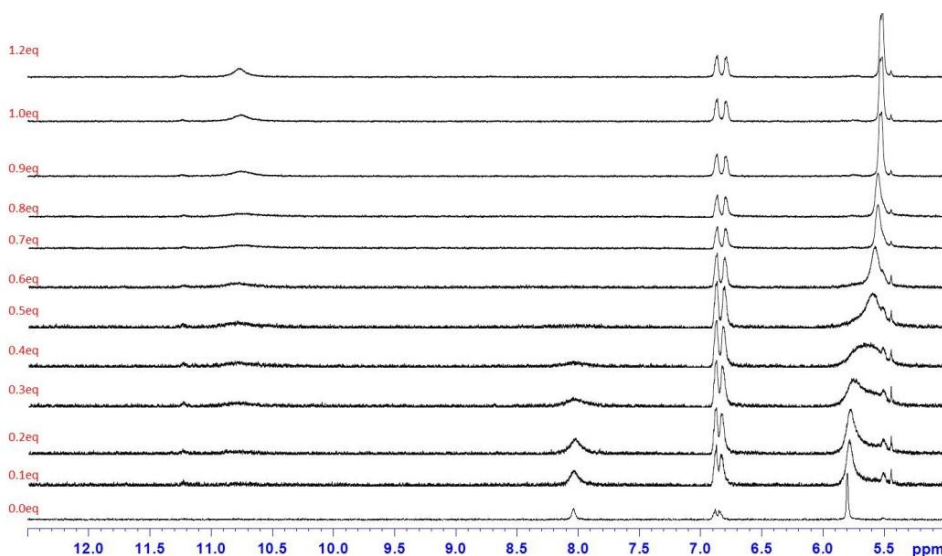


Figure 3.21 ^1H NMR titration of **R3** with TBABr in CD_3CN .

Preliminary binding study with these halide ions showed that **R3** converted to its bound form with ~ 1.2 equiv. of fluoride, chloride or bromide ions and the complexation process follows slow exchange kinetics on NMR time scale, and hence the binding constants could not be evaluated, however it can be concluded that the complexation follow 1:1 stoichiometry. Another notable point was found that interaction of anions with benzene ring is very less.

In order to evaluate the binding affinities, isothermal titration calorimetry (ITC) was performed for the anions. As we know there is several difficulties associated with ITC studies involving fluoride ion i.e. i) TBAF stays in its hydrated form ($\text{TBAF} \cdot 3\text{H}_2\text{O}$), it is extremely hygroscopic and attempted drying can result in decomposition of the salt,²⁸ ii) sometimes titration with fluoride associated with some other processes related to heat change.¹⁰ For these reasons, we started with our experiments with TBACl. It was found that the binding process form TBACl is enthalpy-driven and entropy-opposed. In case of bromide ion, same trend was also observed.

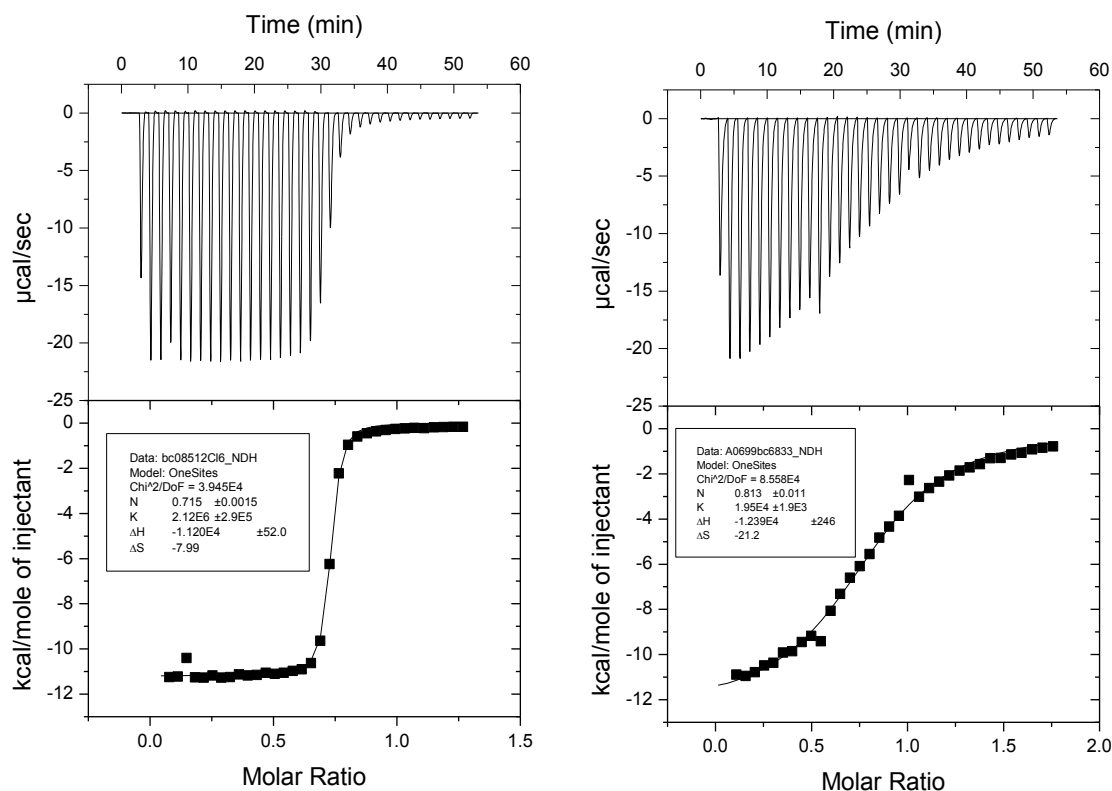


Figure 3.22 ITC study of **R3** in acetonitrile at 303 K with left: TBACl; right: TBABr. The curve shows the fit of the experimental data to a 1:1 binding profile.

Although overall change in enthalpy for bromide is higher than chloride ion, but larger negative entropy change resulted in more than 100 times weaker association constant for bromide compared to chloride ion (table 3.5). When these values are compared to closest literature

Table 3.5 Association Constant K_a , and thermodynamic parameters for the binding of fluoride, chloride, bromide, acetate and dihydrogenphosphate ions by **R3**, as measured by ITC in acetonitrile at 303 K, using the corresponding TBA salts (^a in presence of 0.5 % water).²⁹

TBA-salt	$K_a (M^{-1})$	$\Delta G (kcal\ mol^{-1})$	$\Delta H (kcal\ mol^{-1})$	$T\Delta S (kcal\ mol^{-1})$
Chloride	2.12×10^6	-8.78	-11.2	-2.42
Bromide	1.95×10^4	-5.97	-12.39	-6.42
Acetate	1.28×10^5	-7.09	-10.45	-3.36
$H_2PO_4^-$	1.07×10^5	-6.97	-14.48	-7.51
Fluoride ^a	1.17×10^6	-8.42	-6.27	2.15
Chloride ³⁰	1.37×10^6	-8.51	-7.43	1.08
Bromide ³⁰	3.10×10^4	-6.24	-7.10	-0.86

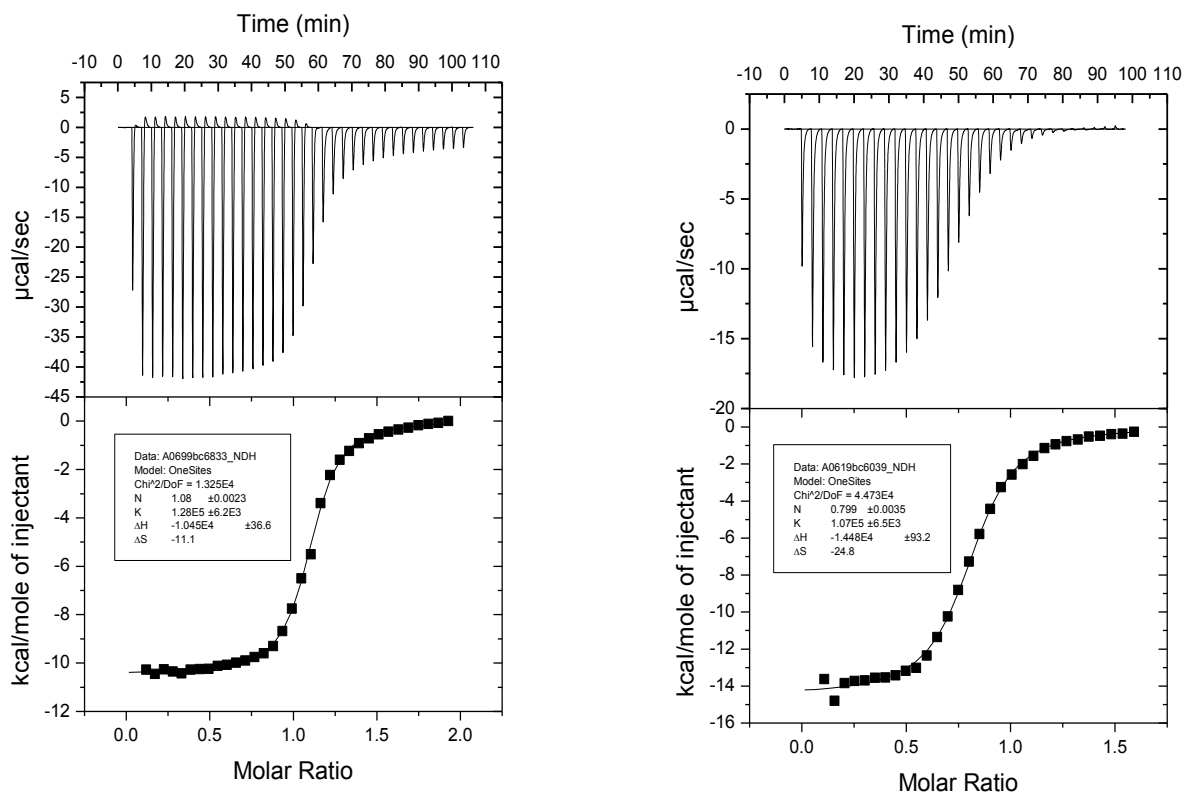


Figure 3.23 ITC study of **R3** in acetonitrile at 303 K with left: TBAOAc; right: TBAH₂PO₄. The curve shows the fit of the experimental data to a 1:1 binding profile.

reported 1,3-analogue of **R3** (i.e. **L125**), we found that association constants were quite similar,³⁰ which led us to assume that may be the role of inner aromatic –CH is not that substantial. For the two measured oxo-anions acetate and dihydrogenphosphate, we found that the heat change patterns were quite similar for both the anions (Figure 3.23). But in case of dihydrogenphosphate, change in enthalpy and negative entropy change both were higher than acetate ion, as a result of these antiparallel effect association constant were found all most same for both the ions.

After these finding, we thought of checking the association constant of fluoride ion for **R3** by ITC. At first we were unable to get reliable heat change in acetonitrile. That may be due to very strong interaction between host-guest, or with surroundings (solvent). So to minimize these effects and to obtain reliable and reproducible heat change (as TBAF is highly hygroscopic) for evaluation of association constant, we added 0.5 % water in the acetonitrile to use as the solvent. This led to quite consistent data (Figure 3.24). It was found that the binding process is favored by

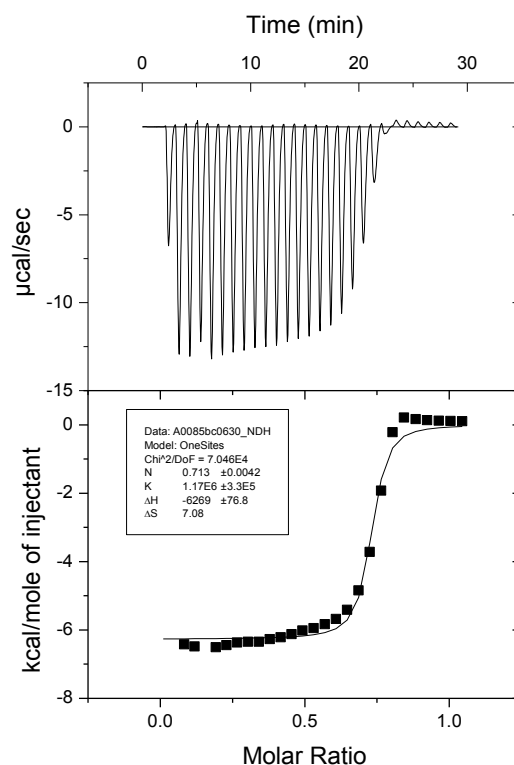


Figure 3.24 ITC study of **R3** in acetonitrile (with 0.5 % H₂O) at 303 K, with TBAF.3H₂O. The curve shows the fit of the experimental data to a 1:1 binding profile.

both enthalpy and entropy. It can be noticed that association constant for fluoride is less than that of chloride ion and it may be due to the water content in the solvent, which can diminish binding efficiency of host due to the greater solvation of the anion. So to check the authenticity of this conclusion further, we performed a competition experiment in $^1\text{H NMR}$. Addition of equimolar ratio of fluoride ion to already complexed chloride ion solution (1:1 molar ratio in CD_3CN), we observed complete ejection of chloride ion, with the onset of signals corresponding to fluoride complex only (Figure 3.25). Therefore, even if the exact K_a in acetonitrile could not be evaluated, however we can still presume that the K_a for fluoride must be higher than that of the

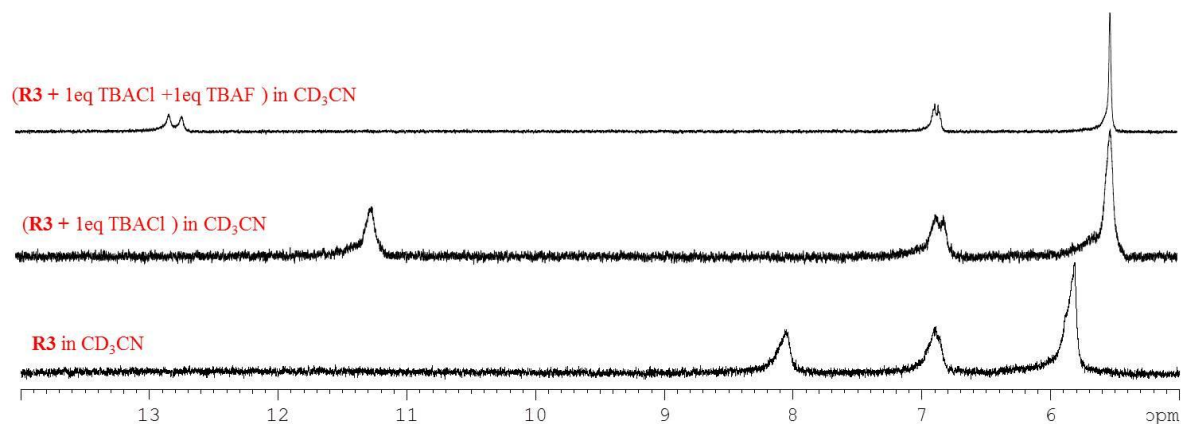


Figure 3.25 Competitive $^1\text{H NMR}$ experiment between TBACl and TBAF with **R3** CD_3CN .

diester-strapped calix[4]pyrrole²⁹ **L124** (highest so far reported to our knowledge), in which case a 6.3:1 ratio of fluoride to chloride complexation observed during competition experiment, although it was measured in DMSO-d_6 .²³

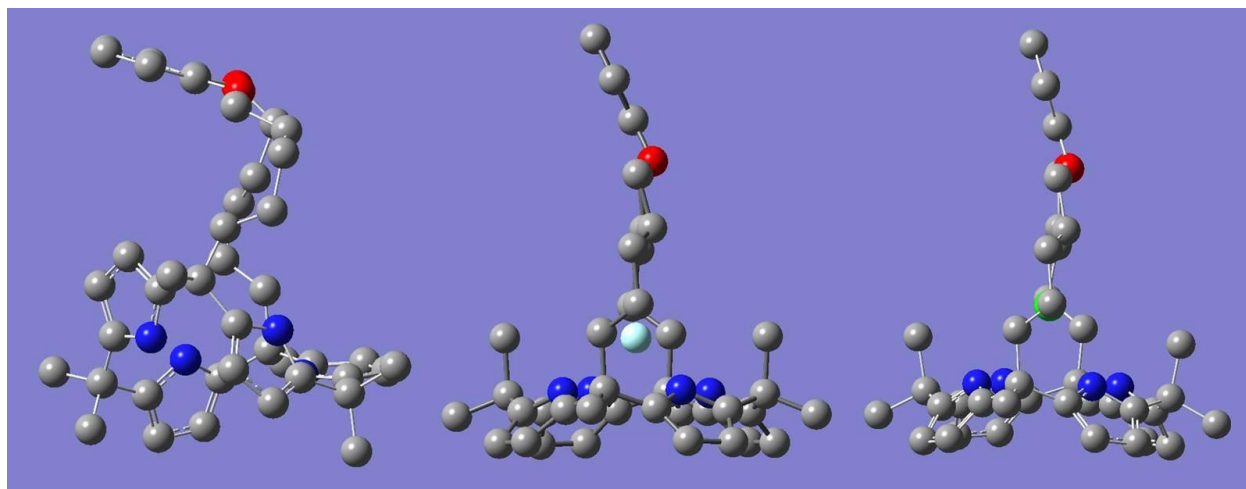


Figure 3.26 DFT optimized structures of **R3** (left), **R3.F⁻** (middle) and **R3.Cl⁻** (right).

To investigate further, we have performed DTF calculations for **R3**, **R3.F⁻** and **R3.Cl⁻** complex.³¹ DFT optimized structure (Figure 3.26) showed that in the free form **R3** existed in a 1,3-alternate conformation, where the benzene ring is tilted towards one side of the calix[4]pyrrole core (as seen in the solid state structure). But upon complexation with fluoride and chloride ions, the strap comes to an almost perpendicular position. This may be due to the more constrained structure of 1,2-diether linkage. Also this relatively restricted binding domain could stabilize the fluoride and chloride ions more effectively than the bromide ion. Further, we can assume that observed strong association constant towards acetate and dihydrogenphosphate ions may be due to the additional hydrogen bonding of oxygen atoms of the catechol derived flexible strap, which can rearrange itself to the periphery of the anion that might be at an appropriate structural environment.

3.6 Conclusion

In conclusion, we have synthesized a novel catechol derived diether linked strapped calix[4]pyrrole **R3** having an, benzene moiety linked through its 1,2-positions. Due to this structural environment, this receptor hosts two methanol molecules, which was not observed before for the 1,3-benzene (orcinol) derived strapped derivatives. This observation also led us to believe that suitable design of strap can also enhance the binding towards neutral guest molecules apart from anions.

We can further conclude that the calix[4]pyrrole having a strap derived from 1,2-linked aromatic moiety can act as good a receptor towards anion, like its 1,3-derived analogue. This investigation further suggested that in spite of strong CH-anion interaction, the role of inner aromatic CH may be not that important, or absence of inner aromatic proton may be compensated by more restricted binding domain in the former case. This constrained binding domain could help the receptor to bind acetate and dihydrogenphosphate ions more strongly.

3.7 Experimental Details

3.7.1.1 Synthesis of 7-[2-(6-oxo-heptyloxy)phenoxy]-2-heptanone (**R1**)

A mixture of catechol (330 mg; 3 mmol) and K₂CO₃ (4.14 g; 30 mmol) in acetone (80 mL) was stirred well for about 1 h, and then 7-bromo-2-heptanone (2.89 g; 15 mmol) was added. The mixture was refluxed for 3 days and then filtered and solvent was removed under reduced pressure. The crude product was purified by column chromatography over silica gel with

increasing ratio of ethyl acetate in hexane. The excess bromoketone was removed first (with 15 % ethyl acetate in hexane) and the desired product was collected as the next major band and vacuum dried to yield compound **R1** as a viscous liquid, which solidifies when kept in refrigerator (700 mg; 70 %). IR (neat): ν (cm^{-1}) 2944-2865, 1715; ^1H NMR (CDCl_3): δ in ppm 6.88 (s, 4H), 3.98 (t, 4H, $J = 12$ Hz), 2.46 (t, 4H, $J = 16$ Hz), 2.14 (s, 6H), 1.82 (m, 4H), 1.65 (m, 4H), 1.50 (m, 4H); ^{13}C NMR (CDCl_3): δ in ppm 209.00, 149.23, 121.28, 114.36, 69.06, 43.7, 29.95, 29.24, 25.75, 25.64. LCMS m/z , $M+H$: 335.4 (calculated for $\text{C}_{20}\text{H}_{31}\text{O}_4+H = 335.2$).

3.7.1.2 Synthesis of 1,2-bis[6,6-di(pyrrol-2-yl)heptyloxy]benzene (**R2**)

To a mixture of **R1** (650 mg; 1.94 mmol) and pyrrole (5.35 mL; 77.72 mmol), trifluoroacetic acid (150 μL ; 1.94 mmol) was added at about 60 $^\circ\text{C}$. The mixture was stirred for about 1.5 h and the reaction mixture was quenched with triethylamine (1 mL). Excess reagents were removed under reduced pressure to get the crude product, which was purified by column chromatography over silica gel (10 % EtOAc in hexane) to obtain the pure product **R2** (1 g, 65 %). IR(neat): ν (cm^{-1}) 3341, 2926-2870; ^1H NMR (CDCl_3): δ in ppm 7.59 (s, 4H), 6.98 (s, 4H), 6.56 (s, 3H), 6.17-6.13 (m, 9H), 4.03 (t, 4H, $J = 12\text{Hz}$), 2.04 (m, 4H), 1.8 (m, 4H), 1.6 (s, 6H), 1.4 (m, 4H), 1.35 (m, 4H); ^{13}C NMR (CDCl_3): δ in ppm 149.20, 138.37, 121.28, 117.26, 114.34, 107.58, 104.78, 69.27, 41.06, 38.99, 29.26, 26.58, 26.42, 24.17; LCMS m/z ($M+H$): 567.6 (calculated for $\text{C}_{36}\text{H}_{46}\text{N}_4\text{O}_2+H = 567.4$).

3.7.1.3 Synthesis of strapped calix[4]pyrrole (**R3**)

To a solution of **6** (750 mg; 1.32 mmol) and acetone (150 mL), $\text{BF}_3\cdot\text{OEt}_2$ (1 μL ; 0.38 mmol) was added. The solution was stirred at room temperature for 10 min, after which product formation was confirmed by TLC. The reaction was quenched by triethylamine (1 mL) and solvent was removed. The crude mass was subjected to column chromatography over silica gel (10% EtOAc in hexane) to obtain the product as a colored species, which upon subsequent washing with methanol yielded the pure macrocycle **R3** as an off-white powder (27 mg, 8 %). ^1H NMR (CDCl_3): δ in ppm 7.42 (s, 4H), 6.89 (s, 4H), 5.94 (m, 8H), 3.97 (t, 4H, $J = 16$ Hz), 1.95 (m, 4H), 1.82 (s, 4H), 1.68 (s, 6H), 1.52-1.50 (m, 16H), 1.24 (m, 4H); ^{13}C NMR (CDCl_3): δ in ppm 149.42, 137.73, 136.9, 121.31, 114.37, 104.31, 103.69, 69.23, 41.48, 39.47, 35.63, 30.24, 29.50, 28.53, 26.68, 25.37; LCMS m/z ($M-H$): 645.75 (calculated for $\text{C}_{42}\text{H}_{54}\text{N}_4\text{O}_2 - H = 645.42$).

3.7.2 Crystallographic Details

Crystallographic data for **R3** (methanol solvate) was collected at 298 K on Oxford Gemini A Ultra diffractometer with dual source. Pertinent crystallographic data collection and refinement parameter are shown in table 3.6.

Table 3.6 Crystallographic parameters of crystal of **R3**.

Crystal data	R3
CCDC No.	798911
Formula unit	C ₄₄ H ₆₂ N ₄ O ₄
Formula wt.	710.48
Crystal system	Monoclinic
T [K]	298 (2)
a [Å]	12.7028(15)
b [Å]	9.8713(7)
c [Å]	32.070(4)
α [°]	90.00
β [°]	91.157(10)
γ [°]	90.00
volume [Å ³]	4020.5(7)
Space group	P 2 ₁ /C
Z'	0
Z	4
D _{calc} [g.cm ⁻³]	1.175
μ /mm ⁻¹	0.075
Reflns collected	15609
Unique reflns	6840
Observed reflns	1975
R(int)	.1131
R ₁ [I > 2 σ (I)], wR ₂	0.0525, 0.0589
GOF	0.703

3.8 References

1. Baeyer, A. *Ber. Dtsch. Chem. Ges.* **1886**, *19*, 2184.
2. Chelintzev, V. V.; Tronov, B. V. *J. Russ. Phys. Chem. Soc.* **1916**, *48*, 105.
3. Rothmund, P.; Gage, C. L. *J. Am. Chem. Soc.* **1955**, *77*, 3340.
4. (a) Chelintzev, V. V.; Tronov, B. V. *J. Russ. Phys. Chem. Soc.* **1916**, *48*, 1197. (b) Brown, W. H.; Hutchinson, B. J.; MacKinnon, M. H. *Can. J. Chem.* **1971**, *49*, 4017.
5. (a) Floriani, C.; Floriani-Moro, R. In *The Porphyrin Handbook*; Kadish, K. M., Smith, K. M., Guillard, R., Eds.; Academic Press: New York, 2000, *3*, 385. (b) Floriani, C.; Floriani-Moro, R. In *The Porphyrin Handbook*; Kadish, K. M., Smith, K. M., Guillard, R., Eds.; Academic Press: New York, 2000, *3*, 405.
6. (a) Gale, P. A.; Sessler, J. L.; Kra'1, V.; Lynch, V. *J. Am. Chem. Soc.* **1996**, *118*, 5140. (b) Allen, W. E.; Gale, P.A.; Brown, C. T.; Lynch, V.; Sessler, J. L. *J. Am. Chem. Soc.* **1996**, *118*, 12471.
7. (a) Van Hoorn, W. P.; Jorgensen, W. L. *J. Org. Chem.* **1999**, *64*, 7439. (b) Wu, Y. -D.; Wang, D. F.; Sessler, J. L. *J. Org. Chem.* **2001**, *66*, 3739.
8. Blas, J. R.; Márquez, M.; Sessler, J. L.; Luque, F. J.; Orozco, M. *J. Am. Chem. Soc.* **2002**, *124*, 12796.
9. (a) Anzenbacher Jr., P.; Jursíková, K.; Lynch, V. M.; Gale, P. A.; Sessler, J. L. *J. Am. Chem. Soc.* **1999**, *121*, 11020. (b) Namor, A. F.; Shehab, M. *J. Phys. Chem. B* **2003**, *107*, 6462. (c) Sessler, J. L.; An, D.; Cho, W. S.; Lynch, V. *Angew. Chem. Int. Ed.* **2003**, *42*, 2278. (d) Sessler, J. L.; An, D.; Cho, W. S.; Lynch, V. *J. Am. Chem. Soc.* **2003**, *125*, 13646. (e) Sessler, J. L.; An, D.; Cho, W. S.; Lynch, V.; Marquez, M. *Chem. Eur. J.* **2005**, *11*, 2001. (f) Nielsen, A. K.; Cho, W. S.; Lyskawa, J.; Levillain, E.; Lynch, V.; Sessler, J. L.; Jeppesen, J. O. *J. Am. Chem. Soc.* **2006**, *128*, 2444.
10. Schmidtchen, F. P. *Org. Lett.* **2002**, *4*, 431.
11. (a) Sessler, J. L.; Gross, D. E.; Cho, W. S.; Lynch, V. M.; Schmidtchen, F. P.; Bates, G. W.; Light, M. E.; Gale, P. A. *J. Am. Chem. Soc.* **2006**, *128*, 12281. (b) Gross, D. E.; Schmidtchen, F. P.; Antonius, W.; Gale, P. A.; Lynch, V.; Sessler, J. L. *Chem. Eur. J.* **2008**, *14*, 7822. (c) Gross, D. E. ITC and NMR Spectroscopy Binding Studies of meso-octamethylcalix[4]pyrrole and its derivatives. Ph.D. Dissertation, The University of Texas at Austin, Austin, Texas 78712, 2009.

12. Shriver, J. A.; Westphal, S. G. *J. Chem. Educ.* **2006**, 83, 1330.
13. Anzenbacher Jr., P.; Jursíková, K.; Lynch, V.; Gale, P. A.; Sessler, J. L. *J. Am. Chem. Soc.*, **1999**, 121, 11020.
14. Aydogan, A.; Akar, A. *Chem. Eur. J.* **2012**, 18, 1999.
15. Mahanta, S. P.; Kumar, B. S.; Panda, P. K. *Chem. Commun.* **2011**, 47, 4496.
16. Mahanta, S. P.; Panda, P. K. *Org. Biomol. Chem.* **2014**, 12, 278.
17. Gale, P. A.; Sessler, J. L.; Allen, W. E.; Tvermoes, N. A.; Lynch, V. *Chem. Commun.* **1997**, 665.
18. Anzenbacher Jr., P.; Jursíková, K.; Shriver, J. A.; Miyaji, H.; Lynch, V. M.; Sessler, J. L.; Gale, P. A. *J. Org. Chem.* **2000**, 65, 7641.
19. (a) Miyaji, H.; Anzenbacher Jr., P.; Sessler, J. L.; Bleasdale, E. R.; Gale, P. A. *Chem. Commun.* **1999**, 1723. (b) Miyaji, H.; Sato, W.; Sessler, J. L. *Angew. Chem. Int. Ed.* **2000**, 39, 1777. (c) Liu, Y.; Minami, T.; Nishiyabu, R.; Wang, Z.; Anzenbacher Jr., P. *J. Am. Chem. Soc.* **2013**, 135, 7705.
20. a) Scherer, M.; Sessler, J. L.; Gebauer, A.; Lynch, V. *Chem. Commun.* **1998**, 1. (b) Gale, P. A.; Anzenbacher, Jr., P.; Sessler, J. L. *Coord. Chem. Rev.* **2006**, 250, 3004. (c) Gale, P. A. *Chem. Soc. Rev.*, **2010**, 39, 3746. (d) Lee, C. H. *Bull. Korean Chem. Soc.*, **2011**, 32, 768. (e) Sharma, A.; Obrai, A.; Kumar, A. *J. Chem. Bio. Phy. Sci. Sec. A*, **2013**, 3, 91. (f) Wenzel, M.; Hiscock, J. R.; Gale, P. A. *Chem. Soc. Rev.* **2012**, 41, 480. (g) Gale, P. A.; Busschaert, N.; Haynes, C. A. J.; Karagiannidis, A. E.; Kirby, I. L. *Chem. Soc. Rev.*, **2014**, 43, 205.
21. (a) Woods, C. J.; Camiolo, S.; Light, M. E.; Coles, S. J.; Hursthouse, M. B.; King, M. A.; Gale, P. A.; Essex, J. W. *J. Am. Chem. Soc.* **2002**, 124, 8644. (b) Namor, A. D.; Shehab, M.; Abbas, I.; Withams, M. V.; Zvietcovich-Guerra, J. *J. Phys. Chem. B* **2006**, 110, 12653. (c) Namor, A. D.; Shehab, M.; Khalife, R.; Abbas, I. *J. Phys. Chem. B* **2007**, 111, 12177. (d) Gil-Ramírez, G.; Escudero-Adán, E. C.; Benet-Buchholz, J.; Ballester, P. *Angew. Chem. Int. Ed.* **2008**, 47, 4114. (e) Ballester, P.; Gil-Ramírez, G. *Proc. Natl. Acad. Sci. U.S.A.* **2009**, 106, 10455.
22. (a) Gil-Ramírez, G.; Chas, M.; Ballester, P. *J. Am. Chem. Soc.* **2010**, 132, 2520. (b) Espelt, M.; Ballester, P. *Org. Lett.* **2012**, 14, 5708. (c) Sokkalingam, P.; Kee, S. Y.; Kim, Y.; Kim, S. J.; Lee, P. H.; Lee, C. H. *Org. Lett.* **2012**, 14, 6234. (c) Kaur, S.; Hwang, H.;

- Lee, J. T.; Lee, C. H. *Tetrahedron Lett.* **2013**, *54*, 3744. (d) Galán, A.; Escudero-Adán, E. C.; Frontera, A.; Ballester, P. *J. Org. Chem.* **2014**, *79*, 5545. (e) Taner, B.; Alici, O.; Deveci, P. *Supramol. Chem.* **2014**, *26*, 119. (f) Chang, K. C.; Minami, T.; Koutnik, P.; Savechenkov, P. Y.; Liu, Y.; Anzenbacher, Jr., P. *J. Am. Chem. Soc.* **2014**, *136*, 1520. Louis, A.; Guzman, G. R.; David, F. A. Q.; Eduardo, C. E. D.; Ballester, P. *J. Am. Chem. Soc.* **2014**, *136*, 3208. (g) Albano, G.; Eduardo, C. E. D.; Antonio, F.; Ballester, P. *J. Org. Chem.* **2014**, *79*, 5545. (m) Aydogan, A.; Koca, A.; Şener, M. K.; Sessler, J. L. *Org. Lett.* **2014**, *16*, 3764.
23. Yoon, D. W.; Hwang, H.; Lee, C. H. *Angew. Chem. Int. Ed.* **2002**, *41*, 1757.
 24. Lee, C. H.; Miyaji, H.; Yoon, D. W.; Sessler, J. L. *Chem Commun.* **2012**, *48*, 8060.
 25. Park, J. Y.; Skonieczny, K.; Aratani, N.; Osuka, A.; Gryko, D. T.; Leem, C. H. *Chem Commun.* **2008**, *24*.
 26. Bucher, C.; Zimmerman, R. S.; Lynch, V.; Sessler, J. L. *J. Am. Chem. Soc.* **2001**, *123*, 9716.
 27. (a) Lee, C. -H.; Lee, J. S.; Na, H. K.; Yoon, D. W.; Miyaji, H.; Cho, W. S.; Sessler, J. L. *J. Org. Chem.* **2005**, *70*, 2067. (b) Miyaji, H.; Kim, H. K.; Sim, E. K.; Lee, C. K.; Cho, W. S.; Sessler, J. L.; Lee, C. H. *J. Am. Chem. Soc.* **2005**, *127*, 12510. (c) Jeong, S. D.; Yoo, J.; Na, H. K.; Chi, D. Y.; Lee, C. H. *Supramol. Chem.* **2007**, *19*, 271. (d) Yoon, D. W.; Gross, D. E.; Lynch, V. M.; Sessler, J. L.; Hay, B. P.; Lee, C. H. *Angew. Chem. Int. Ed.* **2008**, *27*, 5038. (e) Gross, D. E.; Yoon, D. W.; Lynch, V. M.; Lee, C. H.; Sessler, J. L. *J Incl Phenom Macrocycl Chem.* **2010**, *66*, 81. (f) Fisher, M. G.; Gale, P. A.; Hiscock, J. R.; Hursthouse, M. B.; Light, M.; Schmidtchen, F. P.; Tong, C. C. *Chem Commun.* **2012**, *48*, 3017.
 28. Sharma, R. K.; Fry, J. L. *J. Org. Chem.* **1983**, *48*, 2112.
 29. Samanta, R.; Mahanta, S. P.; Chaudhuri, S.; Panda, P. K.; Narahari, A. *Inorg. Chim. Acta.* **2011**, *372*, 281.
 30. Lee, C. H.; Na, H. K.; Yoon, D. W.; Won, D. H.; Cho, W. S.; Lynch, V. M.; Shevchuk, S. V.; Sessler, J. L. *J. Am. Chem. Soc.* **2003**, *125*, 7301.
 31. Samanta, R.; Mahanta, S. P.; Ghanta, S.; Panda, P. K. *RSC Adv.* **2012**, *2*, 7974.

CHAPTER 4

Isomeric Naphthalene Derived Strapped Calix[4]pyrroles

4.1 Introduction

In the last two decades, the development of anion coordination chemistry saw several new approaches, for example anion recognition sites can be coupled to certain groups that are capable of “reporting” the coordination event.¹ In this case, the binding process is transduced into a signaling event. Receptors specifically designed for sensing purposes are generally called chemosensors.² The basic design principle in these new multicomponent systems is that the sensing event has to be related with an easy to measure signal. In fact, many chemosensors display changes in either color^{3,4} or fluorescence⁵ in the presence of a certain guest, although changes in electrochemical properties such as the oxidation potential of redox active groups has also been widely used.^{6,7} During the sensing process, information at the molecular level, such as the presence or absence of a certain guest in solution, is amplified to a macroscopic level; hence, sensing might open the door to the determination (qualitative or quantitative) of certain guests. These ideas connect in some way with supramolecular concepts such that of molecular devices (in this case sensor devices) in which the final operation (anion signaling), performed by the device, results from the sum of the basic functions of the components i.e. the binding site (coordination), and the reporting unit (transduction of the coordination event).

4.1.1. Design Principles of Chemosensors for Anion Sensing

A general approximation to the development of anion chemosensors is the coupling of at least two units, each one displaying a precise function: the binding site and the signaling subunit. In the former resides the function of coordination to a certain anion(s), whereas the latter undergoes change in certain spectroscopic characteristics (color or fluorescence) upon anion coordination. Binding sites and signaling units can be covalently linked (binding site-signaling subunit approach)⁸ or not (displacement approach).⁹ This general design principle is based on anion coordination events; therefore, both the interaction with the anion and the change in color or fluorescence are in principle reversible. In fact, coordination is a typical reversible chemical reaction, in which, changes in the concentration of the anion determine the relative amount of coordinated and free guest. In addition, anion signaling using fluorescence or color changes can also be observed using irreversible reactions. Here, the term chemosensor should not strictly be applied and terms such as reagents, reactants, or chemodosimeters should be used.^{10,11}

4.1.1.1 Binding Site-Signaling Subunit Approach

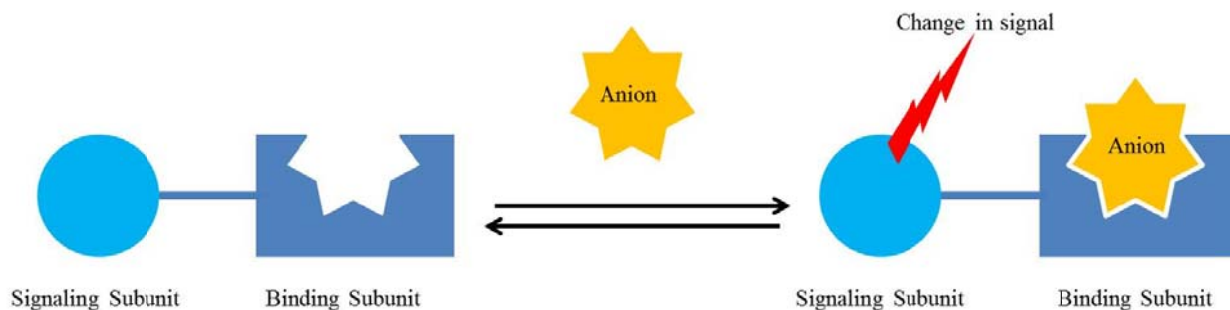


Figure 4.1 Schematic representation of anion chemosensors based on the binding site-signaling subunit approach.

Many chemical sensors follow the approach of the covalent attachment of signaling subunits and binding sites, as schematically shown in Figure 4.1. This has been the most widely used approach in the development of anion chemosensors and will surely be a fundamental approach in future developments. As shown above, the coordination site binds the anion in such a way that the properties of the signaling subunit are changed giving rise to variations, either in the color (chromogenic chemosensor) or in its fluorescence behavior (fluorogenic chemosensor).

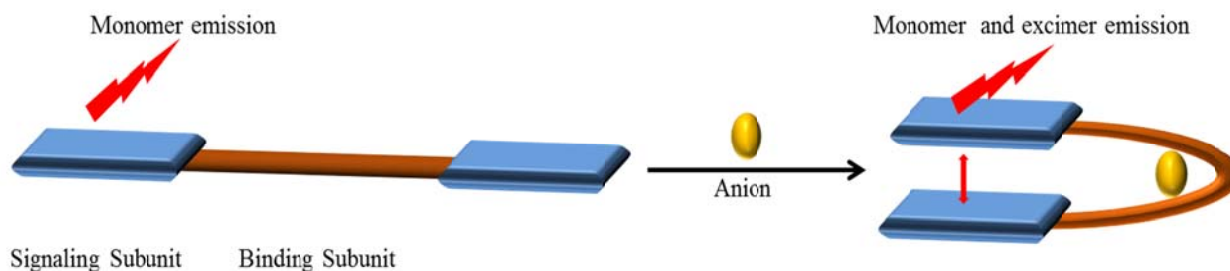


Figure 4.2 Receptor composed of a flexible coordinating subunit and two “flat” fluorophores. Anion coordination induced spatial proximity between the two fluorophores and hence led to dual emission from the monomer and the excimer.

A particular phenomenon that can be observed when using fluorophores as a signaling unit is the formation of excimers. An excimer can be defined as a complex formed by interaction of a fluorophore in the excited state with a fluorophore of the same structure in the ground state.¹² An important aspect is that the emission spectrum of the excimer is red-shifted with respect to that of the monomer, and in many cases, the dual emission of the monomer and the excimer is observed. Therefore, by simple monitoring of the emission excimer band, excimer

formation or excimer rupture upon addition of anion, one can get information about anion coordination. In general, it is assumed that flat, highly π -delocalized systems such as pyrene and anthracene show greater tendency to form excimers. An additional requirement for excimer formation is that two monomers need to be in close proximity in order to give stacking interactions and the molecular excimer state. Figure 4.2 shows a schematic representation of anion-induced excimer formation in which anion coordination favors the proximity between the two fluorophores.

4.1.1.2 Displacement Approach

This approach also involves, as in the above case, the use of anion binding site and signaling subunits. However, in this case, both subunits need not be necessarily covalently attached but form a coordination complex (molecular ensemble). Then, when a target anion is added to the solution containing the binding site signaling unit ensemble, there is a displacement reaction; the binding site coordinates with the anion, whereas the signaling subunit returns to the solution retrieving its non-coordinated spectroscopic behavior (Figure 4.3). If the spectroscopic

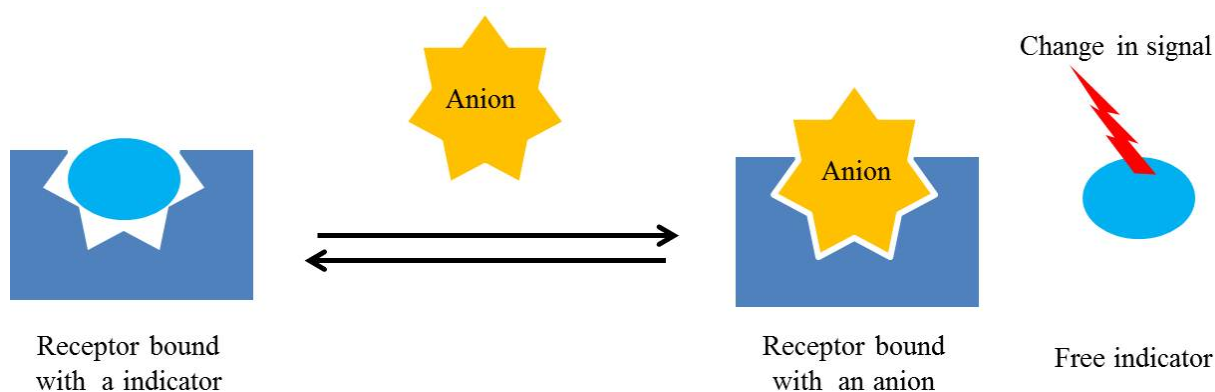


Figure 4.3 Schematic diagram of anion chemosensors based on the displacement approach.

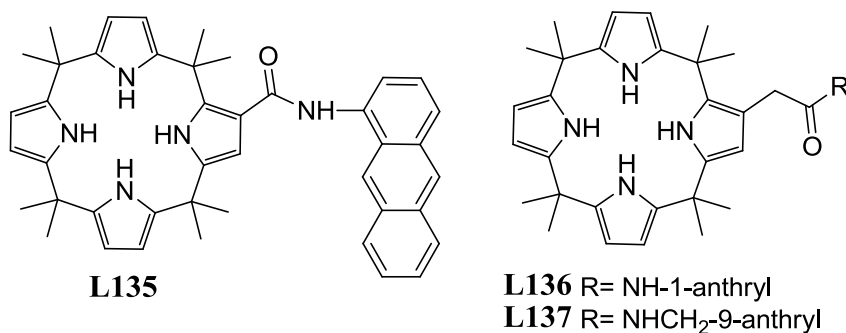
characteristics of the signaling subunit in the molecular ensemble are different to those in its non-coordinated state, then the anion binding process is coupled to a signaling event. Needless to mention, the stability constant for the formation of the complex between the binding site and the signaling subunit has to be lower than that between the binding site and the target anion. Only in this way, the displacement reaction will take place indicating the presence of the target anion, through the signaling event. Additionally, selectivity can be achieved by choosing an indicator-

binding site couple, with a formation (stability) constant, larger than that between the signaling unit and the potentially interfering anions.^{9c}

4.2 Calix[4]pyrrole as Chemosensor

As calixpyrrole is a non-conjugated molecule so it is difficult to use it as chemoreceptor for anions. To make this class of molecule as chemoreceptor, researchers have attached reporter (chromophore or fluorophore) group(s) covalently to this molecule. Some groups have used displacement approach (dye displacement assay) using anionic dyes and simple calix[4]pyrroles. Among the two methods, binding site-signaling subunit approach is the most popular one.

4.2.1 Binding Site-Signaling Subunit Approach



In 1999, Sessler and coworkers first reported fluorescent anthracene–calix[4]pyrrole conjugates **L135-137**, which can detect the presence of anions by a significant quenching of their fluorescence.¹³ They have shown that for these receptors, it was difficult to measure the

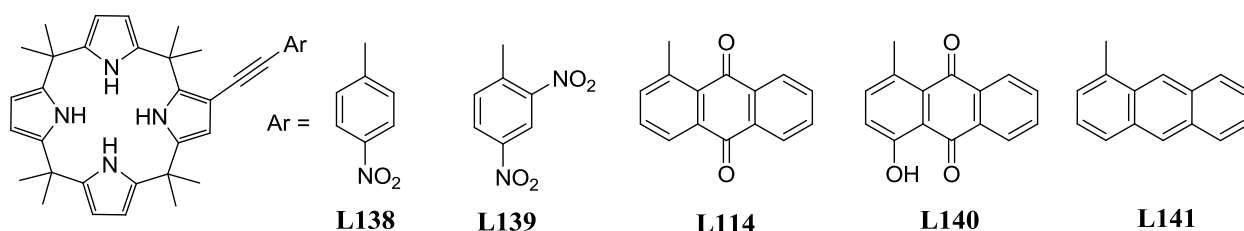
Table 4.1 log K_a of **L135-137** with various anions in the form of tetrabutylammonium salts determined by (a) ¹H NMR titration in CD₃CN and (b) fluorescence quenching analyses in CH₃CN at 298 K.

	L135		L136		L137	
Anion	a	b	a	b	a	b
F [−]	N.D.	5.17	N.D.	4.69	N.D.	4.69
Cl [−]	> 4	4.87	> 4	3.81	> 4	3.71
Br [−]	3.59	3.98	3.00	2.86	2.63	^c
H ₂ PO ₄ [−]	> 4	4.96	3.50	3.90	3.08	^c

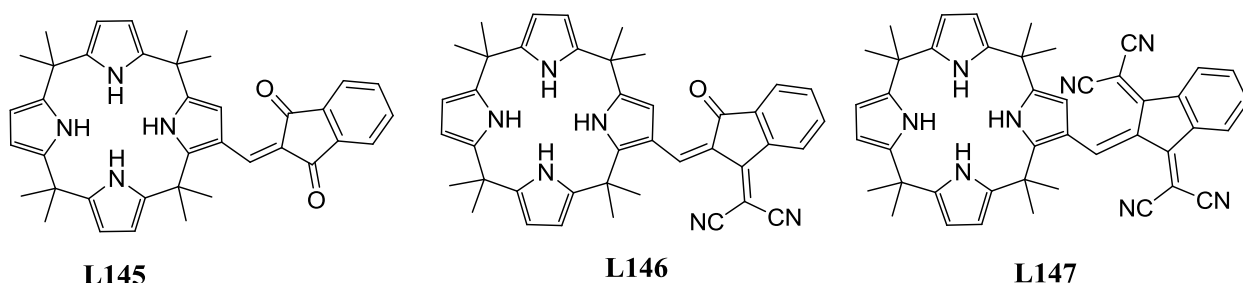
N.D. NH resonance broadened precluding a determination of its value using NMR spectroscopic method.

^c Quenching insufficient to provide an accurate stability constant value.

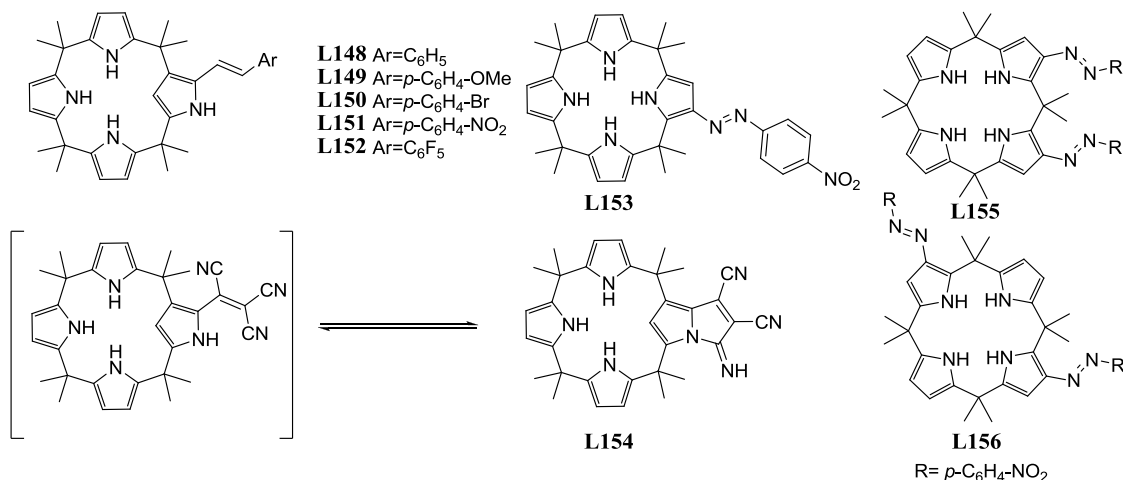
association constant for some anions (fluoride and dihydrogenphosphate ions) by $^1\text{H-NMR}$ titration but by fluorescence quenching experiment one can easily measure the association constant for fluoride ion. They have also demonstrated that quenching efficiency is better, when the fluorophore is conjugated (**L135**) than unconjugated (**L136-137**). One year later, same group have reported a range of arylalkynyl-functionalized calix[4]pyrroles (**L114**, **L138-141**), directly linking chromophores at its one of the β -pyrrolic position. **L138** and **L139** contain 4-nitrobenzene and 2,4-dinitrobenzene group as chromophores, respectively. In case of **L138**, upon addition of 20 equivalent of TBAF the color of the solution changed from pale yellow to intense yellow. The presence of chloride and dihydrogenphosphate ions could also be detected from the intense final yellow color. Whereas, for **L139** color change from yellow to red, upon addition of TBAF and yellow to orange for chloride and dihydrogenphosphate ions (200 equivalents) was reported, for naked eye detection of anion by calix[4]pyrroles.^{14a} In the same year,



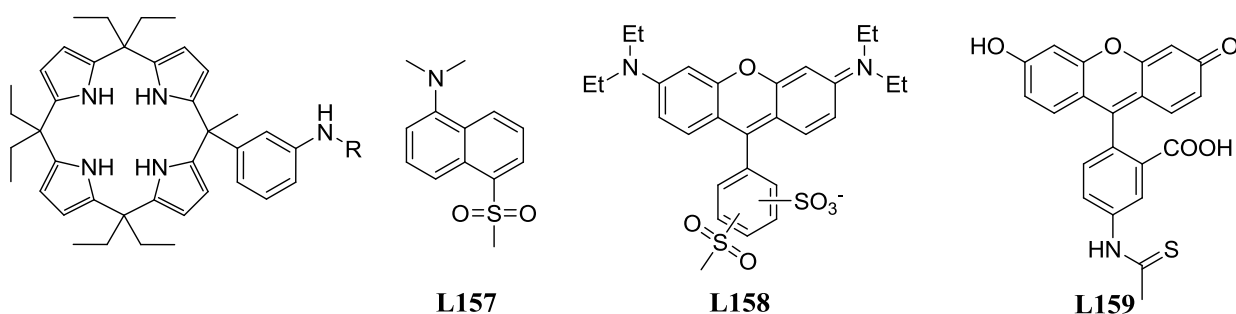
and **L144** were obtained by condensation of **L133** with 1-indanylidene malononitrile and anthrone, respectively. These three receptors showed dramatic color changes in the presence of fluoride, acetate, pyrophosphate, and also phosphate ions but no change in color was observed upon addition of chloride, bromide, iodide, or nitrate ions. They also showed that **L142** can be used for detecting carboxylate ions in aqueous solution of ionic strength and pH corresponding to blood plasma. In 2006, Anzenbacher Jr. and Nishiyabu reported a new set of chromogenic calix[4]pyrroles based on 1,3-indane. These receptors showed effective color change in presence



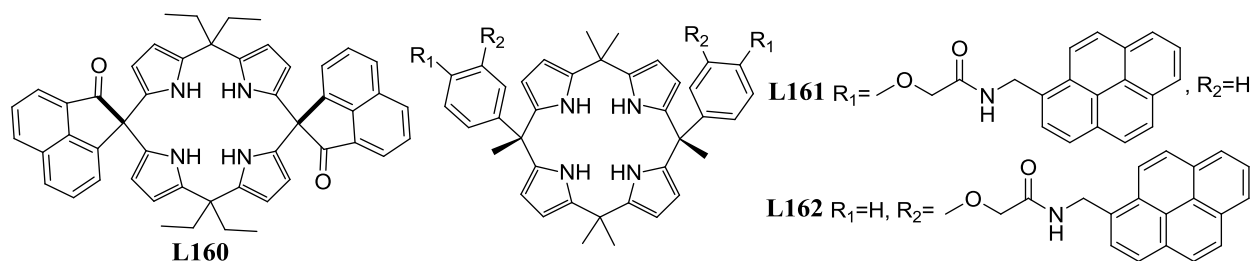
of fluoride, chloride, acetate and dihydrogenphosphate ions. Selectivity was found higher for dihydrogenphosphate over chloride ion (50 times higher when compared to **L72**), which may be due to the presence of the electron withdrawing dicyanomethylidene moieties on the indane ring.¹⁶ As these molecules are quite acidic in nature, use of higher concentration of anion leads to deprotonation of pyrrole-NH (in case of fluoride and acetate ions). In 2005, Dehaen and coworkers showed that α -aryldiazo N-confused calix[4]pyrroles (**L148-152**), prepared by azo-coupling of parent N-confused calix[4]pyrrole with an excess of the corresponding benzenediazonium chlorides or tetrafluoroborates in the presence of a base at low temperature, can be used as chemosensors for anions.¹⁷ These modified receptors can bind to dihydrogenphosphate ion with higher efficiency when compared with **L72**. They have also found



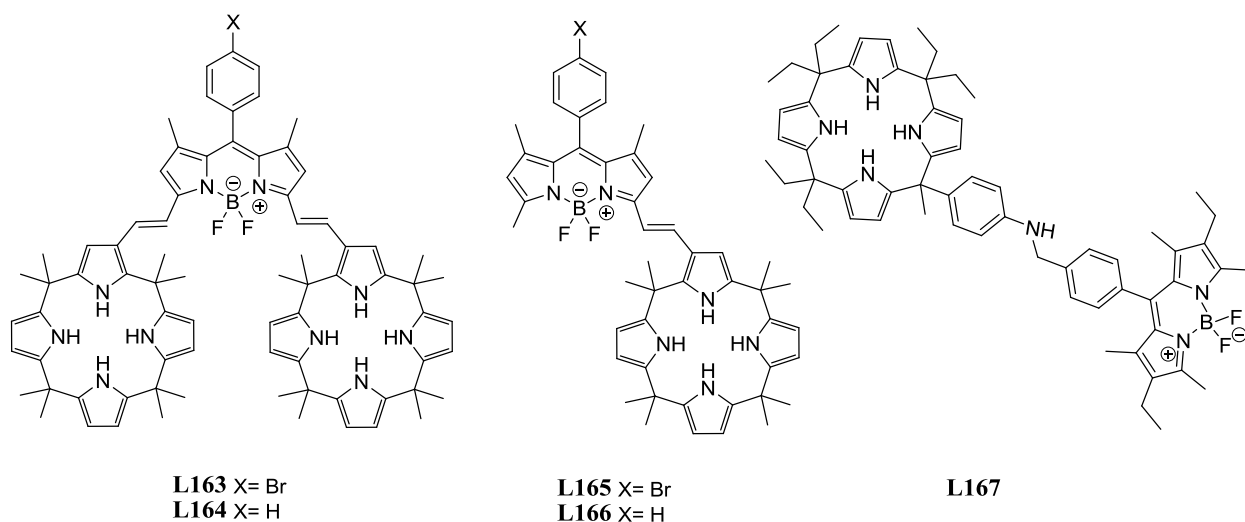
noticeable increase in association constants with the electron-withdrawing character of the side-arm substituents, in dichloromethane. In the case of very basic fluoride ion and acidic ligands with nitrophenyl and fluorophenyl moieties, deprotonation of pyrrole-NH was observed. Later in 2006, Anzenbacher Jr. and Dehaen together reported **L153** and **L154** (cyclized form of N-confused tricyanoethane-calix[4]pyrrole) and compared binding affinity with **L151** and **L142**.¹⁸ They found that N-confused calix[4]pyrrole receptors exhibit a different binding preference compared to the parent octamethylcalix[4]pyrrole receptors. Regular calix[4]pyrrole based materials showed the anion affinity order $F^- > HP_2O_7^{3-} > AcO^- > H_2PO_4^- > Cl^-$, while the materials based on N-confused calix[4]pyrrole showed the order of affinity as $AcO^- > F^- > HP_2O_7^{3-} > H_2PO_4^- > Cl^-$. Few years later, Chauhan and coworkers have synthesized **L155-156**, where both the receptors showed higher affinity towards acetate ion compared to chloride and dihydrogenphosphate ions, in fact even higher than **L151** and **L153**.¹⁹ First chromophore dye linked at *meso*-position of calix[4]pyrrole reported by Sessler and coworkers in 2000, by following a building block approach, they synthesized three fluorescent dye appended calix[4]pyrroles (**L157-L159**). These receptors were the first to show high phosphate/chloride



selectivity (by 2 order). They have shown that presence of appropriate chromophore can enhance the binding affinity towards a particular anion. As hydrogen bonding site is increasing from **L158** to **L159**, binding affinity towards the pyrophosphate ion is also increased. **L159** was first reported as the fluorescence active calix[4]pyrrole that can bind anion in presence of water at physiological pH.²⁰ Cheng and coworkers in 2008, reported synthesis of calix[4]pyrrole **L160** from acenaphthenequinone.²¹ Solid state structure showed that both the remaining ketone group stays in *trans*-orientation. Solution phase UV-vis study in dichloromethane showed that the receptor bind only to fluoride and chloride ions among the measured anions. In 2010, Lee and coworkers synthesized **L161-162** bearing appended pyrenyl groups at two opposite *meso*-positions in *cis*-fashion. Both the receptors showed ability to interact with fluoride and chloride

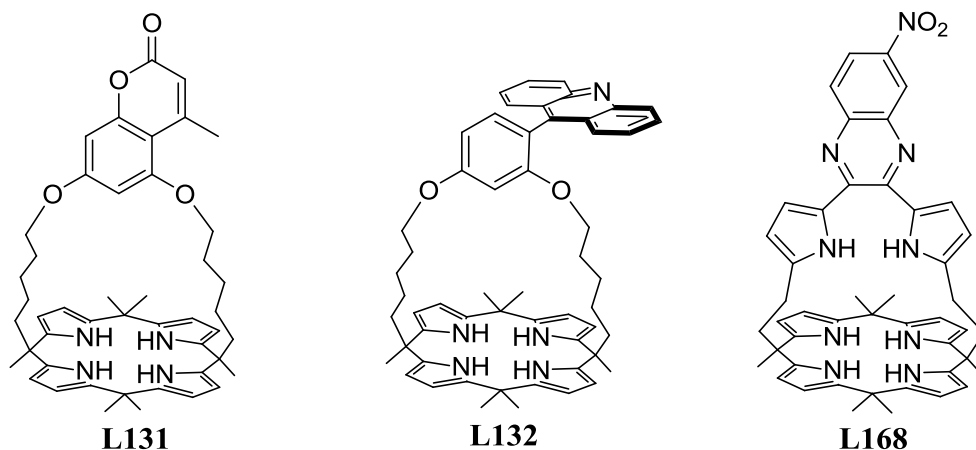


ions. Fluorescence quenching study of **L161** revealed that its binding affinity is slightly higher for chloride ion.²² BODIPY dyes, a popular chromophoric group, have also been attached to calix[4]pyrroles. First sandwich anion receptor, a BODIPY dye bearing two calix[4]pyrrole units **L163**, was reported by Shao and coworkers in 2011.^{23a} As an anion receptor, **L163** displayed a red shift in absorption spectrum and fluorescence quenching of varying degrees in the presence of fluoride, chloride, acetate and dihydrogenphosphate ions and affinity towards these anions also were found better due to the formation of a sandwich complex through multiple hydrogen-bonding interactions. One year later, same group again synthesized mono-BODIPY linked calix[4]pyrrole **L165**, which could able to bind all the previous mentioned anions, however to a



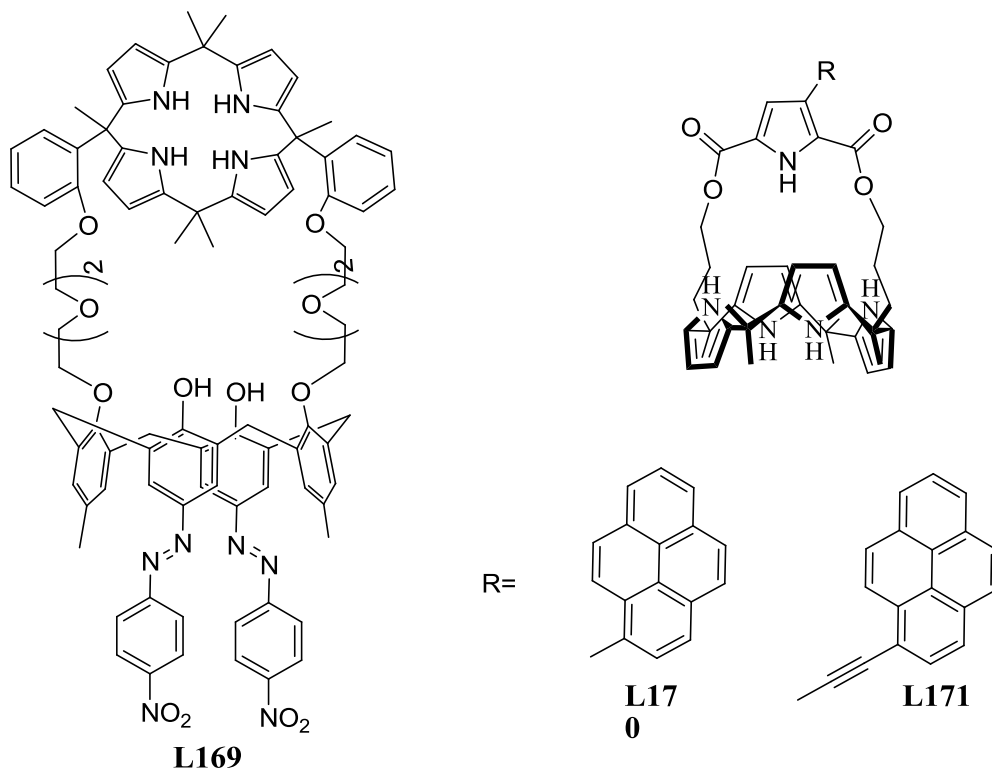
lesser extent.^{23b} Costero and coworkers have reported two very similar BODIPY bridged calix[4]pyrroles **L164** and **L166** towards sensing of aliphatic and aromatic dicarboxylate anions.²⁴ The ditopic receptor, **L164** shows a higher affinity for α,ω -aliphatic dicarboxylates with 7 or 8 methylene groups as spacer (dianions of azelaic acid and sebacic acid), most probably because of the formation of a cyclic 1:1 complex involving coordination of the two carboxylate groups of the guest to both calix[4]pyrrole units of the receptor. When **L166** was

checked for its binding affinity it was found that it can bind to dianions and association constant was quite close to those obtained for the 1:1 complexes between **L164** and the shortest dicarboxylates (and also with acetate), however, for the larger dianions, magnitude of association constants were lower by two order. Very recently Kursunlu and coworkers reported another BODIPY appended calix[4]pyrrole unit **L167**, which could able to show colorimetric and ‘turn-off’ fluorescent response in presence of fluoride ion.²⁵



Apart from the above *meso* and β -modified calix[4]pyrrole chemosensors, researcher also explored strapped calix[4]pyrroles by incorporating the reporting units in the strap. This approach could be beneficial, as we have noticed that strap can interact with anions upon binding, which in return can generate greater spectral response and presence of particular chromophore groups may help in binding. In 2005, Lee and coworkers synthesized coumarin-strapped calix[4]pyrrole **L131** from 5,7-dihydroxy-4-methylcoumarin by using conventional procedure.²⁶ In preliminary study no significant quenching of the fluorescence was observed when anions were added to dilute solutions of **L131** in acetonitrile, but in presence of water (3% v/v) or sodium ion enhancement of fluorescence was observed, which was quenched upon addition of chloride, bromide and acetate ions. This phenomenon was attributed to the ability of sodium ion to interact with coumarin carbonyl group causing hindrance to the PET process, which may be subdued after incorporation of anion into the calix[4]pyrrole core. Another fluorophore linked calix[4]pyrrole **L132** was also reported by Lee and coworkers,²⁷ but determination of association constant by fluorometric measurement was not possible either due to the weak communication between attached fluorophore and the binding event or intermolecular energy quenching by π - π stacking interaction. Moreover, the orthogonal

conformation between acridine and phenyl moiety may also be part of the reason. Two years later same group have reported a calix[4]pyrrole strapped with chromogenic dipyrrolylquinoxaline (**L168**), which can be used as a chromogenic sensor for certain anionic species, notably for fluoride and dihydrogenphosphate ion, that functions well in organic media.²⁸ On the basis of ^1H NMR spectroscopic evidence, it was concluded that the dipyrrolylquinoxaline-containing unit is tilted, such that the bound anions can interact with the dipyrrolylquinoxaline, perhaps through anion- π interactions. A chromogenic calix[4]pyrrole **L169** was successfully synthesized by Pulpoka and coworkers by using azocalix[4]arene as the strap.²⁹ The integration of azobenzene unit onto the calix[4]arene framework, enhanced the anion binding ability of the phenolic-OH groups of the calix[4]arene (owing to the electron deficient nitrobenzene moieties), and provided naked-eye detection of anions. In 2013, Lee and coworkers reported two new pyrrole-strapped calix[4]pyrroles bearing pyrene moiety (**L170** and **L171**) which strongly bind with fluoride, chloride, acetate and dihydrogenphosphate ions and the binding event can be monitored by studying anion-dependent quenching of the fluorescence.³⁰ The quenching was associated with increased electron density on the pyrrole moiety through weak PET process.



4.2.2 Displacement Approach

Apart from the binding site-signaling subunit approach, there are few reports, where displacement approach is used. Intrinsic idea was using the anion binding ability of calix[4]pyrrole; first a dye is taken, which can bind significantly to calix[4]pyrrole so that it can generate a spectral change compared to the unbound dye, then upon addition of the analyte, the

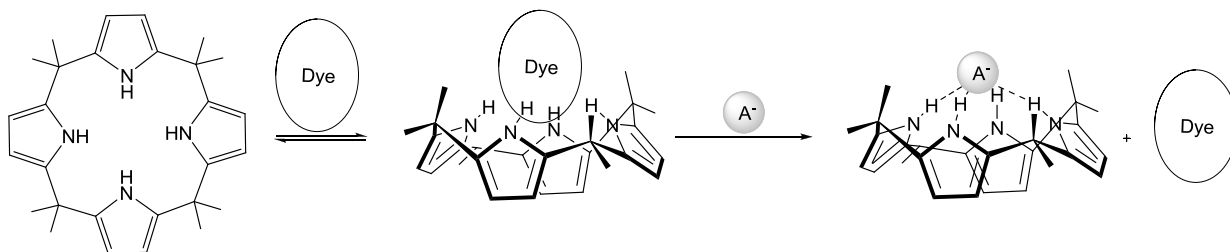
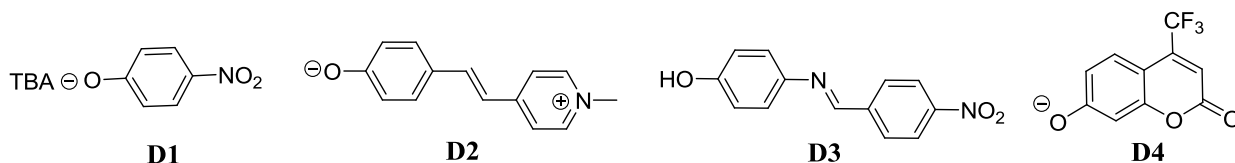


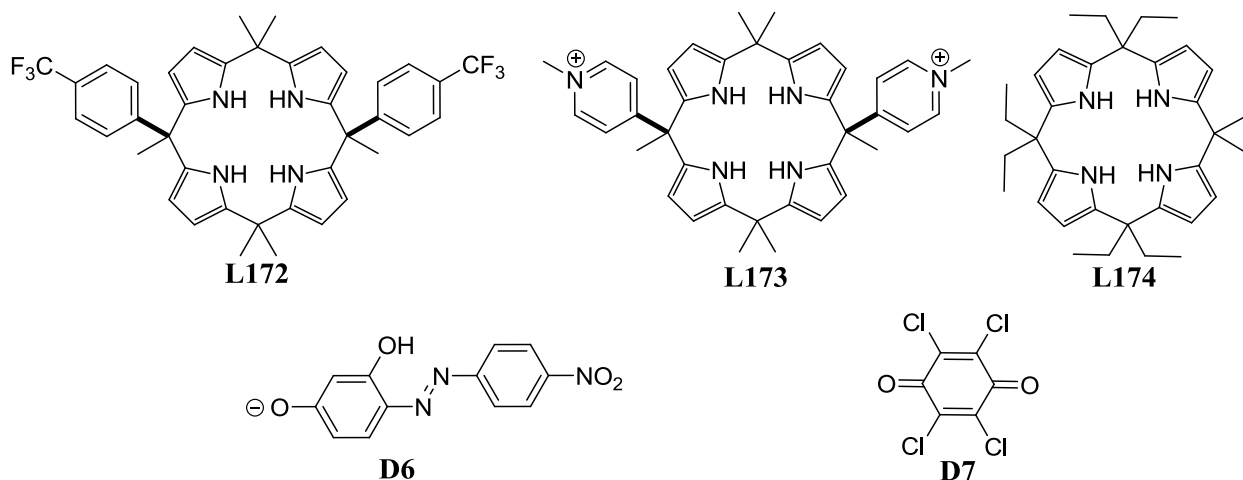
Figure 4.4 Schematic representation of displacement approach used for calix[4]pyrrole based anion receptors.

previously formed dye-calix[4]pyrrole complex dissociates to generate the naked dye (Figure 4.4). In 1999, Sessler and coworkers have reported that intense yellow color of the TBA-4-nitrophenolate (**D1**), in acetonitrile or dichloromethane solution, dissipates upon complex formation with **L72**. The complex may be used as a colorimetric sensor for halide ions, such as fluoride that displaces the phenolate ion, thereby restoring the yellow color, characteristic of free 4-nitrophenolate ion.³¹ Later, very few reports appear in the literature, following this approach.



The interaction of Brooker's merocyanine dye (**D2**), with **L72** was studied in acetonitrile, by Machado and coworkers. **D2** is violet in solution, but on interaction with **L72** changes the color of the solution due to the formation of **L72-D2** species associated through hydrogen bonding. A displacement assay was then carried out in the presence of different anions.³² It was found that fluoride, and to a lesser extent chloride and dihydrogen phosphate ions, displace **D2** through complex formation with **L72**. Few years later same group has reported, anion of 4-(4-

nitrobenzylideneamino)phenol (**D3**) can be used as a dye and act as naked dye detecting agent of fluoride ion in acetonitrile, when clubbed with **L72**, with a drastic color change from colorless to blue.³³ Lee and coworkers used a coumarin dye **D4** [2-oxo-4-(trifluoromethyl)-2H-chromen-7-olate] with various calix[4]pyrroles. When fluoride ion was added to **L172-D4** complex, a full reinstatement of the original indicator fluorescence was observed.³⁴ The **L172**-bound fluoride ion can be easily displaced by treatment with lithium ion resulting in reformation of the indicator complex and a complete quenching of the fluorescence. This switchable “off-on” operation was completely reversible and could be carried out through many repeated cycles. In 2012, using a dicationic calix[4]pyrrole, **L173** and **D4**, Lee and coworkers reported another highly selective fluorescent ‘turn-on’ system for pyrophosphate ion, in presence of water (30%).³⁵ The preference for the pyrophosphate ion is rationalized in terms of its ability to form a stronger complex with **L173**, owing to the combined effect of several favorable interactions, including electrostatic, anion- π and hydrogen bond interactions. Later they have employed **D6** and **L173**, as dye displacement method complex, for the selective detection of pyrophosphate ion in acetonitrile.³⁶ In 2003, Shao and coworkers showed that octamethylcalix[4]pyrrole, **L72** can form a charge

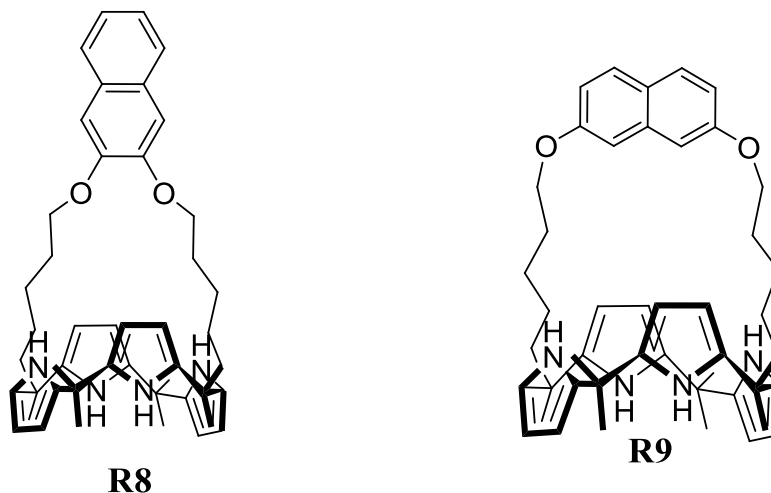


transfer complex with chloranil, in chloroform. This interaction is perturbed in the presence of fluoride and dihydrogenphosphate ions owing to complex formation of **L72** with anion.³⁷ Reversal of this anion induced complexation with **L72** can be performed, by adding water to the mixture, which regenerates the colored **L72-D7** charge transferred species. Few years later same group employed this principle with **L174-D7** assembly for the naked eye detection of some basic amino acids.³⁸ They found that the charge transfer process is hindered by the higher pH of the medium, pH less than 8 is adequate for the formation of this charge transfer complex. Based on

this principle, they could demonstrate that addition of basic amino acids namely; lysine and arginine change the color of the blue complex solution instantly to orange-yellow, whereas color change was not significant for the less basic histidine. This assembly also showed similar colorimetric changes in presence of aliphatic amino acids (e.g. ethylamine, diethylamine, triethylamine, propylamine etc.).

4.3 Research Goal

From the above discussion, we can understand the importance of the calix[4]pyrrole based chemosensors towards sensing of various anions. New developments for the selective recognition of anionic species still remain a challenge. We have noticed very few examples are there where fluorophore have been used as reporter and whenever they are used as a strapping moiety, generally the strap is linked through the '1,3-positions' of aryl moiety (1,3-type) of the reporter (**L131-132**, **L170-171**). As we have seen in the previous chapter that '1,2-type' linking of the strap possess unique structural features, when compared to '1,3 type'. Therefore, here we wish to check the response of fluorophore in '1,2-type' linkage towards anion binding event of



the calix[4]pyrrole moiety. To check the effect of fluorophore, we have synthesized **R8** with the closest fluorophoric homolog, from 2,3-dihydroxynaphthalene. To further check the effect of topological disposition of the fluorophore, we have also synthesized **R9** from 2,7-dihydroxynaphthalene. The two different types of spatial disposition of the reporting unit i.e. the naphthalene moiety may provide varying degree of selectivity towards anions, which further will be affected by the difference in the cavity size of their binding domains.

4.4 Results and Discussion

4.4.1 Synthesis and Characterization

Both the isomeric receptors **R8** and **R9** were synthesized following the slightly modified Lee's method we have used earlier towards the synthesis of **R3**, in the previous chapter (Figure 4.5). First dihydroxy compounds i.e. 2,3-dihydroxynaphthalene and 2,7-dihydroxynaphthalene were alkylated by 7-bromo-2-heptanone in acetone in presence of anhyd. potassium carbonate. The desired diketo compounds **R4** and **R5** were purified from the crude product by column chromatography with 78 and 84% of yields, respectively. The diketones were subsequently converted to respective bisdipyrromethanes **R6** and **R7** using excess pyrrole and TFA at 60 °C with moderate yields, 63 and 55% respectively. Finally, condensation of the bisdipyrromethanes in acetone using catalytic $\text{BF}_3 \cdot \text{etherate}$, we observed the formation of macrocycles after 10-15 min in TLC analysis. Purification of reaction mixtures using column chromatography and washing with methanol, led us to obtain only the *cis*-strapped calix[4]pyrroles **R8** and **R9** as off white powders in 11 and 6% yields, respectively. All the compounds including the desired macrocycle **R8** and **R9** were characterized by IR, ^1H and ^{13}C NMR spectroscopy, mass and

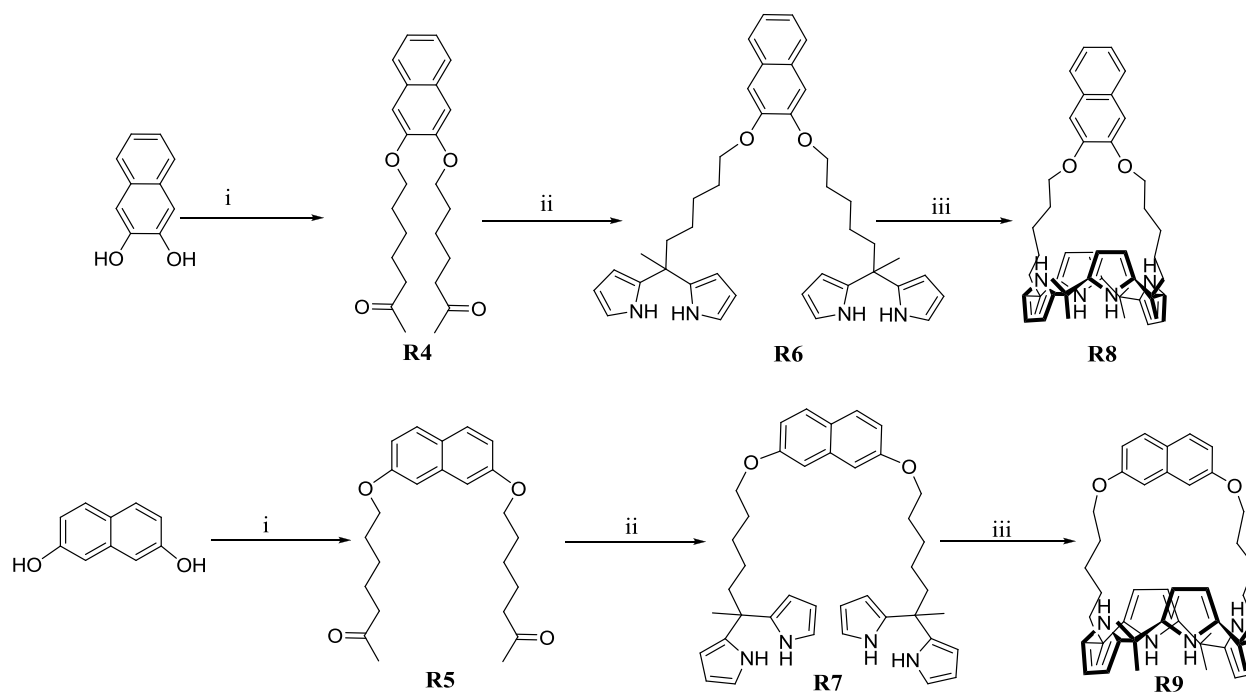


Figure 4.5 Synthetic schemes for **R8** and **R9**. i) 7-bromo-2-heptanone, K_2CO_3 , dry acetone, reflux; ii) pyrrole, TFA, 60 °C; iii) acetone, $\text{BF}_3 \cdot \text{OEt}_2$, R.T.

elemental analysis. ^1H NMR analysis in CDCl_3 of **R8** displayed NH-protons resonating at 7.66 ppm, which was slightly downfield shifted, compared to **R3** (7.42 ppm). Whereas, the corresponding signal for **R9**, was further shifted to downfield region (7.72 ppm). On the other hand, β -pyrrolic protons were upfield shifted for **R9** (5.73 ppm) as compared to **R8** (5.94 ppm). These values indicated the effect of different orientations of the aromatic fluorophore with respect to the calix[4]pyrrole core in the two receptors.

4.4.2 Anion Binding study

Preliminary solution phase anion binding behavior of both the receptors **R8** and **R9** were carried out by ^1H NMR titration studies in CD_3CN with various anions, including F^- and Cl^- as their tetrabutylammonium (TBA) salts and the study revealed that the binding follows a slow complexation-decomplexation process on the NMR time scale. Therefore, measurement of association constant by ^1H NMR spectroscopy was not possible. For both the receptors, it was found that one equivalent of anion was sufficient for the complete conversion of free receptor to their corresponding receptor anion complexes. Shifts for both pyrrolic-NH and β -CH signals were observed. For example, in case of **R8**, upon addition of one equivalent of TBAF in CD_3CN , NH and β -CH signals of pyrrole were shifted from 8.05 and 5.81 ppm to 12.9 and 5.5 ppm, respectively (Figure 4.6). We found that shift for pyrrolic-NH signal was up to 11.25 ppm, upon

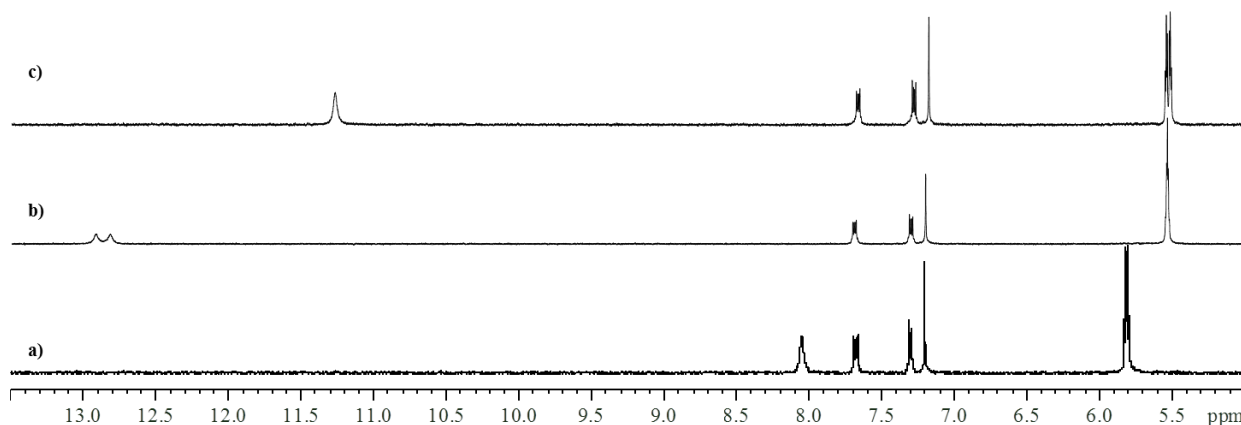


Figure 4.6 Partial ^1H -NMR spectra for a) **R8**; b) **R8** and one equivalent of TBAF; c) **R8** and one equivalent of TBACl in CD_3CN at 25 °C.

addition of one equivalent of TBACl, which is lesser than that in case of TBAF. These observed chemical shifts were indicative of the binding of the anions in the calix[4]pyrrole core through hydrogen bond interaction to pyrrolic-NHs. In both the cases, we did not observe any noticeable shift for the naphthalene-CH signals. In case of **R9**, the nature of the observed chemical shifts for

the pyrrolic-NH and β -CH signals was very similar (Figure 4.7). However, upon careful observation, we could notice an upfield shift for inner naphthalene-CH signal, which is higher for the larger chloride ion than the fluoride (from 7.11 to 7.34 ppm for fluoride and 7.50 ppm for chloride ion), which is indicative of relatively stronger interaction in case of chloride than

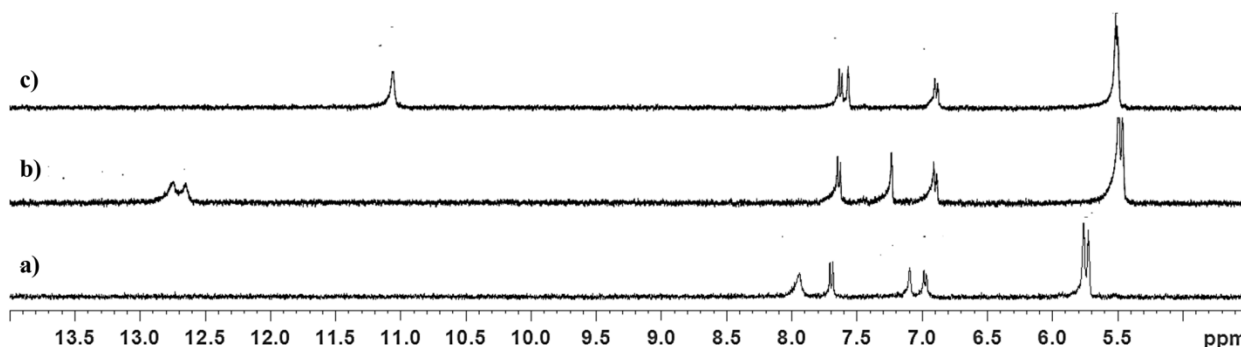


Figure 4.7 Partial ^1H -NMR spectra for a) **R9**; b) **R9** with one equivalent of TBAF; c) **R9** with one equivalent of TBACl in CD_3CN at 25 $^\circ\text{C}$.

fluoride ion. But as the other chemical shift values were similar for both the receptors and previously reported **R3**, we can expect similar kind of binding behavior from these two newly synthesized receptors. As fluorescence spectroscopy method is relatively much more sensitive

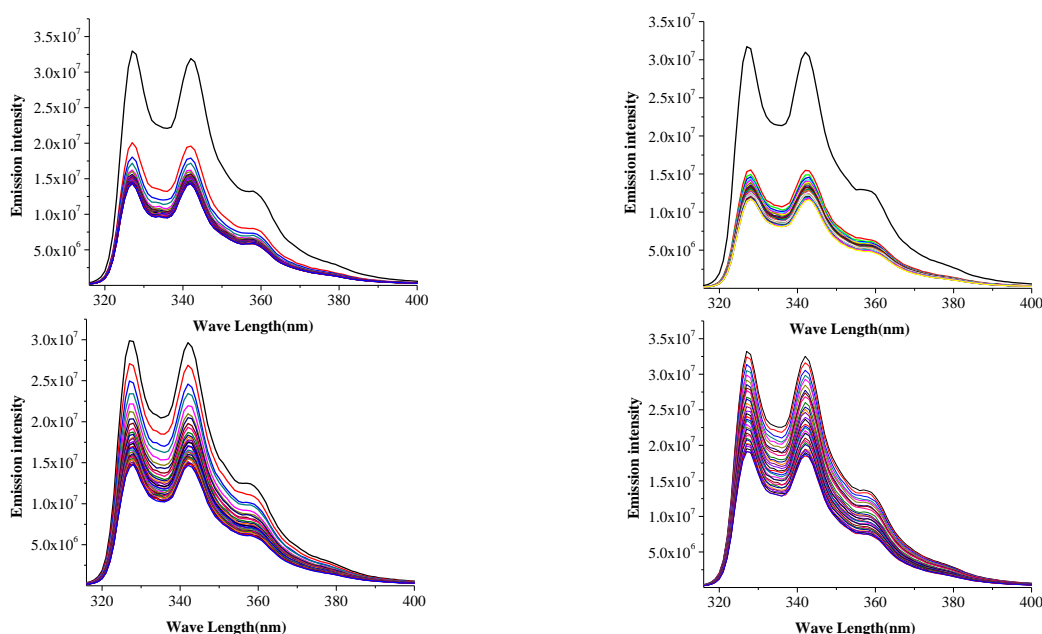


Figure 4.8 Fluorescence titration study of **R8** in CH_3CN (0.0276 mM) excited at 310 nm, showing the changes induced upon the addition of increasing quantities of TBAF (upper left), TBACl (upper right), TBABr (lower left) and TBAI (lower right).

than NMR spectroscopy method, in order to evaluate the reporting ability of the fluorophore toward the binding event, we investigated association of various anions by fluorescence quenching experiments with **R8** and **R9**. Fluorescence titration studies were carried out, by addition of solutions of anions as their tetrabutylammonium (TBA) salts to a $\sim 30 \mu\text{M}$ solution of receptors in acetonitrile. The anion screening experiment of **R8** showed an appreciable quenching upon addition of fluoride, chloride, bromide, cyanide, acetate and dihydrogenphosphate ions, whereas no significant quenching were observed upon addition of nitrate, nitrite, bisulphate and perchlorate ions. Quenching of fluorescence upon addition of anions suggested that the event of binding of anions to **R8** can be monitored by it. The intensity changes (Figure 4.8) display the extent of quenching in case of chloride ion is higher than that of fluoride ion. Further, quenching by bromide ion was much lesser than that of chloride ion (Figure 4.8). Whereas, in case of iodide ion, the observed quenching may be attributed to its

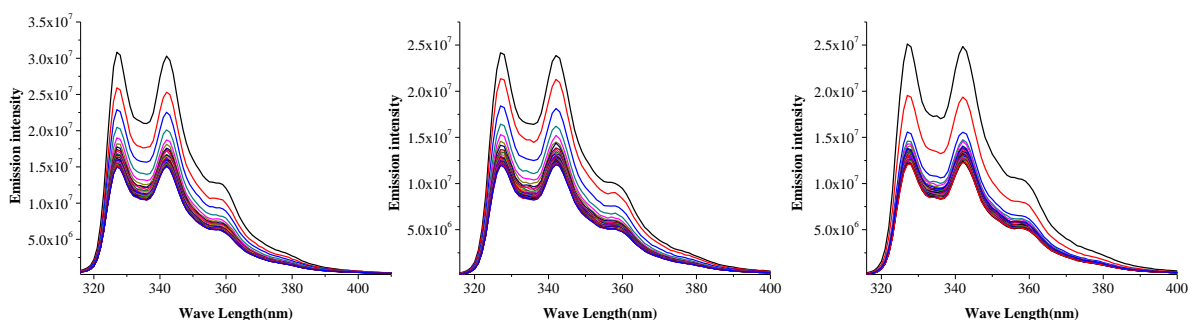


Figure 4.9 Fluorescence titration study of **R8** in CH_3CN (0.0276 mM) excited at 310 nm, showing the changes induced upon the addition of increasing quantities of TBACN (left), TBAH_2PO_4 (middle) and TBAOAc (right).

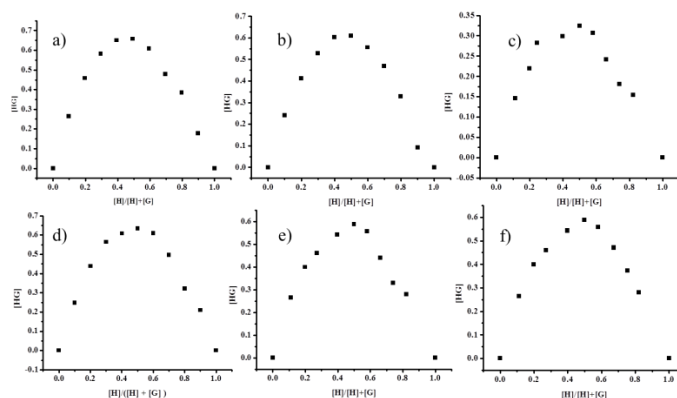


Figure 4.10 Job plot for complexation between **R8** and a) TBAF, b) TBACl, c) TBABr, d) TBACN, e) TBAH_2PO_4 , and f) TBAOAc, by fluorescence spectroscopy. The complex concentration, $[\text{HG}]$ was calculated by the equation $[\text{HG}] = \Delta I/I_0 \cdot [\text{H}]$.

heavy atom effect.³¹ For cyanide, dihydrogenphosphate and acetate ions, the degree of quenching observed was comparable with that in case of bromide ion (Figure 4.9). Job plot analysis revealed that binding stoichiometry is 1:1 in nature for all the bound anions (Figure 4.10).

Interestingly, in case of the receptor **R9**, significant quenching of fluorescence was observed upon addition of fluoride ion, additionally very weak quenching could be noticed upon addition of chloride ion only (Figure 4.11). No significant quenching was observed with any other tested anions. Job plot analysis confirms 1:1 binding stoichiometry for both the anions, upon complexation with **R9** (Figure 4.11). In Figure 4.12, we can see the quenching effect of various anions on **R8** and **R9** in CH₃CN. In order to confirm these fluorescence quenching were induced upon anion binding only, we have carried out control experiments with 2,3-dimethoxynaphthalene and all of the above bound anions and no noticeable quenching were observed. Association constants derived from these fluorescence quenching titrations experiments were tabulated in table 4.2 and a detailed inspection revealed strongest preference of **R8** (quenching response) towards chloride ion compared to other studied anions, including

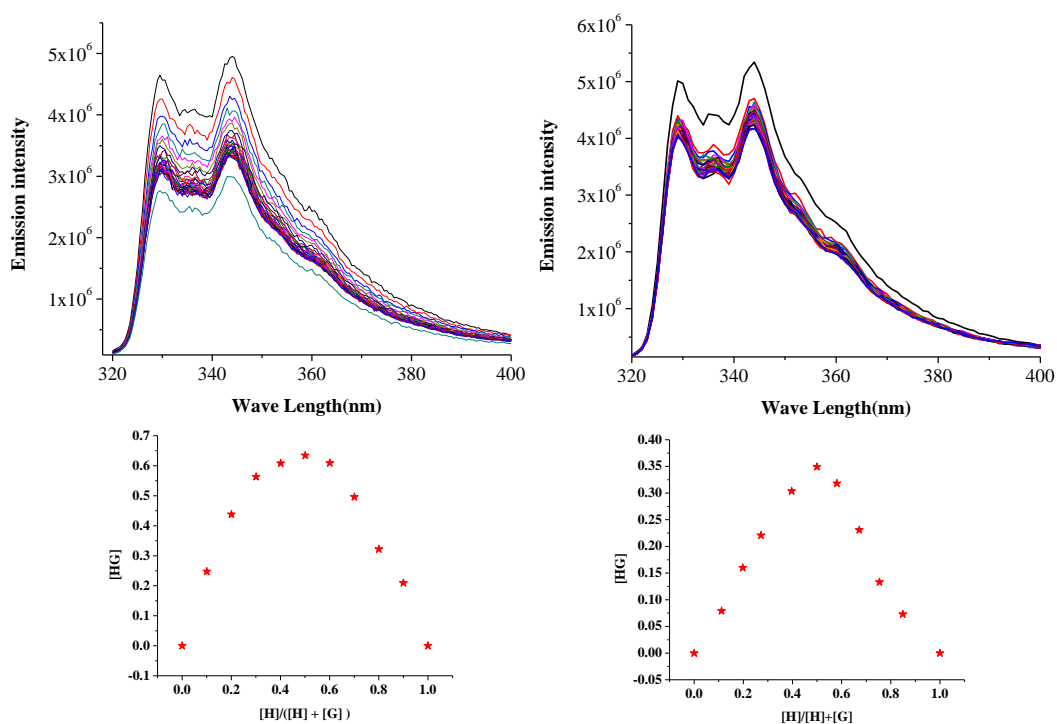


Figure 4.11 Fluorescence titration study of **R9** in CH₃CN (0.0305 mM) excited at 316 nm, showing the changes induced upon the addition of increasing quantities of TBAF (top left) and TBACl (top right); Job plot for complexation between **R9** and TBAF (bottom left) and TBACl (bottom right).

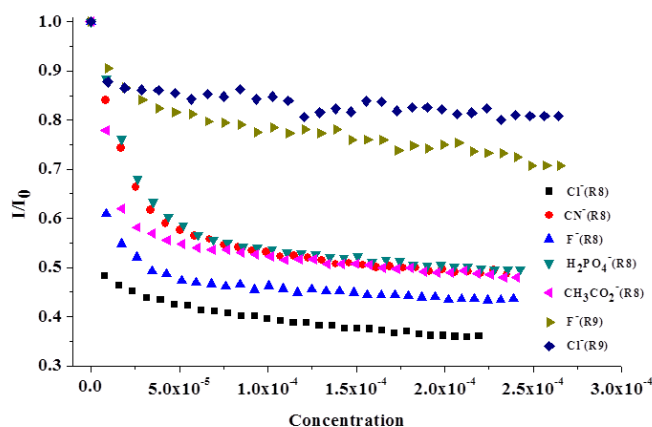


Figure 4.12 The quenching effect of various anions on **R8** and **R9** in CH_3CN .

Table 4.2 K_a (M^{-1}) for the interaction of **R8** and **R9** with different anions in CH_3CN at 303 K determined by fluorescence study.⁴⁰

Anion	F^-	Cl^-	Br^-	CN^-	H_2PO_4^-	CH_3COO^-
R8	2.42×10^5	2.28×10^6	2.92×10^4	6.31×10^4	5.30×10^4	1.21×10^5
R9	4.60×10^4	7.20×10^2	a	a	a	a

^a Binding constants could not be evaluated; all the anions used as their TBA salts.

fluoride ion. The association constant (K_a) for compound **R8** towards chloride ion is about one order higher compared to fluoride ion and K_a decreases in the order: $\text{CH}_3\text{COO}^- > \text{CN}^- > \text{H}_2\text{PO}_4^- > \text{Br}^-$. This type of chloride selectivity over fluoride is hitherto not reported in calixpyrrole chemistry and is also a rare phenomenon in host–guest chemistry.⁴¹ Interestingly, in the case of receptor **R8**, K_a for fluoride ion appears one order less than that observed for the very closely related **R3** under identical conditions.⁴² However, the fluorescence quenching study of **R9** displays maximum quenching by fluoride with K_a about two orders higher than that observed for the chloride ion, albeit weakly (table 4.2).

To check the rightfulness of these measured association constants we have performed, isothermal titration calorimetry (ITC) for various anions. For fluoride ion, we have measured the binding constants in neat acetonitrile and acetonitrile containing 0.5% water, and in both cases we can found association constants were quite similar (Figure 4.14) and in both the cases, the binding processes are exothermic in nature. Addition of water only diminishes the affinity for the fluoride ion, probably owing to greater hydration of the fluoride ion in presence of water. The

ITC analysis of chloride and bromide ions revealed both binding processes were exothermic in nature (Figure 4.15). For pseudo-halide cyanide ion and oxo-anions acetate and dihydrogenphosphate, we found similar exothermic heat changes (Figure 4.16).

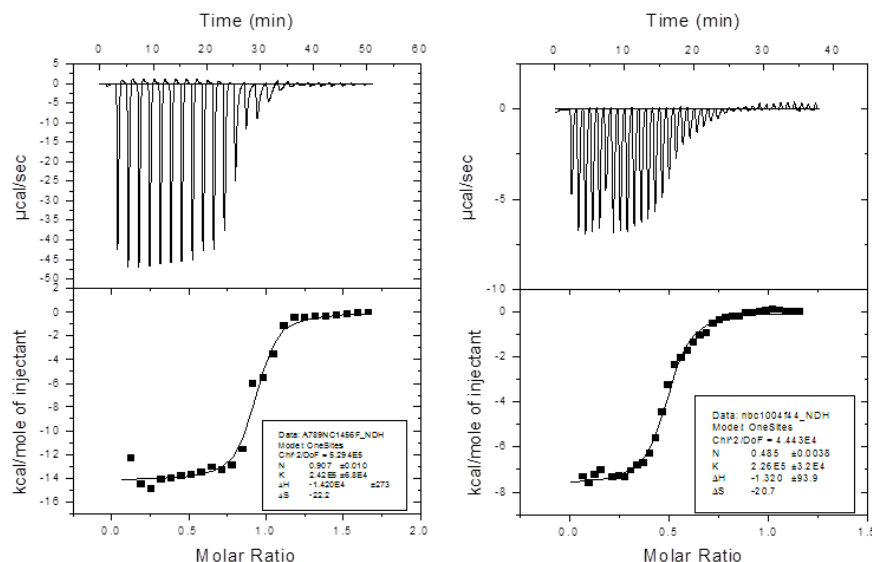


Figure 4.14 Isothermal calorimetric titrations measured at 303 K upon addition of TBAF into the solution of **R8**; measurement was carried out left: in acetonitrile, right: in 0.5% water-acetonitrile

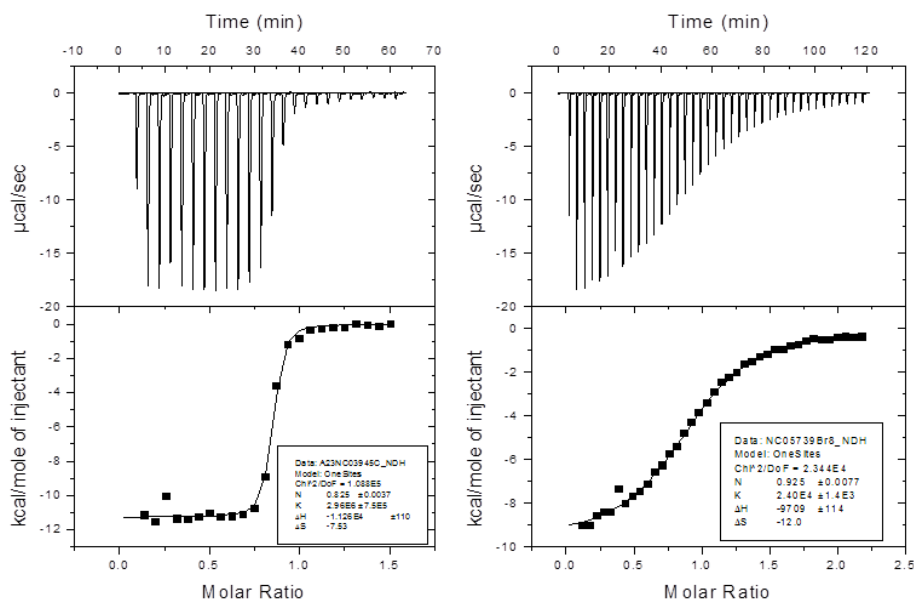


Figure 4.15 Isothermal calorimetric titrations measured at 303 K upon addition of TBACl (left) and TBABr (right) into the solution of **R8** in acetonitrile.

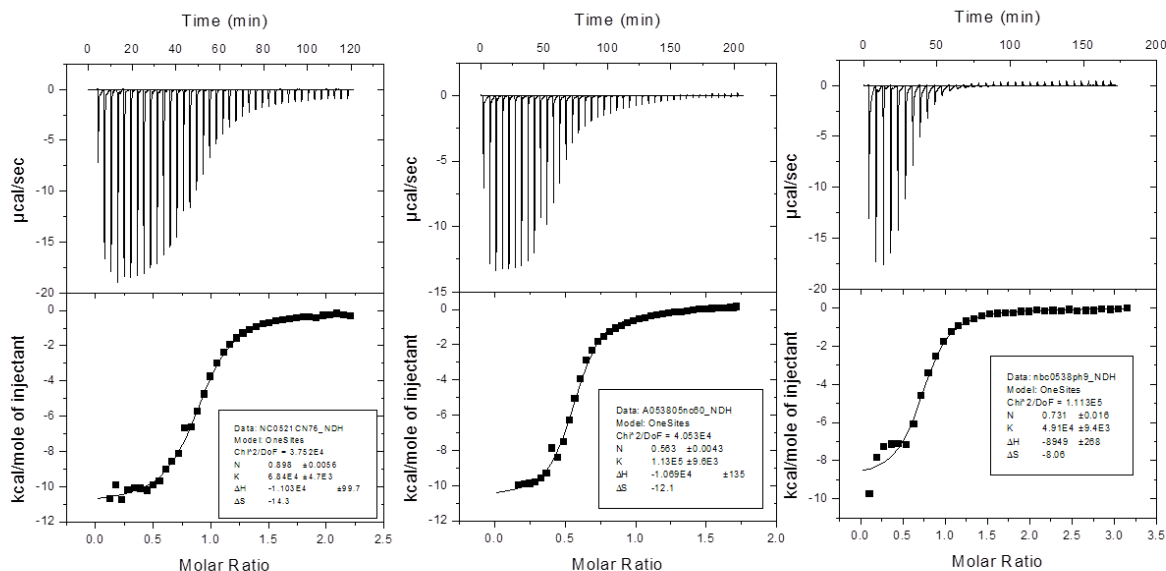


Figure 4.16 Isothermal calorimetric titrations measured at 303 K upon addition of TBACN (left), TBACl (middle) and TBAH_2PO_4 (right) into the solution of **R8** in acetonitrile.

ITC experiment for **R9** showed that it can bind to bromide, cyanide, acetate, dihydrogenphosphate ions (display no fluorescence quenching) along with fluoride and chloride ions. All the binding processes were exothermic in nature (Figure 4.16 and 4.17).

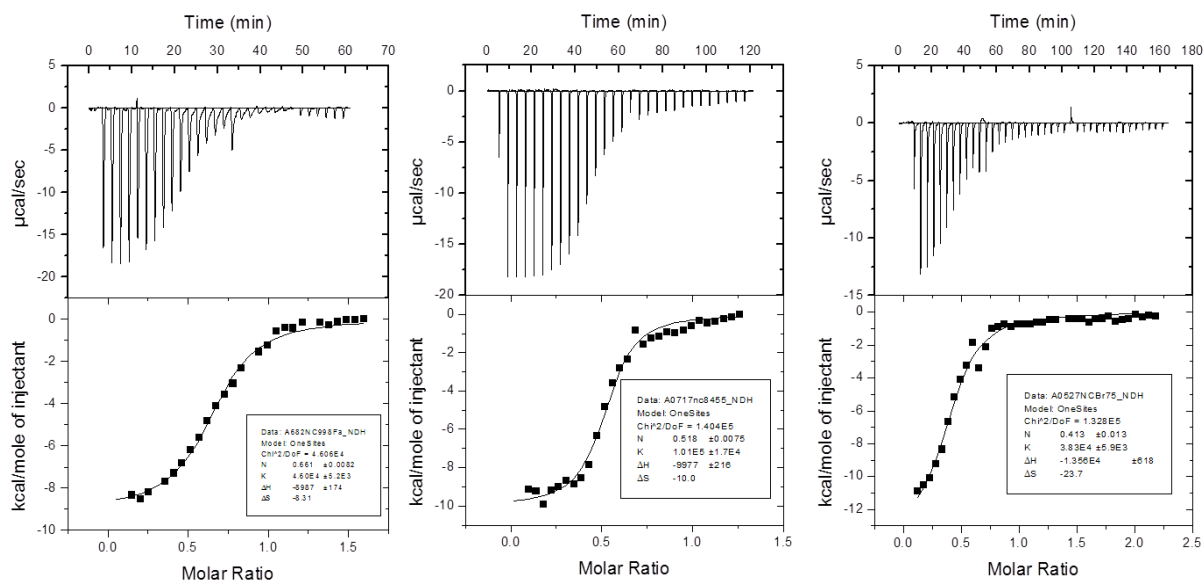


Figure 4.17 Isothermal calorimetric titrations measured at 303 K upon addition of TBAF (left), TBACl (middle) and TBABr (right) into the solution of **R9** in acetonitrile.

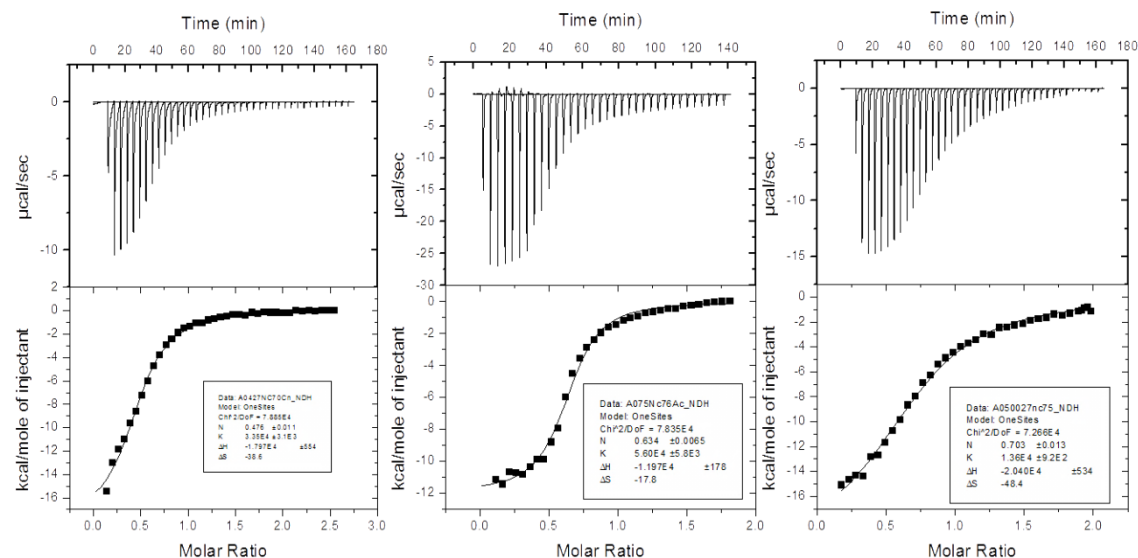


Figure 4.18 Isothermal calorimetric titrations measured at 303 K upon addition of TBACN (left), TBAOAc (middle) and TBAH₂PO₄ (right) into the solution of **R9** in acetonitrile.

Table 4.3 Thermodynamic data derived from isothermal titration calorimetry (ITC) for the interaction of receptors **R8** and **R9** with TBA salts of anions, at 303K in CH₃CN (^a CH₃CN + 0.5 % H₂O).

	Anion	K _a (M ⁻¹)	ΔH (kcal/mol)	TΔS (kcal/mol)	ΔG (kcal/mol)
R8	F ⁻	2.26 × 10 ^{5a}	-13.20	-6.272	-6.928
		2.42 × 10 ⁵	-14.20	-6.507	-7.473
	Cl ⁻	2.96 × 10 ⁶	-11.26	-2.292	-8.968
	Br ⁻	2.40 × 10 ⁴	-9.709	-0.012	-6.073
	CN ⁻	6.84 × 10 ⁴	-11.03	-4.333	-6.697
	H ₂ PO ₄ ⁻	4.91 × 10 ⁴	-8.949	-2.442	-6.507
R9	CH ₃ COO ⁻	1.13 × 10 ⁵	-10.69	-0.0121	-7.0237
	F ⁻	4.20 × 10 ⁴	-8.987	-2.518	-6.577
	Cl ⁻	1.01 × 10 ⁵	-9.977	-3.030	-6.947
	Br ⁻	3.38 × 10 ⁴	-13.56	-7.181	-6.379
	CN ⁻	3.35 × 10 ⁴	-17.97	-11.696	-6.274
	H ₂ PO ₄ ⁻	1.36 × 10 ⁴	-20.40	-14.665	-5.735
	CH ₃ COO ⁻	5.60 × 10 ⁴	-11.97	-5.393	-6.577

From the table 4.3, we can see that all the binding events are thermodynamically favored. For **R8** we can see that enthalpy and entropy contributions are having an antiparallel effect. Association constants were found to be almost similar, derived from both methods (comparing table 4.2 and table 4.3), proving that naphthalene unit acting as fluorescence reporter for the anion binding to calix[4]pyrrole core. In case of **R9**, we found that association constants derived from both the methods, matching only for fluoride ion. For the chloride ion association constant obtained from ITC study, found one order higher than that of fluoride, whereas from fluorescence quenching experiment, the association constant, was found two orders lesser for chloride ion. For some of the non-interactive anions (i.e. bromide, cyanide, acetate and dihydrogenphosphate ions), we could find reasonable association constants from ITC experiments (Table 4.3). As sizes increased for the bound anions, we can observe higher amount of changes in enthalpy and entropy, from which we can presume that binding processes were

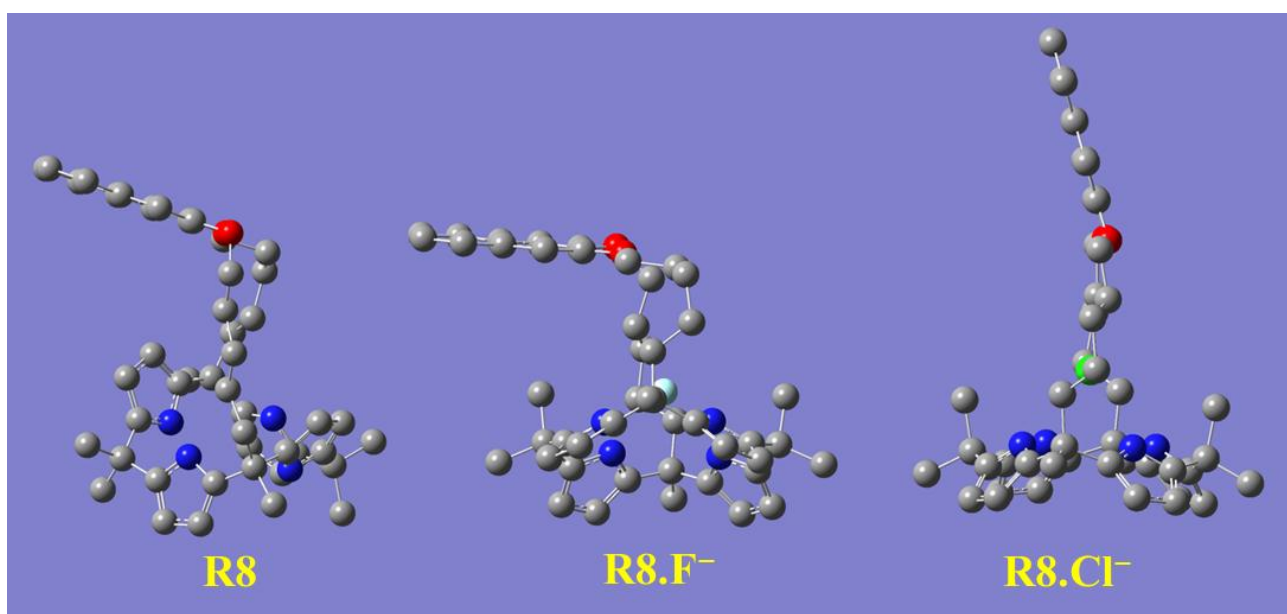


Figure 4.19 DFT minimized structures of **R8**, along with their fluoride and chloride complexes. Color code: red: O, blue: N, grey: C, dark green: Cl, and bluish green: F.

accompanied with large amount of conformational changes for the receptors **R9**. To investigate the discrepancies in association constants, we performed DTF calculation for the receptors **R8** and **R9**, along with their fluoride and chloride ion complexes. Interestingly, the DFT minimized structures showed a tilted disposition for the naphthalene moiety upon binding to fluoride ion, whereas a perpendicular disposition was observed for the chloride ion complex for **R8** (Figure 4.19), as found in case **R3.F⁻** and **R3.Cl⁻** (chapter 3), where the benzene moiety stays almost

perpendicular to the calix[4]pyrrole core in both the cases. Therefore, we presumed that perpendicular disposition of the aromatic moiety in the strap encourage better electronic communication between the aromatic unit and the anion. In our case, the bulkier chloride ion could have effective interaction with the fluorophore (greater quenching), leading it to assume the orthogonal disposition with regard to the calix[4]pyrrole moiety, whereas the relatively smaller fluoride ion could not induce strong interaction with the fluorophore and probably due to the resultant conformation change the calix[4]pyrrole undergoes upon anion binding, resulted in more tilting of the bulky naphthalene moiety and hence displayed reduced anion affinity. On the other hand, for **R9** it was observed that whole strap along with the naphthalene unit remains in a much tilted position, and upon binding to anions, the strap comes to a more perpendicular position, however naphthalene unit remains in a tilted position (Figure 4.20). It was also observed that as size of the anion increases naphthalene unit assumed a more parallel orientation with respect to calix[4]pyrrole core. From the table 4.4, it was perceived that for **R9** as the size of anion increases, anions binds in an unsymmetrical manner to calix[4]pyrrole core, which may be due to the steric hindrance generated from the naphthalene unit in the strap.

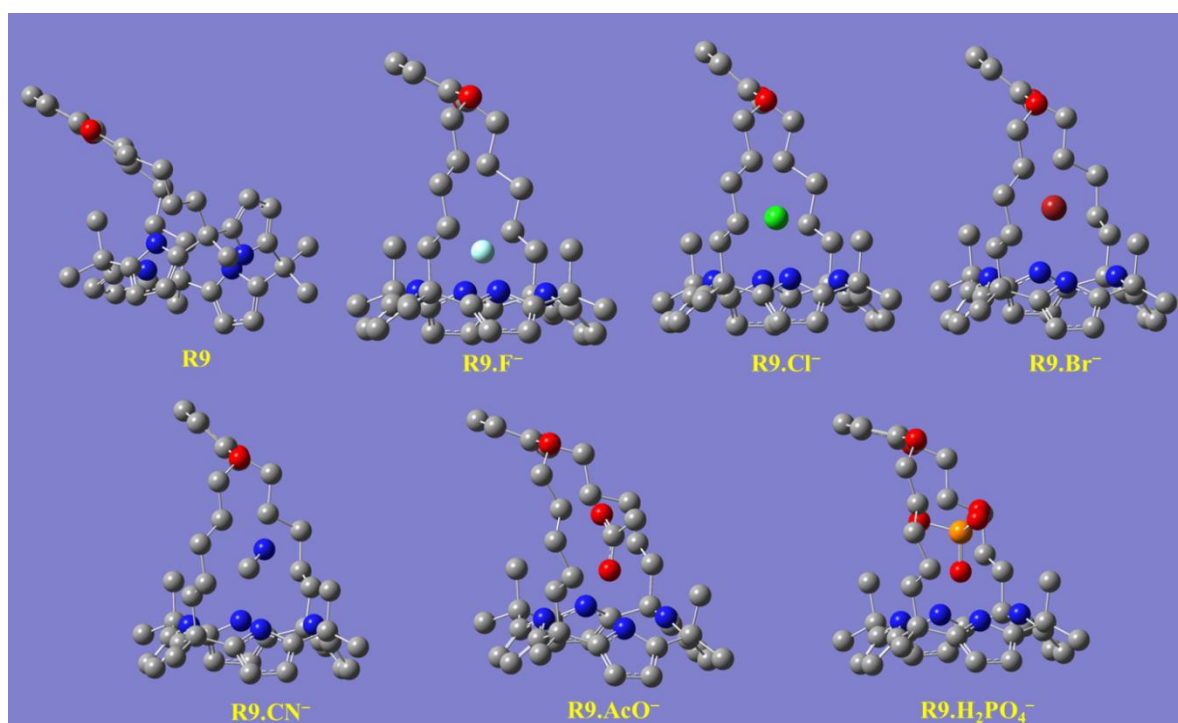


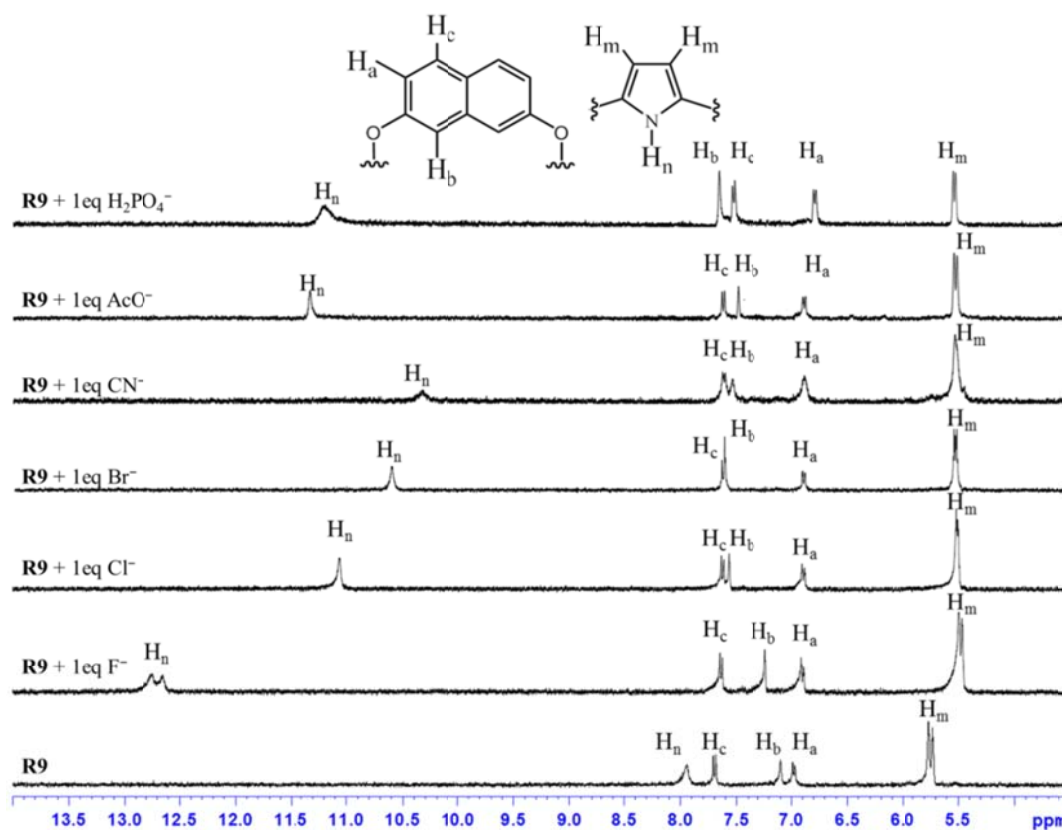
Figure 4.20 DFT minimized structures of **R9**, along with its F^- , Cl^- , Br^- , CN^- , AcO^- and H_2PO_4^- complexes. Color code: red: O, blue: N, grey: C, bluish green: F, dark green: Cl, cherry red: Br, and orange: P.

Table 4.4 Distance of anion from all pyrrole-NHs (obtained from DFT minimized structure).

NH...X (D values, Å)	R8.F ⁻	R8.Cl ⁻	R9.F ⁻	R9.Cl ⁻	R9.Br ⁻	R9.CN ^{-a}	R9-AcO ^{-b}	R9-H ₂ PO ₄ ^{-b}
	2.77	3.32	2.73	3.35	3.55	3.16	2.89	2.88
	2.76	3.28	2.74	3.36	3.53	3.15	2.93	2.97
	2.77	3.28	2.73	3.36	3.55	3.37	3.09	3.03
	2.74	3.29	2.74	3.35	3.56	3.38	3.03	3.95

^a distance measured from anionic oxygen atom. ^b distance measured from anionic carbon atom.

To check the interaction of various anions with the inner aromatic-CH of the naphthalene in ¹H NMR, one equivalent of various anions in acetonitrile-d₃ were added to a solution of **R9** in acetonitrile-d₃. In support of our presumption, stronger downfield shifts, (0.3–0.6 ppm) depending on their proximity to the anions were observed for the inner aromatic-CH of the naphthalene (H_b) (Figure 4.21). For example, fluoride being the smallest in size exerts a very minimal downfield shift compared to the larger dihydrogenphosphate ion, where the inner CH protons (H_b) comes closer to the anion, thereby enhancing the hydrogen bonding interaction.

**Figure 4.21** Changes in ¹H NMR spectrum of **R9** after addition one equivalent of various anions in CD₃CN (partial ¹H-NMR spectra only shown).

From the above association constants and DFT minimized structures, we have proposed a model, which may be able to explain the possible reason for these different kinds of binding behavior of these two receptors **R8** and **R9**. When inspected carefully, one can find the most striking difference between the two receptors, are the two inner aromatic hydrogen atoms in **R9**, pointing towards the calix[4]pyrrole core. The receptor **R8** displays higher association constant for the chloride ion, owing to the perpendicular disposition of naphthalene unit, while in case of fluoride ion, naphthalene unit remains parallel to the calix[4]pyrrole core. On the other hand, in case of **R9**, inner aromatic hydrogens of naphthalene interact with anions and as a result for smaller anions residing somewhat tilted with respect to calix[4]pyrrole core. However, when anions were large, the interaction with these hydrogens were much stronger, as a result of which,

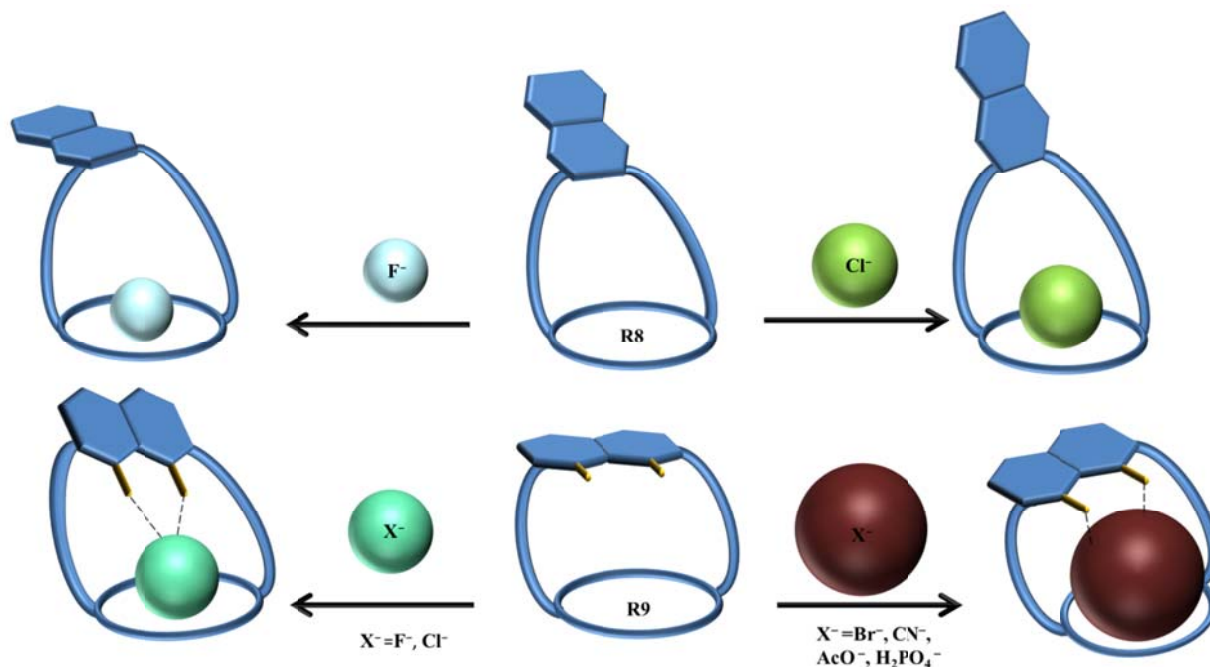


Figure 4.22 Plausible binding modes of different anions for **R8** and **R9**.

naphthalene moiety become tilted to make room for the anion (Figure 4.22). However, the tilting away of the fluorophore probably negates anion–fluorophore interaction and hence the observation of resultant lack of quenching in emission. Chloride seems to be an intermediate case, which probably interacts weakly with the fluorophore and relatively strongly with the calix[4]pyrrole with an overall higher K_a (from ITC). The greater overall affinity for chloride is again supported by enthalpy driven complexation of chloride ion for both the receptors leading to maximum stabilization in ΔG (table 4.3).

4.5 Conclusion

In conclusion, we have designed and synthesized two new isomeric fluorescent strapped calix[4]pyrroles, **R8** and **R9**, containing naphthalene unit as the reporter, in the strap. **R8** is a successful homolog for **R3** which is capable of binding various anions in organic media and the binding processes can be easily monitored by quenching of fluorescence. Higher binding affinity for chloride over fluoride ion is a first of its kind report for this class of receptors. Unique binding behavior of **R9** could lead us to a new way of modifying this class of receptors; where by modulating the spatial disposition of the strap one can tune the receptor-anion interaction.

4.6 Experimental Details

4.6.1.1 Synthesis of **R4**

A mixture of 2,3-dihydroxynaphthalene (480 mg; 3 mmol) and K_2CO_3 (4.14 g; 30 mmol) in acetone (100 mL) was stirred well for about 1 h, and then 7-bromo-2-heptanone (2.89 g; 15 mmol) was added. The mixture was refluxed for 3 days, cooled, filtered and solvent was removed. The crude product was purified by column chromatography over silica gel with increasing ratio of ethyl acetate in hexane. The excess bromoketone is removed first (15 % ethyl acetate in hexane) and the desired product was collected as the next major band and vacuum dried to obtain compound **R4** as a white solid (900 mg; 78 %). Melting point: 76.4 °C; IR(neat): ν (cm^{-1}) 2939.78-2860.69, 1714.87; 1H NMR ($CDCl_3$): δ in ppm 7.65 (m, 2H), 7.31 (m, 2H), 7.10 (s, 2H), 4.10 (t, 4H, $J = 6.4$ Hz), 2.49 (t, 4H, $J = 7.6$ Hz), 2.15 (s, 6H), 1.91 (m, 4H), 1.69 (m, 4H); ^{13}C NMR ($CDCl_3$): δ in ppm 209.11, 149.35, 129.35, 126.35, 108.00, 68.60, 43.75, 30.06, 29.04, 25.82, 23.67. LCMS m/z , $M+H$: 385.5 (calculated for $C_{24}H_{33}O_4 = 385.24$). Elemental analysis for $C_{24}H_{32}O_4$: calcd. C, 74.97; H, 8.39; found: C, 74.84; H, 8.41.

4.6.1.2 Synthesis of **R5**

A mixture of 2,7-dihydroxynaphthalene (480 mg; 3 mmol) and K_2CO_3 (4.14 g; 30 mmol) in acetone (100 mL) was stirred well for about 1 h, and then 7-bromo-2-heptanone (2.89 g; 15 mmol) was added. The mixture was refluxed for 3 days and then filtered and solvent was removed. The crude product was purified by column chromatography over silica gel with increasing ratio of ethyl acetate in hexane. The excess bromoketone is removed first (15 % ethyl acetate in hexane) and the desired product was collected as the next major band and vacuum

dried to yield compound **R5** as a white solid (970 mg; 84 %). Melting point: 61.8 °C; IR (neat): ν (cm^{-1}) 2939.78-2860.69, 1714.87; ^1H NMR (CDCl_3): δ in ppm 7.63 (d, 2H, $J = 9.2$ Hz), 7.01 (s, 2H), 6.98-6.95 (m, 2H), 4.06 (t, 4H, $J = 6.4$ Hz), 2.49 (t, 4H, $J = 7.2$ Hz), 2.15 (s, 6H), 1.85 (m, 4H), 1.67 (m, 4H), 1.51 (m, 4H); ^{13}C NMR (CDCl_3): 209.12, 157.62, 136.00, 129.13, 124.23, 116.29, 106.05, 67.06, 43.66, 30.02, 29.14, 25.80, 23.58. LCMS m/z , $M+H$: 385.5 (calculated for $\text{C}_{24}\text{H}_{33}\text{O}_4 = 385.24$). Elemental analysis for $\text{C}_{24}\text{H}_{32}\text{O}_4$: calcd. C, 74.97; H, 8.39; found: C, 74.84; H, 8.40.

4.6.1.3 Synthesis of R6

To a mixture of **R4** (746 mg; 1.94 mmol) and pyrrole (5.4 mL; 78 mmol), trifluoroacetic acid (150 μL ; 1.94 mmol) was added at about 60 °C and the reaction mixture was stirred for about 4 h at this temperature. Then reaction was quenched with triethylamine (1mL). Excess reagents were removed under reduced pressure to get the crude product, which was purified by column chromatography over silica gel (10 % ethyl acetate in hexane) to obtain the pure product **R6** (750 mg, 63 %). IR (neat): ν (cm^{-1}) 3391.16, 2932.06-2858.76, 1715; ^1H NMR (CDCl_3): δ in ppm 7.79 (br s, 4H), 7.65 (m, 2H), 7.3 (m, 2H), 7.09 (s, 2H), 6.59 (s, 4H), 6.09 (d, 8H, $J = 18$ Hz), 4.05 (t, 4H, $J = 6.2$ Hz), 1.99 (m, 4H), 1.85 (m, 4H), 1.58 (s, 6H), 1.50 (m, 4H), 1.28 (m, 4H); ^{13}C NMR (CDCl_3): δ in ppm 149.43, 138.27, 129.37, 126.36, 124.14, 117.08, 107.83, 104.63, 68.85, 51.03, 41.29, 39.22, 29.03, 26.52, 24.31. LCMS m/z , $M+H$: 617.7 (calculated for $\text{C}_{40}\text{H}_{48}\text{N}_4\text{O}_2 = 617.38$). Elemental analysis for $\text{C}_{40}\text{H}_{48}\text{N}_4\text{O}_2$: calcd. C, 77.89; H, 7.84; N, 9.08.; found: C, 77.95; H, 7.76; N, 8.96.

4.6.1.4 Synthesis of R7

To a mixture of **R5** (746 mg; 1.94 mmol) and pyrrole (5.4 mL; 78 mmol), trifluoroacetic acid (150 μL ; 1.94 mmol) was added at about 60 °C and the reaction mixture was stirred for about 4 h at this temperature. Then reaction was quenched with triethylamine (1 mL). Excess reagents were removed under reduced pressure to get the crude product, which was purified by column chromatography over silica gel (10 % ethyl acetate in hexane) to obtain the pure product **R7** (665 mg; 55 %). IR (neat): ν (cm^{-1}) 3391.16, 2932.06-2858.76, 1715; ^1H NMR (CDCl_3): δ in ppm 7.71 (br s, 4H), 7.63 (d, 2H, $J = 8.8$), 6.98 (m, 4H), 6.60 (s, 4H), 6.13 (m, 8H), 4.01 (t, 4H, $J = 6.4$), 2.02 (m, 4H), 1.81 (m, 4H), 1.59 (s, 6H), 1.48 (m, 4H), 1.28 (m, 4H); ^{13}C NMR (CDCl_3):

δ in ppm 157.60, 138.15, 136.00, 129.07, 124.23, 117.01, 116.26, 107.68, 106.04, 67.88, 41.17, 39.04, 29.20, 26.64, 26.31, 24.28. LCMS m/z , M+H: 617.7 (calculated for $C_{40}H_{48}N_4O_2 = 617.38$). Elemental analysis for $C_{40}H_{48}N_4O_2$: calcd. C, 77.89; H, 7.84; N, 9.08; found: C, 77.75; H, 7.76; N, 9.15.

4.6.1.5 Synthesis of **R8**

To a solution of **R6** (814 mg; 1.32 mmol) and acetone (150 mL), $BF_3 \cdot OEt_2$ (1 μ L; 0.38 mmol) was added. The solution was stirred at room temperature for 15 min, after which product formation was confirmed by TLC. The reaction was quenched by triethylamine (1 mL) and solvent was removed. The crude mass was subjected to column chromatography over silica gel (10 % ethyl acetate in hexane) to obtain the product as a colored species, which upon subsequent washing with methanol yielded the pure macrocycle **R8** as an off white powder (106 mg; 11 %). Melting point: 178 °C (decomp.); 1H NMR ($CDCl_3$): δ in ppm 7.66 (br s, 4H), 7.31 (m, 2H), 7.10 (s, 2H), 5.94 (s, 8H), 4.09 (t, 4H, $J = 6$ Hz), 1.92 (m, 8H), 1.67 (m, 8H), 1.52 (m, 12H), 1.26 (m, 4H); ^{13}C NMR ($CDCl_3$): δ in ppm 149.46, 137.86, 137.21, 129.43, 126.40, 124.18, 108.16, 104.30, 103.69, 68.65, 41.35, 39.53, 35.62, 30.21, 29.21, 28.26, 26.66, 25.17. LCMS m/z , M+H: 697.75 (calculated for $C_{46}H_{56}N_4O_2 = 697.44$). Elemental analysis for $C_{46}H_{56}N_4O_2 \cdot 2CH_3OH$: calcd. C, 75.75; H, 8.48; N, 7.36; found: C, 75.68; H, 8.55; N, 7.31.

4.6.1.6 Synthesis of **R9**

To a solution of **R7** (1.16 g; 2.64 mmol) and acetone (300 mL), $BF_3 \cdot OEt_2$ (5 μ L; 0.04 mmol) was added. The solution was stirred at room temperature for 10 min, after which product formation was confirmed by TLC. The reaction was quenched by triethylamine (1 mL) and solvent was removed. The crude mass was subjected to column chromatography over silica gel (10 % ethyl acetate in hexane) to obtain the product as a colored species, which upon subsequent washing with methanol yielded the pure macrocycle **R9** as an off white powder (78 mg, 6 %). Melting point: 172 °C (decomp.); 1H NMR ($CDCl_3$): δ in ppm 7.71 (d, 2H, $J = 9.2$ Hz), 7.17 (s, 2H), 7.11 (s, 4H), 7.04 (d, 2H, $J = 8.8$ Hz), 5.78 (d, 8H, $J = 27.2$ Hz), 4.20 (t, 4H, $J = 6.8$ Hz), 1.86 (m, 8H), 1.47 (s, 6H), 1.42 (s, 6H), 1.37 (s, 6H), 1.25 (m, 4H); ^{13}C NMR ($CDCl_3$): δ in ppm 157.64, 138.42, 136.93, 136.22, 129.44, 124.66, 116.76, 107.11, 104.01, 102.94, 67.47, 41.76, 39.30, 35.47, 31.00, 29.85, 28.09, 25.09, 23.98. LCMS m/z , M+H: 697.75 (calculated for

$C_{46}H_{56}N_4O_2 = 697.44$). Elemental analysis for $C_{46}H_{56}N_4O_2$: calcd. C, 79.27; H, 8.10; N, 8.04; found: C, 79.21; H, 8.31; N, 8.09.

4.7 References:

1. Lehn, J. M. *Supramolecular Chemistry*; VCH: Weinheim, 1995.
2. Desvergne, J. P.; Czarnik, A. W. *Chemosensors for Ion and Molecule Recognition*; NATO Asi Series, Series C; Kluwer Academic Publishers: London, 1997.
3. Löhr, H. -G.; Vögtle, F. *Acc. Chem. Res.* **1985**, *18*, 65.
4. Takagi, M.; Ueno, K. *Top. Curr. Chem.* **1984**, *121*, 39.
5. Czarnik, A. W. *Acc. Chem. Res.* **1994**, *27*, 302.
6. Beer, P. D. *Chem. Commun.* **1996**, 689.
7. Beer, P. D. *Coord. Chem. Rev.* **2000**, *205*, 131.
8. Bissell, R. A.; de Silva, P.; Gunaratne, H. Q. N.; Lynch, P. L. M.; Maguire, G. E. M.; Sandanayake, K. R. A. S. *Chem. Soc. Rev.* **1992**, *21*, 187.
9. (a) Nielsen, K. A.; Bähring, S.; Jeppesen, J. O. *Chem. Eur. J.* **2011**, *17*, 11001. (b) Bähring, S.; Olsen, G.; Stein, P. C.; Kongsted, J.; Nielsen, K. A. *Chem. Eur. J.* **2013**, *19*, 2768. (c) Wiskur, S. L.; Ait-Haddou, H.; Lavigne, J. J.; Anslyn, E. V. *Acc. Chem. Res.* **2001**, *34*, 963.
10. Chae, M. -Y.; Czarnik, A. W. *J. Am. Chem. Soc.* **1992**, *114*, 9704.
11. Dujols, V.; Ford, F.; Czarnik, A. W. *J. Am. Chem. Soc.* **1997**, *119*, 7386.
12. de Silva, P.; Gunaratne, H. Q. N.; Gunnlaugsson, T.; Huxley, A. J. M.; McCoy, C. P.; Rademacher, J. T.; Rice, T. E. *Chem. Rev.* **1997**, *97*, 1515.
13. Miyaji, H.; Anzenbacher Jr, P.; Sessler, J. L.; Bleasdale, E. R.; Gale, P.A. *Chem. Commun.*, **1999**, 1723.
14. (a) Miyaji, H.; Sato, W.; Sessler, J. L.; Lynch, V. M. *Tetrahedron Lett.* **2000**, *41*, 1369. (b) Miyaji, H.; Sato, W.; Sessler, J. L.; Lynch, V. M. *Angew. Chem. Int. Ed.* **2000**, *39*, 1777.
15. Nishiyabu, R.; Anzenbacher, Jr., P. *J. Am. Chem. Soc.* **2005**, *127*, 8270.
16. Nishiyabu, R.; Anzenbacher, Jr., P. *Org. Lett.* **2006**, *8*, 359.
17. Gu, R.; Depraetere, S.; Kotek, J.; Budka, J.; Wagner-Wysiecka, E.; Biernat, J. F.; Dehaen, W. *Org. Biomol. Chem.* **2005**, *3*, 2921.

18. Nishiyabu, R.; Palacios, M. A.; Dehaen, W.; Anzenbacher, Jr. P. *J. Am. Chem. Soc.* **2006**, *128*, 11496.
19. Garg, B.; Bisht, T.; Chauhan, S. M. S. *New J. Chem.* **2010**, *34*, 1251.
20. Anzenbacher, Jr., P.; Jursíková, K.; Sessler, J. L. *J. Am. Chem. Soc.* **2000**, *122*, 9350.
21. Yang, W.; Yin, Z.; Li, Z.; He, J.; Cheng, J. P. *J. Mol. Struct.* **2008**, *889*, 279.
22. Yoo, J.; Park, I.; Kim, T. Y.; Lee, C. H. *Bull. Korean Chem. Soc.* **2010**, *31*, 630.
23. (a) Lv, Y.; Xu, J.; Guo, Y.; Shao, S. *Chem. Pap.* **2011**, *65*, 553. (b) Lv, Y.; Xu, J.; Guo, Y.; Shao, S. *J. Incl. Phenom. Macrocycl. Chem.* **2012**, *72*, 95.
24. Gotor, R.; Costero, A. M.; Gaviña, P.; Gil, S.; Parra, M. *Eur. J. Org. Chem.* **2013**, 1515.
25. Taner, B.; Kursunlu, A. N.; Güler, E. *Spectrochim Acta A* **2014**, *118*, 903.
26. Miyaji, H.; Kim, H. K.; Sim, E. K.; Lee, C. K.; Cho, W. S.; Sessler, J. L.; Lee, C. H. *J. Am. Chem. Soc.* **2005**, *127*, 12510.
27. Jeong, S. D.; Yoo, J.; Na, H. K.; Chi, D. Y.; Lee, C. H. *Supramol. Chem.* **2007**, *19*, 271.
28. Yoo, J.; Kim, M. S.; Hong, S. J.; Sessler, J. L.; Lee, C. H. *J. Org. Chem.* **2009**, *74*, 1065.
29. Thiampanya, P.; Muangsin, N.; Pulpoka, B. *Org. Lett.* **2006**, *14*, 4050.
30. Park, G.; Park, K.; Lee, C. H. *Bull. Korean Chem. Soc.* **2013**, *34*, 283.
31. Gale, P. A.; Twyman, L. J.; Handlinc C. I.; Sessler, J. L. *Chem. Commun.*, **1999**, 1851.
32. Linn, M. M.; Poncio, D. C.; Machado, V. G. *Tetrahedron Lett.* **2007**, *48*, 4547.
33. Nicoleti, C. R.; Marini, V. G.; Zimmermann, L. M.; Machado, V. G. *J. Braz. Chem. Soc.* **2012**, *23*, 1488.
34. Sokkalingam, P.; Yoo, J.; Hwang, H.; Lee, P. H.; Jung, Y. M.; Lee, C. H. *Eur. J. Org. Chem.* **2011**, 2911.
35. Sokkalingam, P.; Kim, D. S.; Hwang, H.; Sessler, J. L.; Lee, C. H. *Chem. Sci.* **2012**, *3*, 1819.
36. Kaur, S.; Hwang, H.; Lee, J. T.; Lee, C. H. *Tetrahedron Lett.* **2013**, *54*, 3744.
37. Shao, S.; Guo, Y.; He, L.; Jiang, S.; Yu, X. *Tetrahedron Lett.* **2003**, *44*, 2175.
38. Liu, K.; He, L.; He, X.; Guo, Y.; Shao, S.; Jiang, S. *Tetrahedron Lett.* **2007**, *48*, 4275.
39. (a) Thomas III, S. W.; Joly, G. D.; Swager, T. M. *Chem. Rev.* **2007**, *107*, 1339. (b) Shanmugaraju, S.; Joshi, S. A.; Mukherjee, P. S. *J. Mater. Chem.*, **2011**, *21*, 9130.
40. Samanta, R.; Mahanta, S. P.; Ghanta, S.; Panda, P. K. *RSC Adv.* **2012**, *2*, 7974.

41. a) Sessler, J. L.; Camiolo, S.; Gale, P. A. *Coord. Chem. Rev.* **2003**, 240, 17. (b) Schazmann, B.; Alhashimy, N.; Diamond, D. *J. Am. Chem. Soc.* **2006**, 128, 8607. (c) Nam, K. C.; Kang, S. O.; Ko, S. W. *Bull. Korean Chem. Soc.* **1999**, 20, 953. (d) Sessler, J. L.; Mody, T. D.; Ford, D. A.; Lynch, V. *Angew. Chem. Int. Ed. Engl.* **1992**, 31, 452; (e) Sessler, J. L.; Gale, P. A.; Cho, W. S, *Anion Receptor Chemistry*, Royal Society of Chemistry, 2006.
42. Samanta, R.; Mahanta, S. P.; Chaudhuri, S.; Panda, P. K.; Narahari, A. *Inorg. Chim. Acta.* **2011**, 372, 281.

CHAPTER 5

Calix[4]pyrroles with Shortest Possible Strap

5.1 Introduction

The recognition of a guest by a supramolecular host depends on how closely the two partners fit together. One of the most fundamental and first thoughts in this area was the ‘lock-and-key’ concept proposed by Emil Fisher,¹ which is still a stimulating research area in ‘host-guest’ chemistry. With a given host and guest, the thermodynamic stability of the ‘host-guest’ complex is primarily related to host preorganization and ‘host-guest’ complementarity. It follows that host preorganization and complementarity is related to a specific ‘host-guest’ complex. A guest-free host with the same conformation as in the complex with a specific guest is highly preorganised for that particular guest. A structurally complementary host has an ideal size and shape for a specific guest i.e., the spatial distribution of the host atoms in the guest free host, resides in the conformation, which preferably coordinates a specific guest. Fulfilment of these criteria of preorganization and complementarity has evolved from the early days of the anion coordination chemistry. In their first report, Simmons and Park had synthesized seven macrobicyclic diamines and had tested halide katapinosis capability of four of them (**L1-4**). They

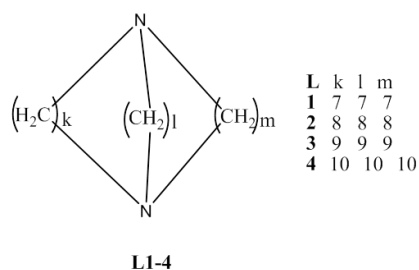
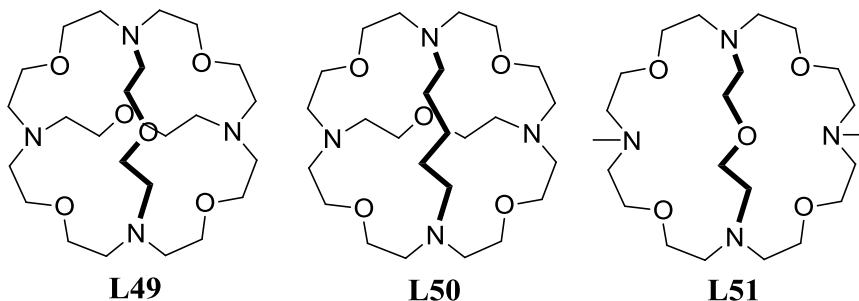


Table 5.1 Equilibrium Constants for Halide Encapsulation by Diazabicyclo [k.l.m]alkaneammonium ions.

Anion	$r_{\text{ionic}} (\text{\AA})$	L1 ($K_{\text{a}}, \text{M}^{-1}$)	L2 ($K_{\text{a}}, \text{M}^{-1}$)	L3 ($K_{\text{a}}, \text{M}^{-1}$)	L4 ($K_{\text{a}}, \text{M}^{-1}$)
Cl⁻	1.81	0	0	4	>10
Br⁻	1.95	0	0	1	>10
I⁻	2.16	0	0	0	>10
Cavity Diameter (Å)		1.6	2.8	3.6	4.5

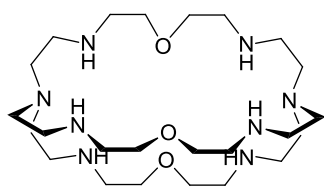
observed that among the four tested receptors only two were capable of interacting with the halides.² When the diameter of the cavities was measured with CPK models, it was found that size of the cavity is an important factor in halide katapinosis (table 5.1). Lehn and coworker's later reported cryptand like receptors (**L49-51**) containing four amine centers, which displayed



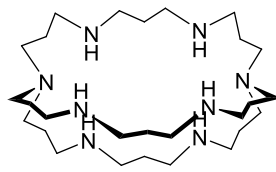
size based selective (table 5.2).³ Reason for high chloride ion selectivity of **L49-50** compared to **L51** was connected with presence of a closed and rigid cavity, which resist to deformation upon changes in anion size. They have also postulated that **L49** and **L50** may have the optimal

Table 5.2 Association constants for **L4**, **L49-51** measured at pH = 1.3 (HNO₃) at 294 K. log K_a determined using chloride and bromide ion selective electrode.³

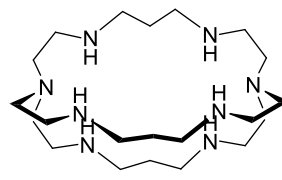
Anion	Solvent	log K _a			
		L4	L49	L50	L51
Cl ⁻	Water	(~0.7)	>4.0	>4.5	1.7 ± 0.1
	Water : MeOH (9:1)	2.1 ± 0.1	—	—	3.1 ± 0.1
Br ⁻	MeOH	<1.0	<1.0	1.55 ± 0.1	<1.0
	MeOH/ Water	~1.2 ± 0.3	1.75 ± 0.2	3.2 ± 0.1	1.72 ± 0.2



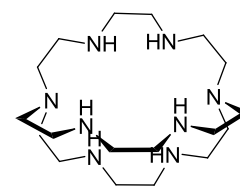
L52



L175



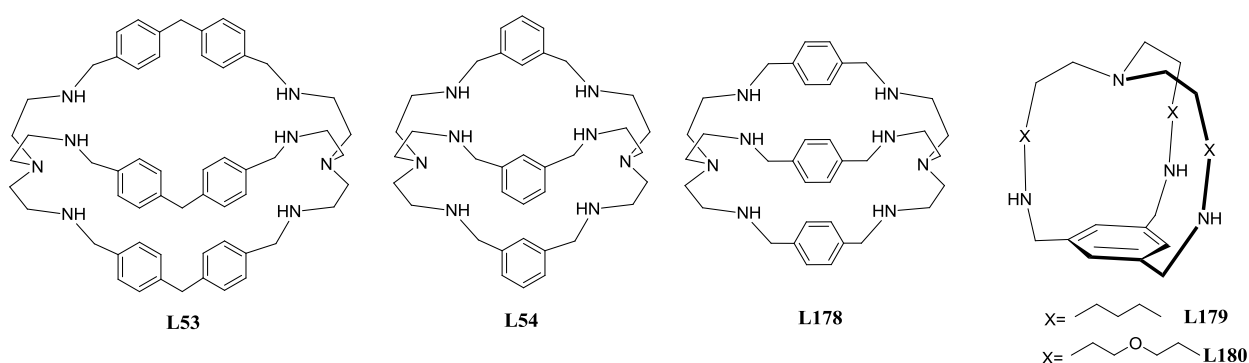
L176



L177

topology for spherical chloride ion. Subsequently, Lehn and coworkers reported a series of cryptand like polyamine based anion receptors, which are capable of showing varying degree of anion affinities depending on their cavity sizes. **L52** showed affinity for mono negative anions in the order $\text{I}^- < \text{Br}^-, \text{Cl}^-, \text{NO}_3^- < \text{N}_3^-$ in its hexaprotonated form.⁴ Whereas, in its hepta or octa-protonated form **L175** have a higher affinity for iodide over other anions ($\text{Cl}^- < \text{Br}^- < \text{I}^-$). This contrasting difference in binding behavior was attributed to the larger and more spherical cavity for **L175** than **L52**.⁵ In another analogous receptor **L176** affinity was found higher for fluoride and chloride ion compared to bromide and iodide ions.⁶ The crystal structure displayed complete encapsulation of chloride ion within the hexaprotonated receptor. Among the series of azacryptand receptors reported by the Lehn group, the bicyclic receptor **L177** was having the smallest cavity and considered well-tailored for the binding of fluoride ion.^{7a} Association constants measured in water showed that receptor is highly selective for fluoride ion ($\log K_a = 10.55$ and < 2 respectively, for the binding of fluoride and chloride ions). Solid state structures for both fluoride and chloride ion encapsulated complexes, reported separately by Lehn and Bowman-James in a time span of eleven years, found similar type of encapsulation of both the anions.⁷ In 1991, Lehn and coworkers reported more extended macrobicyclic receptor **L53**,

which was capable of binding dicarboxylate ions ($\log K_a = 4.4$ for terephthalate and 3.4 for oxalate ions).⁸ Essentially concurrent with the **L53**, Martell and coworkers have reported the synthesis of **L54**.⁹ Later various groups explored its anion binding capabilities by various methods.¹⁰ But only in 2004, Nelson and coworkers found that this receptor can also bind with dicarboxylate ions, viz. oxalate ion ($\log K_a=10.71$) with quite high association constant. The crystal structure revealed that this unprecedented selectivity is a result of overall effect of electrostatic, hydrogen bonding and π -stacking interactions.¹¹ Bowman-James and coworkers in 2002 reported **L178**, which had a little larger cavity size than that of **L54**, and bind to two fluoride ions in the solid state.¹² Potentiometric titration with fluoride ion showed that $\log K_a$ of



L178 is almost two orders higher than that of **L54**, in their hexaprotonated forms (6.54 for **L178** and 3.53 for **L54**).^{10e,12} These two examples have shown that increase or decrease in the size of the cavity can impart a large effect on the selectivity of the receptors. Lehn and coworkers reported another more rigid, preorganised macrobicyclic receptor **L179** having potential to bind dianions, such as sulphate, dithionate and oxalate.¹³ Steed and coworkers reported a very similar kind of receptor **L180** and their solid state structures for fluoride, chloride, bromide and iodide ions.¹⁴ Interestingly, the fluoride ion encapsulated structure displayed the longest distance from the center of the benzene core to the anion, which reflects repulsion between the electron rich π -surface of the benzene ring and the fluoride ion. The potentiometric titration showed a higher selectivity for fluoride ion ($\log K_F : \log K_{Cl} = 9.54 : 4.19$) in their hexaprotonated forms, with no appreciable binding of bromide and iodide ions.

Owing to the effect of the size of the binding domain (cavity size), many remoulding have been performed on the binding domain of every class of anion receptors, mainly in search

of better affinity and selectivity towards a particular anion. Our targeted macrocycle i.e. calixpyrrole also has undergone through various kinds of modification over the years.

5.2 Size Modification of the Binding Domain of Calixpyrrole

Size modification of the binding domain of the calixpyrrole macrocycle was affected generally in two ways: i) modification of the core, and ii) modification of the size of the binding domain, by varying the strap length.

5.2.1 Modification of Core

Subsequent to the discovery of the anion binding properties of the calix[4]pyrrole,¹⁵ it was anticipated that larger calix[n]pyrroles ($n > 4$) may be with their larger cavities will enable selective and effective complexation of larger anionic species. First example of expanded calixpyrrole was reported by Sessler and coworkers, by condensing *p*-*tert*-butylcalix[5]arene pentamethyl ketone with 5 equiv. of pyrrole in the presence of BF_3 .ether, a calix[5]pyrrole-calix[5]arene pseudo-dimer **L181** was formed in 10% yield.^{16a} The intramolecular hydrogen bonding array in **L181** (NH 9.88 ppm) appears to be weaker than that of the calix[4]pyrrole-calix[4]arene (NH 11.22 ppm). This new receptor could able to interact with CD_3OD or chloride ion to cause shifts in the NH proton signal, which was not observed for the tetramer derivative.¹⁶ First only *meso*-substituted, calix[6]pyrrole **L182** was reported by Eichen and coworkers in 1998.¹⁷ ^1H NMR showed a moderate preference for iodide ion by this receptor (table 5.3). The preference for bigger anions was attributed to the larger core size of the molecule, which creates a better geometrical fit for the larger anions. Using a very different kind of approach, Kohnke

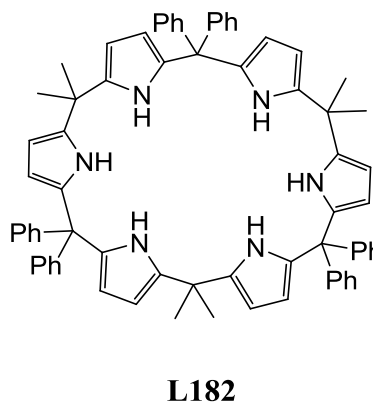
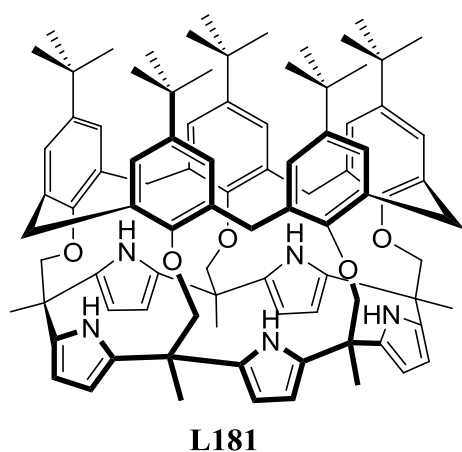


Table 5.3 K_a (M^{-1}) for the binding of **L72** and **L182** with various anions, as determined by 1H NMR spectroscopy in $CD_3CN-CDCl_3$ (1:9) at 298 K. All the anions used as their TBA salts.¹⁷

	F^-	Cl^-	Br^-	I^-	BF_4^-	$CF_3CO_2^-$
L72	23,800	6800	270	<10	<10	70
L182	1080	650	150	6600	2350	1150

and coworkers reported the synthesis of *meso*-decamethylcalix[5]pyrrole **L183**, *meso*-dodecamethylcalix[6]pyrrole **L184**, calix[2]furan[4]pyrrole **L185** and calix[1]furan[5]pyrrole **L186**.¹⁸ These compounds were prepared from calix[n]furans ($n = 5, 6$) by using *m*-CPBA to open the furan heterocycles, and then ammonium acetate to form the obtained pyrrole rings. Crystal structure for **L183** with chloride and bromide ion were quite similar, and $N \cdots Cl$ distances in **L183** were in the range from 3.265 to 3.305 Å, whereas those in case of **L72-Cl** complex,

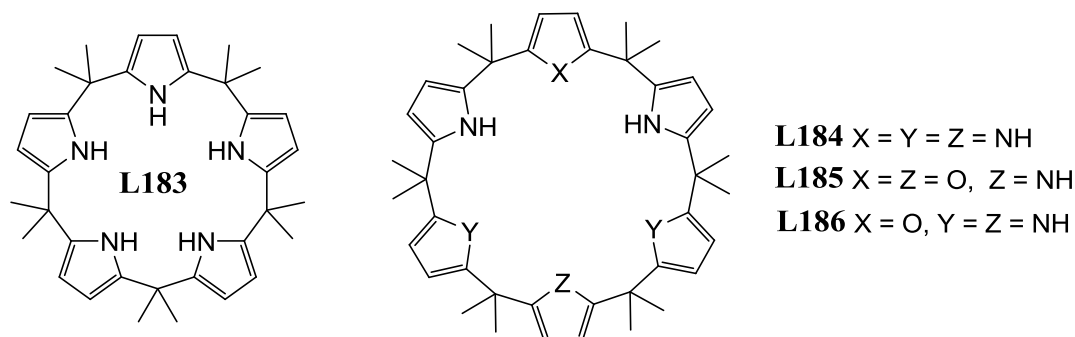


Table 5.4 K_a (M^{-1}) for various 1:1 anion complexes with **L72** and **L183-186**.^{18, 20}

Anion	L72	L183	L184	L185	L186
F^-	2,700 ^a	14,000	<i>ca.</i> 320,000 ^g	57,000 ^g	^f
Cl^-	46 ^a	35 ^b	12,000 ^e	65 ^a	5,500 ^e
Br^-	10 ^d	—	710 ^c	<10 ^a	69 ^c
I^-	<10 ^d	—	ⁱ	ⁱ	ⁱ
$H_2PO_4^-$	97	—	^h	ⁱ	ⁱ
HSO_4^-	<10 ^d	—	<i>ca.</i> 10 ^c	ⁱ	ⁱ
NO_3^-	<10 ^d	—	16 ^c	ⁱ	<10 ^c
CN^-	<10 ^a	—	<i>ca.</i> 100 ^a	ⁱ	^h

^a measured by 1H NMR in D_2O saturated CD_2Cl_2 at 20 °C; ^b measured by 1H NMR in D_2O saturated CD_2Cl_2 at 22 °C; ^c measured by 1H NMR in dry CD_2Cl_2 at 20 °C; ^d measured by 1H NMR in dry CD_2Cl_2 at 25 °C; ^e measured by Crams extraction method at 16 °C using D_2O/CD_2Cl_2 ; ^f Crams extraction method could not be applied; ^g measured competition experiment using **L72** as competing species; ^h NH disappeared upon addition of anion; ⁱ no detectable binding were observed. range from 3.264 to 3.331 Å.¹⁹ The result of anion binding

studies carried out with **L183-186** are shown in table 5.4.^{18,20} Although it is difficult to compare these data as they are collected in different conditions by various methods, however they could provide a qualitative idea about affinities of the various receptors. From the table we can notice that association constant for halide ions increases with the increase in the number of pyrrolic NHs in the receptor. Intrinsic selectivity is seen to change. In case of **L72**, the fluoride to chloride K_a ratio is ~ 59 . On the contrary, the corresponding ratio for **L184** is ~ 27 , indicating lower fluoride selectivity than **L72**. Besides, enhanced selectivity for fluoride over chloride ion was also noticed in case of **L183** and **L185**, with the relevant K_a ratios *ca.* 400 and 877, respectively. Much later, Chacón-García and coworkers reported a direct method for the synthesis of **L183** from pyrrole and acetone, by using $\text{Bi}(\text{NO}_3)_3$ as catalyst with a yield of 25%.²¹ In 2000, a direct synthesis of calix[n]pyrroles (**L73-76**, $n = 4-6, 8$) was discovered by Sessler and coworkers.²² It hinged on the use of 3,4-difluoropyrrole rather than simple pyrrole. Solid state structure displayed cone conformation for the fluoride complex of **L72**, however, for the acetate complex of **L73** considerable distortion was observed, may be due to the presence of interannular $\text{CF}\cdots\text{H}$ hydrogen bonding in this macrocycle. Few years later they reported the

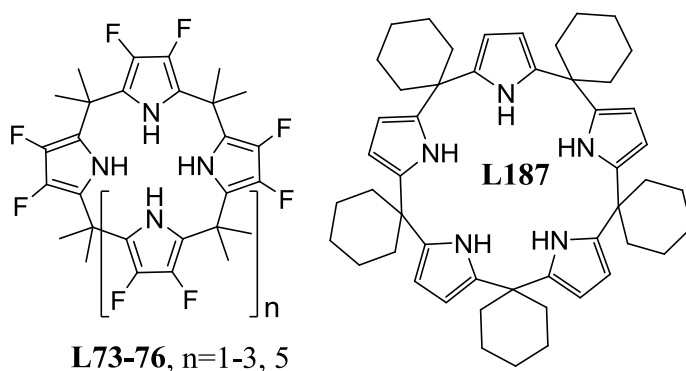
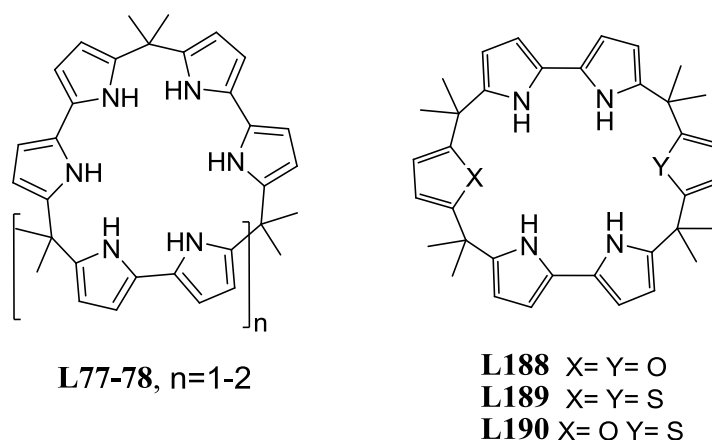


Table 5.5 K_a (M^{-1}) for **L73-75** determined in CH_3CN and DMSO by ITC at 303 K.

Anion	Solvent	L73	L74	L75
Cl^-	CH_3CN	5.30×10^5	4.10×10^4	2.80×10^5
Br^-	CH_3CN	8.50×10^3	8.50×10^5	1.10×10^5
I^-	CH_3CN	^a	^a	6.12×10^2
H_2PO_4^-	DMSO	1.70×10^4	9.60×10^4	1.30×10^4
H_2PO_2^-	DMSO	3.30×10^3	1.30×10^4	3.50×10^4
$\text{C}_6\text{H}_5\text{CO}_2^-$ ^b	CH_3CN	1.39×10^6	8.30×10^4	5.80×10^5
CH_3CO_2^- ^b	CH_3CN	2.36×10^6	5.20×10^5	1.02×10^6

^a no evidence of binding was observed; ^b reverse titration was performed.

macrocycle. Few years later they reported the association constants for some these fluorinated receptors by ITC (table 5.5). It was found that the relative association constants ($K_{\text{rel}} = K_{\text{a(Cl)}}/K_{\text{a(Br)}}$) decreased with increasing macrocycle size, whereas in case of dihydrogenephosphate ion, association constant increased, with the number of pyrrolic-NHs. Very recently, Chacón-García and coworkers reported *meso*-pentaspirocyclohexylcalix[5]pyrrole **L187**, but unfortunately this receptor showed very low affinity for the anions, compared to **L72**.²³ In order to make more efficient receptors for larger anions, many groups have reported extended calixpyrrole type receptors that are based on various combination of bipyrrole, furan, thiophene and pyrrole. For example, in 2003, Sessler and coworkers reported calix[n]bipyrroles **L77-78**. In case of **L77**, crystal structure with chloride ion adopted a cone conformation, with all six pyrrolic-NHs are



involved in hydrogen bonding, however bond distances are larger than that observed in case of **L72**.Cl[−] complex.^{24a} On the other hand, solid state structure of chloride complex of **L78** showed that anion seats in V-shaped cleft of the receptor.^{24b} From table 5.5 we can see that affinity for larger anions increased moderately for **L77** compared to **L72**. In case of **L78**, association

Table 5.5 K_{a} (M^{−1}) for **L77-78** determined in CH₃CN by ITC at 303 K.^{24b}

Anion	Cl [−]	Br [−]	I ^{−a}	NO ₃ ^{−a}
L72	1.40×10^5	3.40×10^3	17	52
L77	1.10×10^5	1.00×10^5	9.30×10^3	1.10×10^4
L78	2.90×10^6	1.10×10^5	56	450

^a value obtained from ¹H NMR titration in CD₃CN at 294 K.

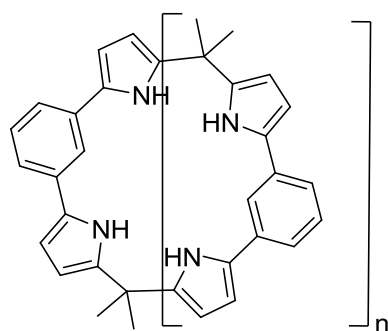
constant for chloride ion was found much higher than that of bromide ion, which is also higher than that of **L72**. The above observation reflects on the fact that along with size- and geometry-

based matching between host and guest, number of pyrrolic-NHs are important in terms of regulating the anion binding affinity. Few calixbipyrrole hybrid receptors containing furan and thiophene were also reported (**L188-190**).²⁵ These receptors showed higher affinity for ‘Y’-shaped anions, whereas their affinity for spherical anions were quite less (table 5.6). The reason was understood upon solving the crystal structure of acetate and chloride complexes of **L188**. The crystal structure showed that for acetate ion, the receptor adopted a cone conformation, whereas for chloride ion 1,3-alternate conformation was observed with only one bipyrrole unit forming hydrogen bond with the chloride ion. These examples also highlighted that proper shape and size of the receptor, can play crucial role in optimizing the selectivity of a receptor towards certain class of anions. Calix[n]bispyrrolybenzenes **L79-81** synthesized by Sessler and coworkers in 2001, showed interesting binding behavior for various anions.²⁵ Solid state

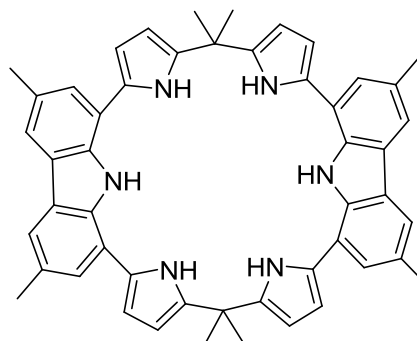
Table 5.6 K_a (M^{-1}) for **L72**, **L188-190** determined in CH_3CN by ITC at 303 K.²⁵

Anion	Cl^-	Br^-	HSO_4^-	$H_2PO_4^-$	$C_6H_5CO_2^-$ ^b	$CH_3CO_2^-$ ^c
L72	1.40×10^5	3.40×10^3	^a	1.51×10^4	1.20×10^5	3.50×10^5
L188	960 ^b	37 ^b	130 ^b	240 ^b	6.30×10^4	1.10×10^4
L189	1.54×10^3 ^b	100 ^b	28 ^b	$>1 \times 10^4$ ^b	1.00×10^5	1.40×10^5
L190	6.70×10^3 ^b	150 ^b	36 ^b	^a	6.70×10^5	7.10×10^5

^a no evidence of binding was observed; ^b value obtained from 1H NMR in CD_3CN at 297 K.



L79-81, $n=1-3$



L94

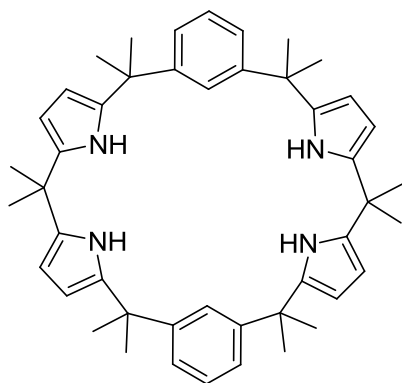
Table 5.7 K_a (M^{-1}) for **L79-81** determined in CH_2Cl_2 by ITC.

Anions	L79	L80	L80
Cl^-	5.60×10^6	8.20×10^4	2.40×10^5
Br^-	2.10×10^7	5.60×10^3	4.40×10^4
HSO_4^-	1.20×10^6	1.10×10^4	7.60×10^4
NO_3^-	2.50×10^6	3.80×10^3	2.20×10^5

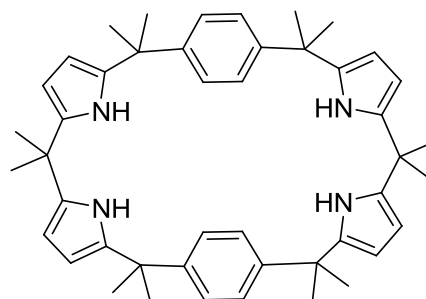
structures for chloride and nitrite ions for **L79** unveiled that it adopted a cone conformation. Selectivity of **L79** towards bromide ion over chloride ion is fully congruous with the size of binding domain present in **L79**, furnishing a better fit for the bromide ion than its congeners (table 5.7). In 2004, **L94**, an expanded calixpyrrole containing carbazole unit was reported, which displayed a clear preference for the oxyanions, measured by fluorescence quenching experiment (table 5.8).²⁶ Few years later, Cafeo and coworkers reported two novel calix[2]benzo-[4]pyrroles **L191-192**.²⁷ Among the tested anions, **L192** could bind only fluoride and acetate to an appreciable extent (table 5.9). However, excluding fluoride ion, the selectivity of **L192** towards acetate was remarkably higher than that observed for **L191**. For **L192** there was

Table 5.8 K_a (M^{-1}) for **L94** determined by fluorescence quenching in CH_3CN .

Anion	$CH_3CO_2^-$	$C_6H_5CO_2^-$	Oxalate	Succinate	$H_2PO_4^-$	$H_2PO_7^{-2}$	Cl^-
L94	2.3×10^5	7.7×10^4	3.1×10^4	9.5×10^3	7.2×10^4	6.4×10^4	3.5×10^4



L191



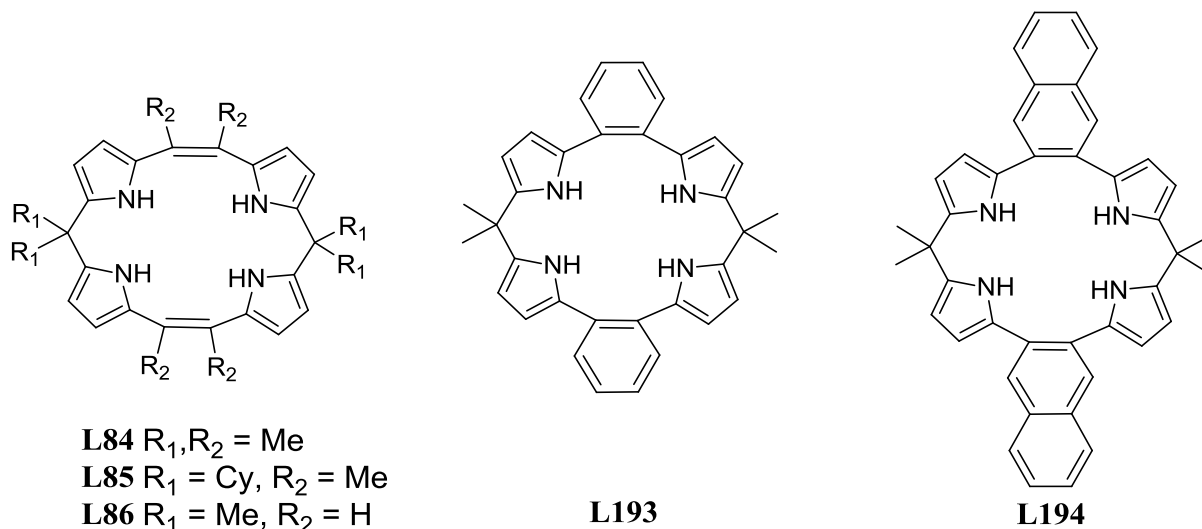
L192

Table 5.9 Association constants K_a (M^{-1}) for the 1:1 complexes of the various anions with **L191-192** by 1H NMR titration.

Anion	L191	L192
F^-	$\sim 2,000^a$	2,246
Cl^-	4,975	^b
Br^-	296	^b
CH_3COO^-	755	597
$H_2PO_4^-$	1,711	^b

^a K_a value was estimated by competitive binding among **L192** and **L72**. ^b no evidence of binding was observed.

a “shape” mismatch with spherical or tetragonal anions, thus, only the planar Y- shaped acetate and nitrate are bound (the latter weakly) by this receptor. **L191** proved to be a better anion receptor than **L72** towards all of the anions tested. Very recently our group also reported some new meso-expanded calix-[4]pyrroles **L84-86**, where the two dialkyldipyrromethane units are linked via C–C double bonds.²⁸ These calix[2]bispyrrolylethenes represented a new class of the



smallest expanded calix[4]pyrrole reported so far. Among these receptors, **L86** displayed colorimetric sensing of fluoride ion (colorless to dark red) in polar aprotic solvents, through anion– π interaction. Subsequently, extending this concept our group again reported **L193-194** with extended π -conjugation, by ‘2 + 2’ cyclocoupling, using the Suzuki coupling protocol.²⁹ While **L193** showed a ‘turn-on’ fluorescence upon addition of fluoride and acetate ions, **L194** exhibited ‘turn-off’ fluorescence, in same condition. Detection sensitivity of **L193** for fluoride ion was found to be quite good (80 nM) compared to **L193** (300 nM).

5.2.2 Modification of the Size of the Binding Domain

Immediately after the discovery of strapped calix[4]pyrrole **L124** in 2002 by Lee and coworkers,³⁰ it was recognized that by varying the nature of the strap, fundamental insights into the relationship between the structure of the receptor, the size and shape of anion, and the binding affinities might be obtained. To fulfill this aspiration, they synthesized two sets of new strapped calix[4]pyrrole bridged by ether-containing straps (**L125**) and amide-containing straps (**L130**), of varying length.³¹ Table 5.10 summarized the association constants corresponding to the binding of chloride, bromide and iodide ions with **L125** and **L130** receptors, as determined

by ITC in dry acetonitrile. Inspection of this table underscores the advantages that accrue as the result of strapping of one side of the calix[4]pyrrole. For instance, the use of tight C-4 ether strap

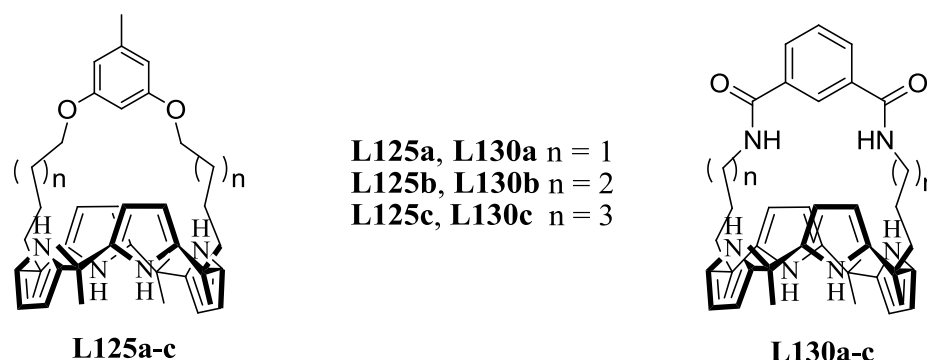


Table 5.10 Association constants K_a (M^{-1}) for the 1:1 complexes of the various anions with **L125** and **L192**, by ITC at 303 K.

Anion	L125a	L125b	L125c	L130a	L130b	L130c
Cl^-	3.63×10^6	1.37×10^6	1.37×10^6	3.89×10^6	3.35×10^6	3.24×10^6
Br^-	3.00×10^4	3.10×10^4	1.20×10^5	1.41×10^6	1.25×10^6	7.00×10^5
I^-	a	a	a	a	2.30×10^3	3.00×10^3

^a no evidence of binding was observed.

in **L125a** provided an extremely high chloride ion affinity. In contrast, the use of C-6 ether strap in **L125c** resulted with an enhanced bromide ion affinity, relative to the previously reported **L124**. In case of C-3, C-4 and C-5 amide strapped calix[4]pyrrole **L130**, the chloride ion affinity were found to be almost identical, however still higher than that of **L124** and **L125**, may be due to the presence of additional hydrogen bonding sites from amide groups. Unlike **L125**, all three **L130** receptors, displayed more or less similar binding nature and thus do not show any kind of anion to receptor, size matched selectivity, which may be assignable to the more flexible nature of the strap that can tilt upon anion coordination. Further, receptors **L130b** and **L130c** were found to bind with iodide ion to some extent.

5.3 Research Goal

From the above discussion it was obvious that size and nature of the cavity/binding domain, plays an enormous role to the overall affinity/selectivity of a calix[4]pyrrole receptor towards a particular anion. Though many studies have been performed by varying the core sizes, to the best of our knowledge, there is only two reports, which deals with anion binding with regard

to variable strap sizes.^{30,31} No insight was found about the minimum or maximum length of the strap. Herein, we try to make calix[4]pyrrole with shortest strap and its consequences on anion binding and selectivity. If we strap a calix[4]pyrrole with a very short strap some interesting things can happen. For example, a shorter binding domain will try to discriminate between the smaller and bigger anions on the basis of their size. This has been schematically illustrated in Figure 5.1, for calix[4]pyrrole with a large strap (**L**) and with a shorter strap (**S**) interacting with small and large anions. For **L**, there may be hardly any difference in the interaction between the large and small anions, as with a large strap the favorable binding

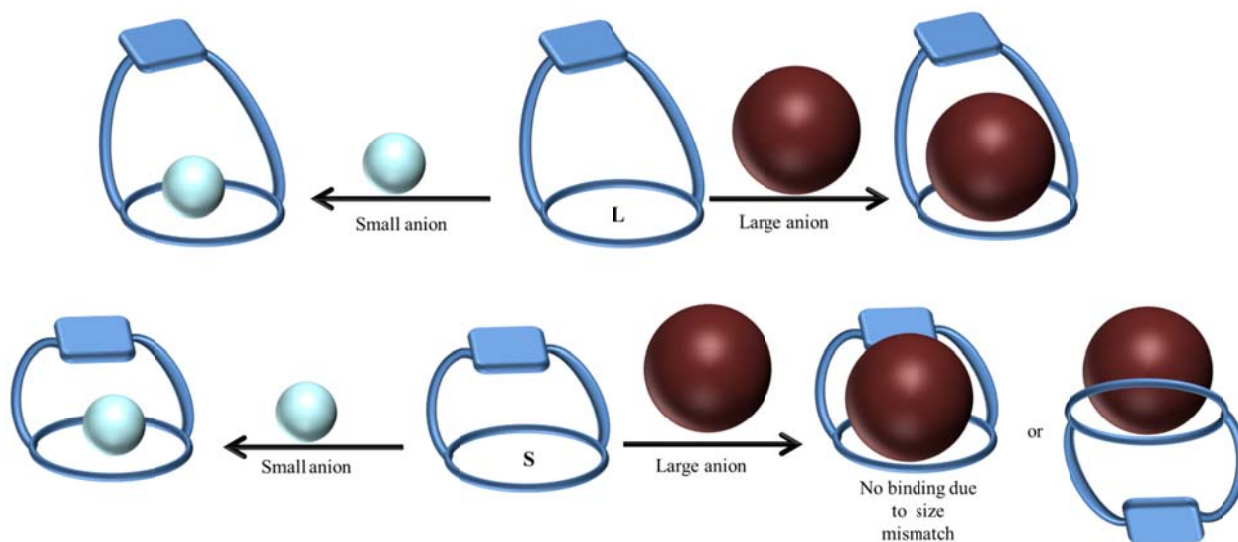


Figure 5.1: Schematic representation of possible modes of interaction between a long (**L**) and short (**S**) strapped calix[4]pyrrole with a small and a large anion.

domain may have enough space i.e. under the strap, to incorporate both the anions. However, in case of **S**, owing to steric hindrance caused by the shorter strap, the larger anion cannot fit into the binding domain, whereas, smaller anion may not have any such difficulty in binding. This size imposed discrimination may eventually lead to the selectivity for the smaller anions. However, another event can happen with **S** and large anion, where anion can go to the other side of calix[4]pyrrole i.e. opposite side of the strap, hence may not display any size based discrimination between anions. To achieve **S** type calix[4]pyrrole, we intended to prepare strapped calix[4]pyrroles with only $-\text{OCH}_2-$ unit as a spacer between the calix[4]pyrrole core and the strapping aromatic unit, e.g. **L18-21** (Figure 5.2). In all the receptors aromatic units were linked via '1,2-position' of the aromatic ring. Motivation for the synthesis of the **R20** and **R21** is

to minimize the repulsion between the bound anion and the lone pairs of oxygen atoms, by introducing electron withdrawing substituents on the strap.

5.4 Results and Discussion

5.4.1 Synthesis and Structural Characterization

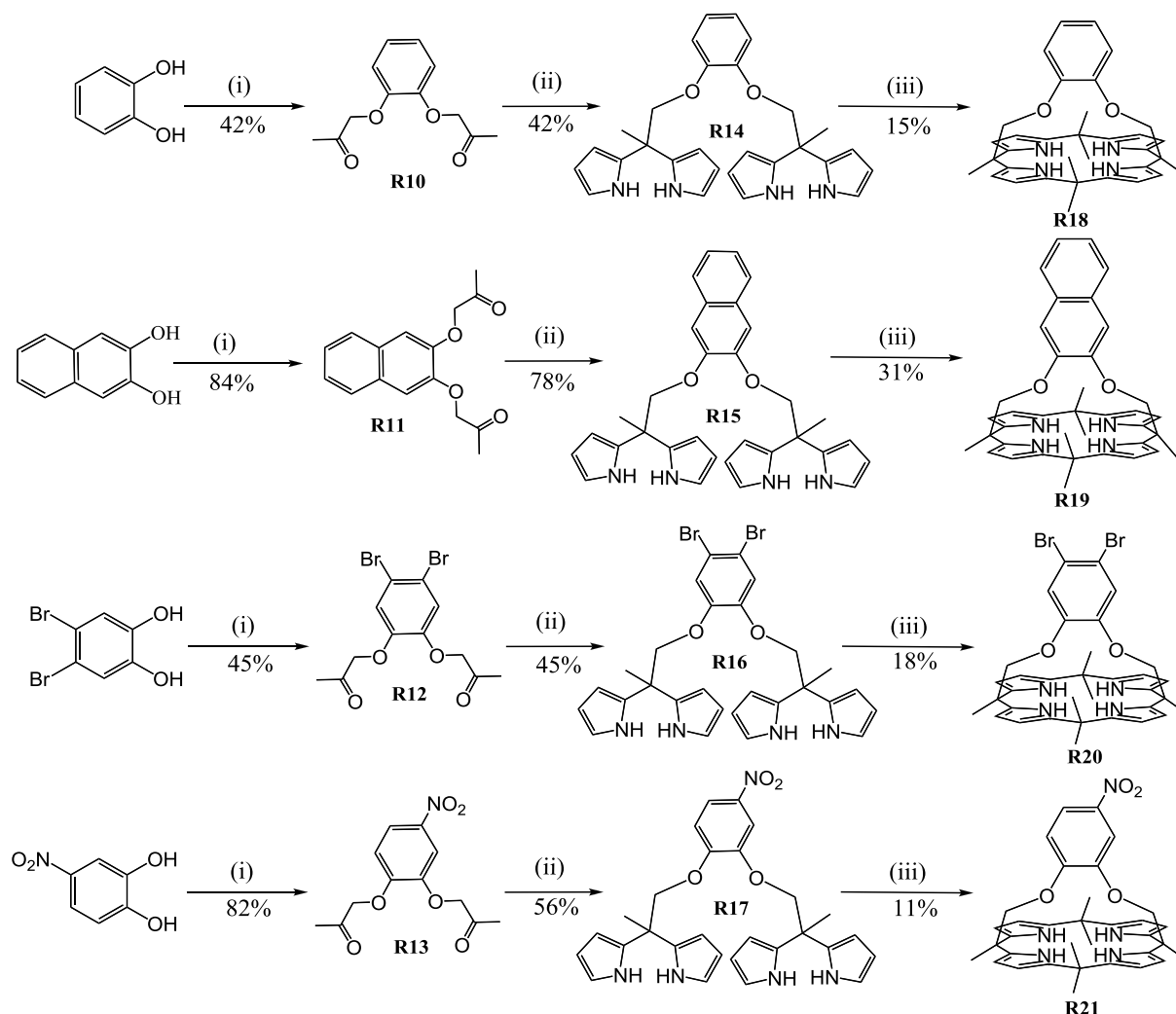


Figure 5.2: Synthetic schemes for **R18-21**. i) 1-bromoacetone, K_2CO_3 , dry acetonitrile, ii) pyrrole, TFA, 60°C iii) acetone, $\text{BF}_3\cdot\text{OEt}_2$, R.T.

All strapped calix[4]pyrrole receptors were synthesized, by slightly modifying the method we have used earlier to synthesize **R3**.^{32a} Our attempts to alkylate the dihydroxy aromatic compounds using 1-bromoacetone in dry acetone, in presence anhyd. potassium carbonate did not yield the desired products, probably owing to decomposition of 1-bromoacetone at higher reaction temperature. Reaction at R.T. in acetone also produced some

impurities, along with the product, making the purification very tedious. However, replacing the solvent to acetonitrile, led to most satisfactory yield for the diketo compounds. Desired diketo compounds (**R10-13**) were purified from the crude product by column chromatography with moderate to good yields (Figure 5.2). These diketo compounds were converted to their respective bisdipyrromethanes **R14-17**, using excess pyrrole and TFA at 60 °C with moderate yields, except in case of **R15**, which was obtained in quite good yield (78%). Finally, condensation of the bisdipyrromethanes **R14-17** in acetone, using catalytic BF₃.etherate, we observed the formation of macrocycles after 10 min in TLC analysis. Purification of the reaction mixtures using column chromatography and washing the product with methanol, led to the desired strapped calix[4]pyrroles **R18-21**. However, our attempted synthesis of analogous strapped calix[4]pyrrole from 1,3-dihydroxybenzene, met with failure in the final macrocyclization step, possibly indicating the strap length is not sufficient. Further, we have also tried to replace the connecting oxygen atom with carbon (to reduce the repulsion with the incoming anion) by using 4,4'-(1,2-phenylene)dibutan-2-one as the starting diketone compound, however, again the final condensation step leading to macrocyclization could not be accomplished successfully, possibly

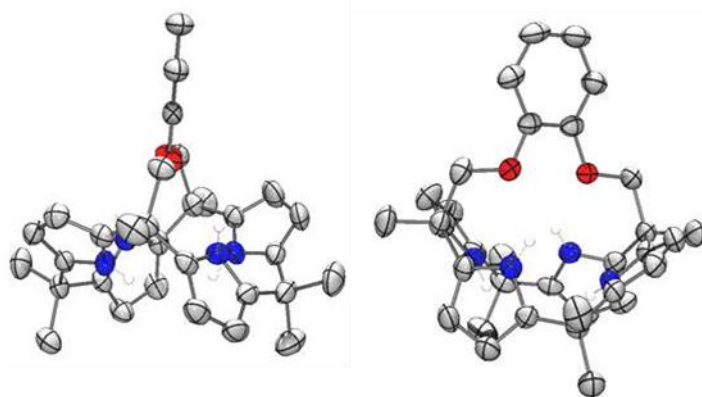


Figure 5.3: Two views of the solid state structure of **R18**. Thermal ellipsoids are scaled to the 50 % probability level. All hydrogen atoms bound to carbon atoms are omitted for clarity. Color code: blue, N; gray, C; red, O; white, H.

indicating a lack of convergence by the sp³-Cs at the 1,2- positions of the benzene. All the compounds, including the desired macrocycles were characterized by IR, ¹H and, ¹³C NMR spectroscopy and high resolution mass analysis. ¹H NMR analysis of the receptors, in CDCl₃ showed that pyrrolic-NH signals were resonating around ~8.0 ppm for all the receptors. Single

crystals were obtained by slow evaporation of ethylacetate-hexane mixture of **R18** and **R20** and from dichloromethane-methanol mixture in case of **R19** (Figure 5.3 - 5.5). All macrocycles display 1,3-alternate orientation of the pyrrole units and the strap resides almost orthogonal to the calix[4]pyrrole cores. It was found that the methylene units are pointed outwardly in all the crystal structures.

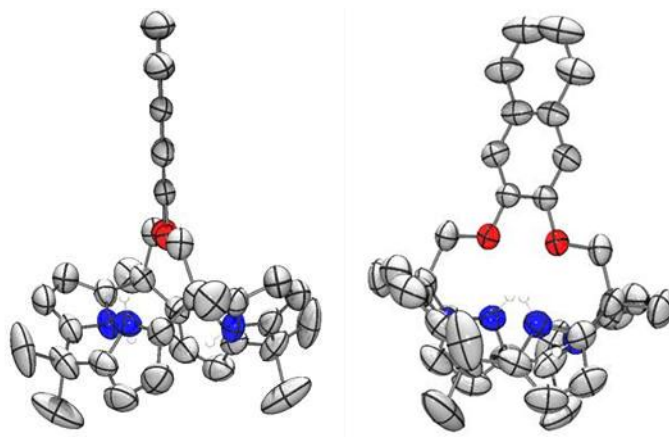


Figure 5.4: Two views of the solid state structure of **R19**. Thermal ellipsoids are scaled to the 50 % probability level. All hydrogen atoms bound to carbon atoms are omitted for clarity. Color code: blue, N; gray, C; red, O; white, H.

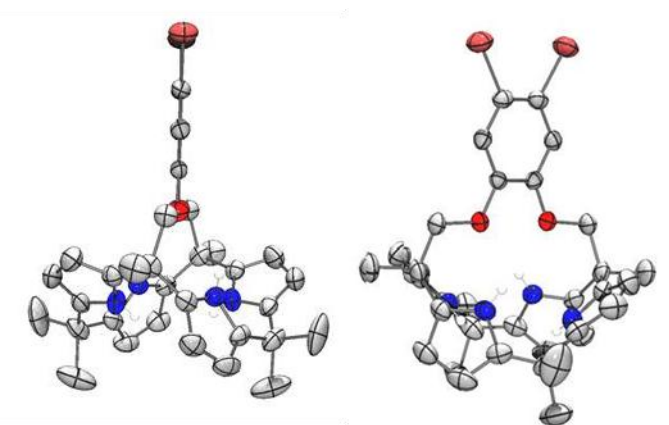


Figure 5.5: Two views of the solid state structure of **R20**. Thermal ellipsoids are scaled to the 50 % probability level. All hydrogen atoms bound to carbon atoms are omitted for clarity. Color code: blue, N; gray, C; red, O; orange, Br; white, H.

5.4.2 Anion Binding Study

Preliminary solution phase anion binding behavior of **R18-20** were carried out by ^1H NMR titration studies in CD_3CN with various anions as their tetrabutylammonium (TBA) salts

(i.e. F^- , Cl^- , Br^- , I^- , CN^- , HSO_4^- , $H_2PO_4^-$, $CH_3CO_2^-$, N_3^- , NO_2^- , NO_3^- and ClO_4^-) and the study revealed that all the three tested receptors showed interaction only with fluoride ion, indicating complexation with fluoride ion occurs only inside the cavity of the strap, not the other way around. For all the three receptor it was found that one equivalent of anion was sufficient for the complete conversion of free receptor to receptor anion complex. Interestingly, very less shift of pyrrolic-NH signals were observed, whereas those in case of β -pyrrolic-CH signals were almost negligible (Figure 5.6).

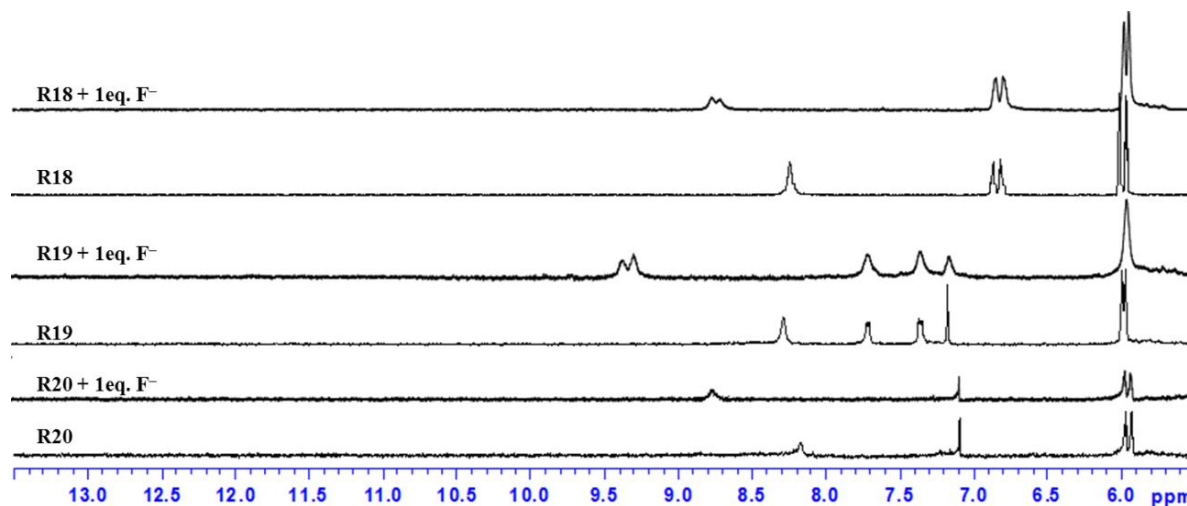


Figure 5.6 Partial 1H NMR spectra for the receptors **R18**, **R19** and **R20** and their complexes with fluoride ion, upon addition of one equivalent of TBAF.3H₂O in CD₃CN at 25 °C.

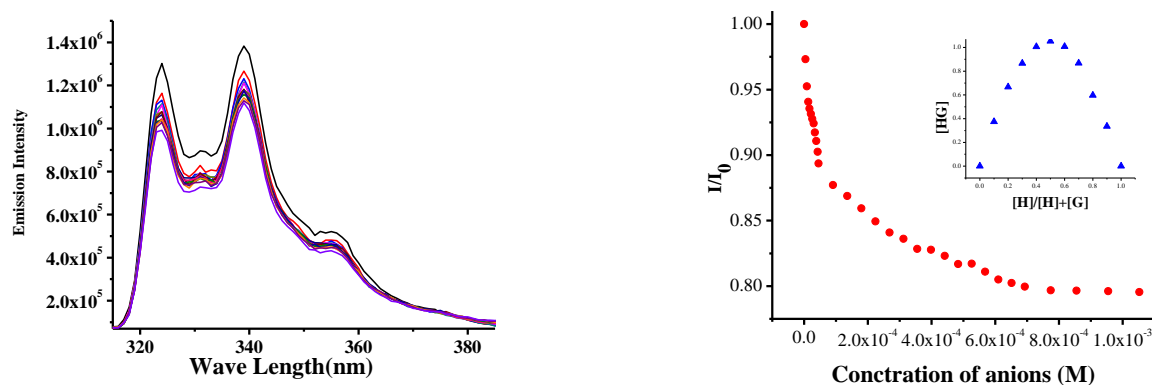


Figure 5.7: Left: Fluorescence spectra of **R19** in CH₃CN (0.04 mM) excited at 310 nm showing the induced changes, upon the addition of increasing quantities of TBAF.3H₂O. Right: Quenching effect of TBAF.3H₂O upon gradual addition to **R19**; (inset) Job plot analysis of **R19** vs TBAF.3H₂O.

When fluorescence active **R19** was checked for its anion binding affinities with various anion it was found that quenching of fluorescence was observed only in case of fluoride ion. However, the amount of quenching was found to be less than that observed in case of **R8**. Job plot analysis for this binding event found to follow 1:1 binding stoichiometry (Figure 5.7). Association constant derived from this quenching experiment is 1.16×10^4 , which is again found to be less by an order than that observed for its higher homolog **R8**.^{32b} In order to evaluate the binding affinities, isothermal titration calorimetry (ITC) was performed for the receptors **R18-20** with fluoride ion. The binding isotherm was found to follow 1:1 binding stoichiometry in all cases. Binding processes are found to be exothermic in nature, with maximum heat change occurred for **R20** upon complexation, and followed by **R19** and **R18** (Figure 5.8). All the

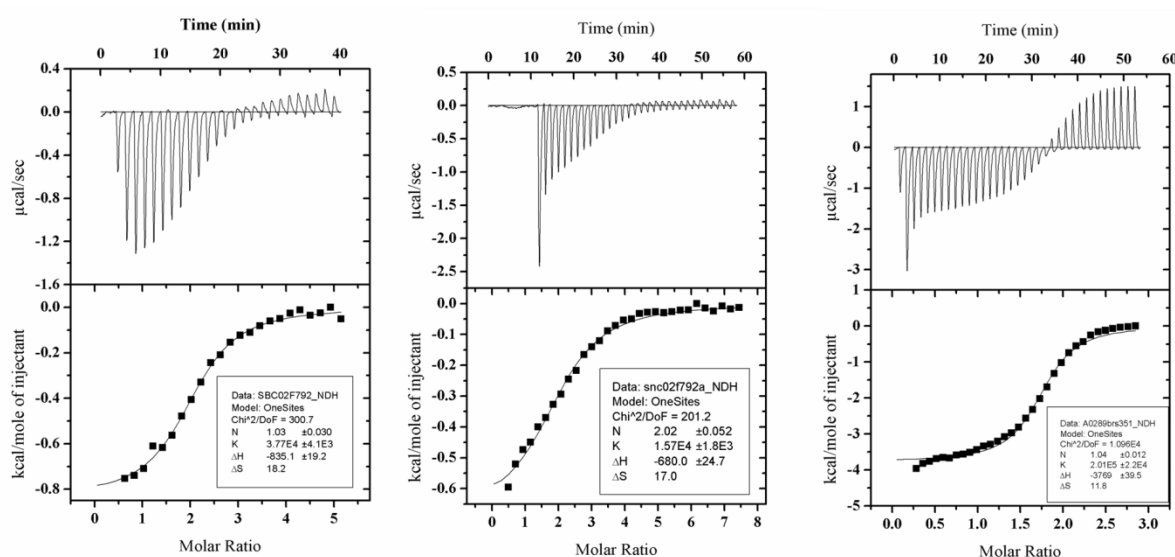


Figure 5.8: Isothermal calorimetric titration performed at 303 K, with solution of TBAF.3H₂O in acetonitrile added into the solution of **R18** (left) **R19** (middle) and **R20** (right) in acetonitrile.

processes were found thermodynamically favored. In all cases, entropy contribution is major, except for **R20**, in which case the binding is favored by enthalpy, in addition. Association constants and thermodynamic parameters are tabulated in table 5.11. The data clearly indicates association constants are lesser compared to the previously reported strapped calix[4]pyrroles with larger straps and this may be attributed to the repulsive interaction between lone pairs of oxygen atoms present in the strap and the anion. For example, receptor **R18** displayed about two order weaker association constant with fluoride ion as compared to analogous calix[4]pyrrole with longer strap (**R3**). Further, the selective affinity towards fluoride ion could be enhanced

further by one order, by introducing two bromine atoms onto the benzene moiety of the strap (in **R20**), probably owing to their electron withdrawing nature, which helps in reducing the repulsion between the lone pairs on oxygen atoms and the anion. This indicates introduction of more electron withdrawing group in aromatic ring of the strap may increase the association constants further. To lend further credence to this conclusion, anion binding study of **R21** could not be performed at this stage. Association constant derived for **R19** from two methods (fluorescence quenching and ITC) were found in good agreement with each other.

Table 5.11 Association constants (K_a) and thermodynamic data derived from ITC experiments, for the interactions of receptors **R18-R20** with TBAF.3H₂O in CH₃CN at 303 K.

	R3 ^{32a}	R8 ^{32b}	R18	R19	R20
K_a (M ⁻¹)	1.17×10^6	2.42×10^5 2.42×10^5 ^a	3.77×10^4	1.57×10^4 1.16×10^4 ^a	2.01×10^5
ΔH (kcal/mole)	-6.27	-14.20	-0.84	-0.68	-3.77
$T\Delta S$ (kcal/mole)	2.16	-6.50	5.45	5.15	3.58
ΔG (kcal/mole)	-8.42	-7.47	-6.29	-5.83	-7.34

^a determined by fluorescence spectroscopy.

5.5 Conclusion

In conclusion, we have synthesized four new calix[4]pyrroles with shortest possible strap. Anion binding study revealed that these receptors display exclusive selectivity towards fluoride ion, albeit weakly compared to the analogous calixp[4]yrroles with longer strap, which can be attributed to the very small binding domain of these receptors. The relatively weaker affinity can be explained on the basis of ‘lone pair-lone pair’ interaction between the oxygen atoms and the anion. Incorporation of electron withdrawing bromine atoms in the benzene ring of the strap increased the association constants by an order, without compromising on the anion selectivity.

5.6 Experimental Details

5.6.1 Crystallographic Details

Crystallographic data for **R18-20** was collected at 298 K on BRUKER SMART-APEX CCD diffractometer. Pertinent crystallographic data collection and refinement parameter are shown in table 5.12

Table 5.12 Crystallographic parameters of crystal of **R18-20**

Crystal data	R18	R19	R20
Formula unit	C ₃₄ H ₃₈ N ₄ O ₂	C ₃₈ H ₄₀ N ₄ O ₂	C ₃₄ H ₃₆ Br ₂ N ₄ O ₂
Formula wt.	534.69	584.75	692.48
Crystal system	monoclinic	monoclinic	monoclinic
T [K]	298 (2)	298 (2)	298 (2)
a [Å]	9.9443 (6)	15.9269 (17)	16.046 (14)
b [Å]	17.8590 (11)	13.3215 (14)	12.8353 (11)
c [Å]	16.3522	16.1486 (17)	16.4376 (14)
α [°]	90.00	90.00	90.00
β [°]	91.515 (10)	111.399 (2)	112.073 (2)
γ [°]	90.00	90.00	90.00
volume [Å ³]	2903.1 (3)	3190.05 (6)	3137.28 (5)
Space group	P 2 ₁ /n	C2/c	C2/c
Z'	0	0	0
Z	4	4	4
D _{calc} [g.cm ⁻³]	1.427	1.433	1.468
μ /mm ⁻¹	0.128	0.129	0.655
Reflns collected	30041	16838	16123
Unique reflns	5768	3289	3110
Observed reflns	3864	1689	1781
R(int)	0.0526	0.0474	0.0586
R ₁ [I > 2 σ (I)], wR ₂	0.0457, 0.1090	0.0464, 0.1135	0.0439, 0.1009
GOF	1.025	0.990	1.001

5.6.2.1 Synthesis of 1,2-bis-(acetoxyloxy)benzene (R10)

In a 3 necked 250 mL round bottom flask, 1,2-dihydroxybenzene (2.75 g; 25 mmol) and acetonitrile (200 mL) were taken. To this anhyds. K_2CO_3 (13.8 g; 100 mmol) was added with constant stirring. After 20 min, 1-bromoacetone (7.48 g; 55 mmol) in acetonitrile (15 mL) was added dropwise to the reaction mixture at 0 °C. After completion of the addition, the reaction mixture was stirred at room temperature for 24h and subsequently, the reaction mixture was filtered through Celite[®], solvent was evaporated and remaining residue was purified by column chromatography over silica gel (eluent: CH_2Cl_2) to obtain **R10** (2.32 g; 42 %) as yellow low melting solid. IR (KBr): ν (cm^{-1}) 1736.1; 1H NMR ($CDCl_3$): δ in ppm 6.96-6.93 (m, 2H), 6.84 - 6.80 (m, 2H), 4.61 (s, 4H), 2.30 (s, 6H); ^{13}C NMR ($CDCl_3$) δ in ppm 205.70, 147.81, 122.48, 114.71, 74.20, 26.60; HRMS m/z , $[M+1]$: 223.0975 (calculated for $C_{12}H_{15}O_4 = 223.0970$).

5.6.2.2 Synthesis of 1,1'-(naphthalene-2,3-diylbis(oxy))dipropan-2-one (R11)

A mixture of 2,3-dihydroxynaphthalene (1.60 g; 10 mmol) and anhyds. K_2CO_3 (5.50 g; 40 mmol) in dry acetonitrile (100 mL) was stirred well for about 20 min, and then 1-bromoacetone (3.14 g; 22 mmol) was added dropwise to the reaction mixture at 0 °C. After addition was over, the reaction mixture was stirred at room temperature. After 24 h reaction mixture was filtered through Celite[®], solvent was evaporated and remaining residue was purified by column chromatography over silica gel (25 % ethyl acetate in hexane) and the desired product was collected as the first major band and vacuum dried, to obtain compound **R11** as a white solid (2.28 g; 84 %). Melting point: 77 °C; IR (KBr): ν (cm^{-1}) 2940.78-2860.69, 1714.87; 1H NMR ($CDCl_3$): δ in ppm 7.65 (m, 2H), 7.37-7.35 (m, 2H), 7.04 (s, 2H), 4.70 (s, 4H), 2.36 (s, 6H); ^{13}C NMR ($CDCl_3$) δ in ppm 205.54, 147.67, 129.43, 126.56, 125.05, 109.00, 73.75, 26.75; HRMS m/z , $[M+H]$: 273.1128 (calculated for $C_{16}H_{17}O_4 = 273.1127$).

5.6.2.3 Synthesis of 1,1'-(4,5-dibromo-1,2-phenylene)bis(oxy)dipropan-2-one (R12)

A mixture of 4,5-dibromobenzene-1,2-diol (2.68 g; 10 mmol) and anhyds. K_2CO_3 (5.50 g; 40 mmol) in dry acetonitrile (100 mL) was stirred well for about 20 min, and then 1-bromoacetone (3.14 g, 22 mmol) was added dropwise to the reaction mixture at 0 °C. After addition was completed, reaction mixture was stirred at room temperature for 24 h. Subsequently, the reaction mixture was filtered through Celite[®], solvent was evaporated and remaining residue was purified by column chromatography over silica gel (30 % ethyl acetate in

hexane) and the desired product was collected as the first major band and vacuum dried, to obtain compound **R12** as a white solid (1.71 g; 45 %). Melting point: 135 °C; IR (neat): ν (cm⁻¹) 1724.45; ¹H NMR (CDCl₃): δ in ppm 7.03 (s, 2H), 4.62 (s, 4H), 2.30 (s, 6H); ¹³C NMR (CDCl₃) δ in ppm 203.92, 147.67, 125.34, 119.32, 116.62, 74.20, 26.66; HRMS m/z , [M+1]: 378.9192 (calculated for C₁₂H₁₂Br₂O₄ = 378.9181).

5.6.2.4 Synthesis of 1,1'-(4-nitro-1,2-phenylene)bis(oxy)dipropen-2-one (R13)

A mixture of 4-nitrobenzene-1,2-diol (1.55 g; 10 mmol) and anhyds. K₂CO₃ (5.50 g; 40 mmol) in dry acetonitrile (100 mL) was stirred well for about 20 min and then 1-bromoacetone (3.14 g; 22 mmol) was added dropwise to the reaction mixture at 0 °C. After addition was finished, reaction mixture was stirred at room temperature for 24 h. Subsequently, the reaction mixture was filtered through Celite®, solvent was evaporated and remaining residue was purified by column chromatography over silica gel (30 % ethyl acetate in hexane) and the desired product was collected as the first major band and vacuum dried, to yield compound **R12** as a light yellow solid (2.19 g; 45 %). Melting point: 145 °C; IR (neat): ν (cm⁻¹) 1738.45; ¹H NMR (CDCl₃): δ in ppm 7.92 (d, 1H, J = 11.2 Hz), 7.68 (s, 1H), 6.83(d, 1H, J = 8.4 Hz), 4.75 (s, 4H), 2.34 (s, 6H); ¹³C NMR (CDCl₃) δ in ppm 203.38, 203.17, 153.08, 147.41, 142.26, 118.75, 112.76, 109.30, 73.77, 73.74, 26.68, 26.65; HRMS m/z , [M+Na]: 290.0638 (calculated for C₁₂H₁₃NNaO₆ = 290.0641).

5.6.2.5 Synthesis of 1,2-bis(2,2-di(1H-pyrrol-2-yl)propoxy)benzene (R14)

In a 2 necked 100 mL round bottom flask, 1,2-bis-(acetonyloxy)benzene (500 mg; 2.25 mmol) and pyrrole (6.23 mL; 90 mmol) were added under N₂ atmosphere. After the compound dissolved, TFA (175 μ L; 2.25 mmol) was added slowly and reaction mixture was stirred at 60 °C. After 6 h, the reaction mixture was quenched by adding triethylamine (~2 mL). Then excess pyrrole was removed under reduced pressure and the remaining mass was purified by column chromatography over silica gel (eluent: CH₂Cl₂) to obtain **R14** (500 mg; 45 %) as colorless dense liquid mass. IR (neat): ν = 3416.24 cm⁻¹; ¹H NMR (CDCl₃): δ in ppm 8.28 (brs, 4H), 6.91 (s, 4H), 6.45 (s, 4H), 6.10-6.08 (m, 8H), 4.30 (s, 4H), 1.68 (s, 6H); ¹³C NMR (CDCl₃) δ in ppm 148.14, 135.34, 121.67, 117.74, 113.04, 107.77, 104.75, 76.63, 40.56, 25.27; HRMS m/z , [M⁺]: 454.2365 (calculated for C₂₈H₃₀N₄O₂: 454.2369).

5.6.2.6 Synthesis of 2,3-bis(2,2-di(1H-pyrrol-2-yl)propoxy)naphthalene (R15)

To a mixture of **R11** (272 mg; 1 mmol) and pyrrole (3.0 mL; 43 mmol), trifluoroacetic acid (75 μ L; 1 mmol) was added at about 60 °C and the reaction mixture was stirred for about 4 h at this temperature. Then the reaction was quenched with triethylamine (1 mL). Excess reagents were removed under reduced pressure to get the crude product, which was purified by column chromatography over silica gel (25 % ethyl acetate in hexane) to obtain the pure product **R6** (394 mg; 78 %). Melting point: 155.5 °C; IR (neat): ν (cm^{-1}) 3391.16, 2932.06-2858.76; ^1H NMR (CDCl_3): δ in ppm 8.26 (brs, 4H), 7.66 - 7.64 (m, 2H), 7.34 - 7.32 (m, 2H), 7.15 (s, 2H), 6.48 - 6.46 (m, 4H), 6.11 - 6.09 (m, 8H), 4.43 (s, 4H), 1.73 (s, 6H); ^{13}C NMR (CDCl_3) δ in ppm 148.27, 135.26, 129.36, 126.51, 126.69, 117.89, 107.89, 107.81, 104.84, 76.39, 40.11, 25.38; HRMS m/z , $[\text{M}+\text{H}]$: 505.2604 (calculated for $\text{C}_{32}\text{H}_{33}\text{N}_4\text{O}_2$: 505.2604).

5.6.2.7 Synthesis of 1,2-bis(2,2-di(1H-pyrrol-2-yl)propoxy)-4,5-dibromobenzene (R16)

To a mixture of **R12** (380 mg; 1 mmol) and pyrrole (3.0 mL; 43 mmol), trifluoroacetic acid (75 μ L; 1mmol) was added at about 60 °C and the mixture was stirred for about 4 h at this temperature. Then the reaction mixture was quenched with triethylamine (1 mL). Excess reagents were removed under reduced pressure to get the crude product, which was purified by column chromatography over silica gel (25 % ethyl acetate in hexane) to obtain the pure product **R16** (276 mg; 45 %). Melting point: 165.5 °C; IR (neat): ν (cm^{-1}) 3395.16; ^1H NMR (CDCl_3): δ in ppm 8.12 (brs, 4H), 7.07 (s, 2H), 6.49 - 6.47 (m, 4H), 6.11 - 6.06 (m, 8H), 4.24 (s, 4H), 1.66 (s, 6H); ^{13}C NMR (CDCl_3) δ in ppm 148.00, 134.82, 117.93, 117.46, 115.56, 108.0, 104.96, 40.17, 29.85, 25.19; HRMS m/z , $[\text{M}^+]$: 610.0582 (calculated for $\text{C}_{28}\text{H}_{28}\text{Br}_2\text{N}_4\text{O}_2$: 610.0579).

5.6.2.8 Synthesis of 1,2-bis(2,2-di(1H-pyrrol-2-yl)propoxy)-4-nitrobenzene (R17)

To a mixture of **R13** (267 mg; 1 mmol) and pyrrole (3.0 mL; 43 mmol), trifluoroacetic acid (75 μ L; 1mmol) was added at about 60 °C and mixture was stirred for about 4 h at this temperature. Then reaction the reaction mixture was quenched with triethylamine (1 mL). Excess reagents were removed under reduced pressure to get the crude product, which was purified by column chromatography over silica gel (40 % ethyl acetate in hexane) to obtain the pure product **R17** (280 mg; 56 %). Melting point: 185.5 °C; IR (KBr): ν (cm^{-1}) 3400.28; ^1H NMR (CDCl_3): δ in ppm 8.07 (brs, 4H), 7.91 - 7.88 (m, 1H) 7.76 (s, 1H), 6.92 (d, 1H, $J = 9.2$ Hz), 6.51 (s, 4H),

6.11 - 6.09 (m, 8H), 4.38 (s, 4H), 1.70 (s, 6H); ^{13}C NMR (CDCl_3) δ in ppm 153.34, 147.86, 141.65, 139.60, 134.43, 118.20, 118.07, 117.90, 117.11, 110.98, 107.98, 107.98, 107.67, 104.9, 104.39, 76.62, 40.07, 25.06, 25.02; HRMS m/z , $[\text{M}+\text{H}]$: 500.2293 (calculated for $\text{C}_{28}\text{H}_{30}\text{N}_5\text{O}_4$: 500.2298).

5.6.2.9 Synthesis of R18

To a solution of compound **R14** (330 mg; 0.73 mmol) in acetone (85 mL), $\text{BF}_3\cdot\text{OEt}_2$ (3 μL ,) was added. The solution was stirred at room temperature for 15 min and quenched by triethylamine (~1 mL) and solvent was evaporated and remaining mass was purified by column chromatography over silica gel (10 % ethyl acetate in hexane) to yield **R18** (78 mg; 20 %) as off-white solid. Melting point: 185.5 °C (decomposed); IR (KBr): ν (cm^{-1}) 3404.67, 3096.03; ^1H NMR (CDCl_3): δ in ppm 8.00 (brs, 4H), 6.86 - 6.85 (m, 2H), 6.75 - 6.72 (m, 2H), 6.03 - 6.02 (m, 4H), 5.98 - 5.96 (m, 4H), 4.18 (s, 4H), 1.72 (s, 6H), 1.54 (s, 6H), 1.50 (s, 6H); ^{13}C NMR (CDCl_3) δ in ppm 147.93, 137.34, 134.79, 120.91, 111.55, 104.79, 104.27, 79.11, 40.42, 36.07, 31.23, 30.71, 23.98; HRMS m/z , $[\text{M}+\text{H}]$: 535.3074 (calculated for $\text{C}_{34}\text{H}_{39}\text{N}_4\text{O}_2$: 535.3073).

5.6.2.10 Synthesis of R19

To a solution of compound **R15** (252 mg; 0.5 mmol) in acetone (60 mL), $\text{BF}_3\cdot\text{OEt}_2$ (2 μL ,) was added. The solution was stirred at room temperature for 15 min and quenched by triethylamine (~1 mL) and solvent was evaporated and remaining mass was purified by column chromatography over silica gel (10 % ethyl acetate in hexane) to obtain **R19** (91 mg; 31 %) as off-white solid. Melting point: 205.5 °C; IR (KBr): ν (cm^{-1}) 3454.67, 3104.07; ^1H NMR (CDCl_3): δ in ppm 7.97 (brs, 4H), 7.65 - 7.63 (m, 2H), 7.34 - 7.31 (m, 4H), 7.00 (s, 2H), 6.03 - 6.01 (m, 4H), 5.99 - 5.98 (m, 4H), 4.31 (s, 4H), 1.77 (s, 6H), 1.53 (s, 6H), 1.51 (s, 6H); ^{13}C NMR (CDCl_3) δ in ppm 148.40, 137.35, 134.65, 129.09, 126.37, 124.36, 107.25, 104.94, 104.37, 79.41, 40.46, 36.07, 31.23, 30.62, 24.11; HRMS m/z , $[\text{M}^+]$: 585.3229 (calculated for $\text{C}_{38}\text{H}_{41}\text{N}_4\text{O}_2$: 585.3230).

5.6.2.11 Synthesis of R20

To a solution of compound **R16** (300 mg; 0.49 mmol) in acetone (60 mL), $\text{BF}_3\cdot\text{OEt}_2$ (2 μL ,) was added. The solution was stirred at room temperature for 15 min and quenched by triethylamine (~1 mL) and solvent was evaporated and remaining mass was purified by column

chromatography over silica gel (10 % ethyl acetate in hexane) to yield **R20** (61 mg; 18 %) as off-white solid. Melting point: 210 °C (decomposed); IR (KBr): ν (cm⁻¹) 3454.67, 3146.58; ¹H NMR (CDCl₃): δ in ppm 7.94 (s, 4H), 6.93 (s, 2H), 6.03 - 6.02 (m, 4H), 5.97 - 5.95 (m, 4H), 4.14 (s, 4H), 1.71 (s, 6H), 1.54 (s, 6H), 1.49 (s, 6H); ¹³C NMR (CDCl₃) δ in ppm 147.77, 137.47, 134.29, 116.50, 115.09, 104.92, 104.45, 79.76, 40.48, 36.06, 31.09, 30.48, 23.97; HRMS *m/z*, [M⁺]: 696.1276 (calculated for C₃₃H₃₄Br₂N₄O₂: 693.1236).

5.6.2.12 Synthesis of R21

To a solution of compound **R17** (300 mg; 0.49 mmol) in acetone (60 mL), BF₃·OEt₂ (2 μ L) was added. The solution was stirred at room temperature for 15 min and quenched by triethylamine (~1 mL) and solvent was evaporated and the residue was purified by column chromatography over silica gel (10 % ethyl acetate in hexane) to obtain **R21** (61 mg; 18 %) as pale yellow solid. Melting point: 230 °C (decomposed); IR (KBr): ν (cm⁻¹) 3454.67, 3146.58; ¹H NMR (CDCl₃): δ in ppm 7.86 (d, 1H, *J* = 2.4 Hz), 7.82 (brs, 4H), 6.81(d, 1H, *J* = 2.4 Hz), 7.63 (d, 1H, *J* = 8.8 Hz), 6.04 - 5.97 (m, 8H), 4.27 (s, 4H), 2.05 (s, 6H), 1.74 (d, 6H), 1.49 (s, 6H); ¹³C NMR (CDCl₃) δ in ppm 153.23, 147.08, 141.64, 137.62, 137.42, 134.21, 133.97, 118.01, 110.97, 107.33, 105.05, 105.02, 104.56, 80.11, 79.88, 40.43, 36.05, 31.14, 30.38, 29.83, 24.00, 23.94; HRMS *m/z*, [M+H]: 580.2926 (calculated for C₃₄H₃₈N₅O₄: 580.2924).

5.7 References

1. Fischer, E. *Chem. Ber.* **1894**, 27, 2985.
2. (a) Simmons, H. E.; Park, C. H. *J. Am. Chem. Soc.* **1968**, 90, 2428. (b) Park, C. H.; Simmons, H. E. *J. Am. Chem. Soc.* **1968**, 90, 2429. (c) Park, C. H.; Simmons, H. E. *J. Am. Chem. Soc.* **1968**, 90, 2431.
3. Graf, E.; Lehn, J. M. *J. Am. Chem. Soc.* **1976**, 98, 6403.
4. Dietrich, B.; Guilhem, J.; Lehn, J. M.; Pascard, C.; Sonveaux, E. *Helv. Chim. Acta* **1984**, 67, 91.
5. Hosseini, M. W.; Lehn, J. M. *Helv. Chim. Acta* **1988**, 71, 749.
6. Dietrich, B.; Dilworth, B.; Lehn, J. M.; Pascard, C.; Souchez, J. P. *Helv. Chim. Acta* **1996**, 79, 569.

7. (a) Dietrich, B.; Lehn, J. M.; Guilhem, J.; Pascard, C. *Tetrahedron Lett.* **1989**, 30, 4125.
(b) Hossain, M. A.; Llinares, M.; Miller, C. A.; Seib, L.; Bowman-James, K. *Chem. Commun.* **2000**, 2269.
8. Lehn, J. M.; Meric, R.; Vigneron, J. P.; Bkouche-Waksman, I.; Pascard, C. *J. Chem. Soc., Chem. Commun.* **1991**, 62.
9. Menif, R.; Reibenspies, J.; Martell, A. E. *Inorg. Chem.* **1991**, 30, 3446.
10. (a) Mason, S.; Clifford, T.; Seib, L.; Kuczera, K.; Bowman-James, K. *J. Am. Chem. Soc.* **1998**, 120, 8899. (b) Mason, S.; Llinares, J. M.; Morton, M.; Clifford, T.; Bowman-James, K. *J. Am. Chem. Soc.* **2000**, 122, 1814. (c) Arnaud-Neu, F.; Fuangswasdi, S.; Maubert, B.; Nelson, J.; McKee, V. *Inorg. Chem.* **2000**, 39, 573. (d) Hynes, M. J.; Maubert, B.; McKee, V.; Town, R. M.; Nelson, J. *J. Chem. Soc., Dalton Trans.* **2000**, 2853. (e) Aguilar, J. A. Clifford, T.; Danby, A.; Llinares, J. M.; Mason, S.; García-Espana, E.; Bowman-James, K. *Supramol. Chem.* **2001**, 13, 405. (f) Maubert, B. M.; Nelson, J.; McKee, V.; Town, R. M.; Pál, I. *J. Chem. Soc., Dalton Trans.* **2001**, 1395. (g) Nelson, J.; Nieuwenhuyzen, M.; Pál, I.; Town, R. M. *Chem. Commun.* **2001**, 2266. (h) Farrell, D.; Gloe, K.; Gloe, K.; Goretzki, G.; McKee, V.; Nelson, J.; Nieuwenhuyzen, M.; Pál, I.; Stephan, H.; Town, R. M.; Wichmann, K. *Dalton Trans.* **2003**, 1961.
11. Nelson, J.; Nieuwenhuyzen, M.; Pál, I.; Town, R. M. *Dalton Trans.* **2004**, 229.
12. Hossain, M. A.; Llinares, J. M.; Mason, S.; Morehouse, P.; Powell, D.; Bowman-James, K. *Angew. Chem. Int. Ed.* **2002**, 41, 2335.
13. Heyer, D.; Lehn, J. M. *Tetrahedron Lett.* **1986**, 27, 5869.
14. Llioudis, C. A.; Tocher, D. A.; Steed, J. W. *J. Am. Chem. Soc.* **2004**, 126, 12395.
15. (a) Gale, P. A.; Sessler, J. L.; Král, V.; Lynch, V. *J. Am. Chem. Soc.* **1996**, 118, 5140. (b) Allen, W. E.; Gale, P. A.; Brown, C. T.; Lynch, V.; Sessler, J. L. *J. Am. Chem. Soc.*, **1996**, 118, 12471.
16. (a) Gale, P. A.; Genge, J. W.; Král, V.; McKervery, M. A.; Sessler, J. L.; Walker, A. *Tetrahedron Lett.* **1997**, 38, 8443. (b) Gale, P. A.; Sessler, J. L.; Lynch, V.; Sansom, P. I. *Tetrahedron Lett.* **1996**, 37, 7881.
17. Turner, B.; Botoshansky, M.; Eichen, Y. *Angew. Chem. Int. Ed.* **1998**, 37, 2475.

18. (a) Cafeo, G.; Kohnke, H.; La Torre, G. L.; White, A. J. P.; Williams, D. J. *Angew. Chem. Int. Ed.* **2000**, *39*, 1496. (b) Cafeo, G.; Kohnke, H.; Parisi, M. F.; Nascone, R. P.; La Torre, G. L.; Williams, D. J. *Org. Lett.* **2002**, *4*, 2695.
19. Cafeo, G.; Kohnke, H.; La Torre, G. L.; White, A. J. P.; Williams, D. J. *Chem. Commun.* **2000**, 1207.
20. Cafeo, G.; Kohnke, H.; La Torre, G. L.; Parisi, M. F.; Nascone, R. P.; White, A. J. P.; Williams, D. J. *Chem. Eur. J.* **2002**, *8*, 3148.
21. Chacón-García, L.; Chávez, L.; Cacho D. R.; Altamirano-Hernández, J. *Beilstein J. Org. Chem.* **2009**, *5*, No. 2.
22. (a) Sessler, J. L.; Anzenbacher Jr., P.; Shriver, J. A.; Jursíková, K.; Lynch, V. M.; Marquez, M. *J. Am. Chem. Soc.* **2000**, *122*, 12061. (b) Anzenbacher Jr., P.; Try, A. C.; Miyaji, H.; Juriskova, K.; Lynch, V. M.; Marquez, M.; Sessler, J. L. *J. Am. Chem. Soc.* **2000**, *122*, 10268.
23. Bedolla-Medrano, M.; Chacón-García, L.; Contreras-Celedón, C. A.; Campos-García, J. *Tetrahedron Lett.* **2011**, *52*, 136.
24. (a) Sessler, J. L.; An, D.; Cho, W. -S.; Lynch, V. *Angew. Chem. Int. Ed.* **2003**, *42*, 2278. (b) Sessler, J. L.; An, D.; Cho, W. -S.; Lynch, V.; Marquez, M. *Chem. Commun.* **2005**, 540.
25. Sessler, J. L.; An, D.; Cho, W. -S.; Lynch, V.; Marquez, M. *Chem. Eur. J.* **2005**, *11*, 2001.
26. (a) Sessler, J. L.; An, D.; Cho, W. -S.; Lynch, V. *J. Am. Chem. Soc.* **2003**, *125*, 13646. (b) Sessler, J. L.; An, D.; Cho, W. -S.; Lynch, V.; Yoon, D. W.; Hong, S. J.; Lee, C. H. *J. Org. Chem.* **2005**, *70*, 1511.
27. Cafeo, G.; Kohnke, F. H.; White, A. J. P.; Garozzo, D.; Messina, A. *Chem. Eur. J.* **2007**, *13*, 649.
28. Mahanta, S. P.; Kumar, B. S.; Baskaran, S.; Sivasankar, C.; Panda, P. K. *Org. Lett.* **2012**, *14*, 548.
29. Chandra, B.; Mahanta, S. P.; Pati, N. N.; Baskaran, S.; Kanaparthi, R. K.; Sivasankar, C.; Panda, P. K. *Org. Lett.* **2013**, *15*, 306.
30. Yoon, D. W.; Hwang, H.; Lee, C. H. *Angew. Chem. Int. Ed.* **2002**, *41*, 1757.

31. (a) Lee, C. H.; Na, H. K.; Yoon, D. W.; Won, D. H.; Cho, W. S.; Lynch, V. M.; Shevchuk, S. V.; Sessler, J. L. *J. Am. Chem. Soc.* **2003**, *125*, 7301. (b) Lee, C. -H.; Lee, J. S.; Na, H. K.; Yoon, D. W.; Miyaji, H.; Cho, W. S.; Sessler, J. L. *J. Org. Chem.* **2005**, *70*, 2067.
32. (a) Samanta, R.; Mahanta, S. P.; Chaudhuri, S.; Panda, P. K.; Narahari, A. *Inorg. Chim. Acta.* **2011**, *372*, 281. (b) Samanta, R.; Mahanta, S. P.; Ghanta, S.; Panda, P. K. *RSC Adv.* **2012**, *2*, 7974.

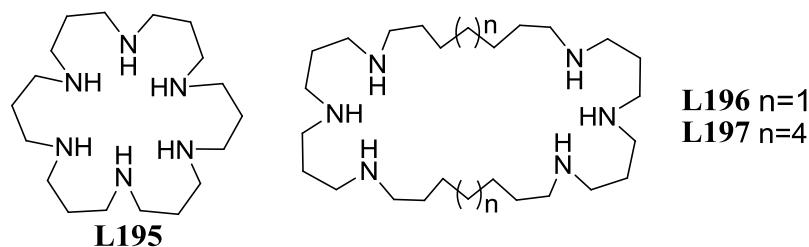
CHAPTER 6

Strapping One Calix[4]pyrrole with Another: a Flexible Biscalix[4]pyrrole

6.1 Introduction

Di- and tri-carboxylates are critical components of numerous metabolic processes including, for instance, the citric acid and glyoxylate. They also play an important role in the generation of high energy phosphate bonds and in the biosynthesis of important intermediates.¹ A large number of carboxylic acids are of critical biological relevance and are important metabolites that may have altered proportions in pathological tissues such as tumors.² For example, *trans,trans*-muconic acid is a metabolite of carcinogenic benzene in humans.³ Dicarboxylic acids of chain length C6–C10 have been identified in the urine of patients with glycogen storage disease type I and type III as a result of inadequate gluconeogenesis with consequent alteration in the metabolic oxidative pathway of fatty acids.⁴ Maleate is a well-known inhibitor of the Krebs cycle and its implication in different kidney diseases has been widely described.⁵ Thus, the di- and tri-carboxylate ions are important species for recognition for the chemists. Selective recognition of monovalent and polyvalent anions differs mainly due to their nature in the distribution of charges. Sometimes total charge of these polyvalent anions is distributed evenly throughout the anion (i.e. carbonate, sulfate, sulfite, phosphate etc.) and sometimes this charge distribution is not possible mainly due to their structural nature (i.e. di-carboxylates, tri-carboxylates). As a result single binding domain is not sufficient for the recognition of these di and tri-carboxylates ions and this requirement was understood in the very early days of anion receptor chemistry.

In 1981, Lehn and coworkers demonstrated that aza crown ether **L195** was capable of binding di- and poly anions in its hexaprotonated form (log K_a = 4.0, 3.8, 3.3, 2.4, 4.7, 3.9, 3.4,



6.5, and 8.9 for sulphate, oxalate, malonate, succinate, citrate, Co(CN)_6^{3-} , AMP, ADP and ATP respectively in 0.1 M TMACl).⁶ Whereas, with monovalent anions no interactions were observed may be due to competition with chloride ion. In order to improve the selectivity towards the dicarboxylate, Lehn and coworkers prepared several isomeric hexamine receptors, **L196** and **L197** in which bridges of different length are used to link the tripod-like subunits.⁷ Where

receptor **L195** shows preference for oxalate ion in its various protonated forms ($\log K_a = 3.8, 3.2, 2.6$ for H_6L195^{6+} , H_5L195^{5+} , H_4L195^{4+} , respectively in 0.01 M TMACl) over anionic malonate, glutarate, adipate and pimelate. On the other hand, **L196** shows preference for succinate ($\log K_a = 3.4, 2.85, 2.45$ for H_6L196^{6+} , H_5L196^{5+} , H_4L196^{4+} , respectively in 0.1 M TMACl) and glutarate ions ($\log K_a = 3.4, 2.9, 2.5$ for H_6L196^{6+} , H_5L196^{5+} , H_4L196^{4+} , respectively in 0.01 M TMACl) over anionic oxalate, malonate, adipate and pimelate. Receptor **L197** shows high selectivity for the oxalate ion ($\log K_a = 6.3, 4.7, 2.85$ for H_6L197^{6+} , H_5L197^{5+} , H_4L197^{4+} , respectively in 0.01 M TMACl). It also showed appreciable selectivity towards pimelate ($\log K_a = 3.4, 2.85, 2.70$ for H_6L197^{6+} , H_5L197^{5+} , H_4L197^{4+} , respectively in 0.01 M TMACl) and suberate ions ($\log K_a = 3.45, 3.0, 2.65$ for H_6L197^{6+} , H_5L197^{5+} , H_4L197^{4+} , respectively in 0.01 M TMACl). The selectivity for certain dicarboxylate presents a striking structural dependence. Each receptor, **L196** and **L197** showed a marked selectivity peak among the homologous dicarboxylate substrates (Figure 6.1). Furthermore, the selectivity peak shifts from $m = 2, 3$ to $m = 5, 6$ on going from **L196** to **L197** this corresponds to the same increase in length, by three

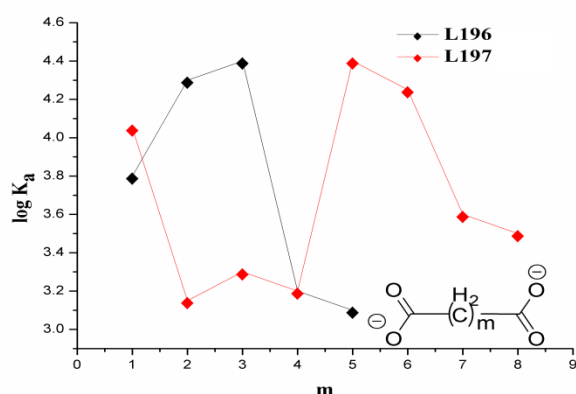


Figure 6.1: Graphical representation of the stability constants ($\log K_a$) of the complexes formed by **L196** to **L197** with the various dicarboxylates as a function of chain length.

methylene groups, both for the most strongly bound dicarboxylates and for the $(CH_2)_n$ bridges separating the triammonium binding units in **L196** ($n = 7$) and **L197** ($n = 10$). Though, no explanation was provided for the higher affinity of **L197** for the oxalate ion. The chain length selection observed describes a linear molecular recognition process, which may be attributed to structural complementarity. Two binding subunits cooperate for substrate binding. The anionic groups of the dicarboxylate would each interact with a triammonium unit of the receptor, the

polymethylene chain stretching between the polymethylene bridges of the macrocycle. Highest stability of the complex corresponds to the best fit between substrate length and site separation of the receptor (Figure 6.2). Few years later same group have reported **L198** which displayed

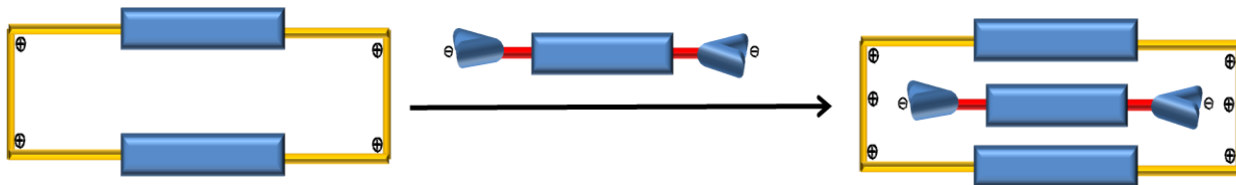
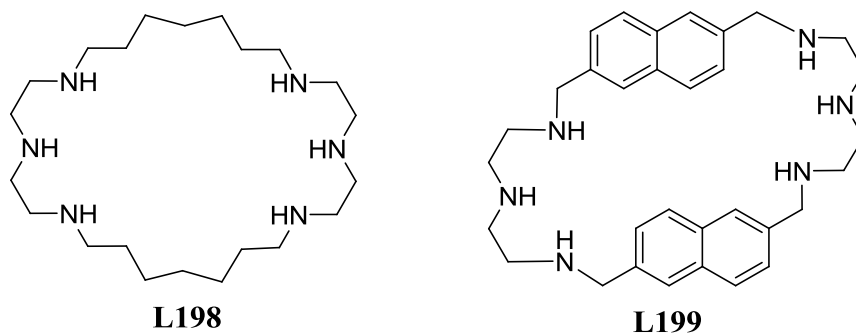


Figure 6.2 Schematic representation of length based recognition of α,ω -dicarboxylates.

selectivity towards glutarate ($\log K_a = 6.1, 5.5, 2.95$ for H_6L198^{6+} , H_5L198^{5+} , H_4L198^{4+} , respectively in 0.1 M TMACl).⁸ In 1993, **L199** containing two flat naphthalene subunits that can provide π -stacking along with two charged diethylenetriamine subunits was reported, where complexation with a dianion could thus be formed via a combination of hydrophobic (π -stacking), electrostatic and hydrogen bonding interactions.^{9c} According to the NMR spectroscopic analysis result, tetraprotonated **L199** displays a preference for terephthalate (\log



$K_a = 5.2$), ATP ($\log K_a = 5.2$), ADP ($\log K_a = 5.1$) and isophthalate ($\log K_a = 5$), over the other anions such as malate ($\log K_a = 4.3$), fumarate ($\log K_a = 4.4$), AMP ($\log K_a = 4.3$), CMP ($\log K_a = 3.7$) and UMP (4.1) in aqueous solution at pH 6. The stronger binding for the aromatic dicarboxylates are mainly due the π - π stacking interaction between benzene and naphthalene rings (Figure 6.3). Subsequent to this work from Lehn and coworkers, many groups have developed various ways to prepare dicarboxylate receptors. So far approaches based on the use of positively charged binding sites, such as protonated polyammonium macrocycles⁷⁻⁹ and guanidinium units¹⁰ have been extensively explored by the groups of Lehn, Kimura, Schmidtchen, and Anslyn. The use of Lewis acids has also been extensively investigated by

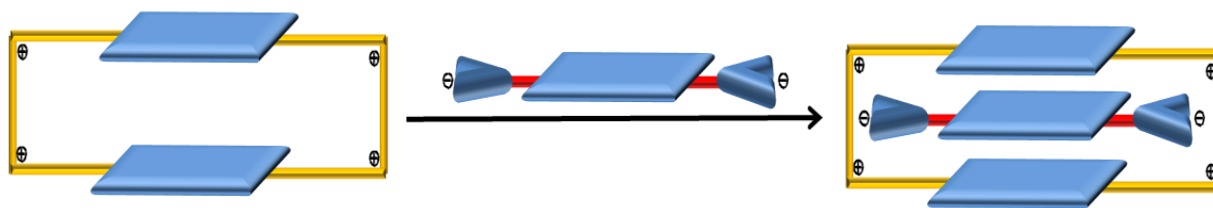


Figure 6.3: Schematic representation of the proposed interaction process involved in the binding of dianionic aromatic substrates by **L199**.

Beer¹¹ and Reinhoudt.¹² In addition, Hamilton has developed neutral receptors featuring hydrogen-bonding donors derived from urea- and thiourea-binding subunits.¹³ While, the detailed approaches used vary, in all cases, chelation of the dicarboxylate substrates is achieved via the formation of several, often cooperative, noncovalent bonds. In many cases, it has been proved necessary to add extra stabilizing interactions, in order to increase binding efficacy and selectivity. Further, in the case of chiral dicarboxylates, enantiomeric recognition has been achieved only at the neutral, deprotonated (i.e., free acid) level, not with the dianionic form, existent at physiological pH.¹⁴ However, one fundamental aspect understood very clearly is the presence of two separate binding domains in a single receptor is an useful way. Almost immediately after the discovery of anion binding properties of protonated polypyrrolic macrocycle (sapphyrin) researcher implemented the idea of two binding domain receptors. As a result, novel sapphyrin dimer **L200** synthesized by Sessler, produced supramolecular complexes, which could be sustained under experimental condition with 4-nitrophthalate, 5-nitroisophthalate, and nitroterephthalate.^{15a} Detailed inspection of binding constants for anions revealed that **L200** is both an excellent and inherently selective receptor for dicarboxylate ions (table 6.1). Higher affinity for the benzoate was ascribed to π - π interaction between receptor and

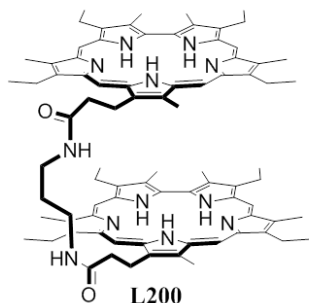
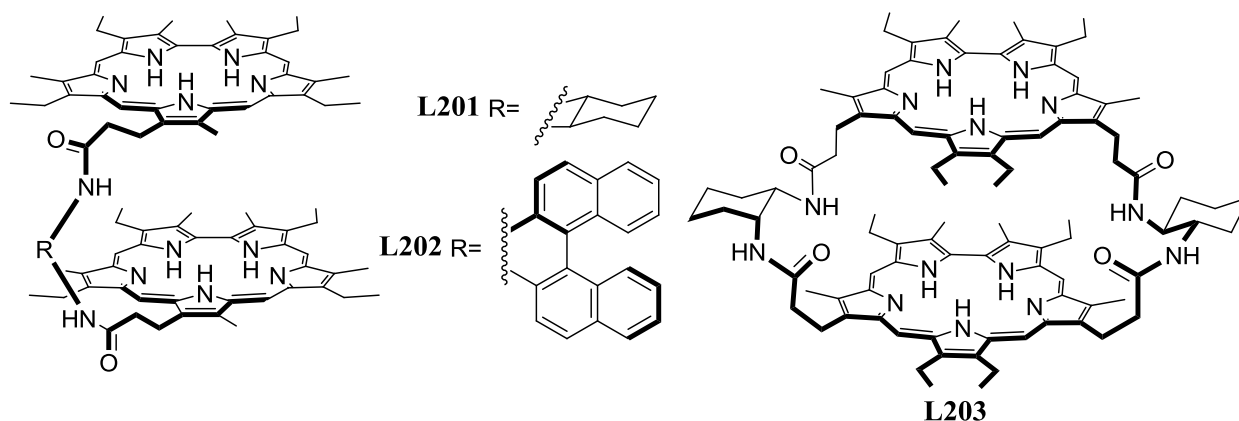


Table 6.1 K_a (M^{-1}) for **L200** and various anions in methanol at 293 K.

Anion	K_a	Selectivity ^c
phthalate	$K_1 = 310^a$ $K_2 = 2801^a$	1.2
isophthalate	2400 ^a , 2500 ^b	9.4
5-nitroisophthalate	5300 ^b	20.4
terephthalate	4600 ^a	17.7
nitroterephthalate	9100 ^a	35.0
benzoate	$K_1, K_2 = 1380^a$	5
oxalate	260 ^b	1
malonate	450 ^b	1.7

^a measured by NMR experiment, ^b measured by visible spectroscopy ^c Relative to the worst bound substrate, oxalate.

anion, which could be clearly observed from ^1H NMR study. Interestingly, this receptor also displayed a preference for linear over bent substrates and aromatic over aliphatic substrates that is remarkable given the inherently flexible nature of this receptor. Two years later much detailed study along with three new receptors; **L201**, **L202** and **L203** were also reported.^{15b} Two different chiral diamines, namely, (S)-2,2'-diamino-1,1'-binaphthalene and (1S,2S)-1,2-diaminocyclohexane were used to serve as stereogenic linkers for these chiral receptors. These receptors were used for chiral recognition of few dicarboxylate ions. All the dimers formed strong complexes with N-Cbz-aspartate and N-Cbz-glutamate and displayed excellent selectivity



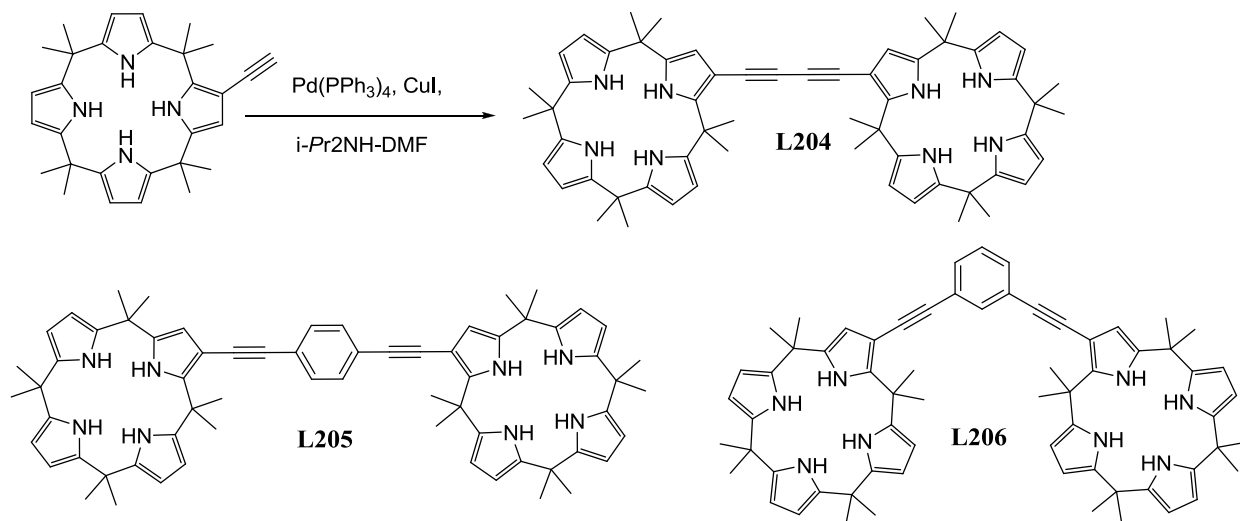
towards substrates that differ in length by only one carbon atom (table 6.2). It was found that the open chain receptors **L201** and **L202** (as well as congener **L200**) bind glutamate and aspartate anions with high affinity (and show a selectivity for the former substrate). The enantioselectivity of the binaphthalene-containing receptor **L202** is higher than that of the diaminocyclohexane-derived dimer **L201**. The cyclic dimer **L203**, on the other hand, displays a lower affinity for these anionic substrates. Although, shows excellent chiral discrimination for a pair of glutamate enantiomers.

Table 6.2 Dicarboxylate binding properties of sapphyrin dimers in dichloromethane solutions containing 5% methanol (protected amino acid substrates were used as their bis-TMA salts).

Anion	L200	L201	L202	L203
N-Cbz-L-Asp	159,100	45,000	20,600	16,700
N-Cbz-D-Asp		38,900	43,500	9,700
N-Cbz-L-Glu	224,000	112,700	324,500	3,800
N-Cbz-D-Glu		119,900	217,100	16,200

6.2 Calix[4]pyrrole Dimers and Anion Recognition

After the discovery of the anion binding property of the calix[4]pyrrole in 1996, first dimeric calix[4]pyrroles **L204-206** was reported by Sessler and coworkers in 2000.¹⁶ However, only **L204** was employed for the anion binding study with isophthalate, phthalate and benzoate ions using ¹H NMR experiments. They have used octamethylcalix[4]pyrrole, **L72** as monomeric



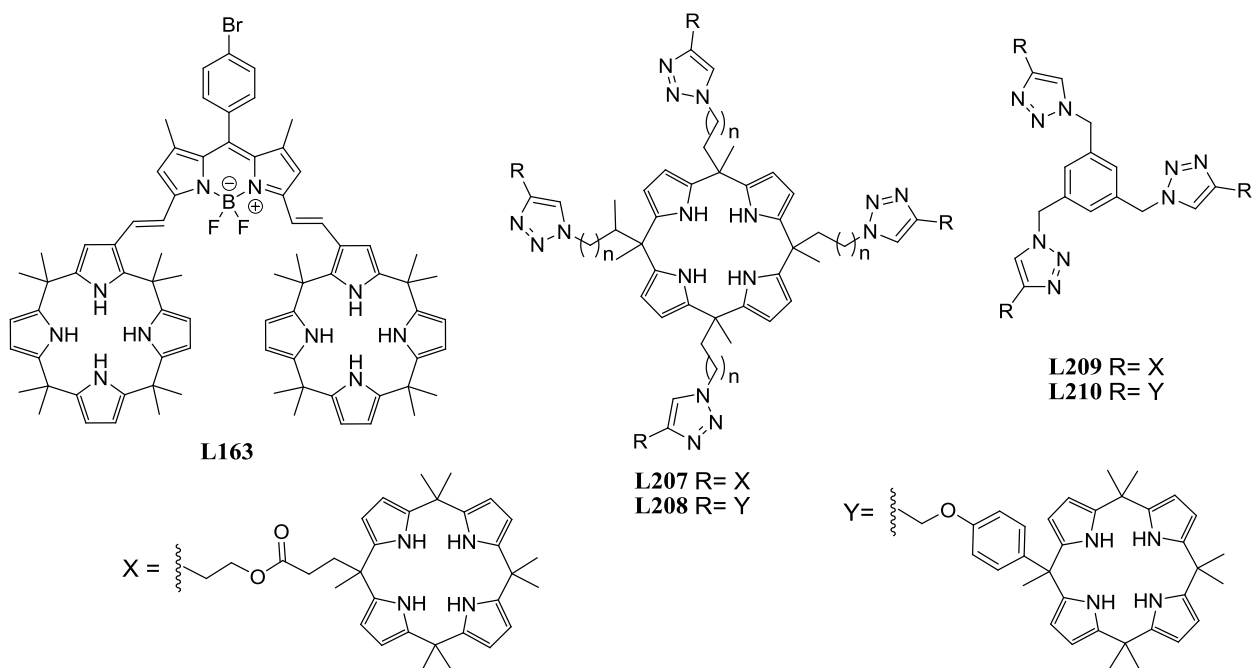
control system. From table 6.3 it was clear that although isophthalate and phthalate ions are bound better than benzoate in the case of the monomer and dimer, the interaction between **L204** and isophthalate ion is especially quite strong. It was found that upon binding with isophthalate ion, six of the eight possible pyrrolic NH signals of **L204** are shifted downfield, from 7.27–6.91 ppm to 11.00–10.60 ppm. Presumably, this reflects the fact that, for each of the calix[4]pyrrole subunits, the three pyrrolic NH moieties not directly linked to the acetylene spacer can point ‘in’

Table 6.3 Association constants (K_a) and binding stoichiometries for the interaction of **L204** and **L72** with various anionic guests in CD_2Cl_2 at 298 K.

Anion	L72	Host : Guest (for L72)	L204	Host : Guest (for L204)
isophthalate	700	1 : 1	4180	1 : 1
phthalate	390	1 : 1	90	1 : 2
benzoate	230	1 : 1	70	1 : 2

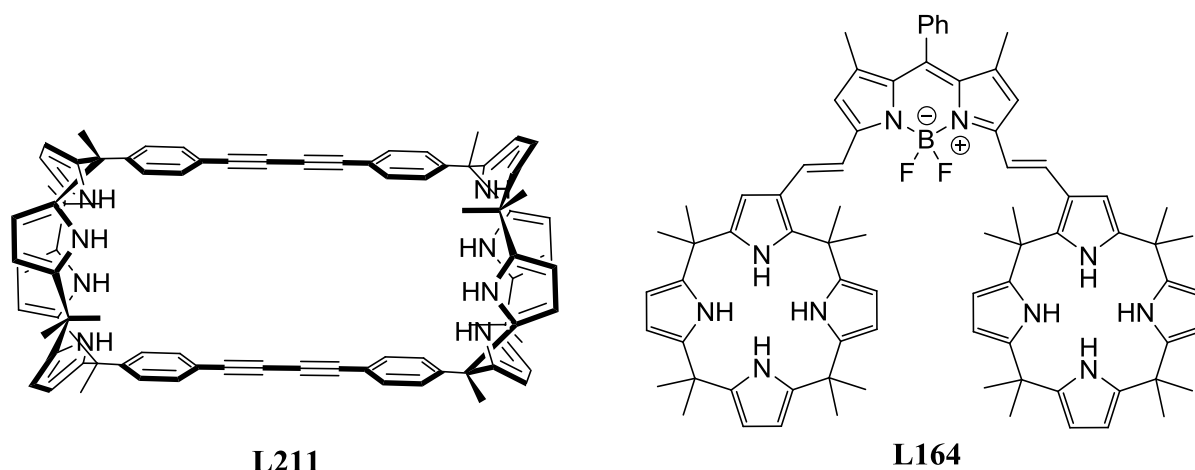
towards the carboxylate substrate, thus showing effective binding. By contrast, the NH of the β -substituted pyrrole is forced to point ‘outwards’ and hence plays little role in mediating the binding process. Subsequent to this report a decade later, Shao and coworkers in 2011 reported

another type of calix[4]pyrrole dimer **L163**, where two calix[4]pyrrole ring were linked via one BODIPY unit.¹⁷ However, this report deals with only monovalent anions. Recently, Aydogan and Akar synthesized some tri- and penta-calix[4]pyrroles (**L207-210**).¹⁸ They have shown these oligomeric calix[4]pyrrole compounds can be used for the extraction of fluoride and chloride



ions and salts of TBA cations. Extraction experiments revealed that, while pentacalix[4]pyrrole derivatives **L207** and **L208** were extracting both fluoride and chloride ions into the organic phase, the tricalix[4]pyrrole derivatives **L209** and **L210** were just able to extract chloride ion only. In 2012, Ballester and coworker synthesized a cylindrical bis-calix[4]pyrrole **L211** and used it in a general strategy for the quantitative self-assembly of pseudorotaxane-like complexes.¹⁹ At 298 K in CDCl₃ solution, an equimolar combination of TBAOCN or TBAN₃ with **L211** and 2,6-bis(ethylcarbamoyl)pyridine-1-oxide induced the quantitative formation of the ion-paired pseudorotaxane like complex, independent of the addition order of the components. They have extensively studied this molecule as cooperative ion pair dimer receptor. They showed that bis(calix[4]pyrrole) macro-tricyclic receptor **L211** could bind two chloride or cyanate TBA ion pairs yielding complexes through a highly cooperative process (α)10⁵; where α is co-operativity factor).²⁰ The complexes exhibited a structure with a cascade-like arrangement of the ion pairs. One ion pair is bound in ‘close-contact’ geometry, while the other in a receptor-

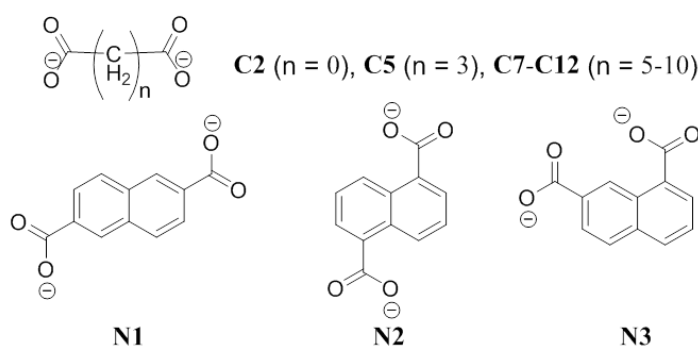
separated arrangement. Derived association constants for cyanate and chloride ions were found very high (1.5×10^{11} and 1.9×10^9 respectively). Very recently, Costero and coworkers have



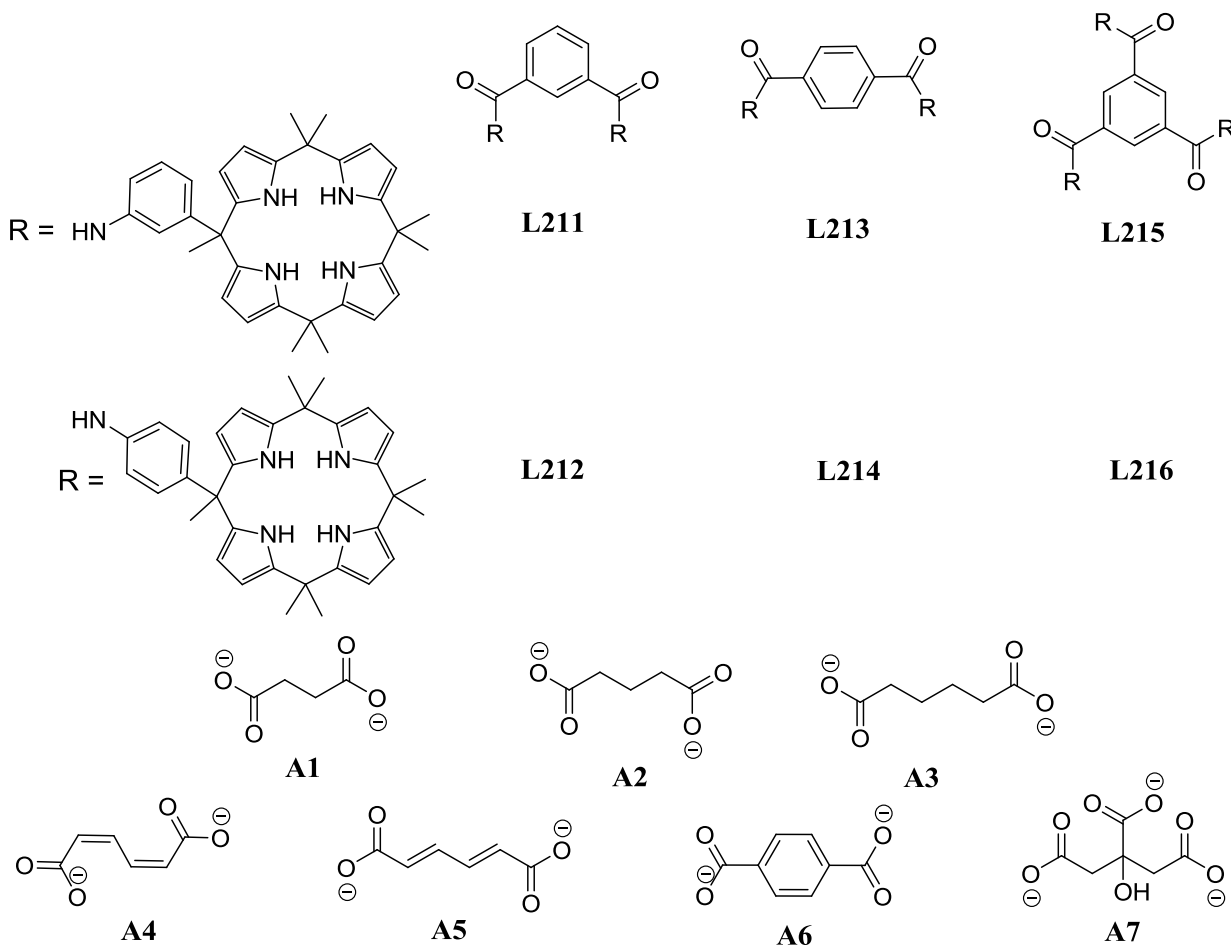
reported a novel BODIPY bases bis-calix[4]pyrrole **L164** and used for the recognition of the dicarboxylate ions.²¹ Association constants derived from UV-Vis spectroscopic analysis showed remarkable increase in $\log K_a$ as chain length extended and reached a maximum for the sebacic dianion, C10 ($n = 8$, $\log K_a = 7.7$), and then slowly decreased again as the size of the dicarboxylate further enlarged. This affinity for sebacate ion was ascribed to size match between dianion and the distance between two calix[4]pyrrole units. Relatively high values of the association constant obtained for the 1:1 complexes between **L164** and the naphthalene dicarboxylate ions, as compared to those obtained with aliphatic dicarboxylate ions of similar

Table 6.4 $\log K_a$ for **L164** with the TBA salts of dicarboxylate (and acetate) anions in THF at 297 K, calculated from UV/Vis titrations by using SPECFIT

Anion	K_a for 1: 1 complex
C2	4.4 ± 0.5
C5	4.7 ± 0.3
C7	5.1 ± 0.1
C8	5.9 ± 0.3
C9	7.1 ± 0.2
C10	7.7 ± 0.3
C11	6.7 ± 0.1
C12	6.5 ± 0.1
N1	7.1 ± 0.6
N2	6.6 ± 0.2
N3	6.8 ± 0.5
AcO ⁻	5.8 ± 0.3



lengths (C5–C8), may be due to the rigidity of the guest and to some additional stabilizing effect involving the aromatic rings. Very recently Kohnke and coworkers have reported aromatic-amide-linked bis- and tris-calix[4]pyrroles **L211–216** and performed binding studies of dicarboxylates in acetonitrile and they have reported quite detailed observations on behavior of these receptors.²² **L211** displayed binding to all the tested anions in 1:1 stoichiometry and for **A7** both the calix[4]pyrrole and the amide groups are involved in binding process. For **L212**, best fit was found for **A3** where one carboxylate group was bound to amide group and the other carboxylate group was shared between two calix[4]pyrroles. As distance increased between the



calix[4]pyrroles in case of **L213** and **L214** as a result binding got weaker. In case of **L216**, interaction with **A5** and **A7** was best when 1.5 and 2 equivalents of anion was used respectively and for the other tested anions broad peaks were generated. **L215** found too much conformationally flexible to study anion binding properties. These reports clearly indicated that receptors with more than one calix[4]pyrrole rings show interesting binding behavior compared to their monomeric analogs. These receptors also displayed not only higher selectivity towards

dicarboxylate ions, but also can bind to some anions with higher cooperativity, in presence of appropriate counter cation. Although they are unique, difficulty in synthesis and complicated binding nature hindered researchers to investigate them in detail.

6.3 Research Goal

It can be noticed that all the above discussed polycalix[4]pyrroles were synthesized by following building block approach i.e. first a functional calix[4]pyrroles was synthesized later using this functionality they are connected to each other or to another substrate. But till now nobody has successfully attempted the direct synthesis of the bis/higher order calix[4]pyrroles. During our previous study for the shortest strapped calix[4]pyrroles, we noticed that bisdipyrromethane generated from catechol derived diketone leads to formation of strapped calix[4]pyrrole, while that derived from resorcinol did not provide the desired strapped macrocycle owing to steric constraint. Therefore, we envisaged that if we can extend this series little further i.e. bisdipyrromethane derived from 1,4-dihydroxybenzene, where intramolecular macrocyclization is completely ruled out, whereas there is a possibility of intermolecular reaction, probably via double (2+2) condensation resulting in a calix[4]pyrrole strapped with another calix[4]pyrrole, i.e. a biscalix[4]pyrrole. However, the chances of linear polymerization as a competing reaction will increase on the other hand.

6.4 Synthesis and Structural Characterization

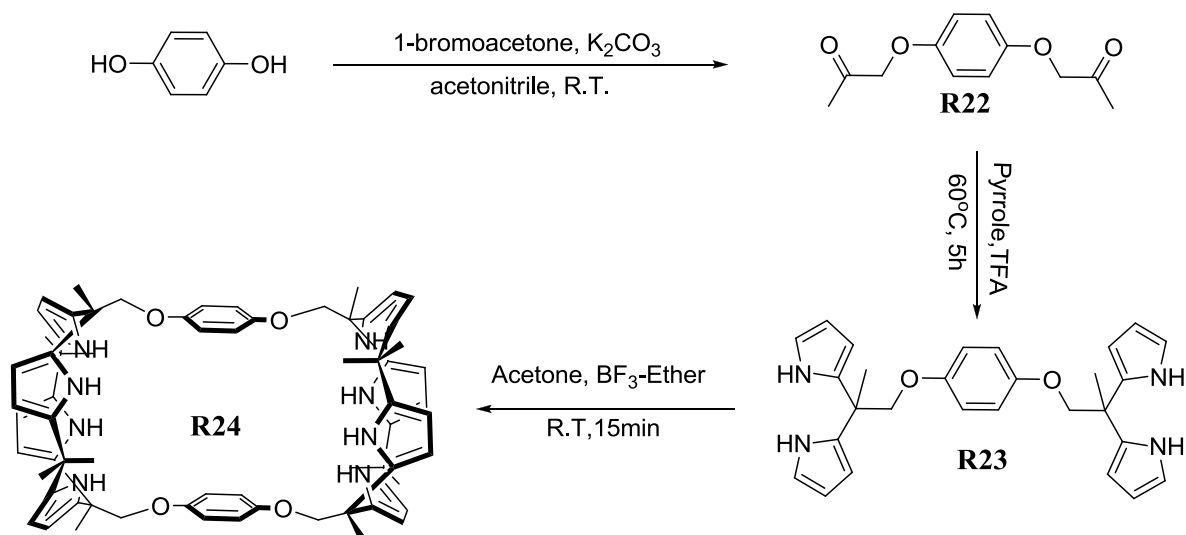


Figure 6.4 Synthetic route for **R24**.

First, 1,4-dihydroxybenzene was alkylated using 1-bromoacetone in presence of anhydrous potassium carbonate in dry acetonitrile. Use of solvent other than acetonitrile such as acetone or DMF decreased the yield of the product, probably owing to the decomposition of the alkylating agent as evident from the TLC of product profile, which was always contaminated with inseparable impurities. Alkylated product **R22** was obtained after the purification by column chromatography as a white solid with a yield of 73 %. Treating diketone **R22** with excess freshly distilled pyrrole in presence of trifluoroacetic acid at 60 °C and subsequent purification provided **R23** in 68%. The resultant bisdipyrromethane **R23** was subjected to react with acetone under various conditions. First we used conditions we have followed previously for the synthesis of strapped calix[4]pyrroles i.e. bisdipyrromethane in acetone (10 mmol/L) and BF₃.ether (0.3 equivalent).²³ But within two min all bisdipyrromethane were polymerized. Therefore, in order to reduce the polymerization rate, we have diluted the bisdipyrromethane concentration (5 mmol/L in acetone), which yielded a new spot after 10 min. After the usual work up and the subsequent purification by column chromatography, the desired biscalix[4]pyrrole **R24** was obtained in 2 % yield. Various attempts to increase the yield by further dilution or using different solvent or mixture of solvents and even use of some templates (e.g. TBACl, TBAI, pyrazine-1,4-dioxide) remain unsuccessful. All the compounds including the desired macrocycle were characterized by IR, ¹H and ¹³C NMR spectroscopy, and high resolution mass analysis. ¹H NMR spectrum in CDCl₃ of the receptor **R24** showed that pyrrole-NH signals are resonating at 7.75 ppm.

6.5 Conclusion

In conclusion, we have synthesized a very novel biscalix[4]pyrrole, where one calix[4]pyrrole unit is strapped by another calix[4]pyrrole moiety with the strap derived from 1,4-dihydroxybenzene, by using double (2+2) condensation pathway. The receptor is characterized by various spectroscopic methods. However, due to lower yield and lack of time, the anion binding study for this receptor could not be completed. But we anticipate interesting and unique anion binding behavior for this receptor.

6.6 Experimental details

6.6.1 Synthesis of 1,4-bis-(acetyloxy)benzene (**R22**)

In a 3 necked 250 mL round bottom flask, 1,4-dihydroxybenzene (2.75 g; 25 mmol) and acetonitrile (200 mL) were taken. To it K_2CO_3 (13.8 g; 100 mmol) was added with constant stirring. After 20 min, 1-bromoacetone (7.48 g; 55 mmol) in acetonitrile (15 mL) was added dropwise to the reaction mixture at 0°C. After addition was completed, reaction mixture was stirred at room temperature for 24 h. The reaction mixture was filtered through Celite®, solvent was evaporated and remaining residue was purified by column chromatography over silica gel (30 % ethyl acetate in hexane) to obtain **R22** (4.1 g, 73 %) as white solid. Melting point: 77 °C; IR (KBr): $\nu = 1756.1\text{ cm}^{-1}$; ^1H NMR ($CDCl_3$): δ in ppm 6.83 (s, 4H), 4.49 (s, 4H), 2.27 (s, 6H); ^{13}C NMR ($CDCl_3$) δ in ppm 205.94, 152.72, 115.79, 73.81, 76.71; HRMS m/z , $[M+Na]$: 245.0790 (calculated for $C_{12}H_{15}NaO_4$: 245.0790).

6.6.2 Synthesis of 1,4-bis(2,2-di(1H-pyrrol-2-yl)propoxy)benzene (**R23**)

In a 2 necked 100 mL round bottom flask 1,4-bis-(acetyloxy)benzene (1 g; 5.5 mmol) and pyrrole (13 mL; 180 mmol) were added under N_2 atmosphere. After the compound dissolved, TFA (350 μL ; 2.25 mmol) was added slowly and reaction mixture was stirred at 60 °C. After 6 h reaction was quenched by adding triethylamine (~2 mL). Then excess pyrrole was removed under vacuum and the remaining mass was purified by column chromatography over silica gel (eluent: CH_2Cl_2) to get **R23** (1.4 g, 68 %) as white solid. Melting point: 157 °C; IR (neat): $\nu = 3466.24\text{ cm}^{-1}$; ^1H NMR ($CDCl_3$): δ in ppm 8.35 (brs, 4H), 6.85 (s, 4H), 6.69 (s, 4H), 6.17 - 6.15 (m, 4H), 6.10 - 6.09 (m, 4H), 4.23 (s, 4H), 1.72 (s, 6H); ^{13}C NMR ($CDCl_3$) δ in ppm 153.42, 135.67, 117.31, 116.16, 108.02, 105.01, 40.26, 25.03; HRMS m/z , $[M+H]$: 455.2447 (Calculated for $C_{28}H_{31}N_4O_2$: 455.2447).

6.6.3 Synthesis of biscalix[4]pyrrole (**R24**)

To a solution of compound **R23** (500 mg; 1.1 mmol) and acetone (220 mL) was added $BF_3 \cdot OEt_2$ (3 μL). The solution was stirred at room temperature for 15 min and quenched by triethylamine (~1 mL) and solvent was evaporated and remaining mass was purified by column chromatography over silica gel (10 % ethyl acetate in hexane) to obtain the desired biscalix[4]pyrrole **R24** (12 mg, 2 %) as off-white solid. Melting point: 209.5 °C (decomposed);

IR (KBr): $\nu = 3404.67, 3096.03, \text{ cm}^{-1}$; $^1\text{H NMR}$ (CDCl_3): δ in ppm 7.75 (s, 8H), 6.63 (s, 8H), 5.98 - 5.97 (m, 8H), 5.92 - 5.91 (m, 8H), 4.20 (s, 8H), 1.57 (s, 12H), 1.53 (s, 12H), 1.49 (s, 12H); $^{13}\text{C NMR}$ (CDCl_3) δ in ppm 153.61, 138.57, 134.99, 116.33, 103.75, 103.08, 40.02, 35.47, 30.39, 29.84, 28.07, 25.26; HRMS m/z , $[\text{M}+\text{H}]$: 1069.5844 (Calculated for $\text{C}_{68}\text{H}_{77}\text{N}_8\text{O}_4$: 1069.6068).

6.7 Reference

1. *Biochemistry*, Stryer, L. W. H. Freeman and Co. New York, 1988.
2. (a) Hori, S.; Nishiumi, S.; Kobayashi, K.; Shinohara, M.; Hatakeyama, Y.; Kotani, Y.; Hatano, N.; Maniwa, Y.; Nishio, W.; Bamba, T.; Fukusaki, E.; Azuma, T.; Takenawa, T.; Nishimura, Y.; Yoshida, M. *Lung Cancer* **2011**, *74*, 284. (b) Hecht, S. S. *Carcinogenesis* **2002**, *23*, 907.
3. Bouchard, G.; Galland, A.; Carrupt, P. A.; Gulaboski, R.; Mirceski, V.; Scholz, F.; Girault, H. H. *Phys. Chem. Chem. Phys.* **2003**, *5*, 3748.
4. Dosman, J.; Crawhall, J. C.; Klassen, G. A.; Mamer, O. A.; Neumann, P. *Clin. Chim. Acta* **1974**, *51*, 93.
5. (a) Tepinski, J.; Pawlowska, D.; Angielski, S. *Acta Biochim. Pol.* **1984**, *31*, 229. (b) Gougoux, A.; Lemieux, G.; Lavoie, N. *Am. J. Physiol.* **1976**, *231*, 1010. (c) Eiam-ong, S.; Spohn, M.; Kurtzman, N. A.; Sabatini, S. *Kidney* **1995**, *48*, 1542.
6. Dietrich, B.; Hosseini, M. W.; Lehn, J. M.; Sessions, R. B. *J. Am. Chem. Soc.* **1981**, *103*, 1282.
7. Hosseini, M. W.; Lehn, J. M. *J. Am. Chem. Soc.* **1982**, *104*, 3525.
8. Hosseini, M. W.; Lehn, J. M. *Helv. Chem. Acta* **1986**, *69*, 587.
9. a) Lehn, J. M.; Meric, R.; Vigneron, J. P.; Bkouche-Waksman, I.; Pascard, C. *J. Chem. Soc., Chem. Commun.* **1991**, 62. (c) Dhaenens, M.; Lehn, J. M.; Vigneron, J. P. *J. Chem. Soc., Perkin Trans. 2* **1993**, 1379. (d) Fenniri, H.; Lehn, J. M.; Marquis-Rigault, A. *Angew. Chem. Int. Ed. Engl.* **1996**, *35*, 337. (e) Kimura, E.; Sakonaka, A.; Yatsunami, T.; Kodama, M. *J. Am. Chem. Soc.* **1981**, *103*, 3041. (f) Kimura, E.; Kuramoto, Y.; Koike, T.; Fujioka, H.; Kodama, M. *J. Org. Chem.* **1990**, *55*, 42. (g) Kimura, E.; Ikeda, T.; Shionoya, M.; Shiro, M. *Angew. Chem. Int. Ed. Engl.* **1995**, *34*, 663.

10. (a) Hannon, C. L.; Anslyn, E. V. *Bioorganic Frontiers*: Springer Verlag: Berlin, **1993**; Vol. 3, pp 143-256. (b) Dietrich, B.; Fyles, D. L.; Fyles, T. M.; Lehn, J. M. *Helv. Chim. Acta* **1979**, 62, 2763. (b) Schiessl, P.; Schmidtchen, F. P. *Tetrahedron Lett.* **1993**, 34, 2449. (c) Albert, J. S.; Goodman, M. S.; Hamilton, A. D. *J. Am. Chem. Soc.* **1995**, 117, 1143.
11. Beer, P. D.; Drew, M. G. B.; Hazlewood, C.; Hesek, D.; Hodacova, J.; Stokes, S. E. *J. Chem. Soc., Chem. Commun.* **1993**, 229.
12. Lacy, S. M.; Rudkevich, D. M.; Verboom, W.; Reinhoudt, D. N. *J. Chem. Soc. Perkin Trans. 2* **1995**, 135.
13. (a) Hamilton, A. D.; Fan, E.; van Arman, S.; Vincent, C.; Garcia-Tellado, F.; Geib, S. J. *Supramol. Chem.* **1993**, 1, 247 and references therein. (b) Fan, E.; van Arman, S. A.; Kincaid, S.; Hamilton, A. D. *J. Am. Chem. Soc.* **1993**, 115, 369. (c) Goodman, M. S.; Jubian, V.; Linton, B.; Hamilton, A. D. *J. Am. Chem. Soc.* **1995**, 117, 11610. (d) Goodman, M. S.; Jubian, V.; Hamilton, A. D. *Tetrahedron Lett.* **1995**, 36, 2551.
14. (a) Webb, T. H.; Wilcox, C. S. *Chem. Soc. Rev.* **1993**, 383. (b) Alcazar, V.; Diederich, F. *Angew. Chem. Int. Ed. Engl.* **1992**, 31, 1521. (c) Garcia-Tellado, F.; Albert, J.; Hamilton, A. D. *J. Chem. Soc., Chem. Commun.* **1991**, 1761. (d) Pieters, R. J.; Diederich, F. *Chem. Commun.* **1996**, 2255. (e) Konishi, K.; Kimata, S.; Yoshida, K.; Tanaka, M.; Aida, T. *Angew. Chem. Int. Ed. Engl.* **1996**, 35, 2823.
15. (a) Král, V.; Andrievsky, A.; Sessler, J. L. *J. Am. Chem. Soc.* **1995**, 117, 2953. (b) Sessler, J. L.; Andrievsky, A.; Král, V.; Lynch, V. *J. Am. Chem. Soc.* **1997**, 119, 9385.
16. Sato, W.; Miyaji, H.; Sessler, J. L. *Tetrahedron Lett.* **2000**, 41, 6731.
17. Lv, Y.; Xu, J.; Guo, Y.; Shao, S. *Chem. Pap.* **2011**, 65, 553.
18. Aydogan, A.; Akar, A. *Chem. Eur. J.* **2012**, 18, 1999.
19. Valderrey, V.; Escudero-Adan, E. C.; Ballester, P. *J. Am. Chem. Soc.* **2012**, 134, 10733.
20. Valderrey, V.; Escudero-Adan, E. C.; Ballester, P. *Angew. Chem., Int. Ed.* **2013**, 52, 6898.
21. Gotor, R.; Costero, A. M.; Gaviña, P.; Gil, S.; Parra, M. *Eur. J. Org. Chem.* **2013**, 1515.
22. Cafeo, G.; Gattuso, G.; Kohnke, F. H.; Papanikolaou, G.; Profumo, A.; Rosano, C. *Chem. Eur. J.* **2014**, 20, 1658.

23. (a) Samanta, R.; Mahanta, S. P.; Chaudhuri, S.; Panda, P. K.; Narahari, A. *Inorg. Chim. Acta.* **2011**, 372, 281. (b) Samanta, R.; Mahanta, S. P.; Ghanta, S.; Panda, P. K. *RSC Adv.* **2012**, 2, 7974.

CHAPTER 7

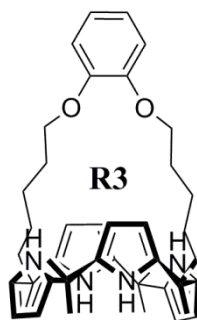
Summary

7.1 Summary

The thesis entitled “*New ways of strapping Calix[4]pyrroles*” describes the syntheses of several strapped calix[4]pyrroles and their anion binding study. The thesis contains seven chapters. The first chapter gives a brief audit regarding anions and their recognition, followed by second chapter dealing with materials and methods employed for the dissertation work. Subsequently, there are four working chapters, which deal with synthesis of several novel strapped calix[4]pyrrole and the anion binding study of most of the newly synthesized calix[4]pyrroles derivatives. The present chapter summarizes the whole investigation.

Chapter one provides a brief account on generalized introduction to anion receptor chemistry with natural anion receptors, historical evolution of artificial anion receptors and classification of anion receptors. In the last few decades anions drew wide attention of researcher owing to the important roles they play in various biological and environmental processes, including health sector. Therefore, the major objective is to carry out selective recognition of anions, if possible with higher affinity. Several synthetic receptors have been reported in literature in this direction. Among them, pyrrole based receptors, mainly calix[4]pyrrole emerged as an attractive neutral receptor, over the last two decades.

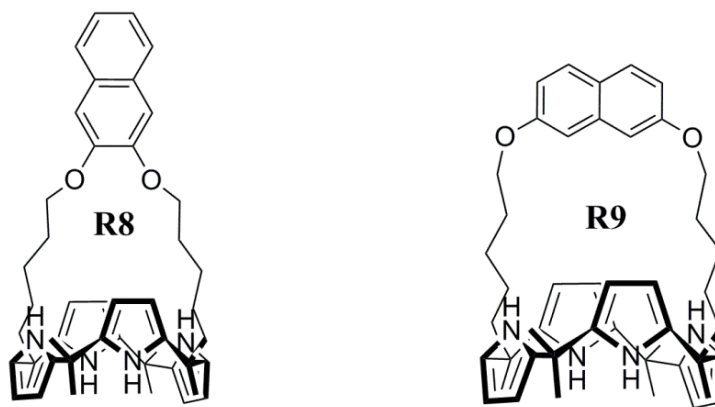
In the third chapter, we have discussed synthesis and characterization of calix[4]pyrrole bearing catechol-derived diether straps, linked via alkyl chains for the first time to investigate the consequences of strap derived from catechol than that derived from resorcinol (1,2- vs 1,3-



linkage) on the anion binding/selectivity of strapped calix[4]pyrrole.¹ The solid state structure reveals two molecules of methanol bound to the host. The strap with 1,2-diether link is providing a relatively constrained geometry on its side of the calix[4]pyrrole moiety. This calix[4]pyrrole also exhibits enhanced binding towards halide anions compared to simple calix[4]pyrrole apart from showing binding towards dihydrogenphosphate and acetate ions. The association constants are quite similar to that found for resorcinol strapped (1,3-linkage) calix[4]pyrrole towards halide

anions in general, but having a higher preference for chloride than bromide ion in particular. Further it shows very strong preference towards fluoride ion. We also found that the role of inner aromatic CH may be is not that important ('1,3-diether' strapped calix[4]pyrrole) or absence of inner aromatic proton may be compensated by more restricted binding domain.

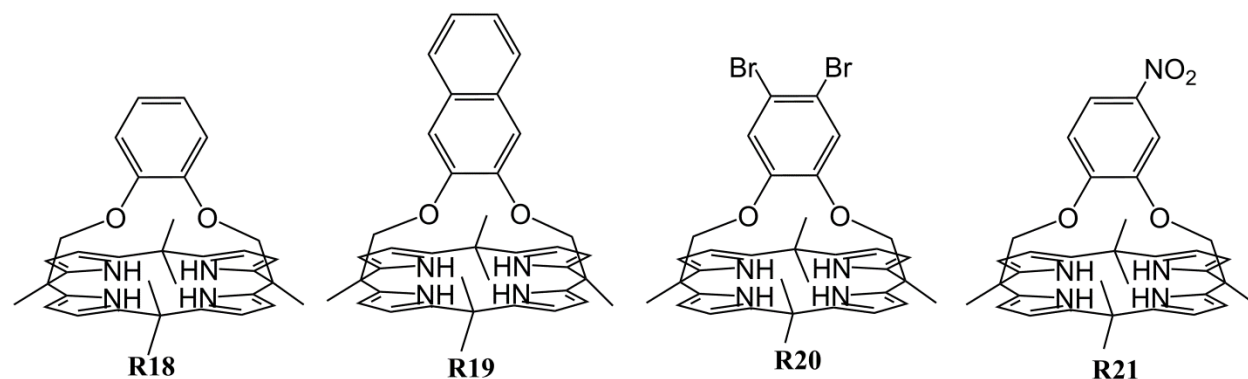
Chapter four deals with the synthesis of two novel isomeric strapped calix[4]pyrroles, derived from naphthalene for the first time, with one derived from 2,3-dihydroxynaphthalene and the other from 2,7-dihydroxynaphthalene.² These naphthalene moieties in the strap act as the fluorescent reporting unit. Anion ion binding event was successfully monitored by the



fluorescence quenching process. Association constants derived from two methods (fluorescence quenching experiment and isothermal titration calorimetry) matched well for the receptor derived from 2,3-dihydroxynaphthalene. It was also observed that difference in spatial disposition of naphthalene unit has a marked effect on the anion affinity and selectivity. The receptor derived from 2,3-dihydroxynaphthalene displays highest sensitivity towards chloride ion, whereas that derived from 2,7-analogue shows highest sensitivity for fluoride ion, albeit weakly. DFT minimized structures for both the cases demonstrated the reason of discrepancies in the derived association constants.

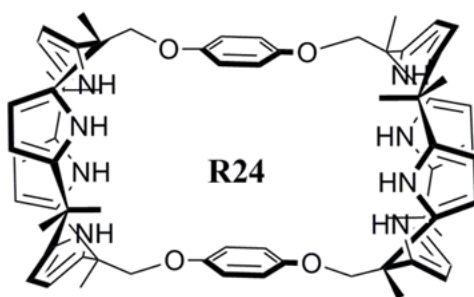
The fifth chapter demonstrates the feasibility of shortest possible strap on calix[4]pyrrole and its consequences on the anion binding properties. In this regards, four new calix[4]pyrroles (**R18-R21**) with shortest possible strap were synthesized.³ Anion binding study revealed that these receptors bind only with fluoride ion, although weakly compared to the analogous calix[4]pyrroles with longer strap. This exclusive selectivity towards fluoride ion is attributed to the very small binding domain of these receptors. The relatively lesser affinity can be explained on the basis of 'lone pair-lone pair' interaction between the oxygen atoms and the anion.

Incorporation of electron withdrawing bromine atoms in the benzene ring of the strap increases



the association constants by an order, without compromising on the anion selectivity. Anion binding behavior for the receptor **R21**, containing one strong electron withdrawing nitro group is still under process.

In the final working chapter i.e. chapter six, we have reported the synthesis of a very novel biscalix[4]pyrrole **R24**, by using double (2+2) condensation path way. In this receptors, a

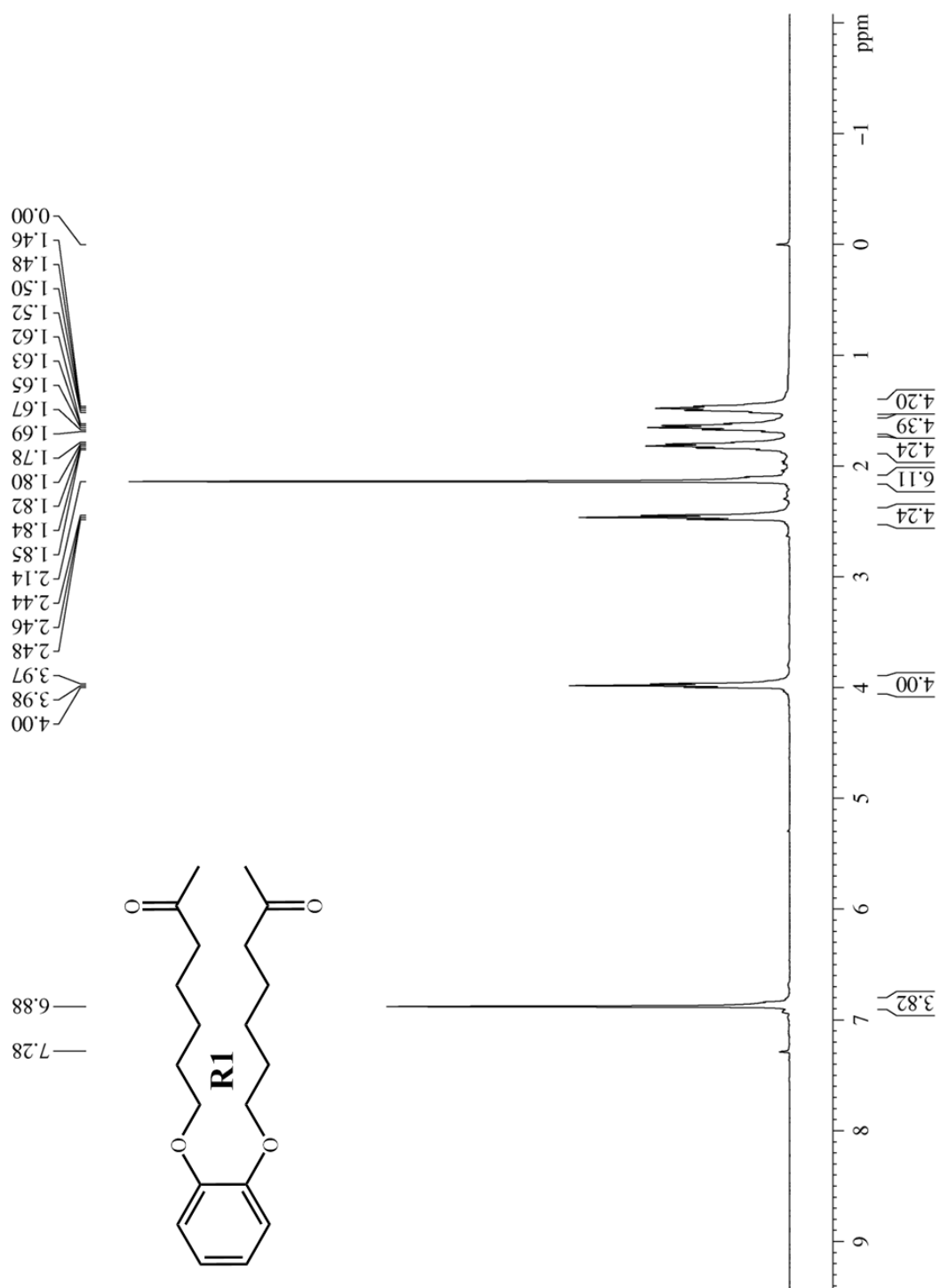


calix[4]pyrrole unit is strapped by another calix[4]pyrrole moiety where the strap is derived from 1,4-dihydroxybenzene. This receptor, possessing relatively flexible bridge between the two calix[4]pyrroles may display interesting binding affinity towards aromatic dicarboxylic acid through ‘ π – π stacking interaction’. The receptor is characterized by various spectroscopic methods. However, due to lack of scope we are not able to study the anion binding properties. We anticipate very interesting and unique host-guest chemistry by this receptor.

7.2 References

1. Samanta, R.; Mahanta, S. P.; Chaudhuri, S.; Panda, P. K.; Narahari, A. *Inorg. Chim. Acta.* **2011**, 372, 281.
2. Samanta, R.; Mahanta, S. P.; Ghanta, S.; Panda, P. K. *RSC Adv.* **2012**, 2, 7974.
3. Samanta, R.; Panda, P. K. (Manuscript under preparation).

Appendix

**Figure A1:** ^1H NMR spectrum of **R1**

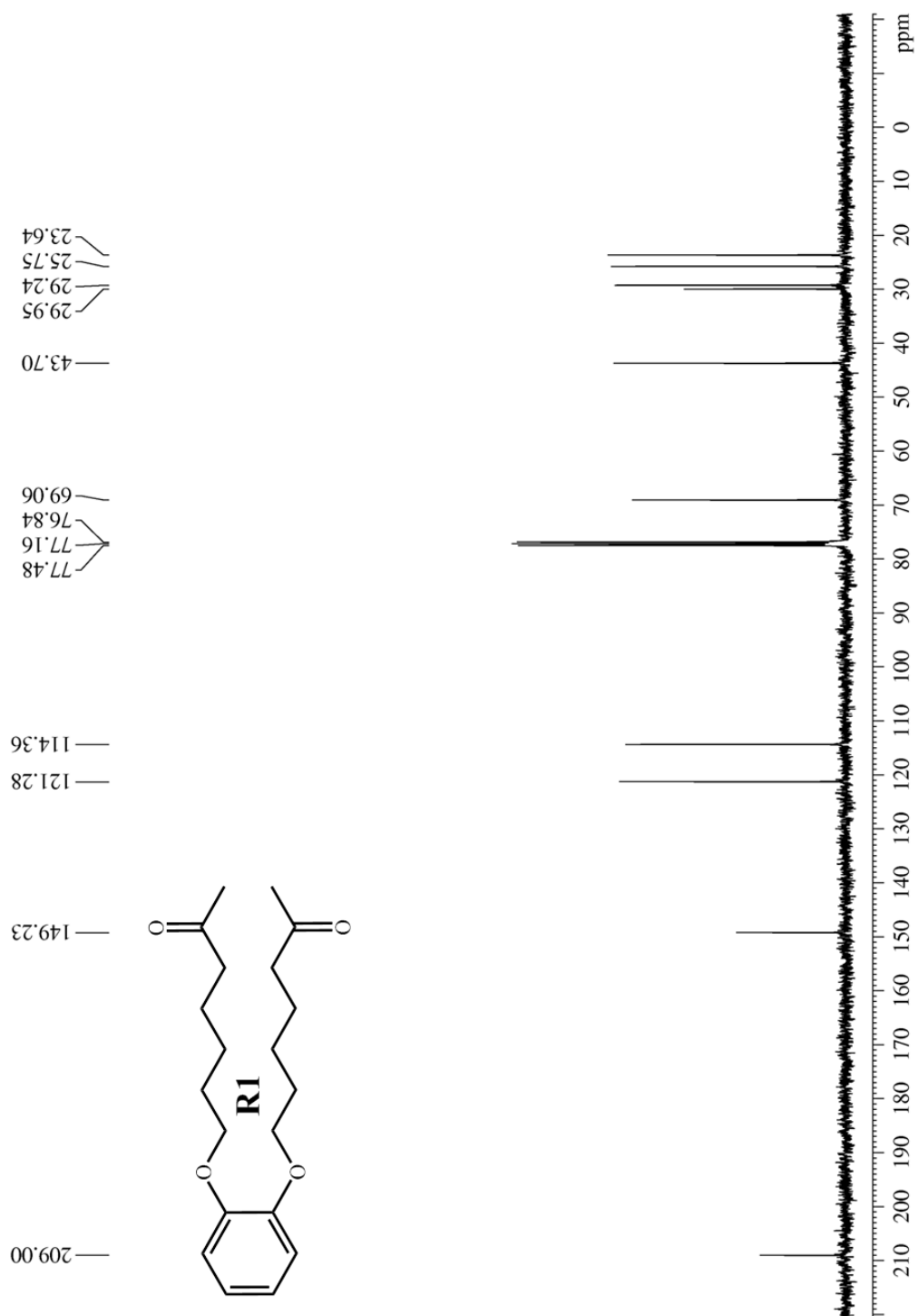


Figure A2: ^{13}C NMR spectrum of **R1**

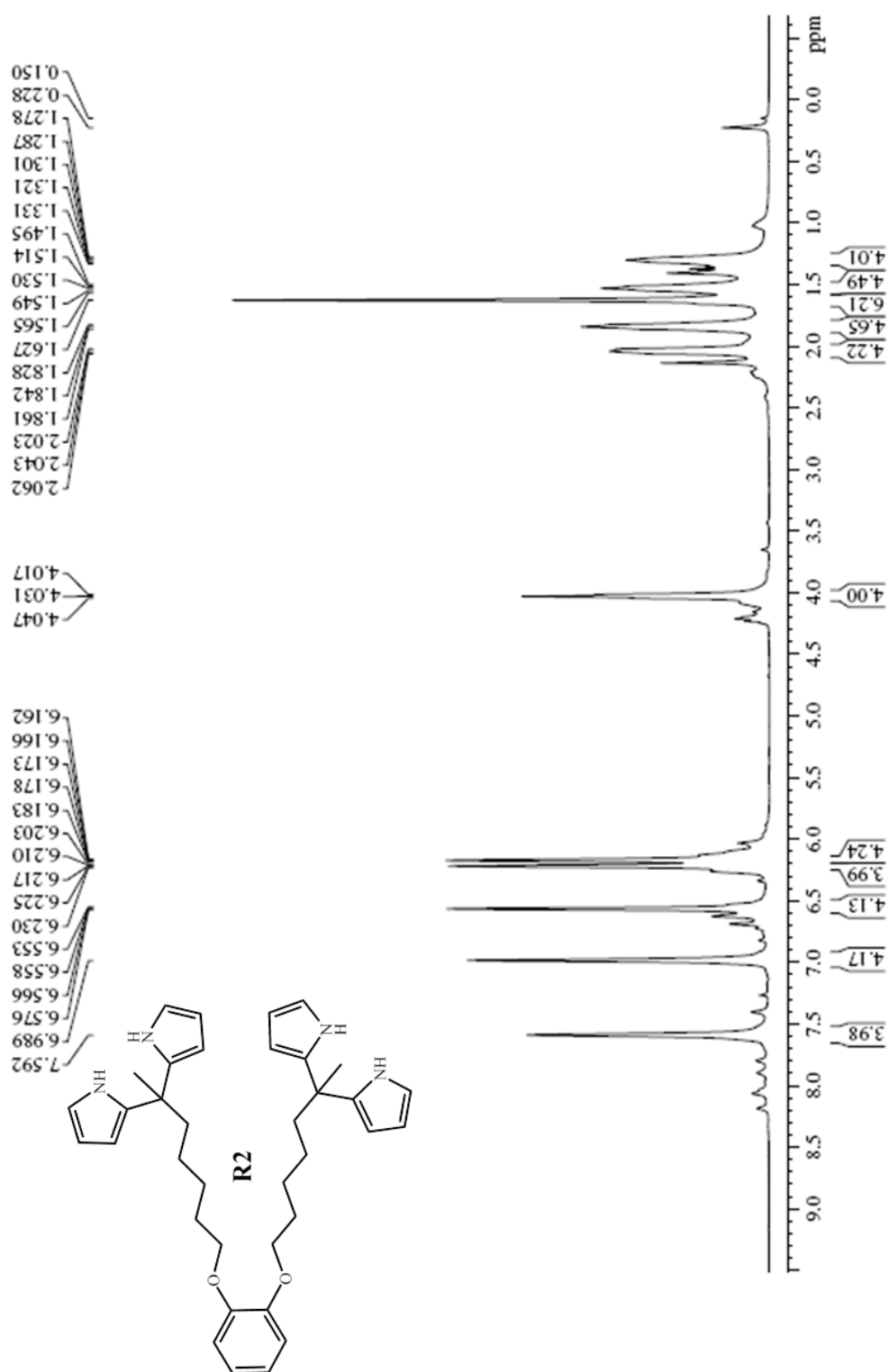


Figure A3: ¹H NMR spectrum of **R2**

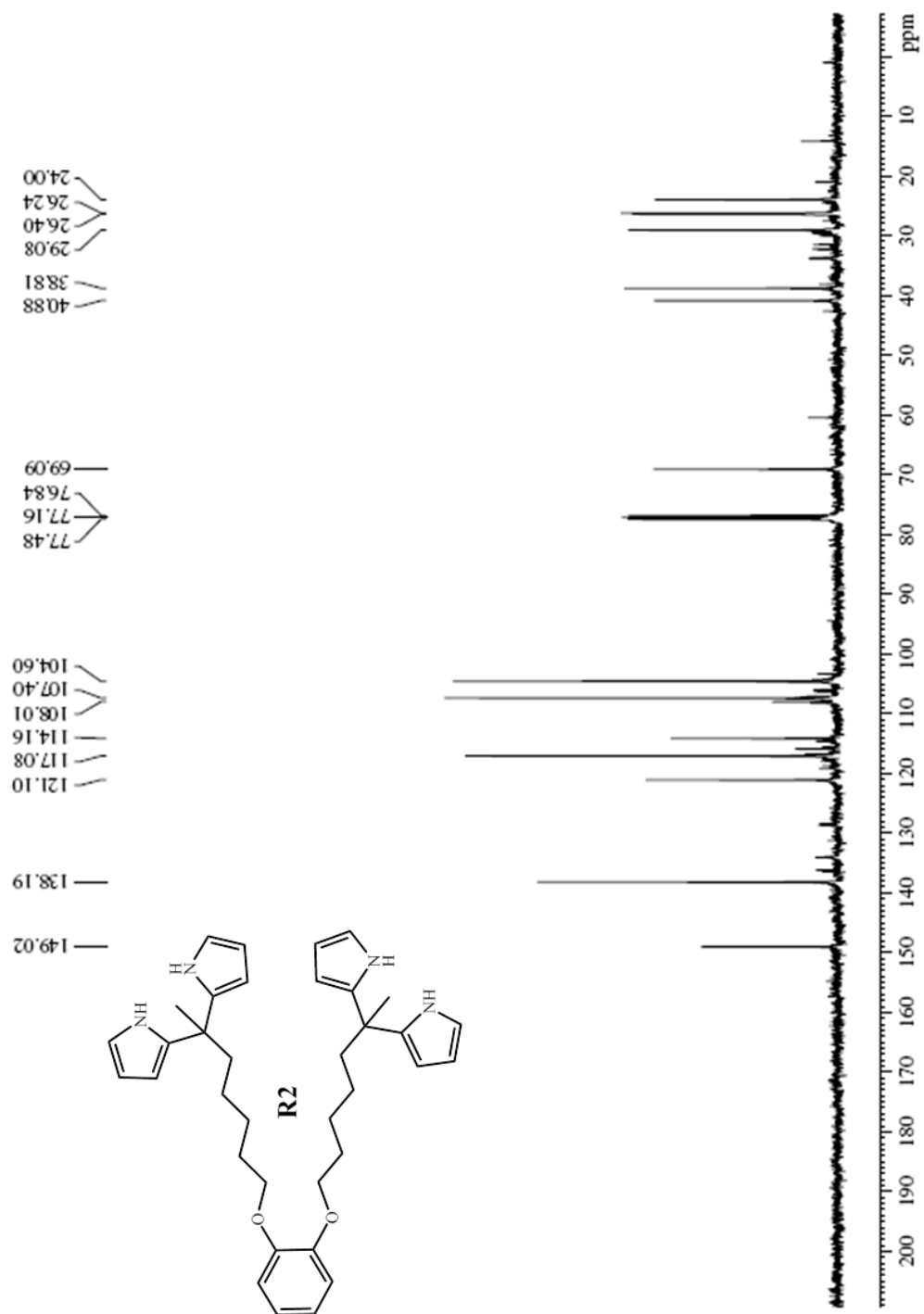
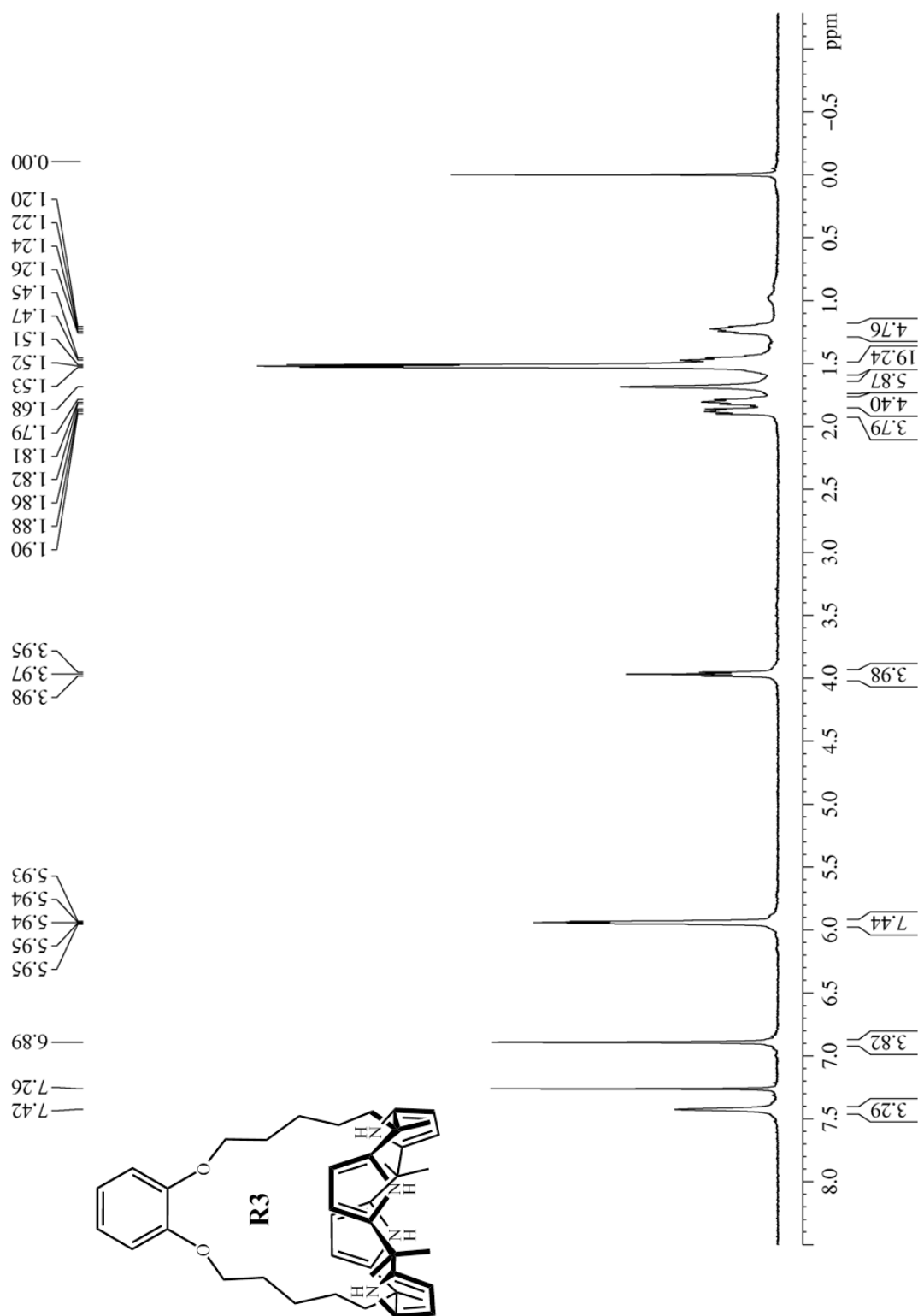


Figure A4: ^{13}C NMR spectrum of **R2**

**Figure A5:** ^1H NMR spectrum of **R3**

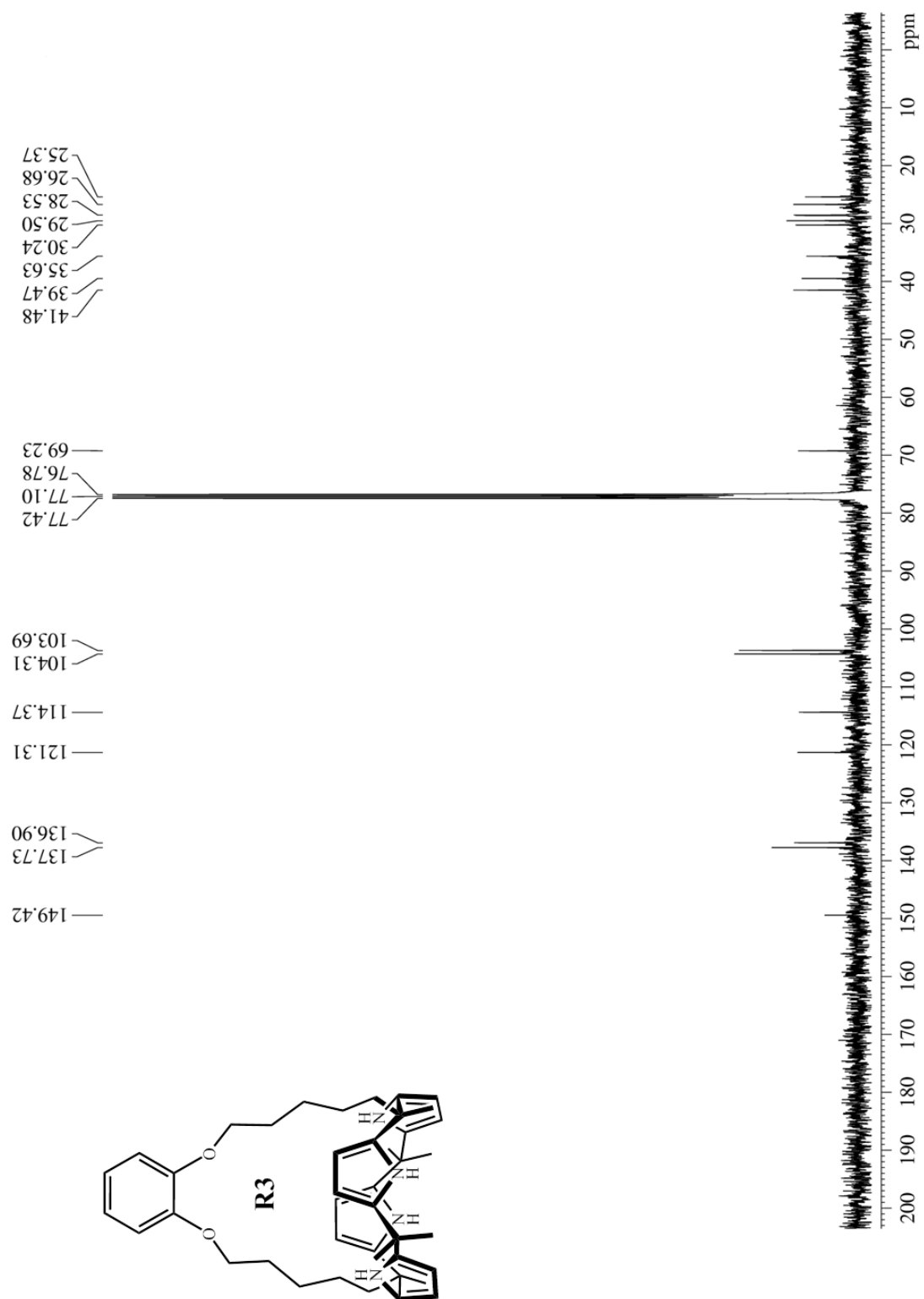


Figure A6: ^{13}C NMR spectrum of **R3**

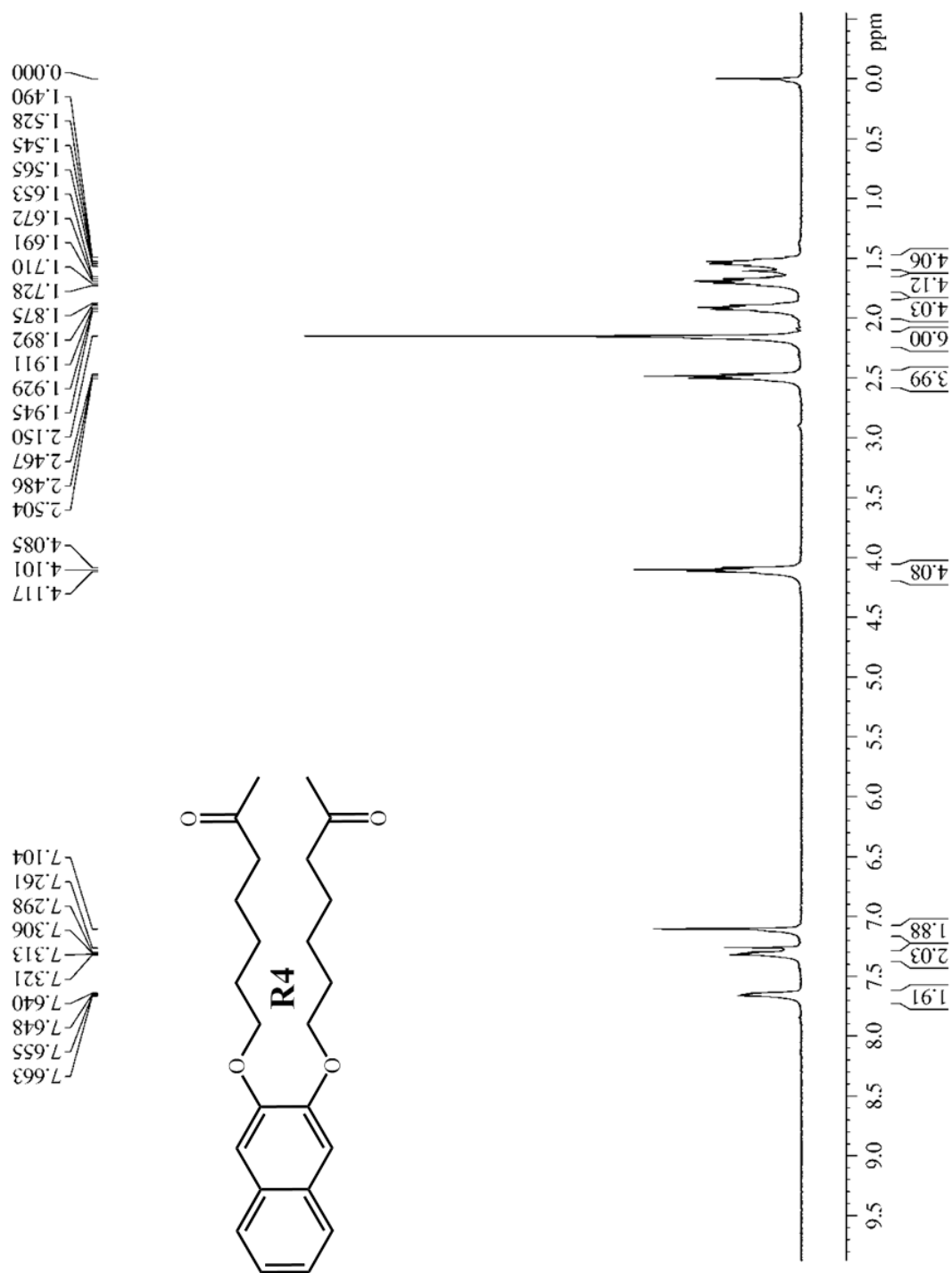


Figure A7: ^1H NMR spectrum of **R4**

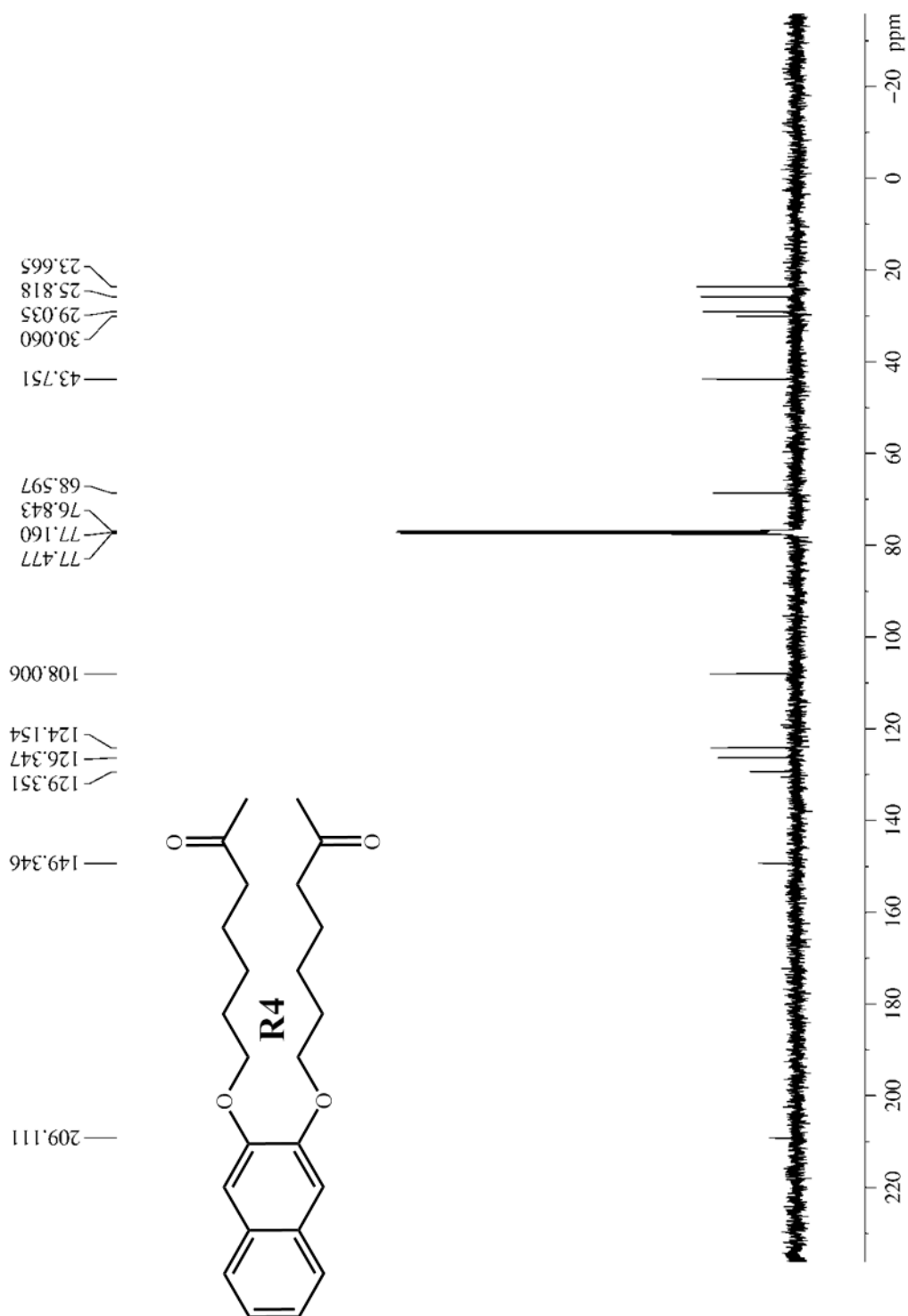


Figure A8: ^{13}C NMR spectrum of **R4**

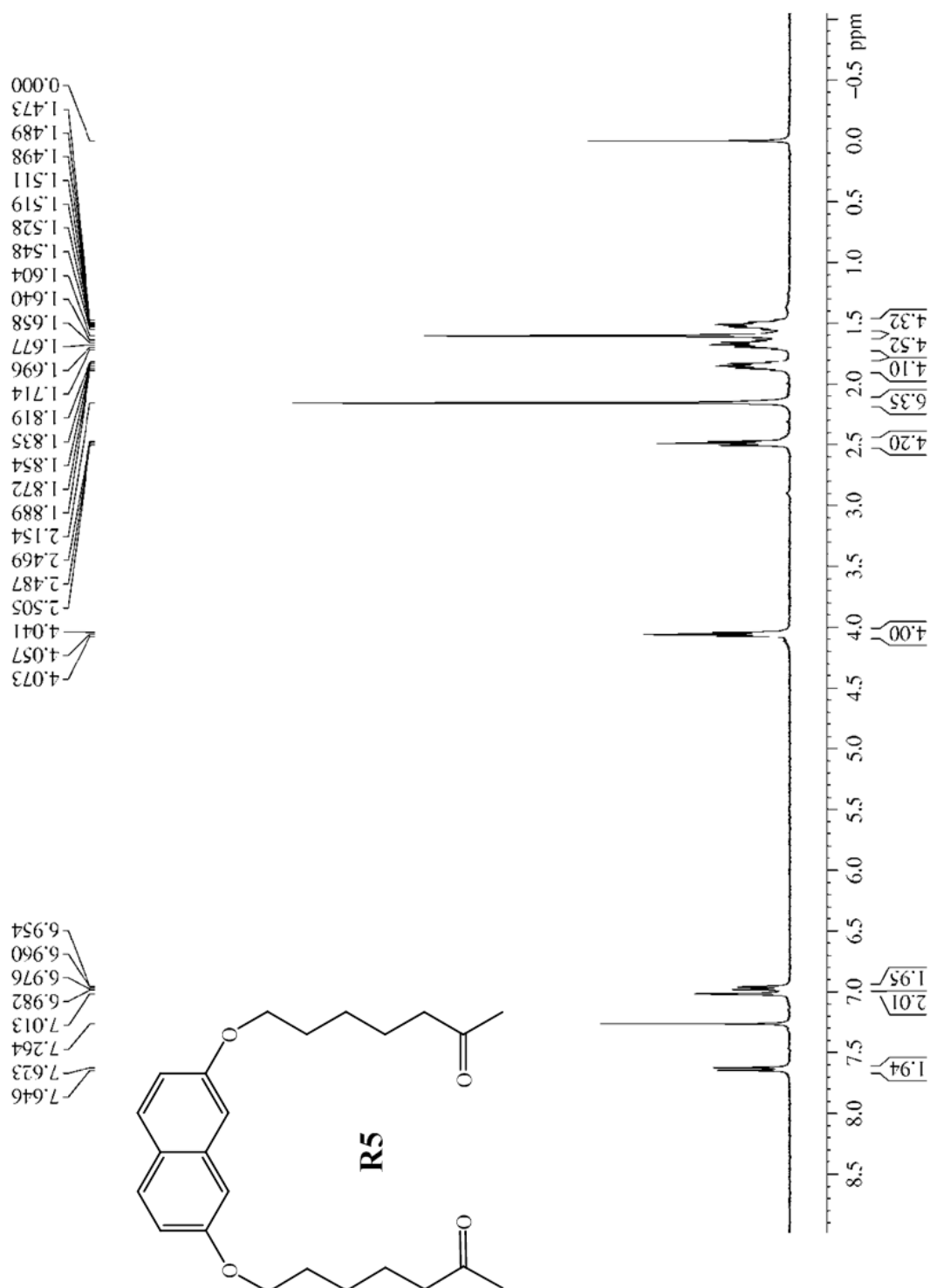


Figure A9: ¹H NMR spectrum of **R5**

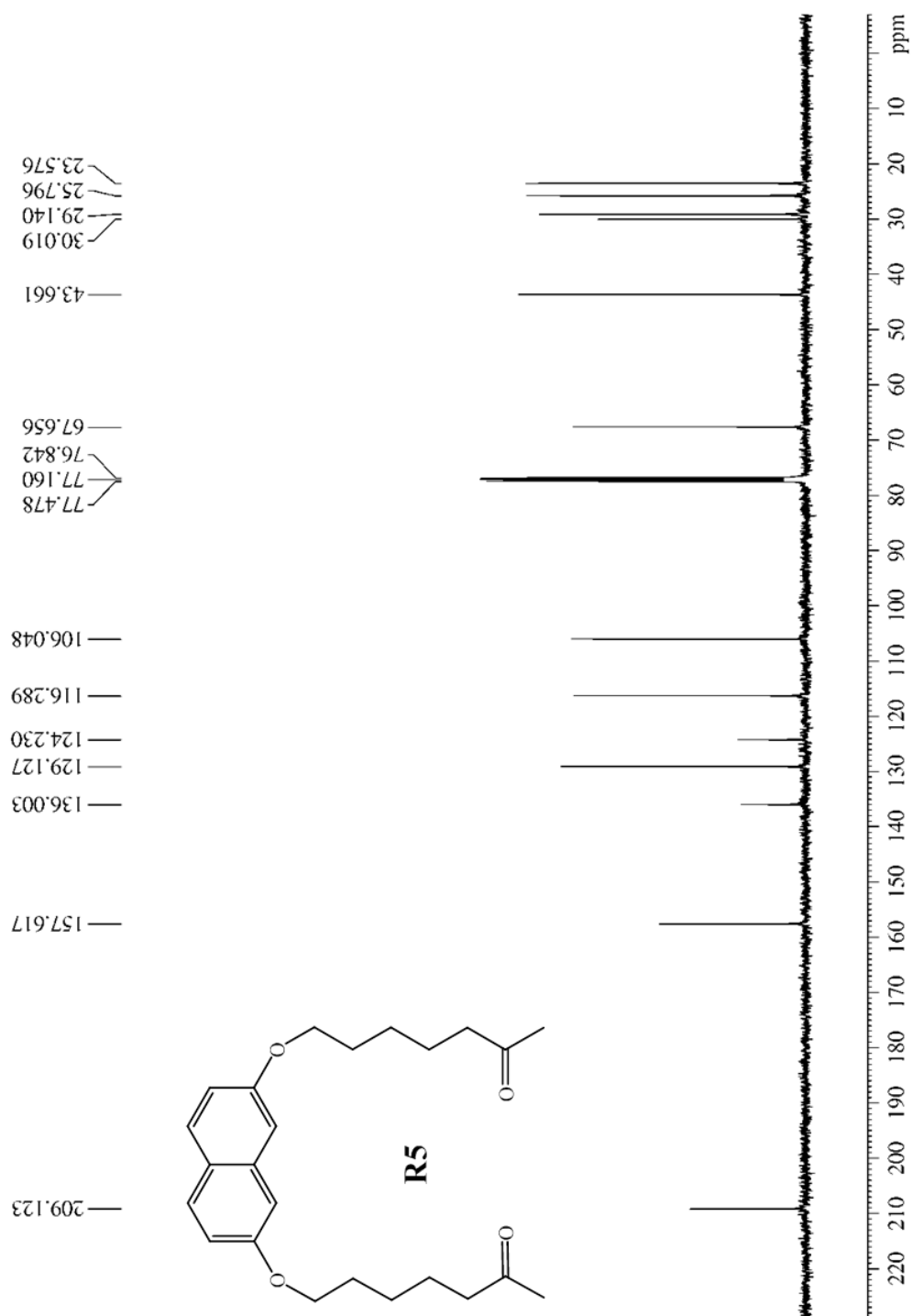


Figure A10: ^{13}C NMR spectrum of **R5**

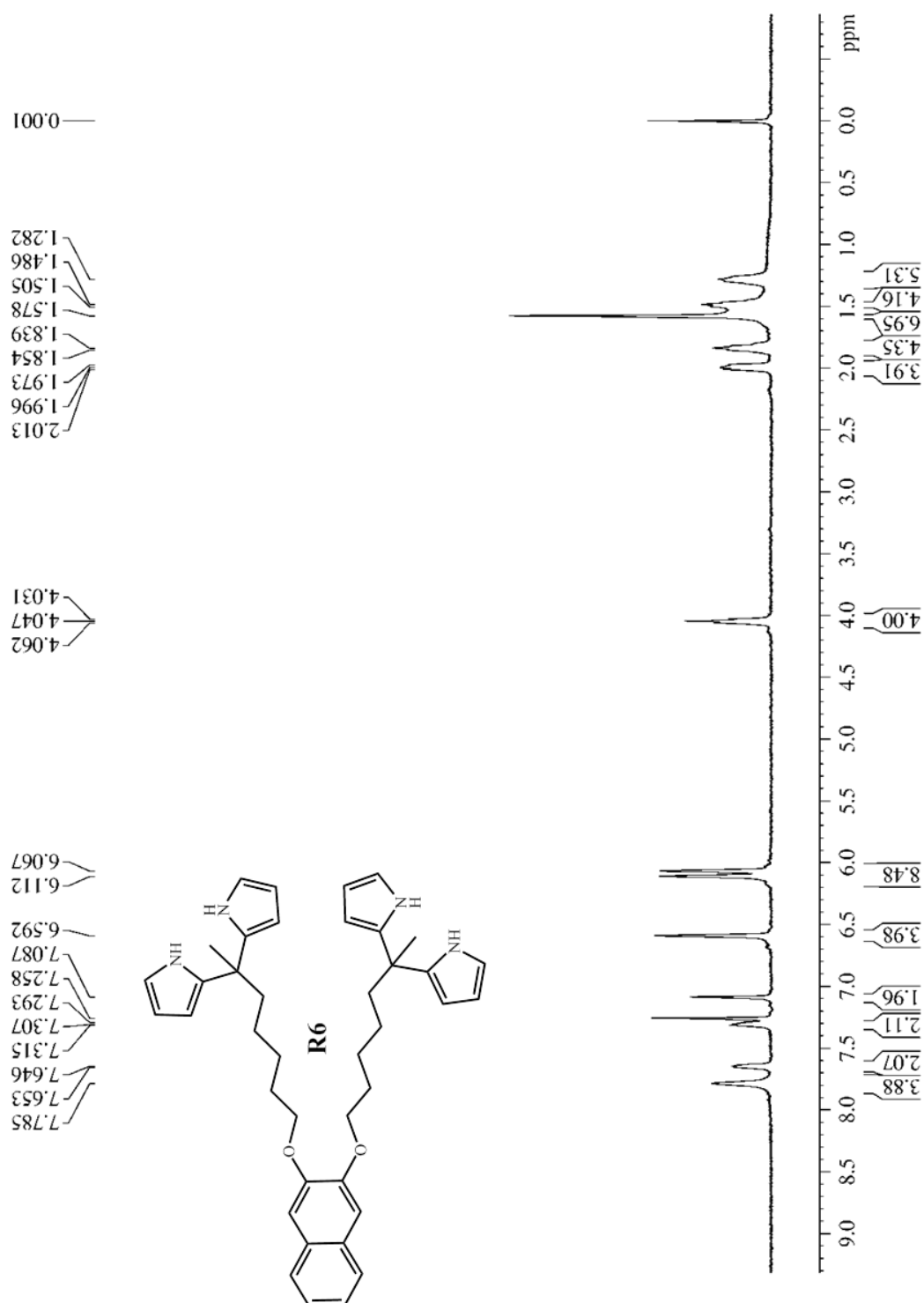


Figure A11: ¹H NMR spectrum of **R6**

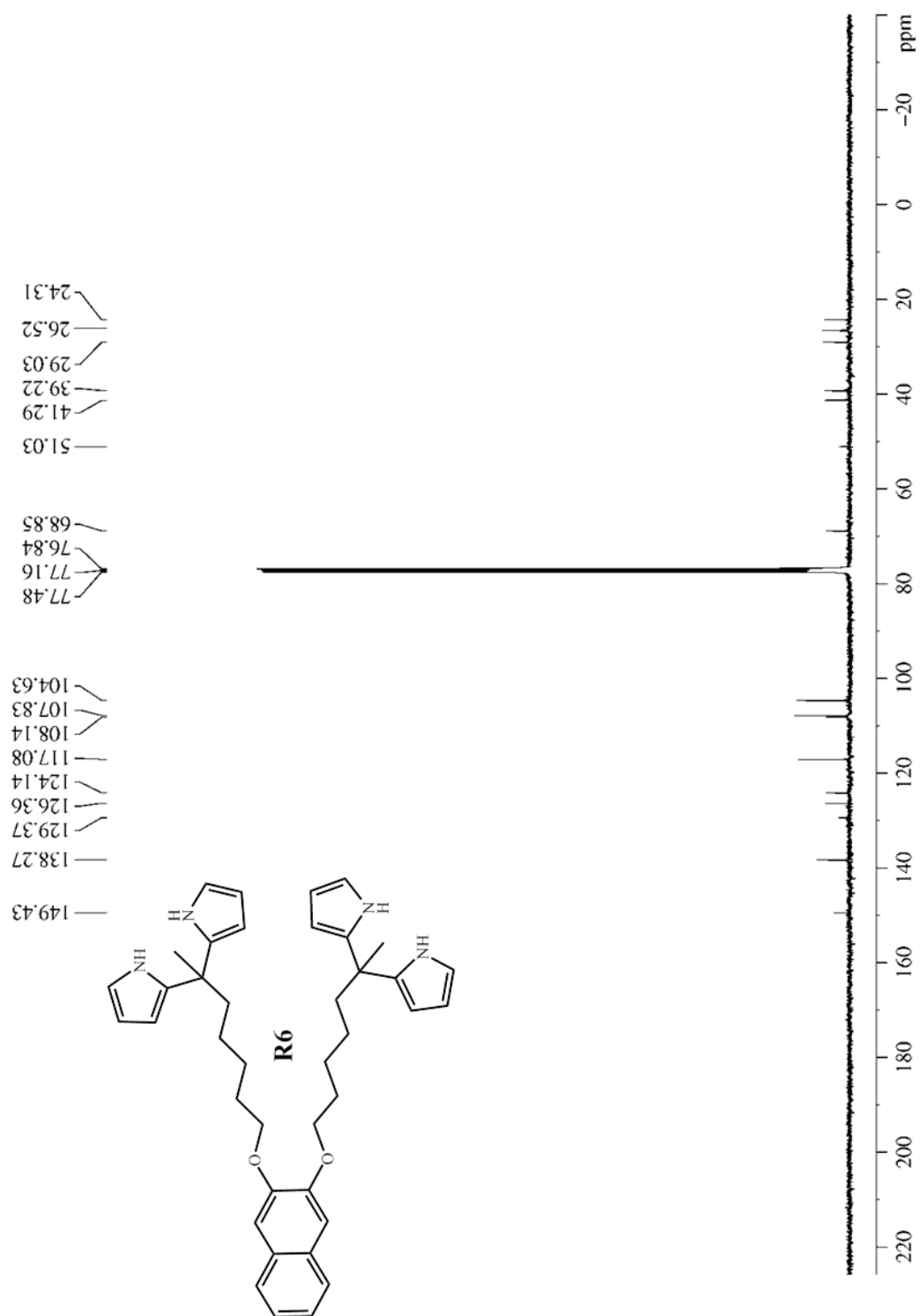
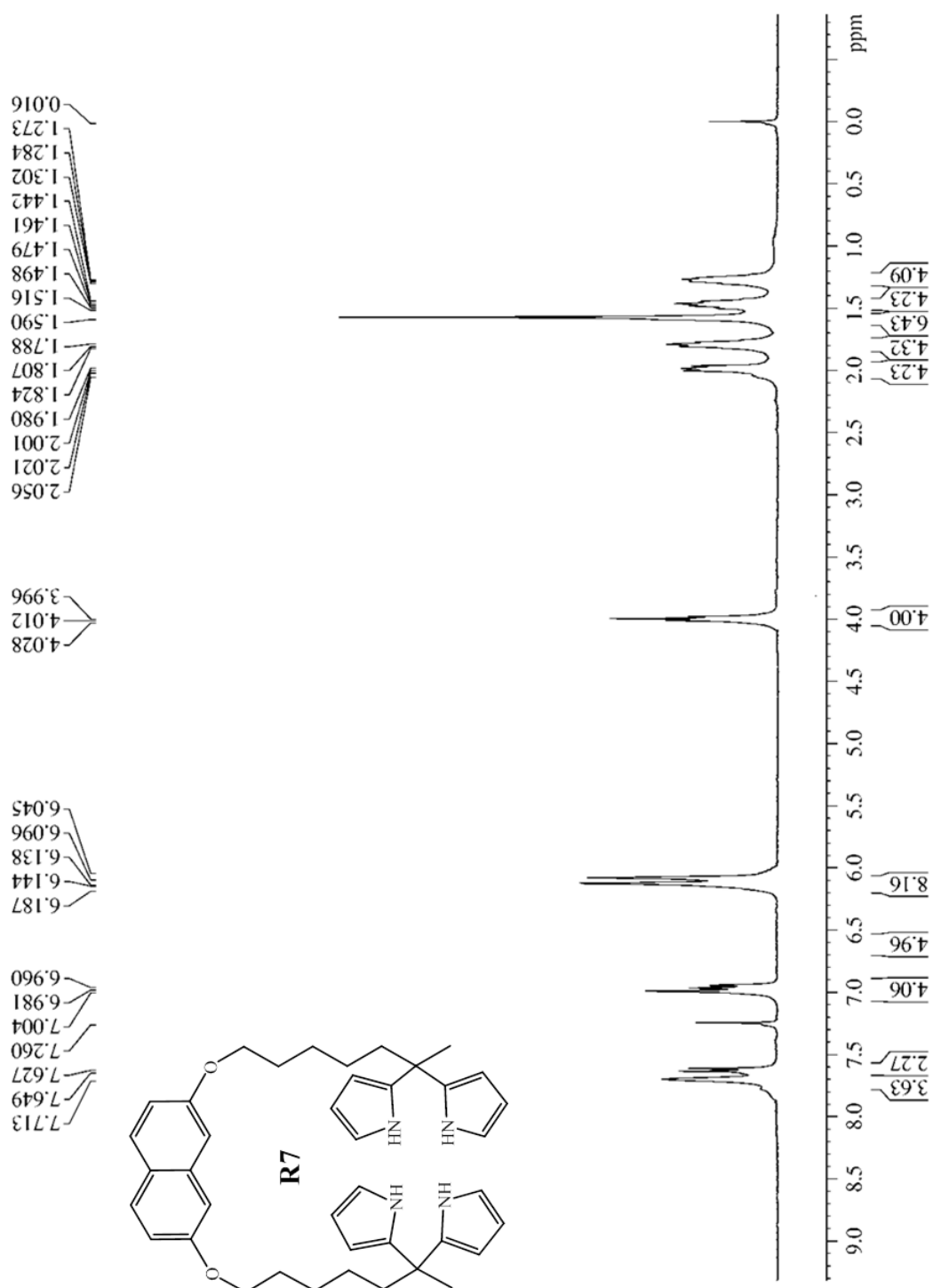


Figure A12: ^{13}C NMR spectrum of **R6**

**Figure A13:** ¹H NMR spectrum of **R7**

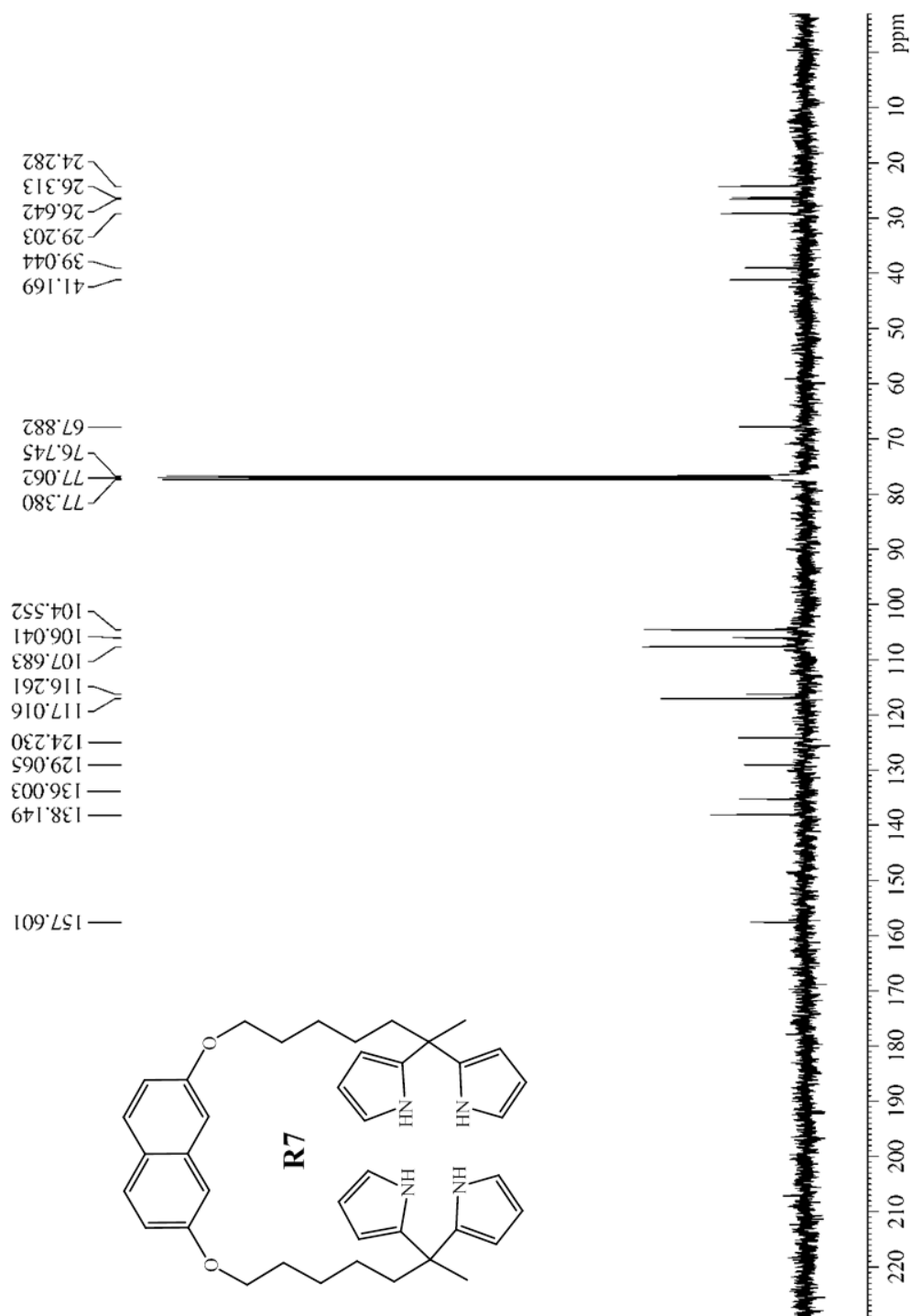
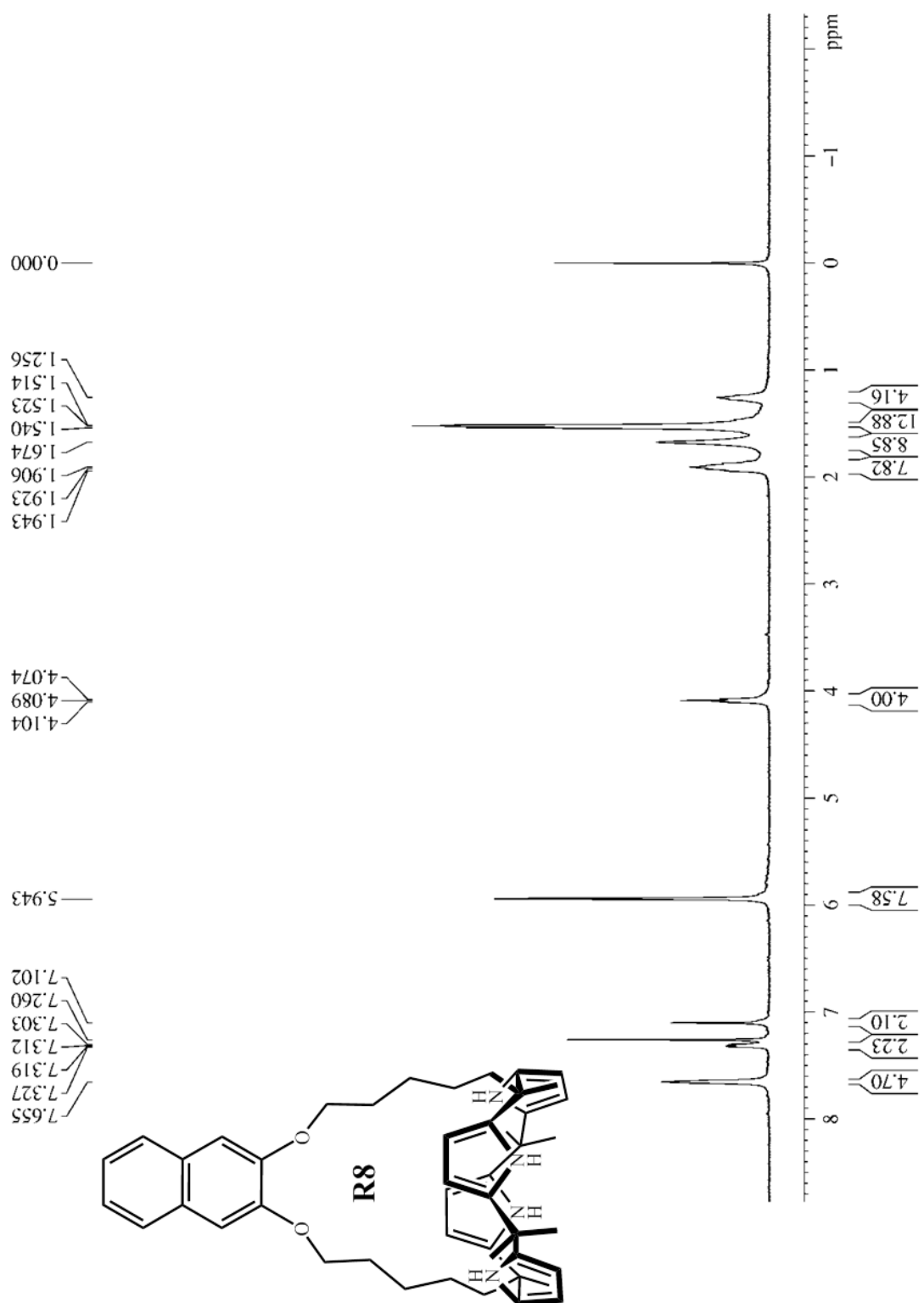


Figure A14: ^{13}C NMR spectrum of **R7**

**Figure A15:** ^1H NMR spectrum of **R8**

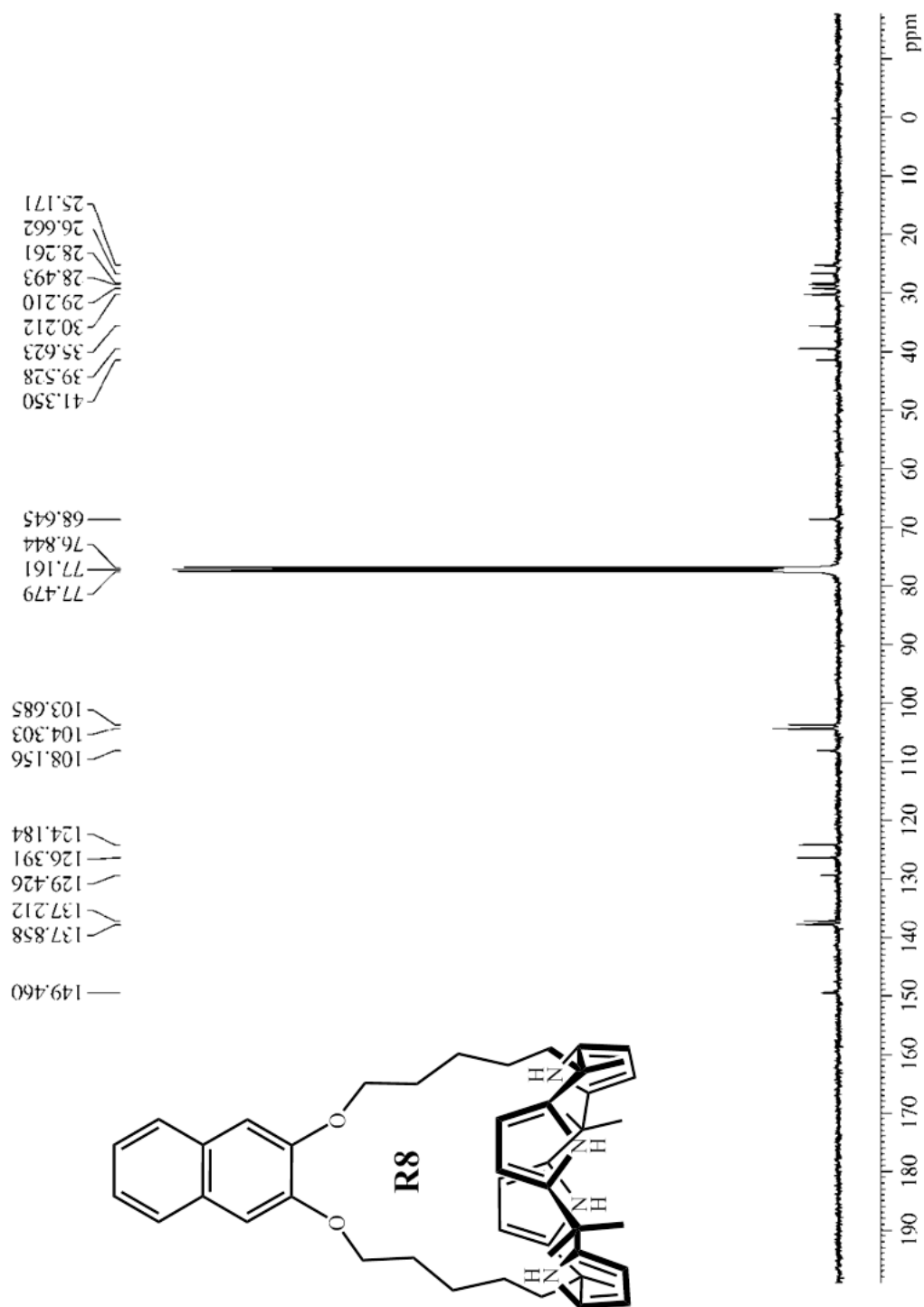


Figure A16: ^{13}C NMR spectrum of **R8**

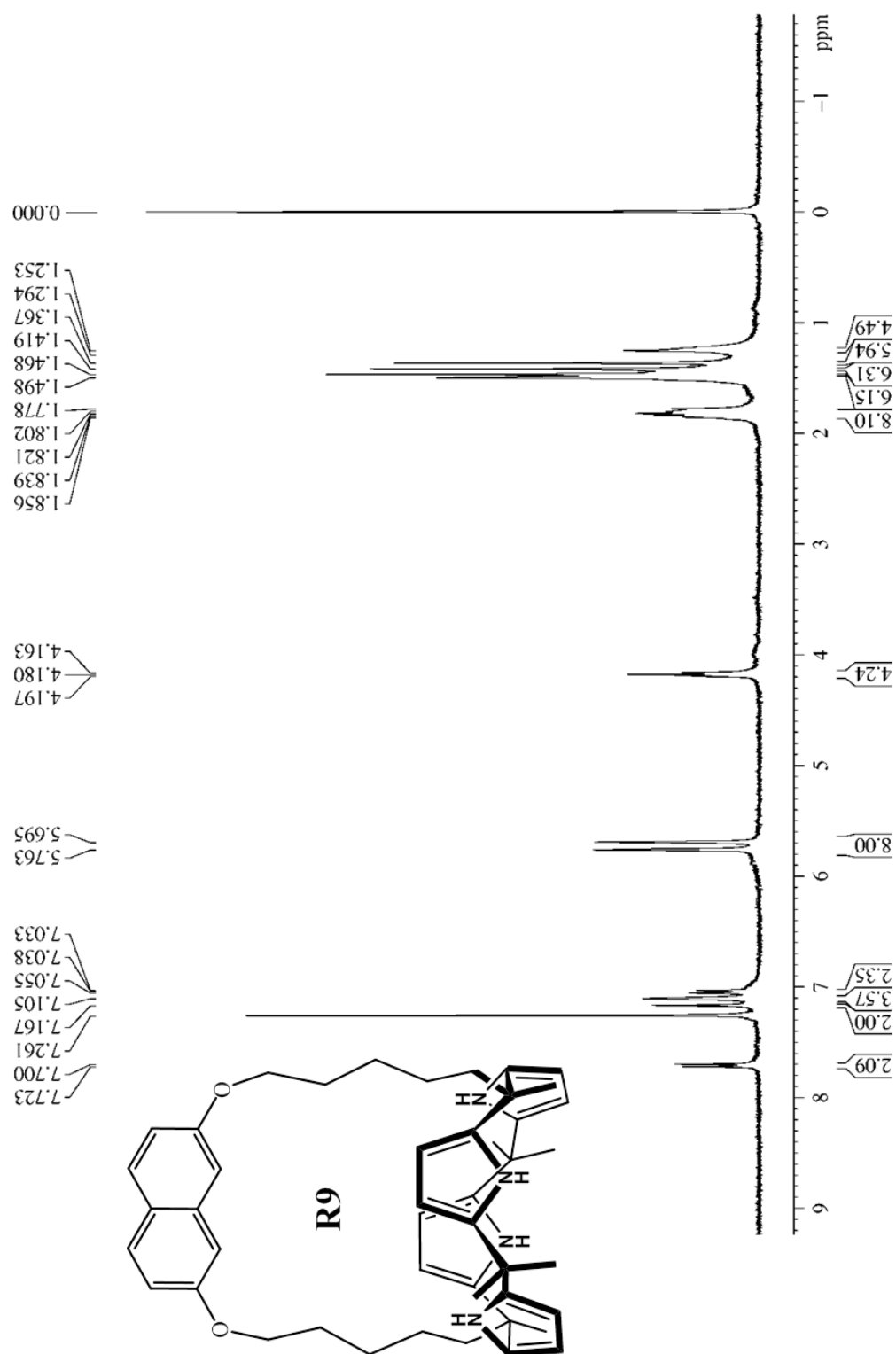


Figure A17: ^1H NMR spectrum of **R9**

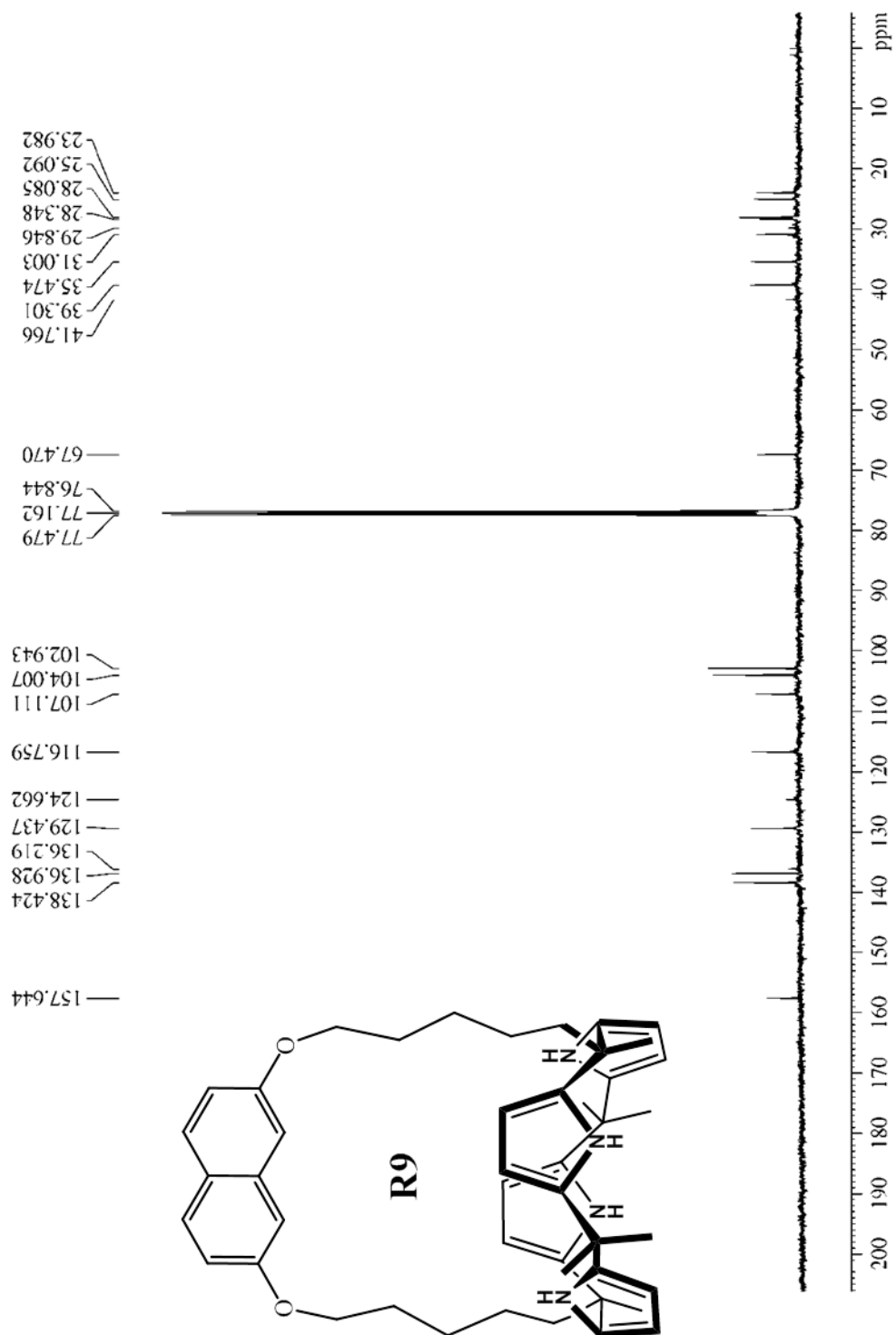


Figure A18: ^{13}C NMR spectrum of **R9**

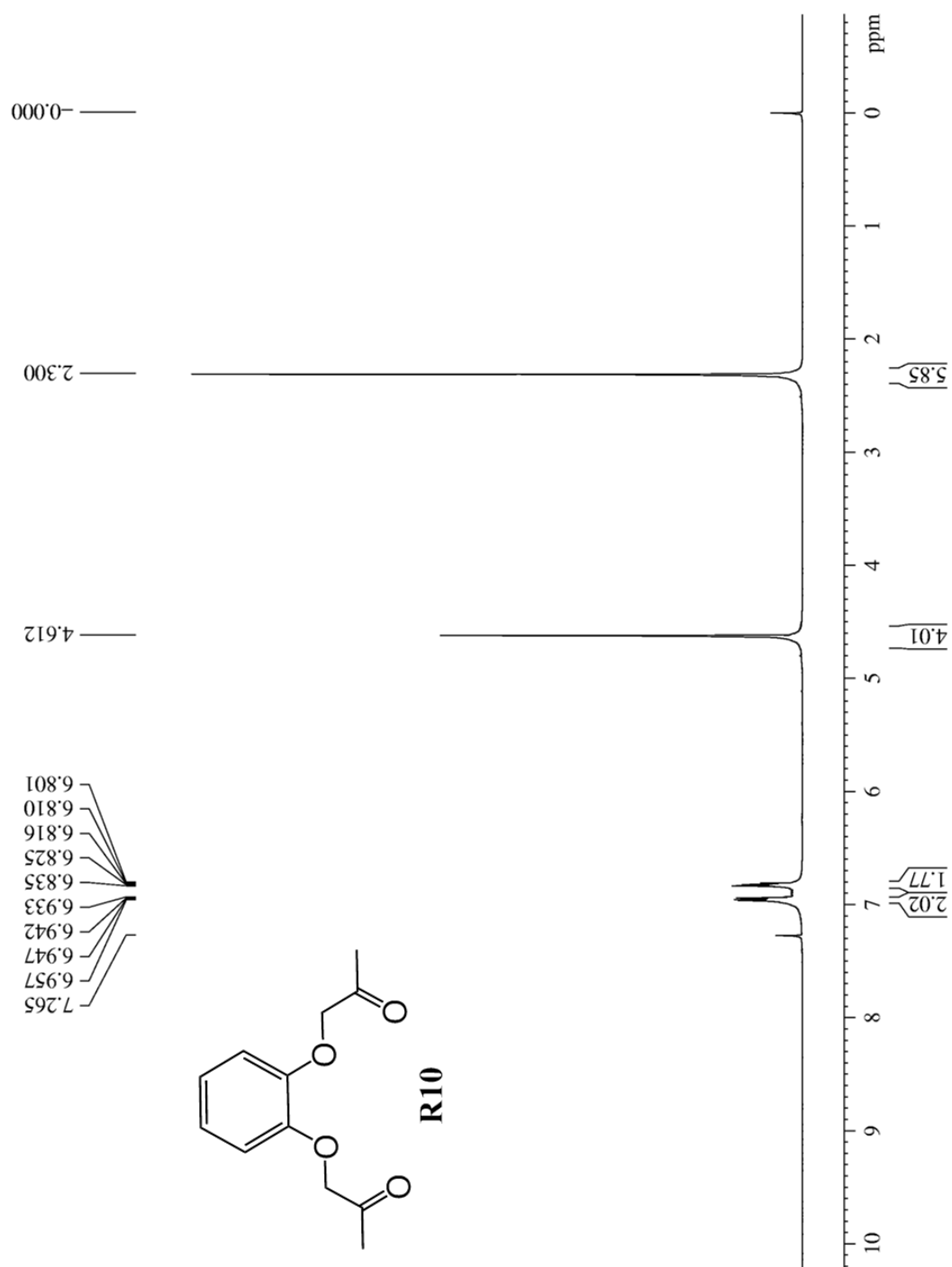


Figure A19: ¹H NMR spectrum of **R10**

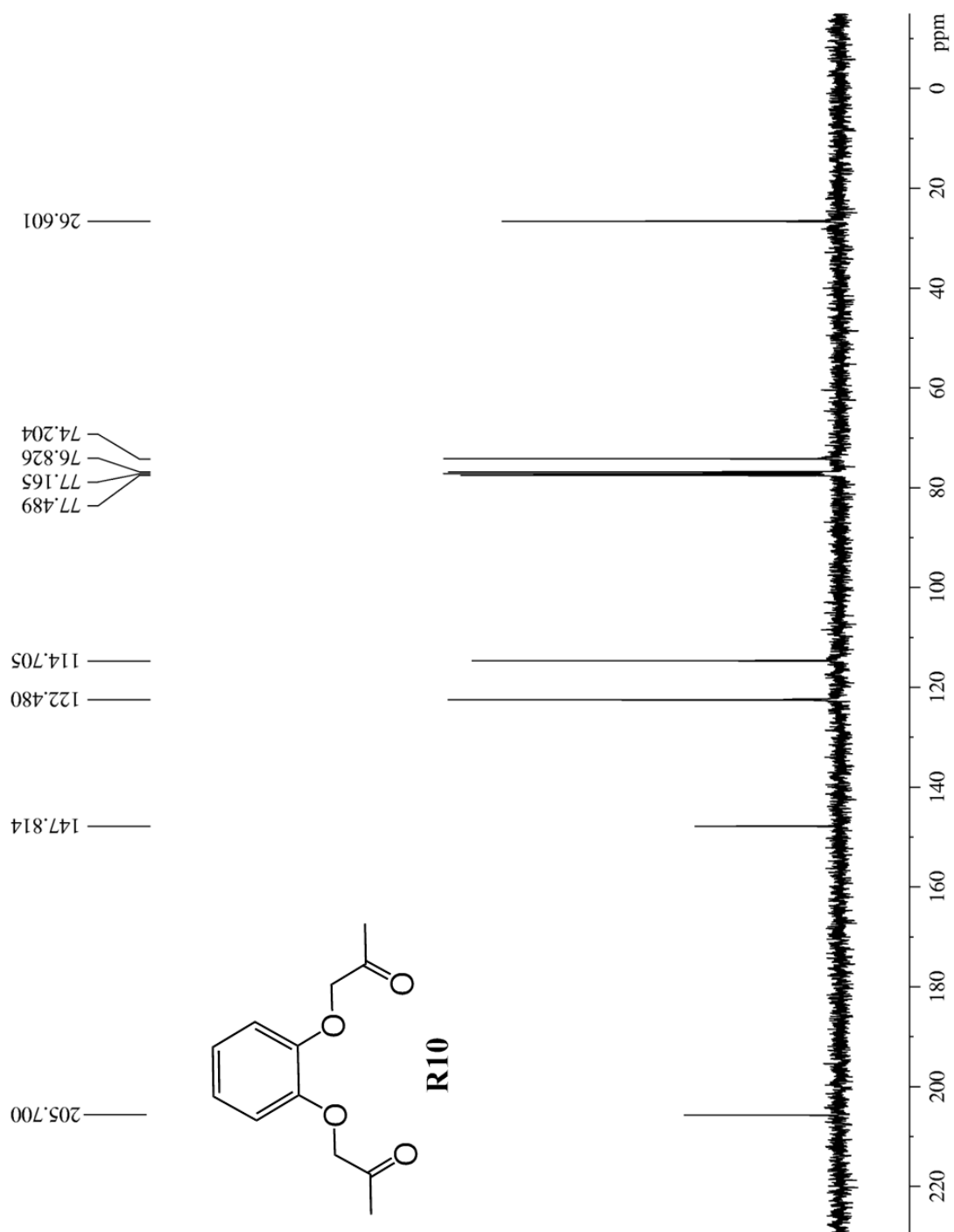


Figure A20: ^{13}C NMR spectrum of **R10**

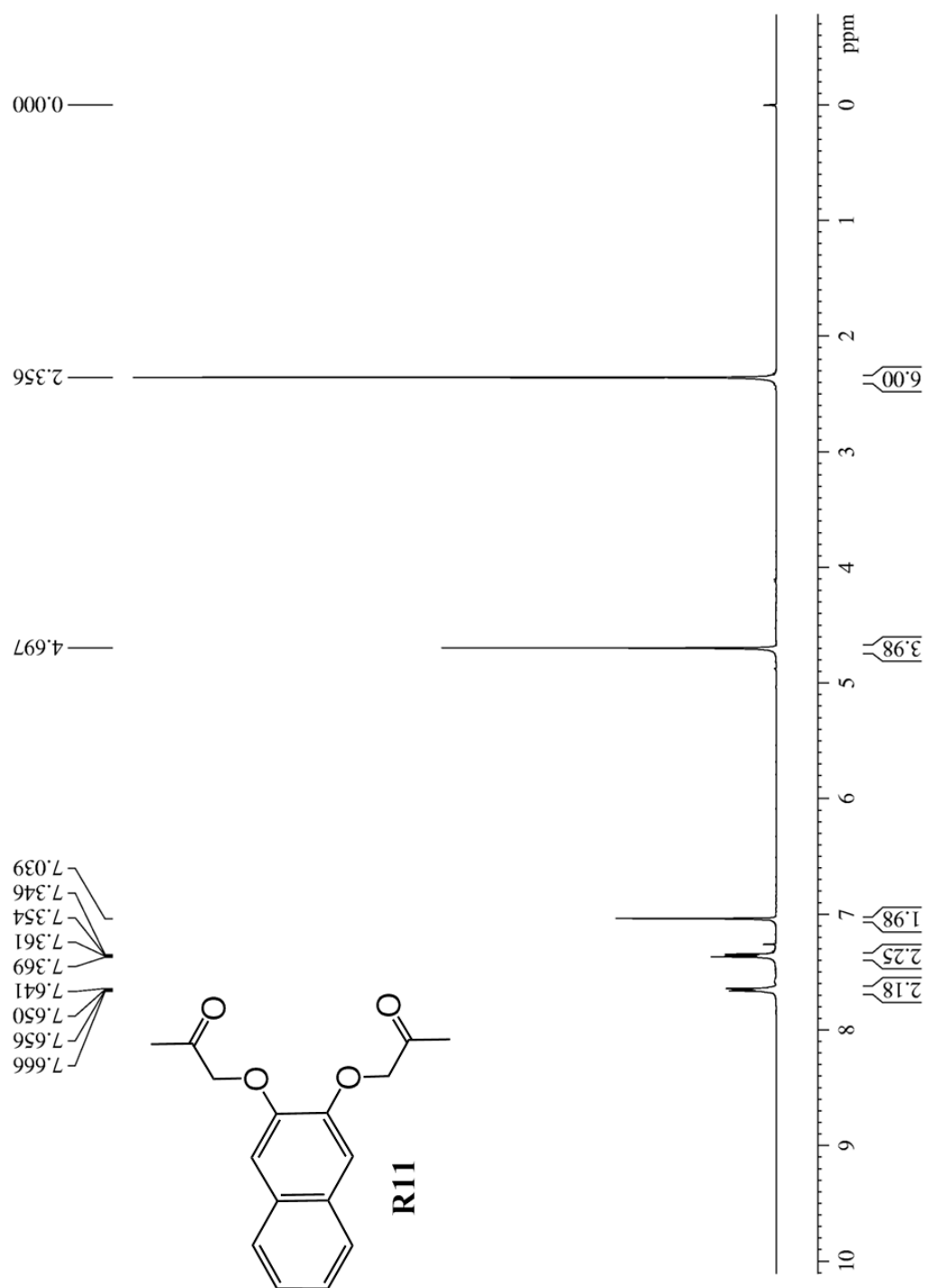


Figure A21: ^1H NMR spectrum of **R11**

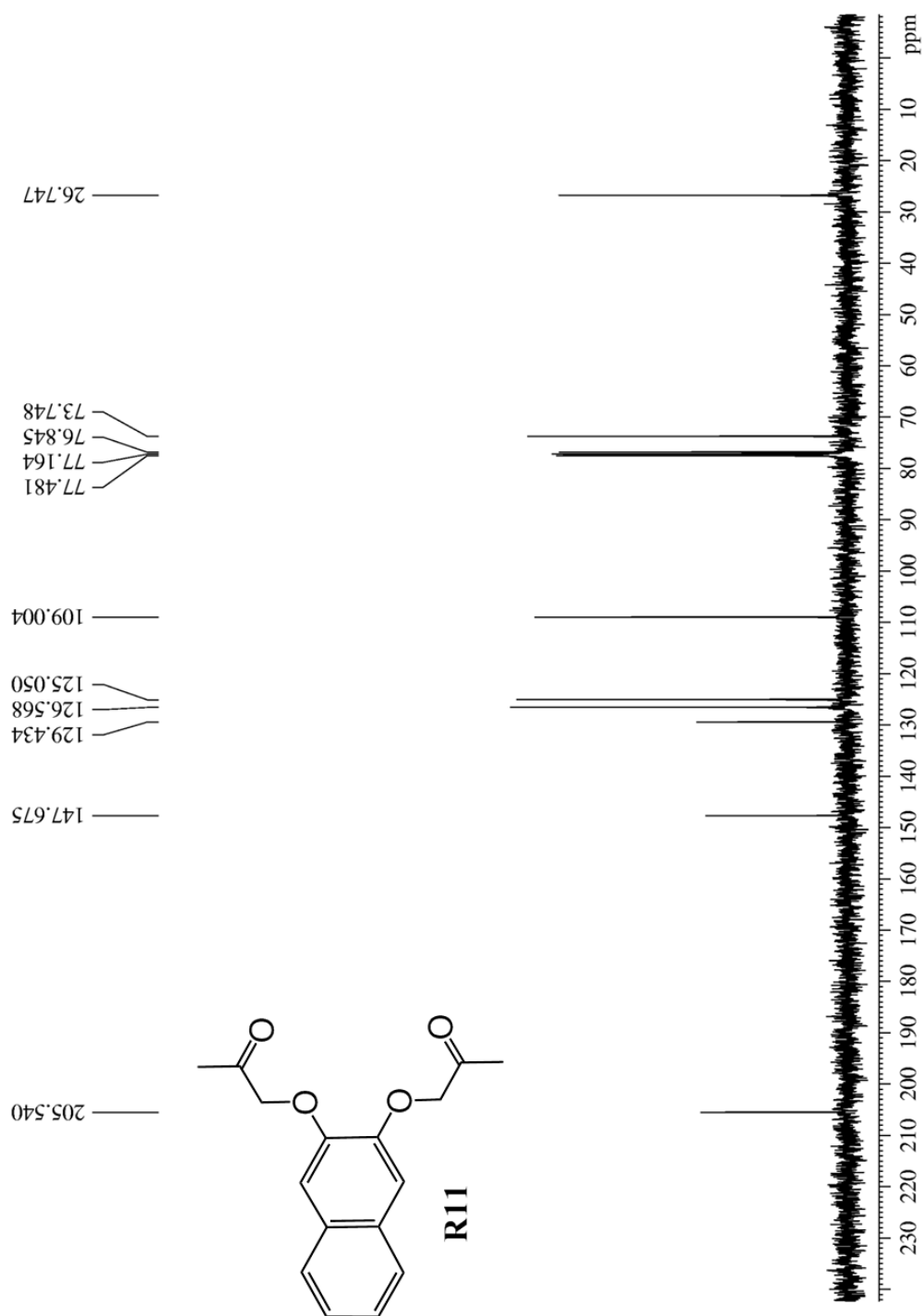
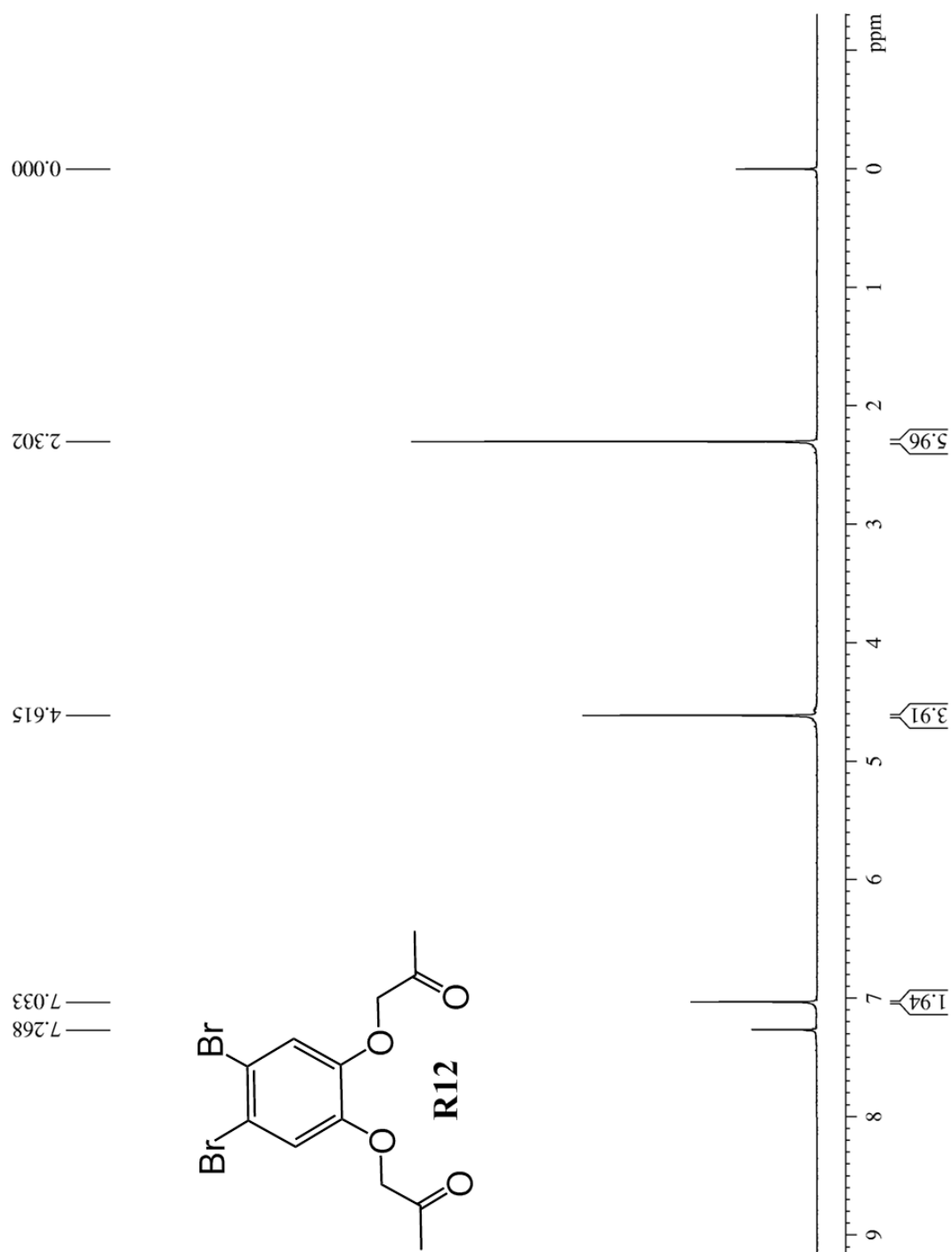


Figure A22: ^{13}C NMR spectrum of **R11**

**Figure A23:** ^1H NMR spectrum of **R12**

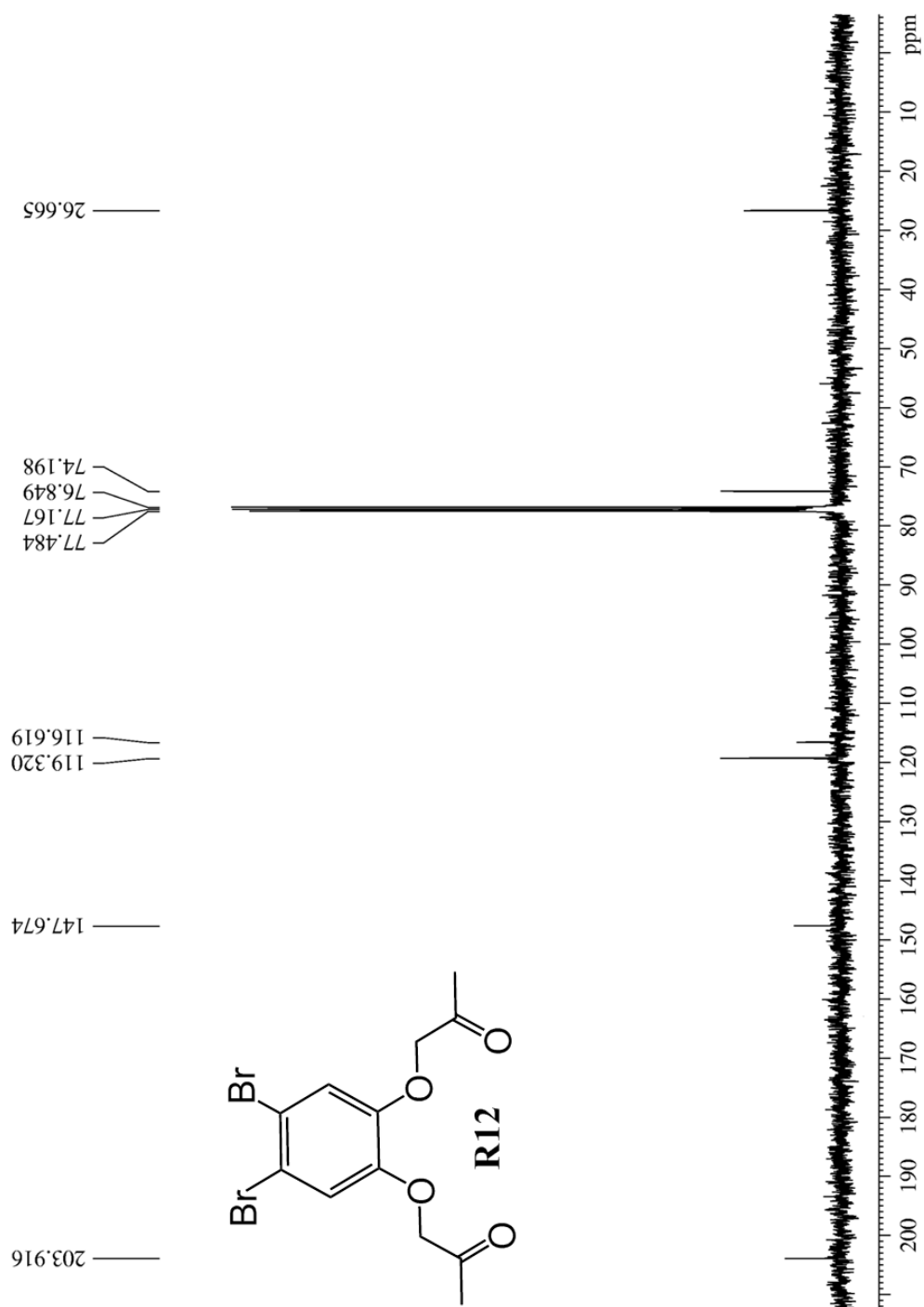


Figure A24: ^{13}C NMR spectrum of **R12**

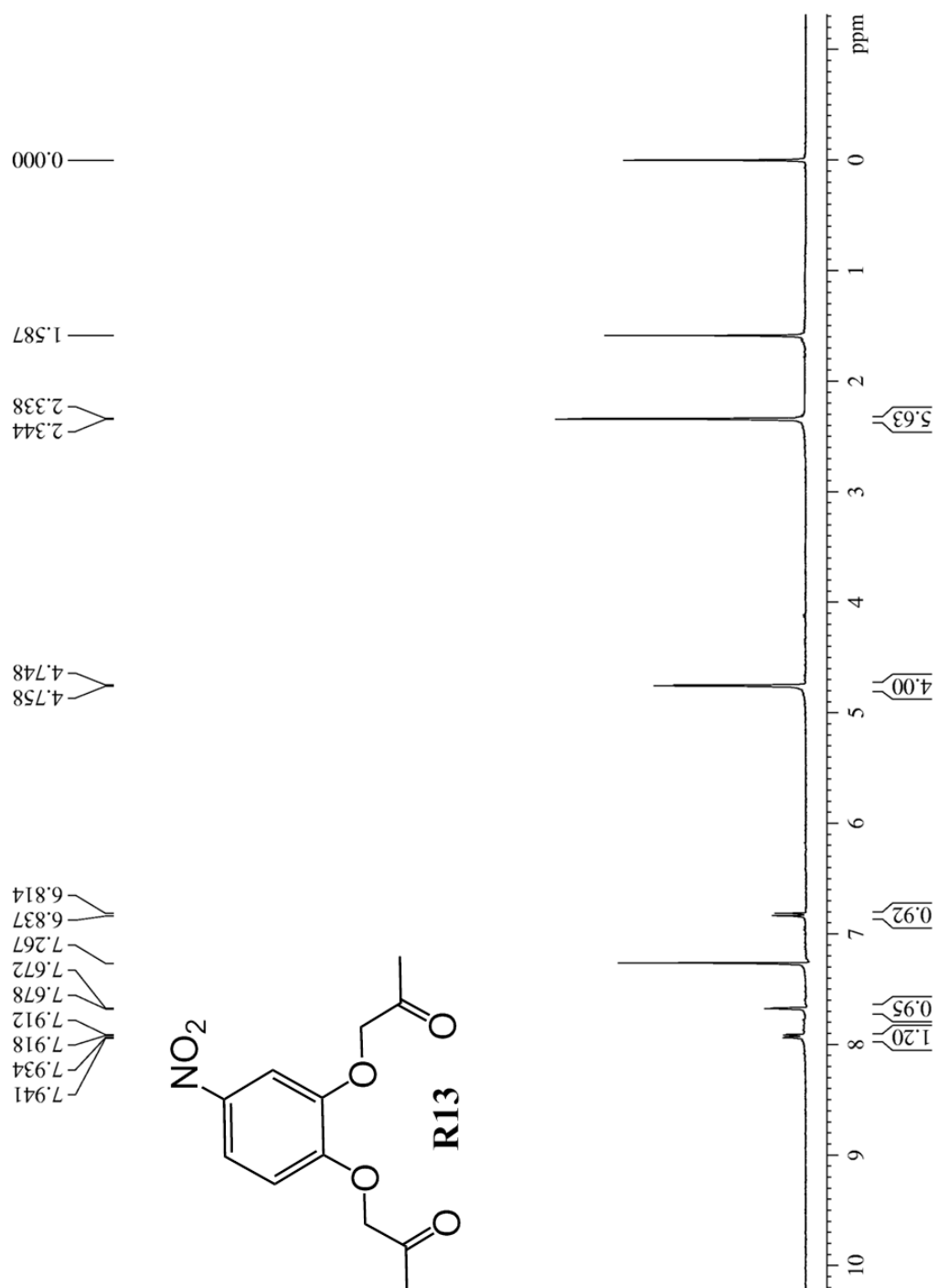


Figure A25: ¹H NMR spectrum of **R13**

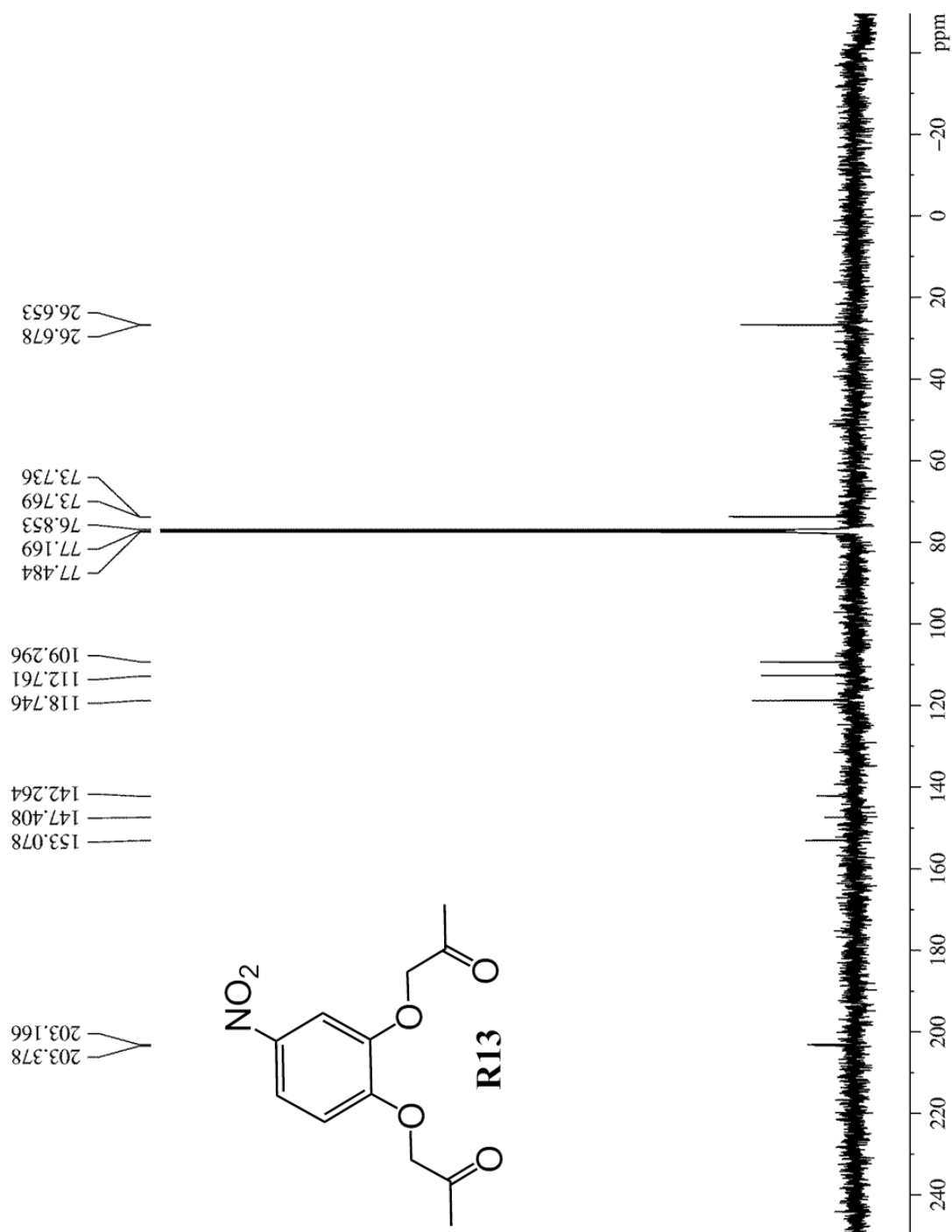
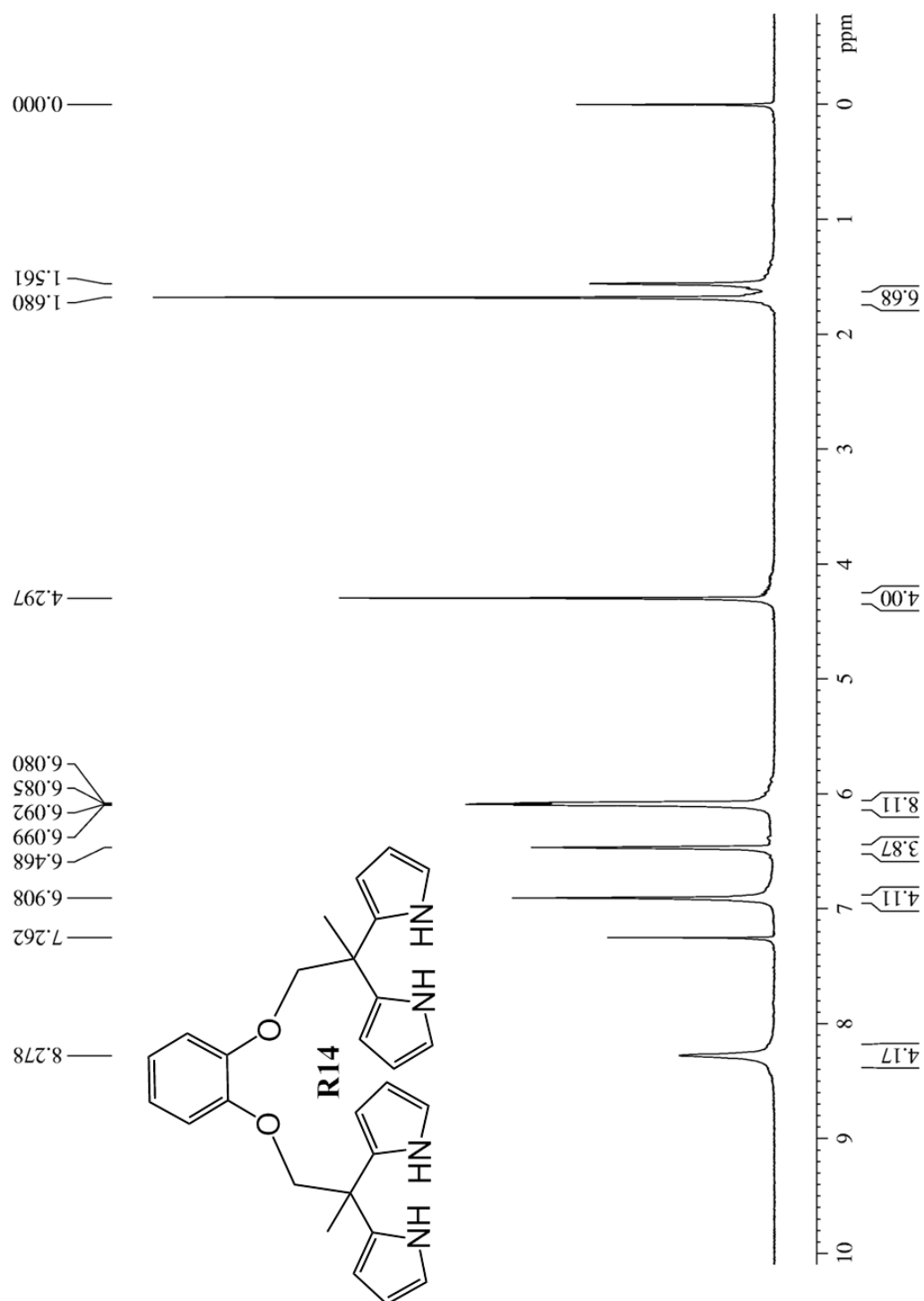
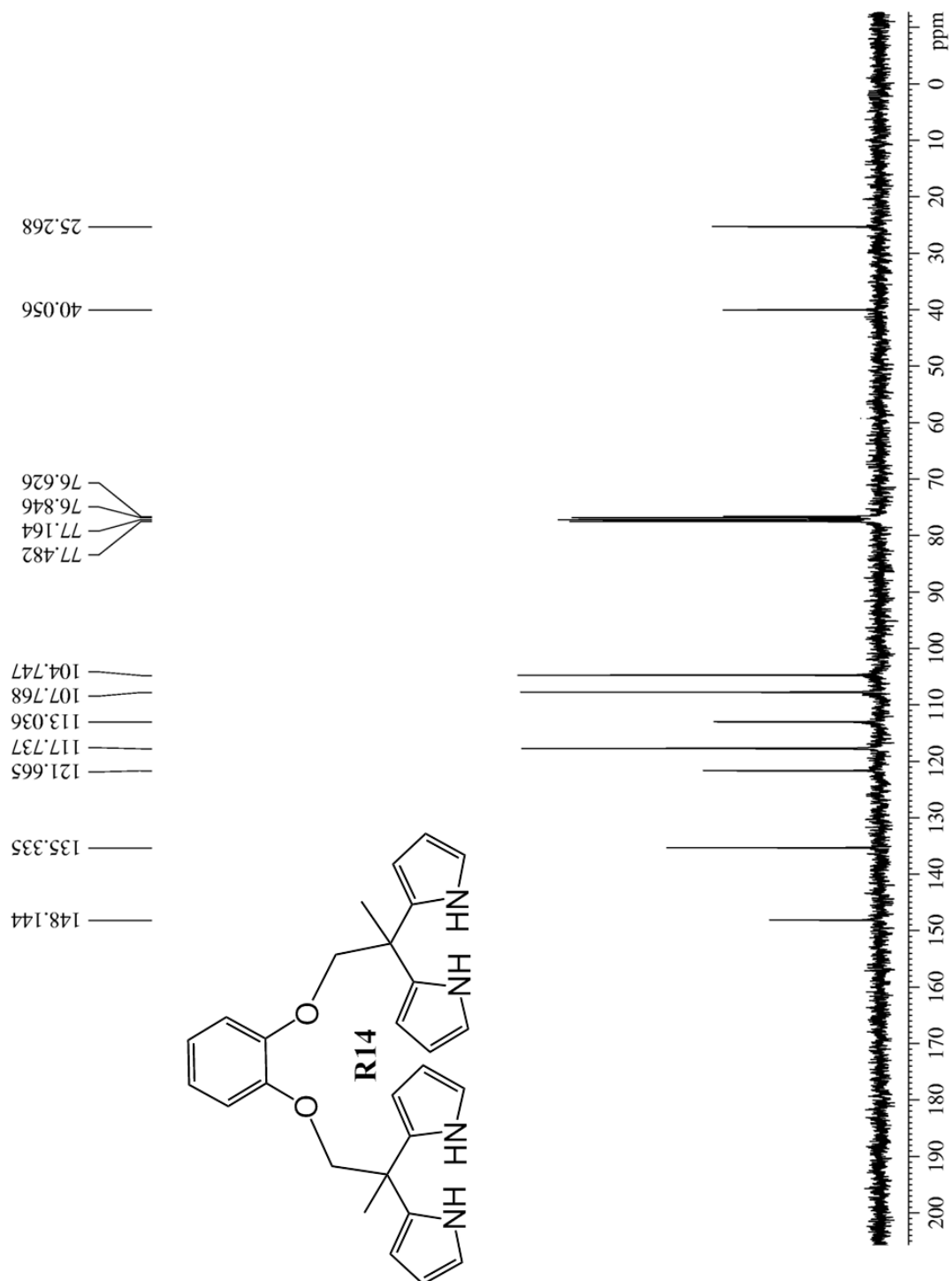


Figure A26: ¹³C NMR spectrum of **R13**

**Figure A27:** ^1H NMR spectrum of **R14**



F
figure A28: ^{13}C NMR spectrum of **R14**

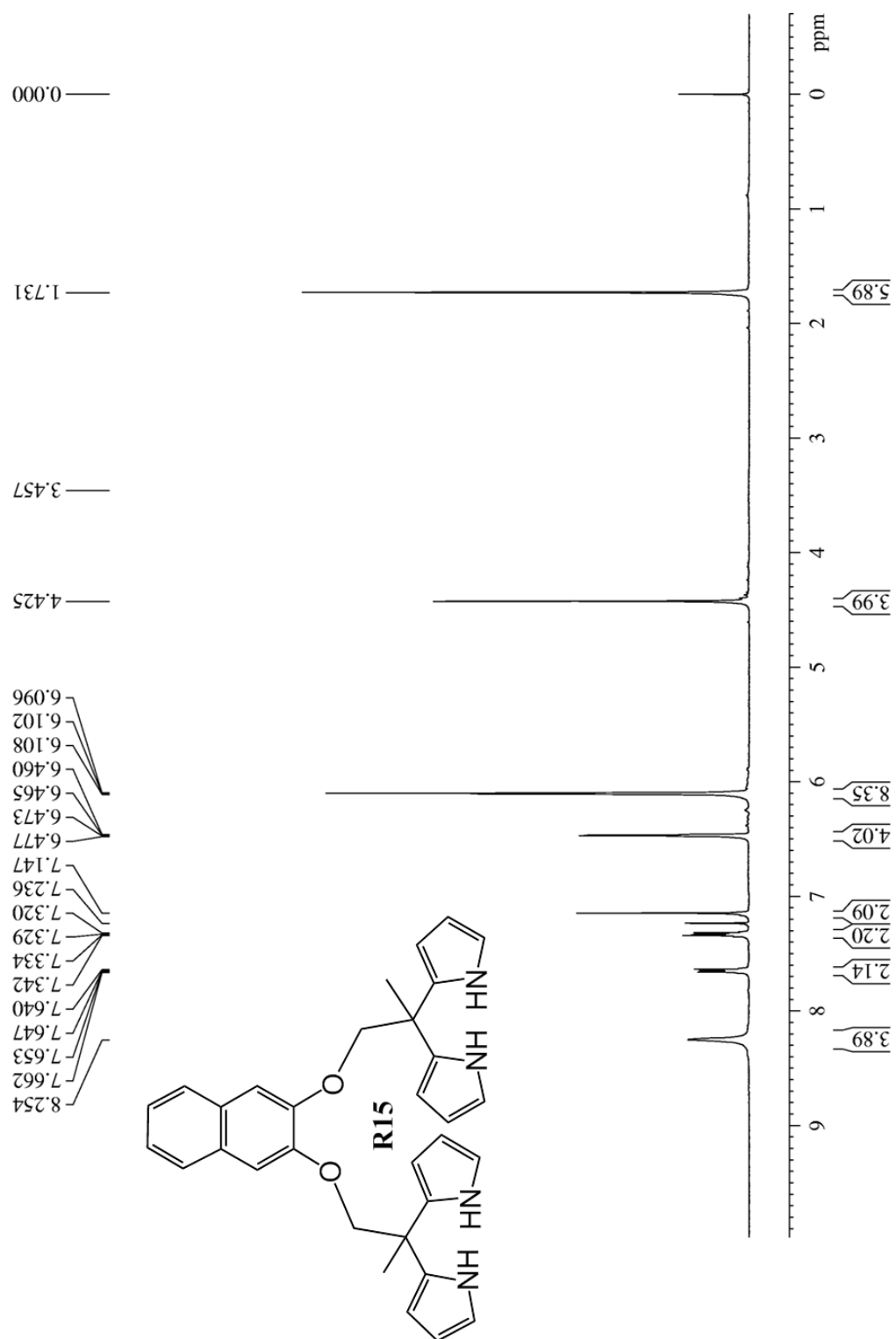


Figure A29: ^1H NMR spectrum of **R15**

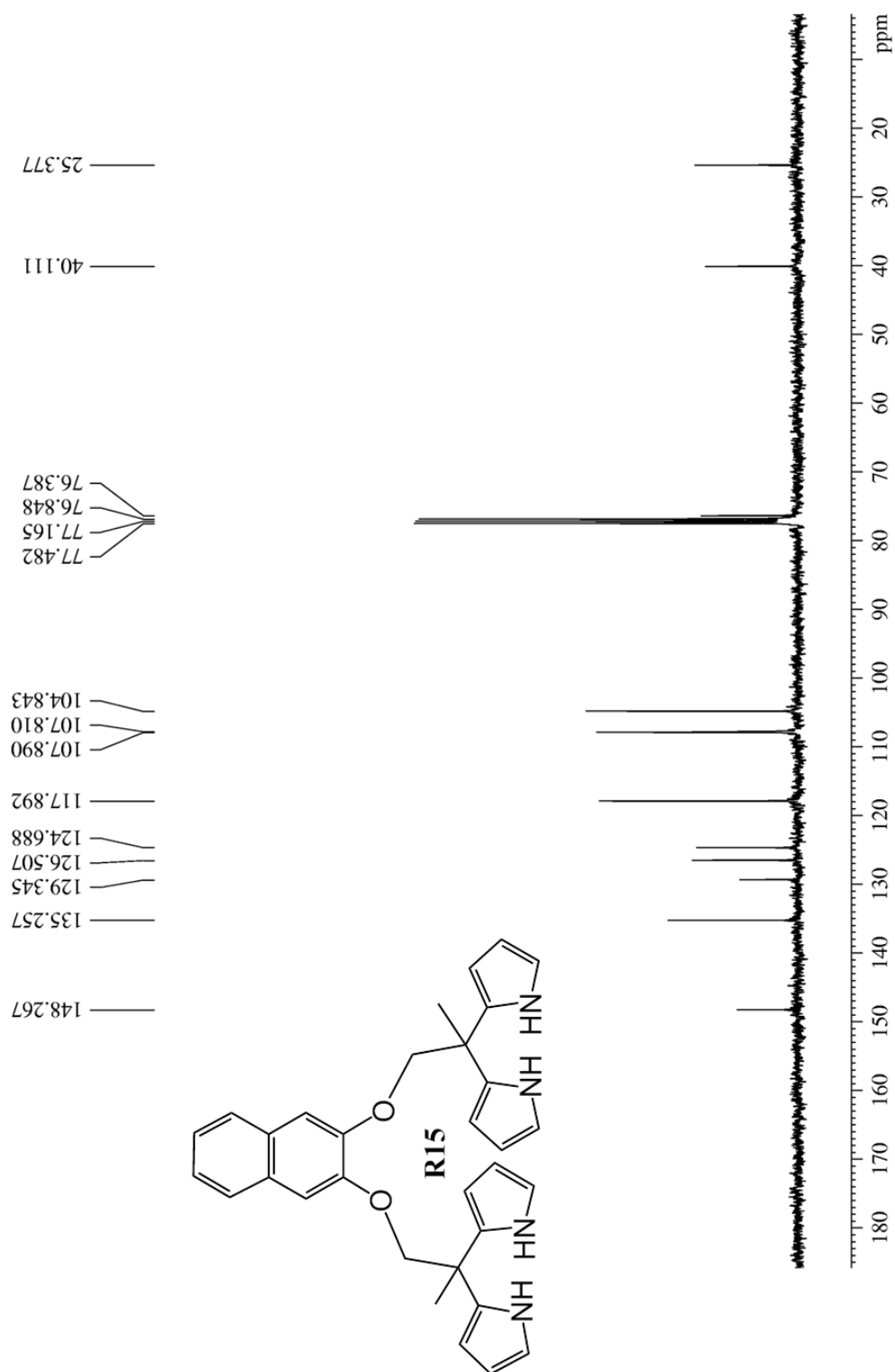


Figure A30: ^{13}C NMR spectrum of **R15**

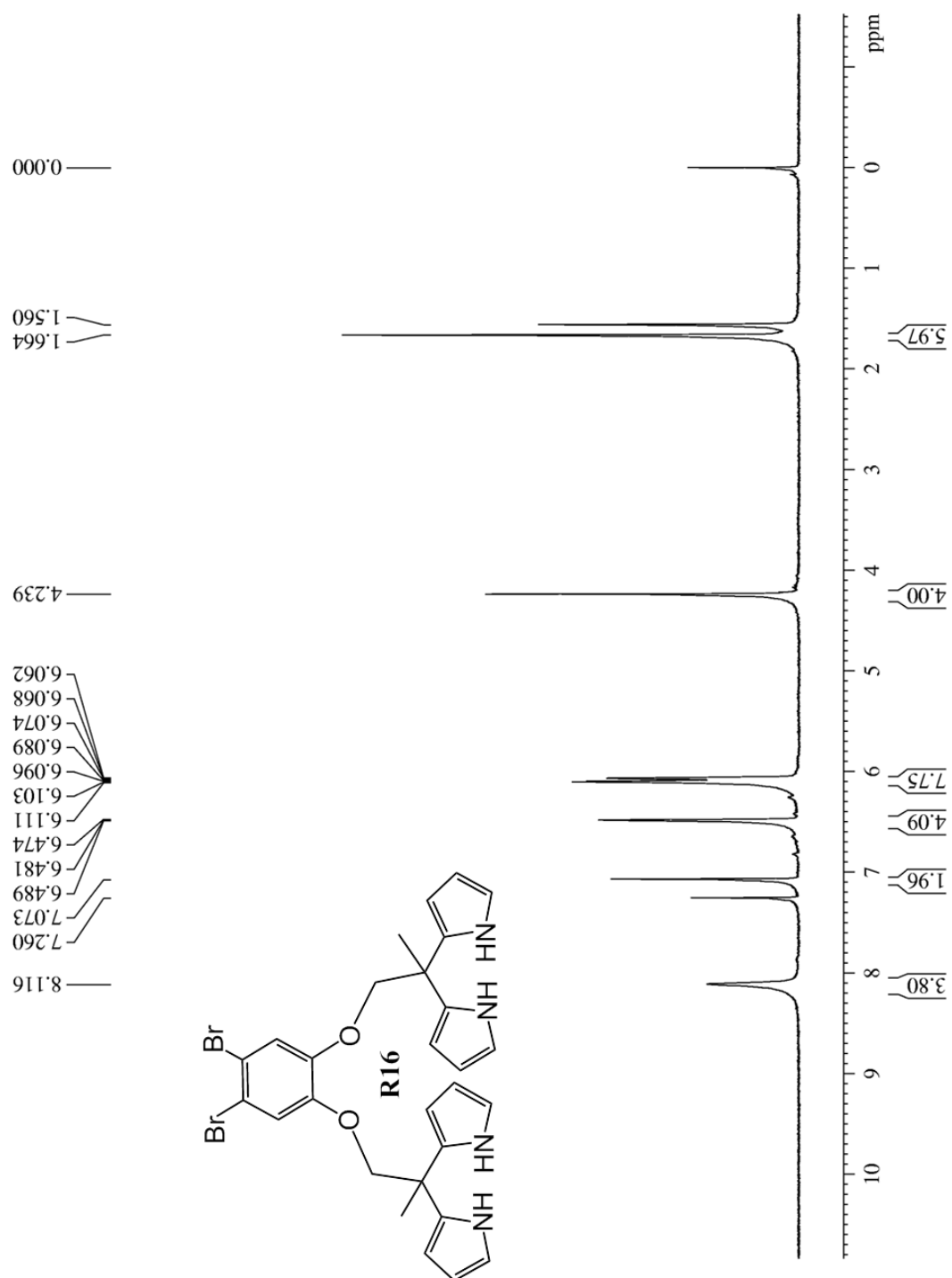


Figure A31: ^1H NMR spectrum of **R16**

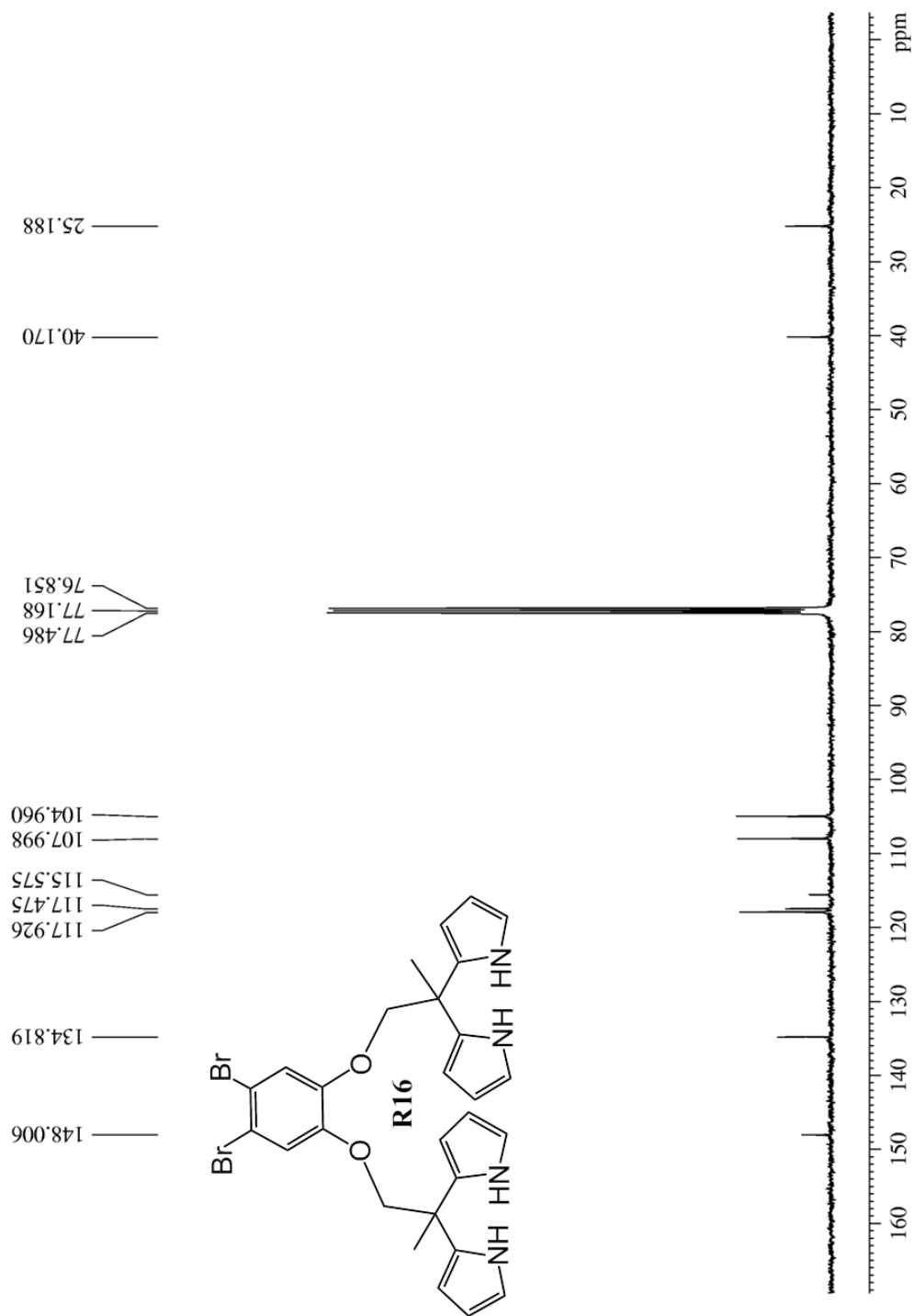
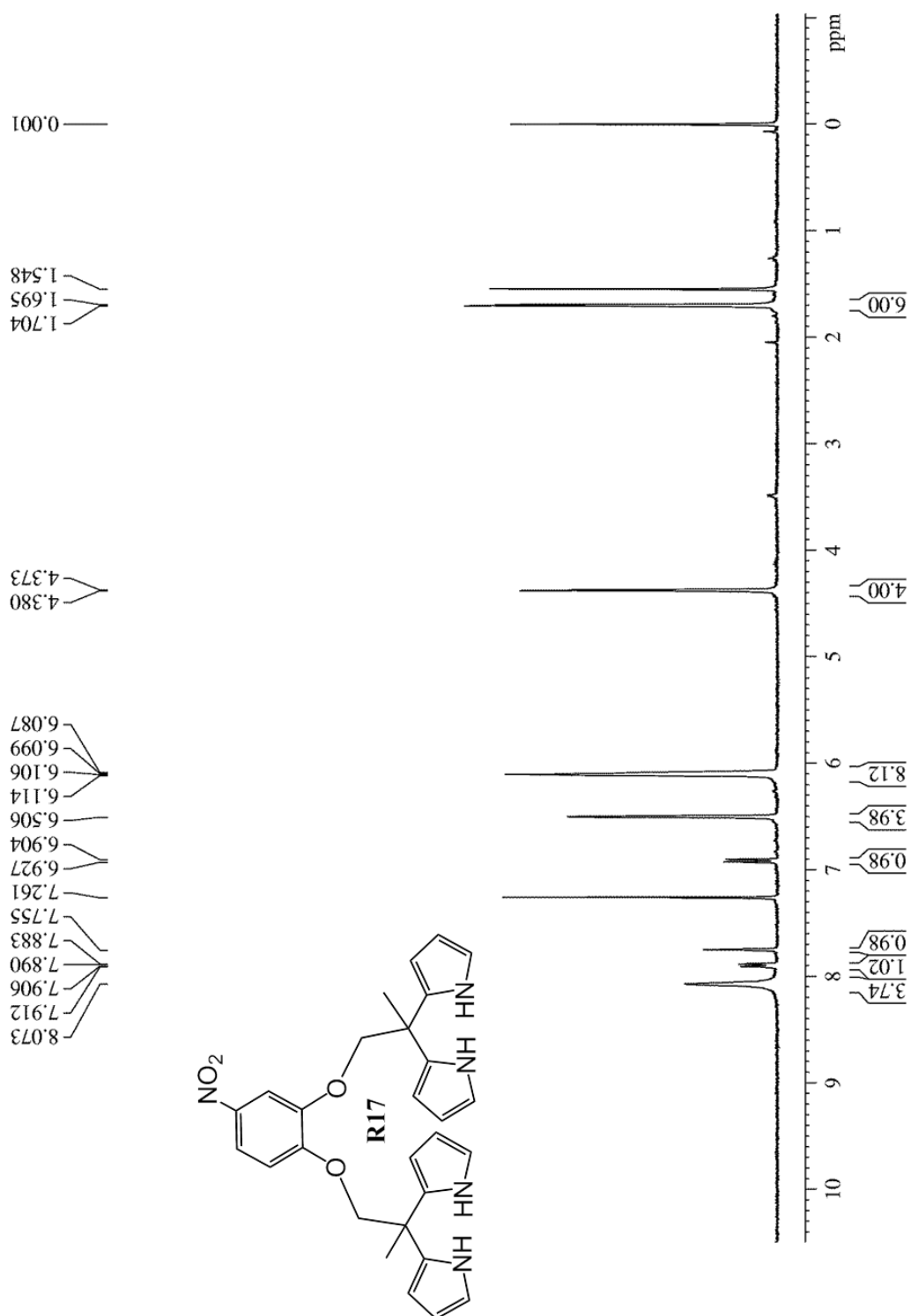


Figure A32: ¹³C NMR spectrum of **R16**

**Figure A33:** ^1H NMR spectrum of **R17**

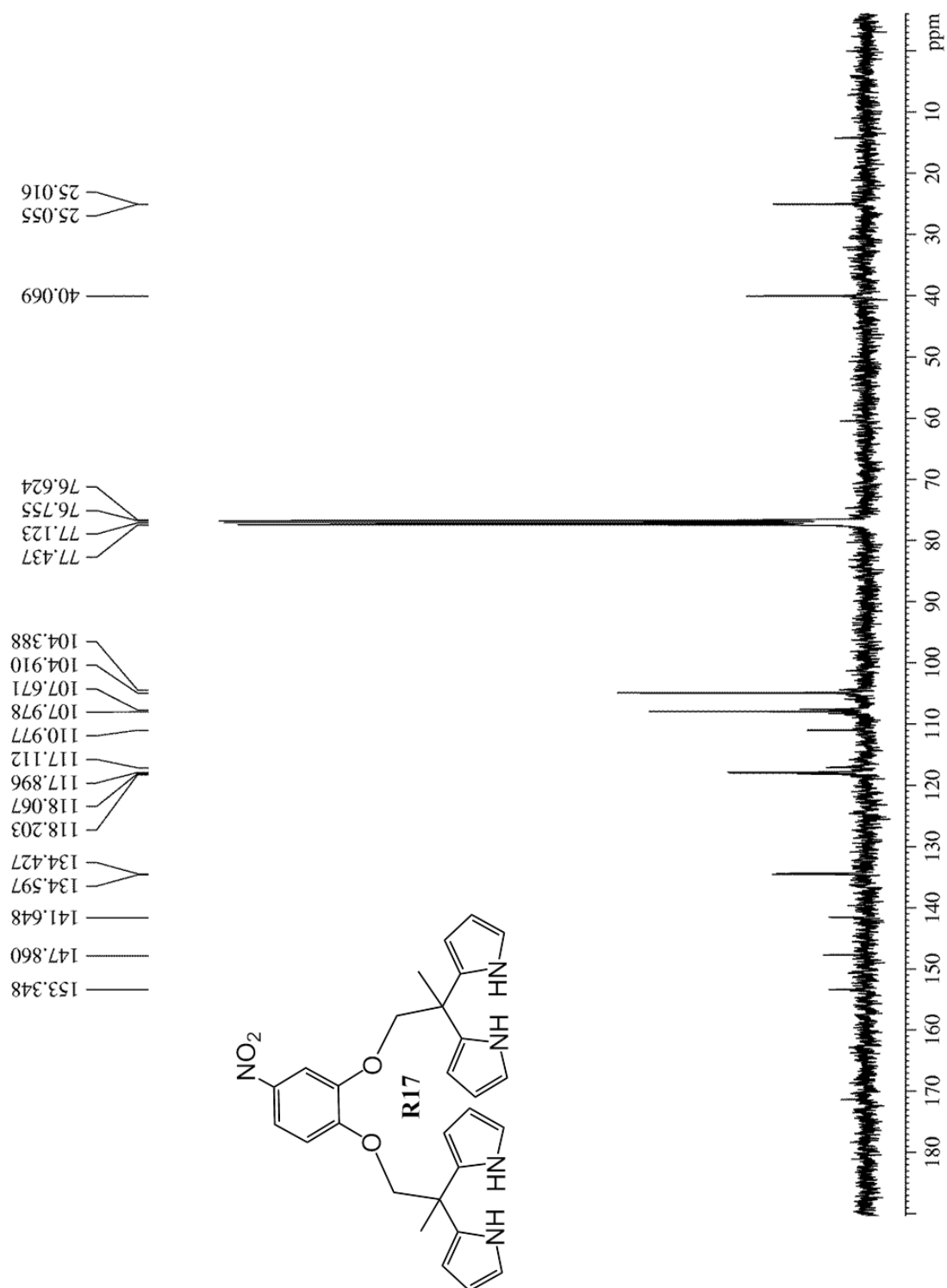


Figure A34: ¹³C NMR spectrum of **R17**

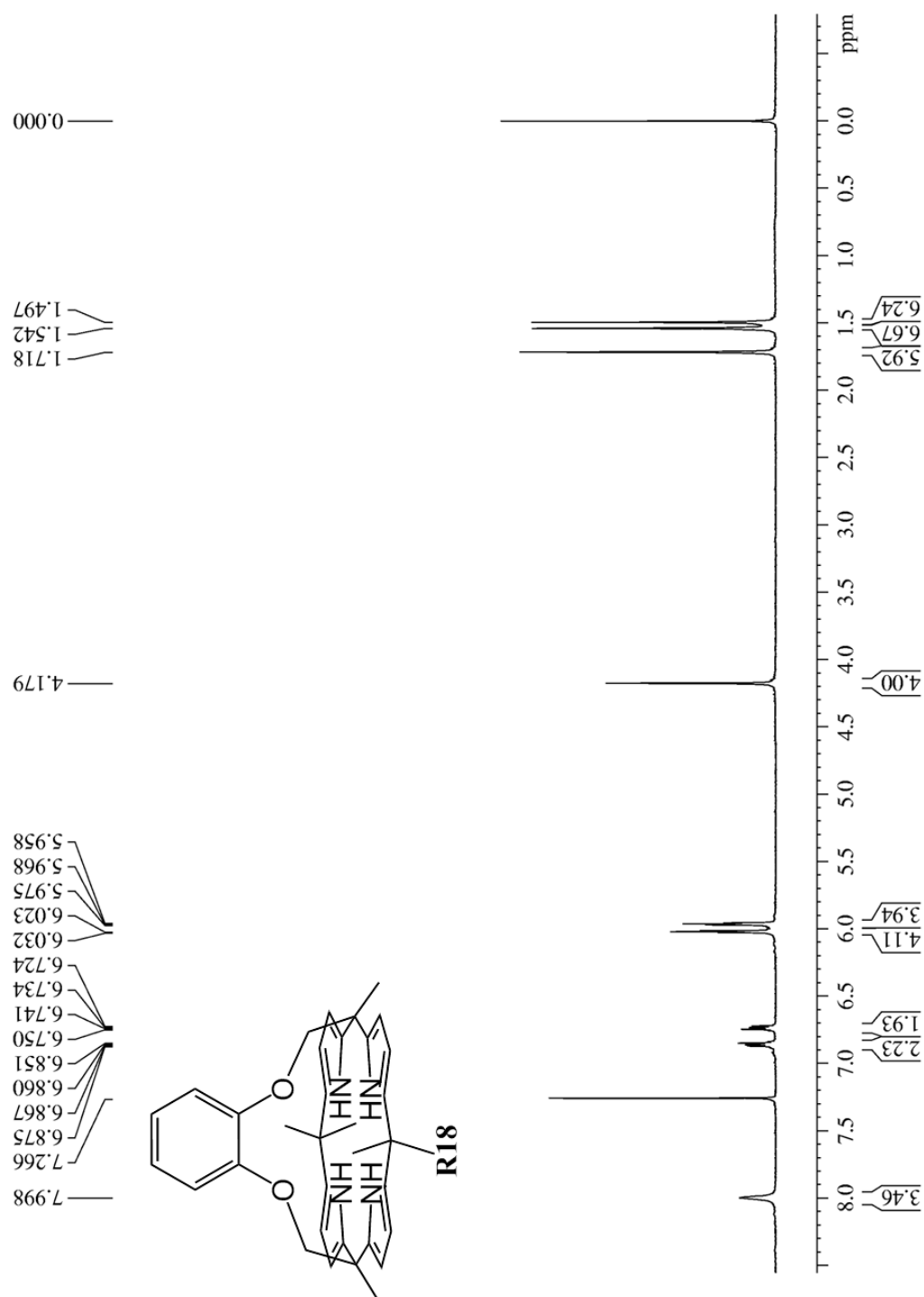


Figure A35: ¹H NMR spectrum of **R18**

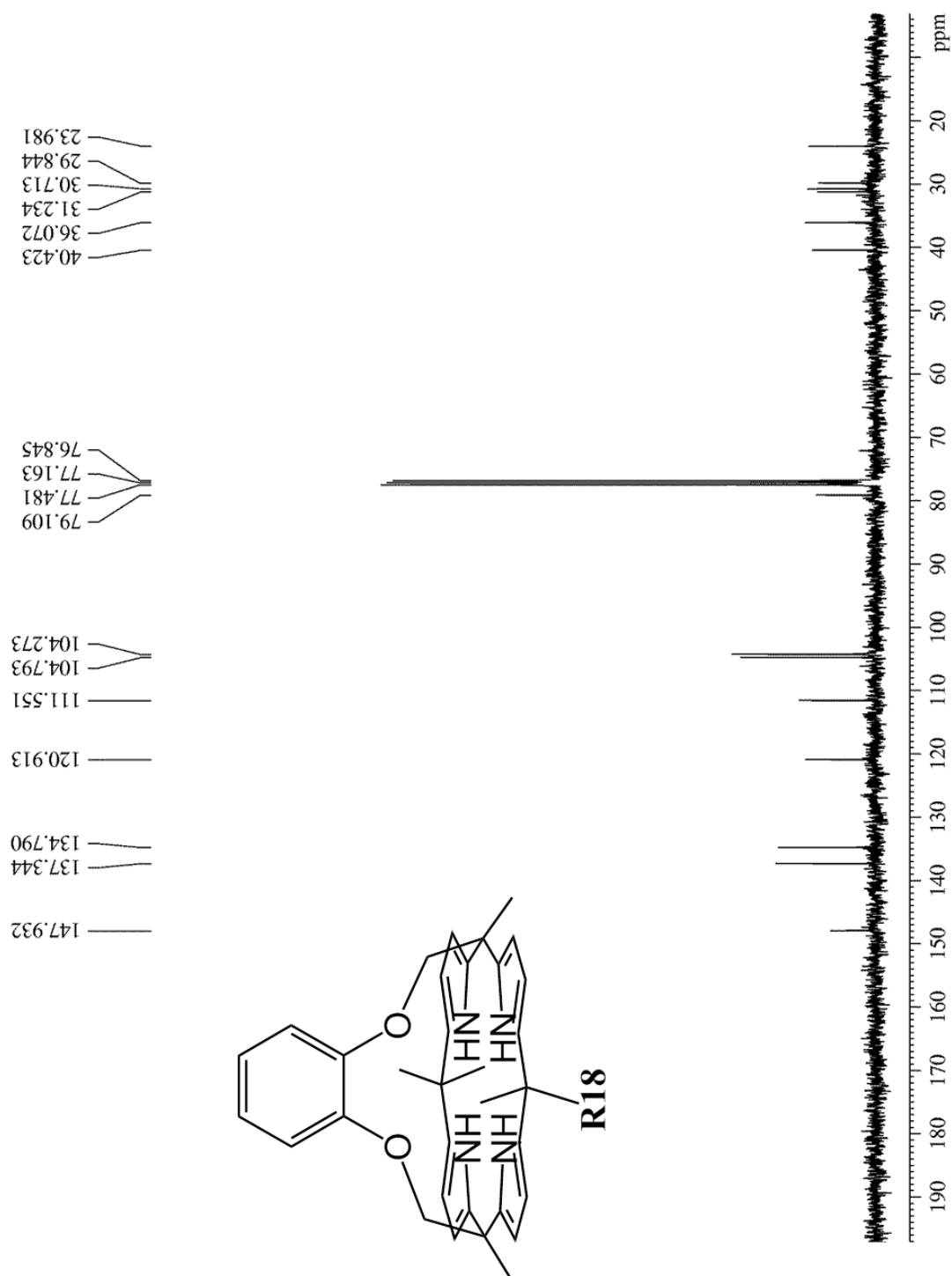
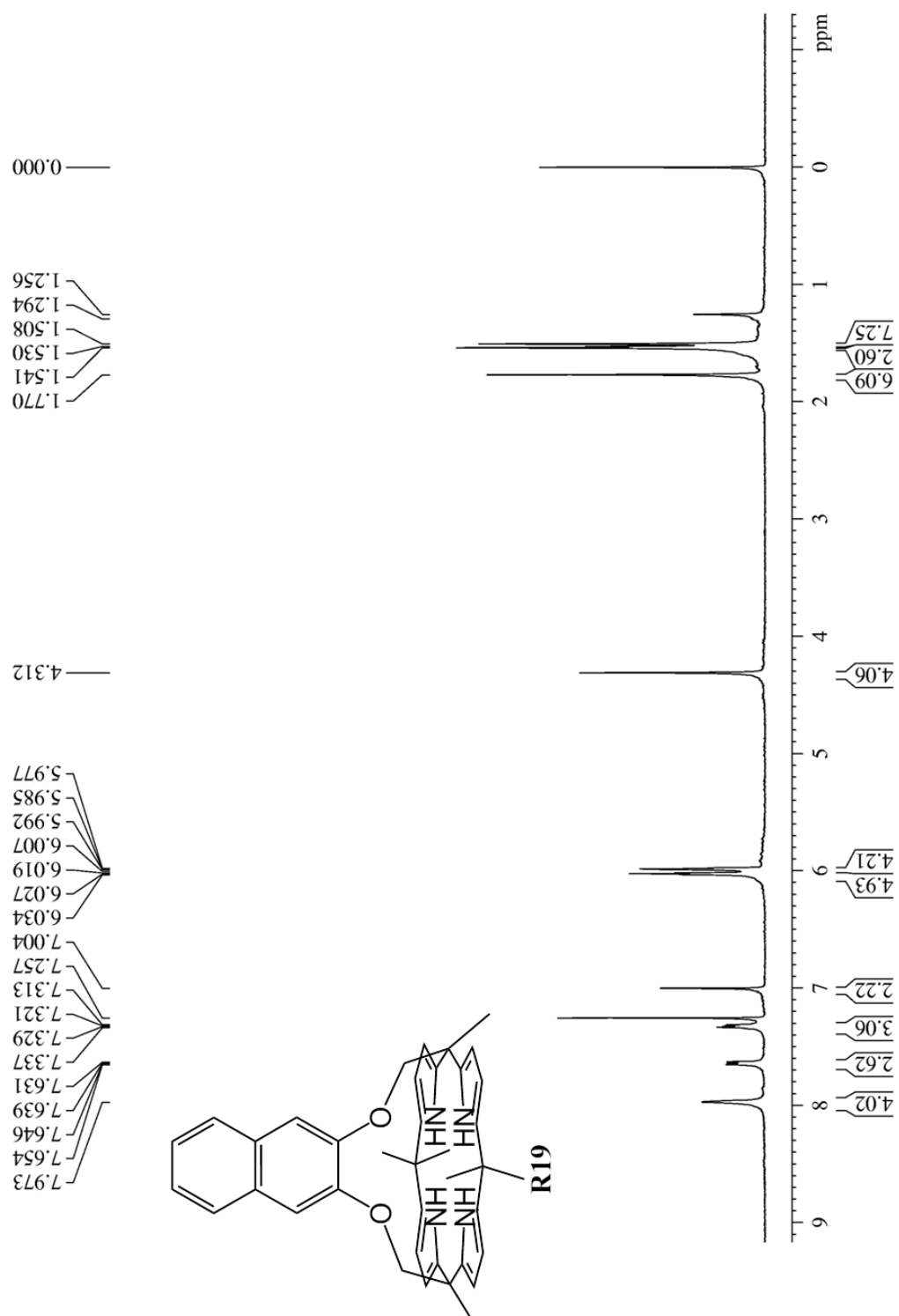


Figure A36: ^{13}C NMR spectrum of **R18**

**Figure A37:** ^1H NMR spectrum of **R19**

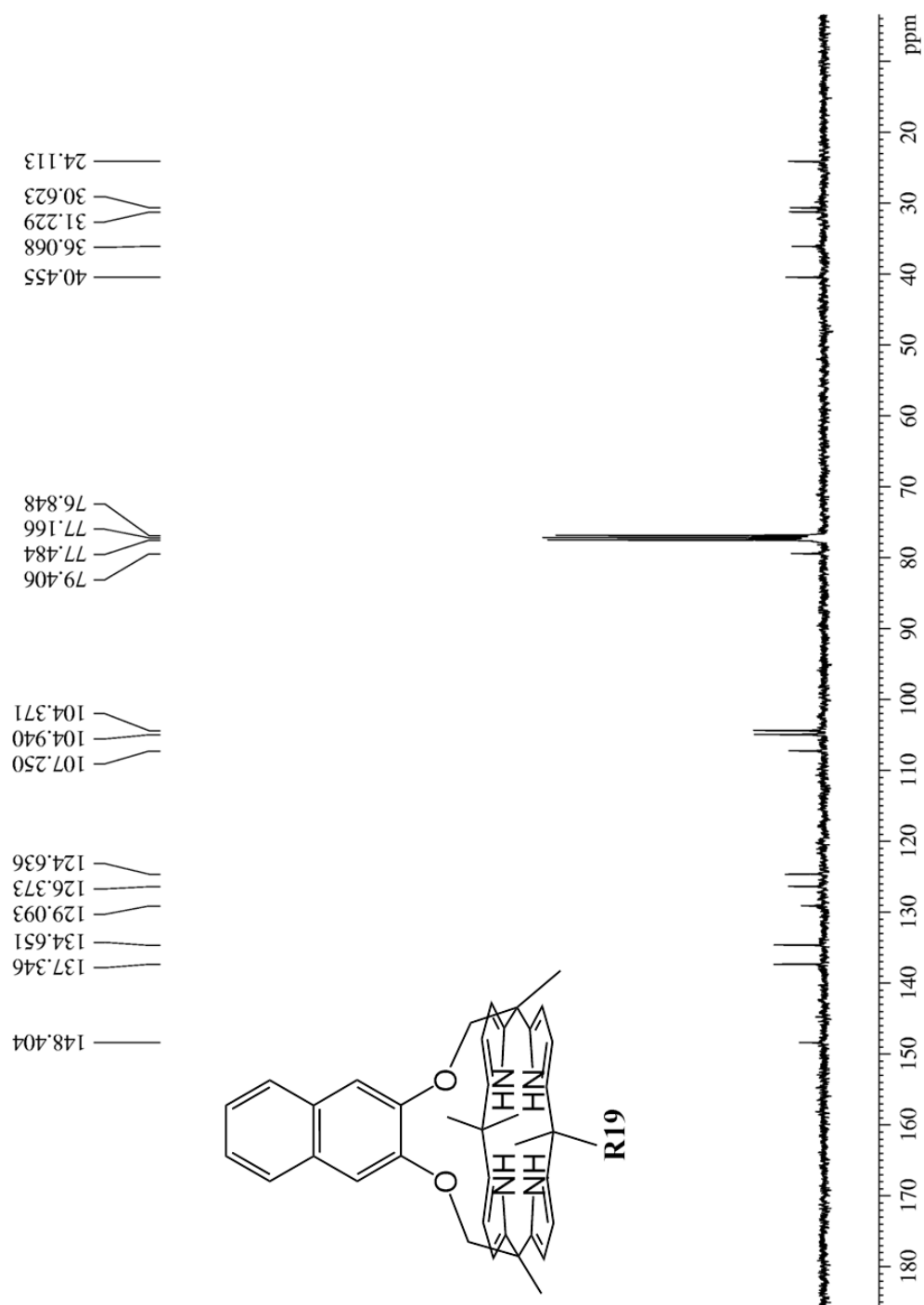


Figure A38: ^{13}C NMR spectrum of **R19**

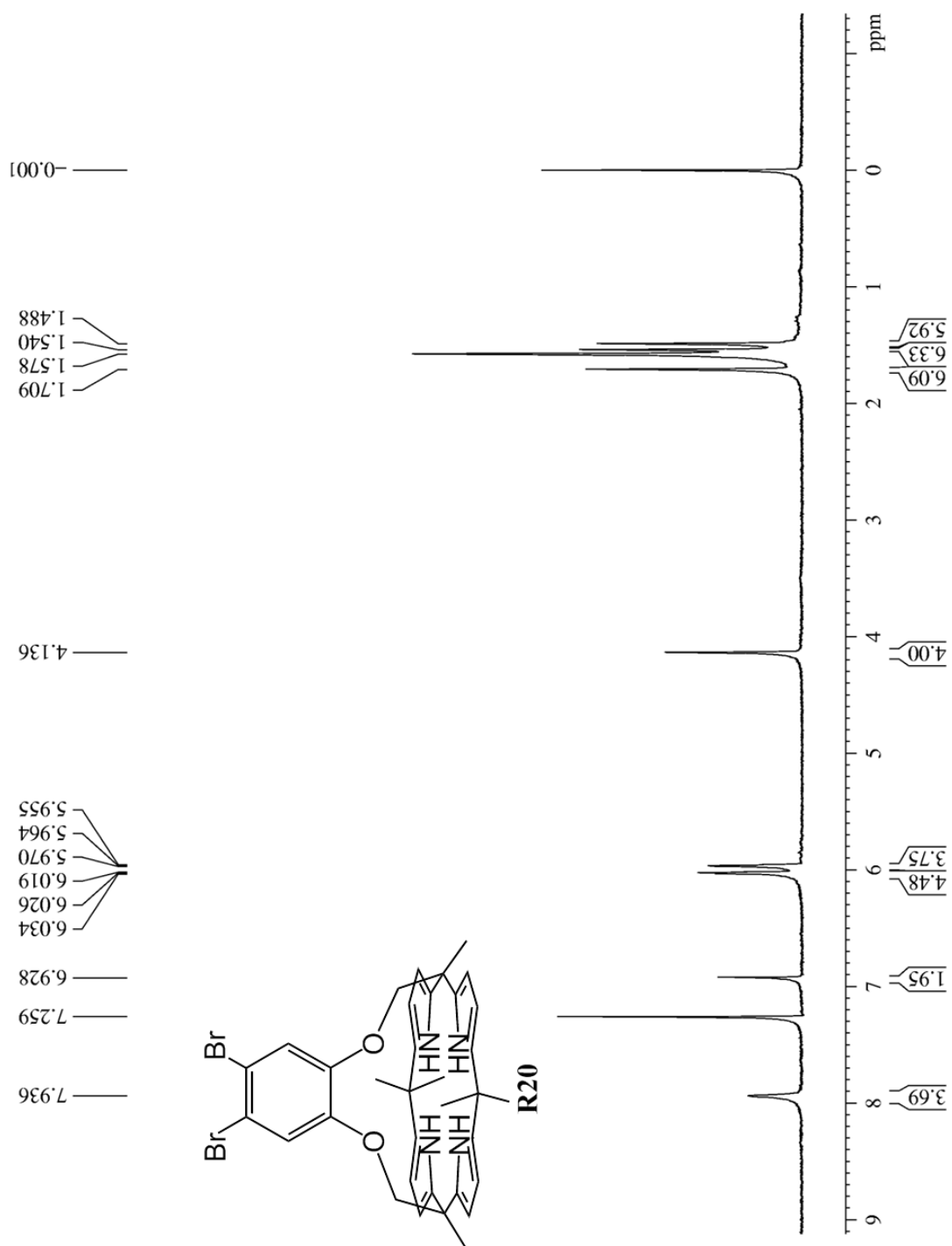


Figure A39: ^1H NMR spectrum of **R20**

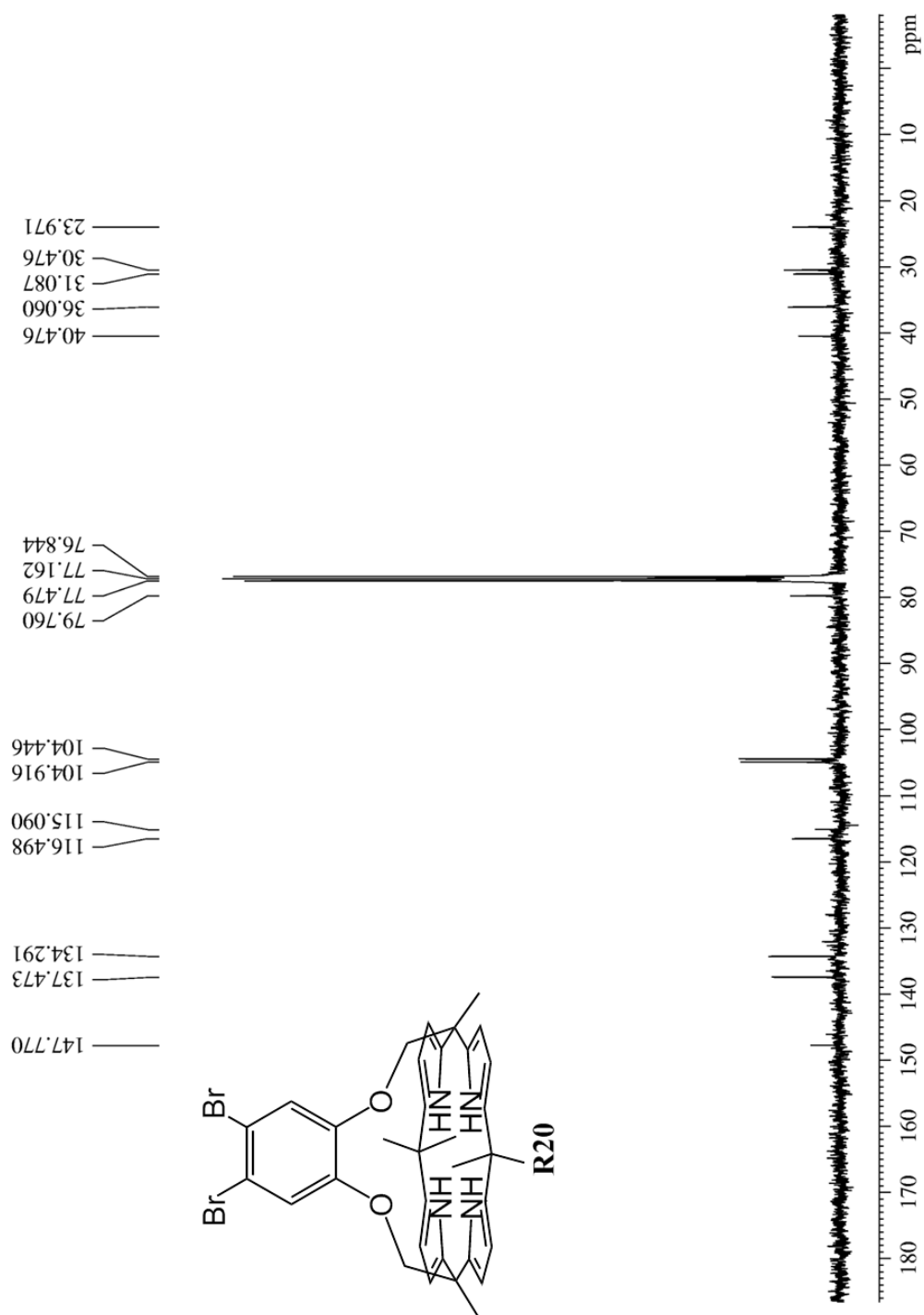


Figure A40: ^{13}C NMR spectrum of **R20**

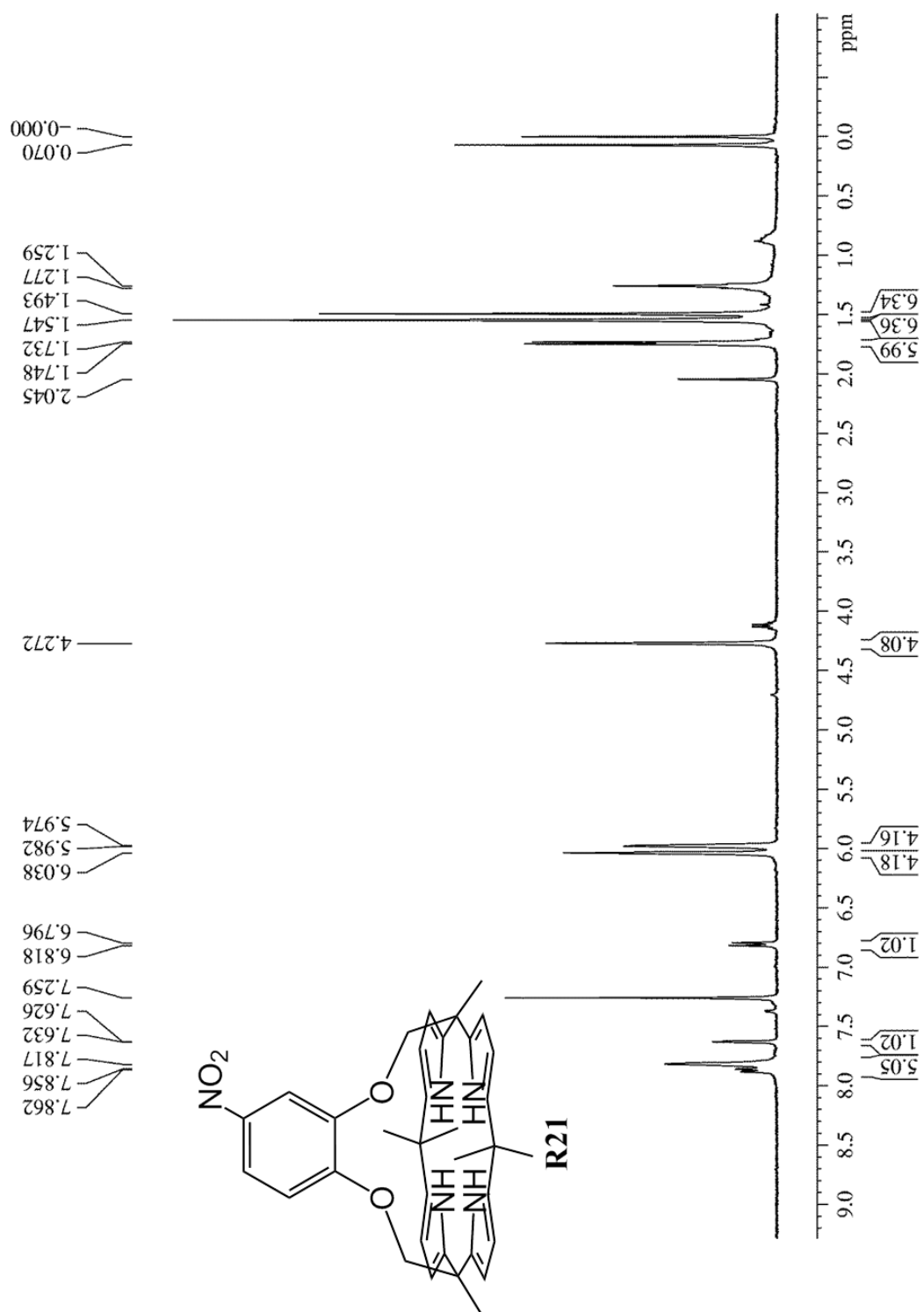


Figure A41: ^1H NMR spectrum of **R21**

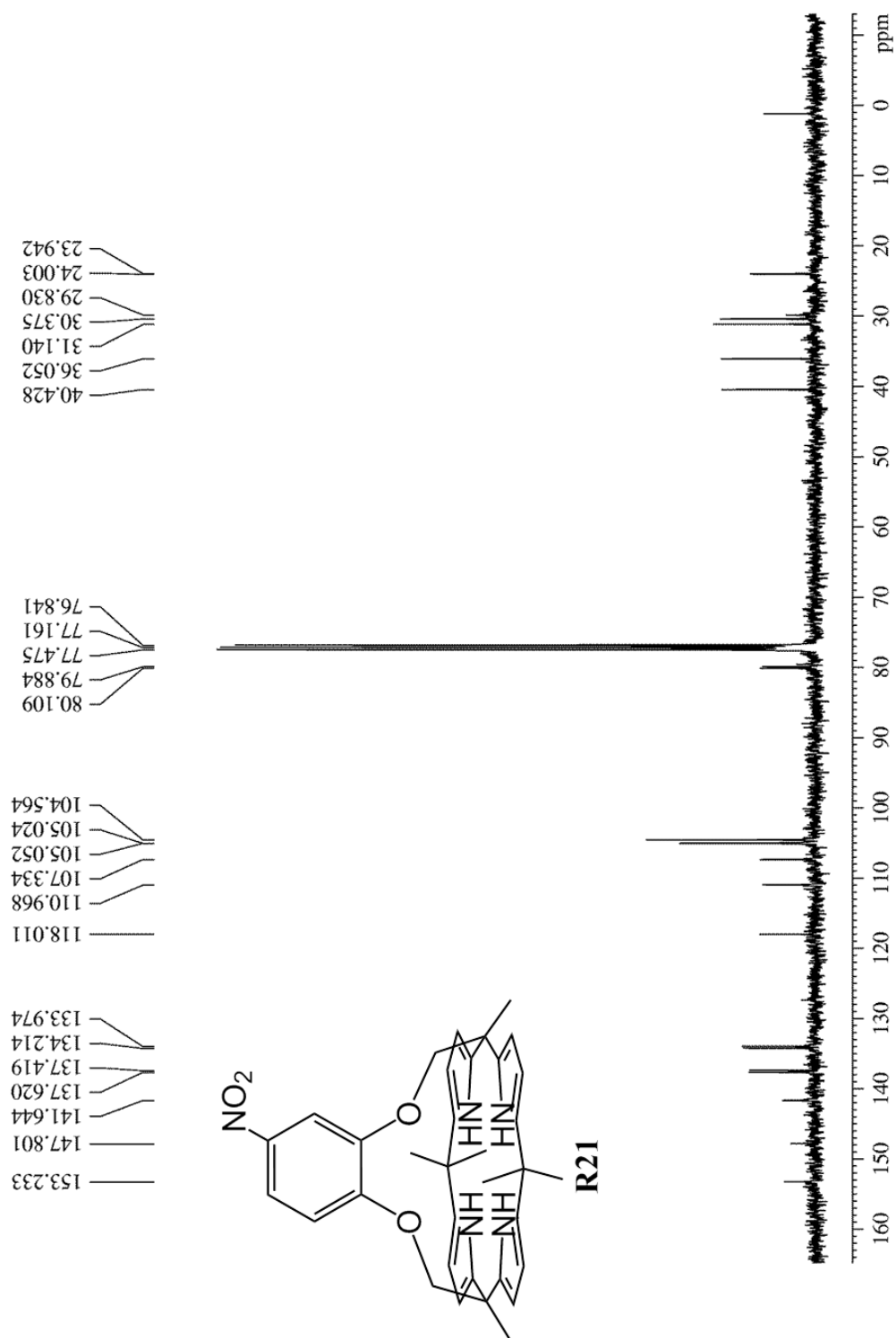


Figure A42: ^{13}C NMR spectrum of **R21**

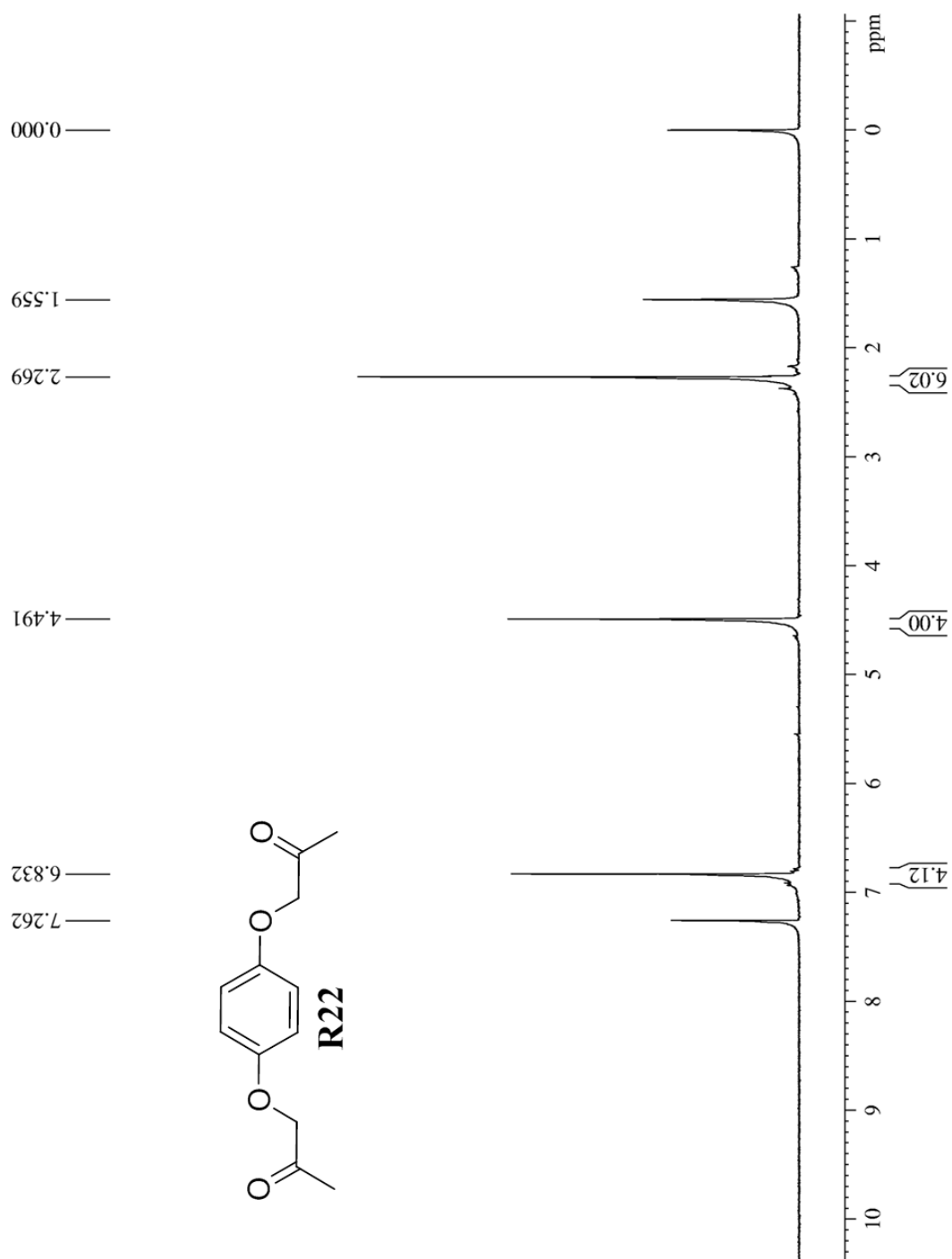


Figure A43: ^1H NMR spectrum of **R22**

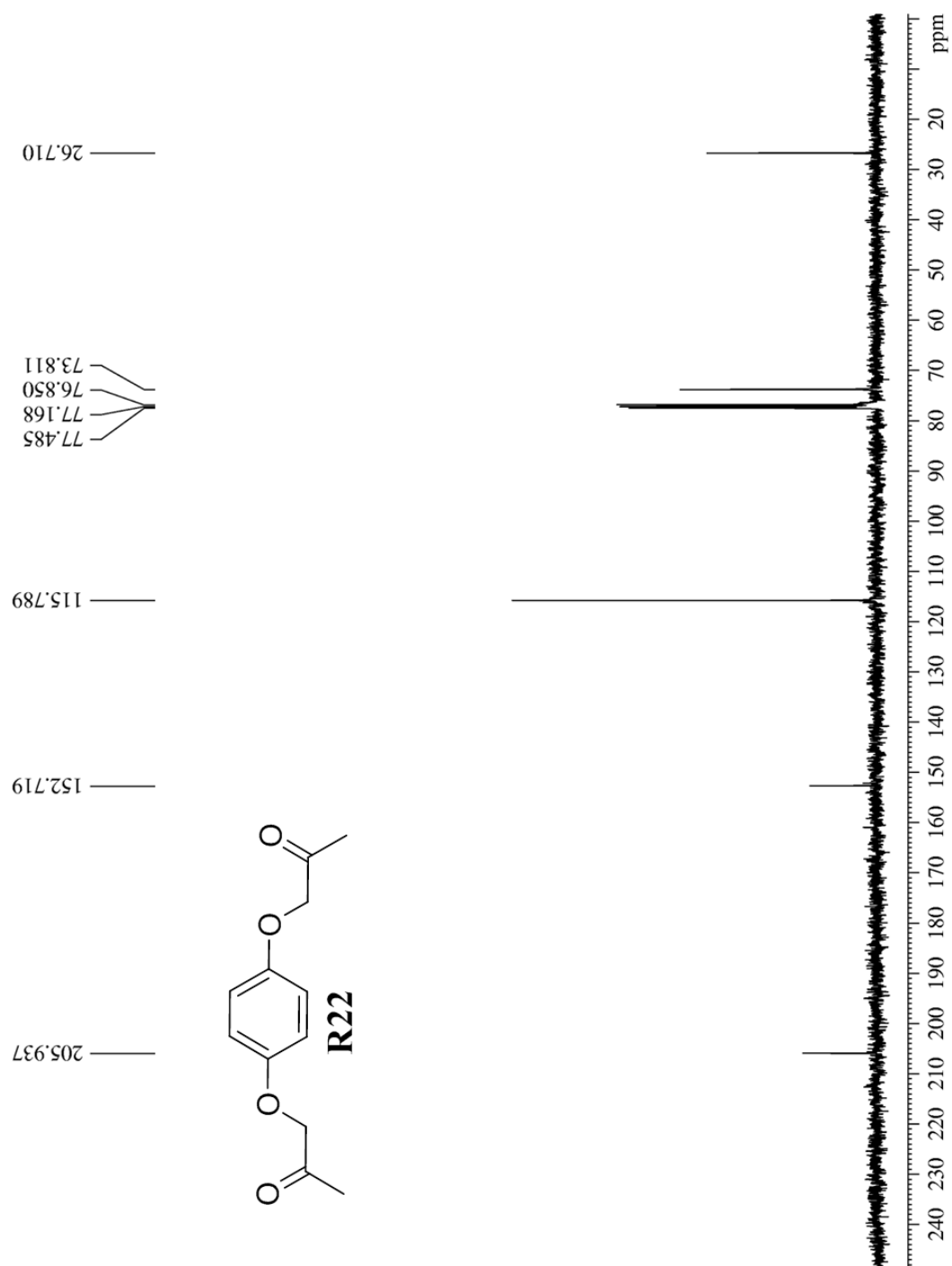


Figure A44: ^{13}C NMR spectrum of **R22**

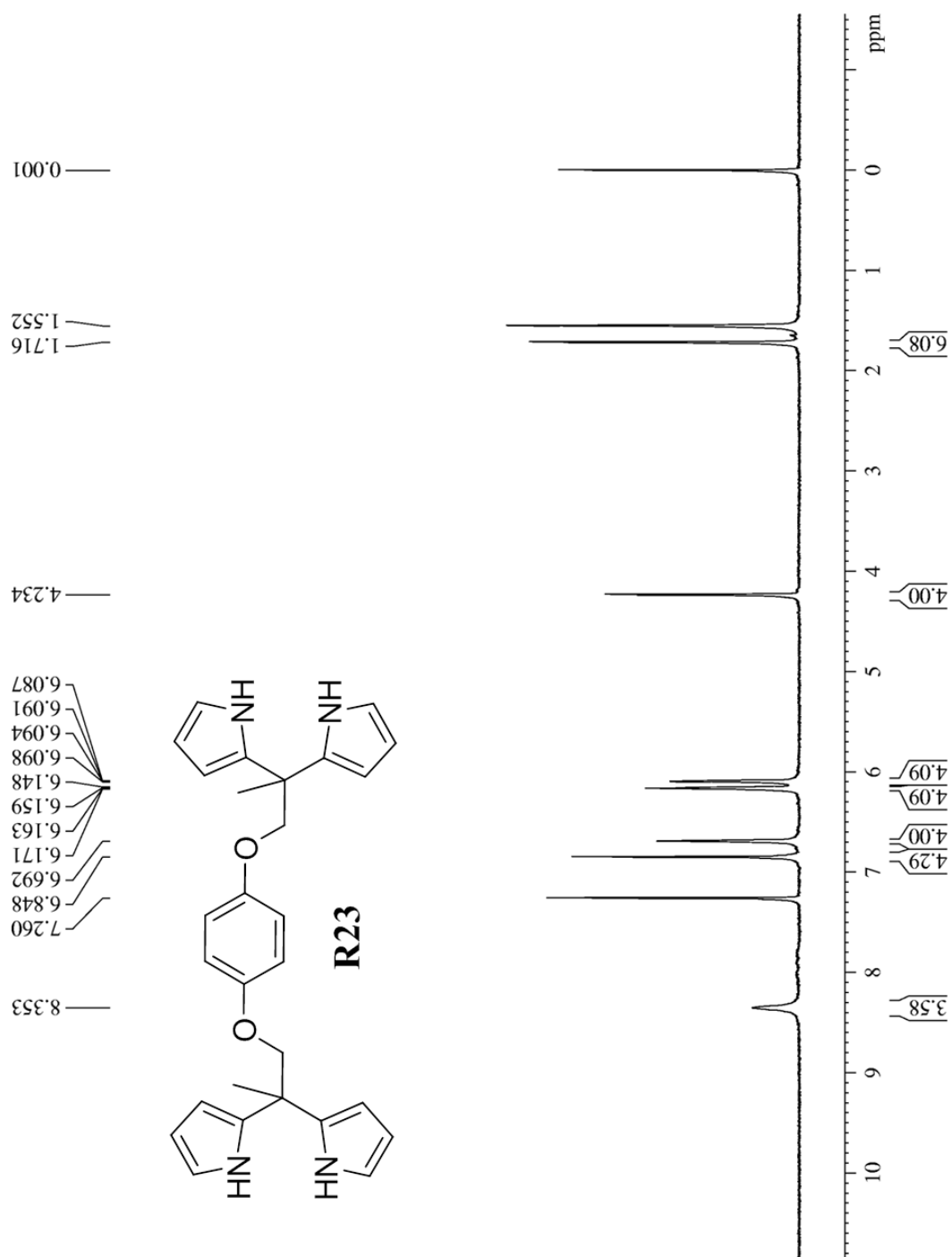


Figure A45: ¹H NMR spectrum of **R23**

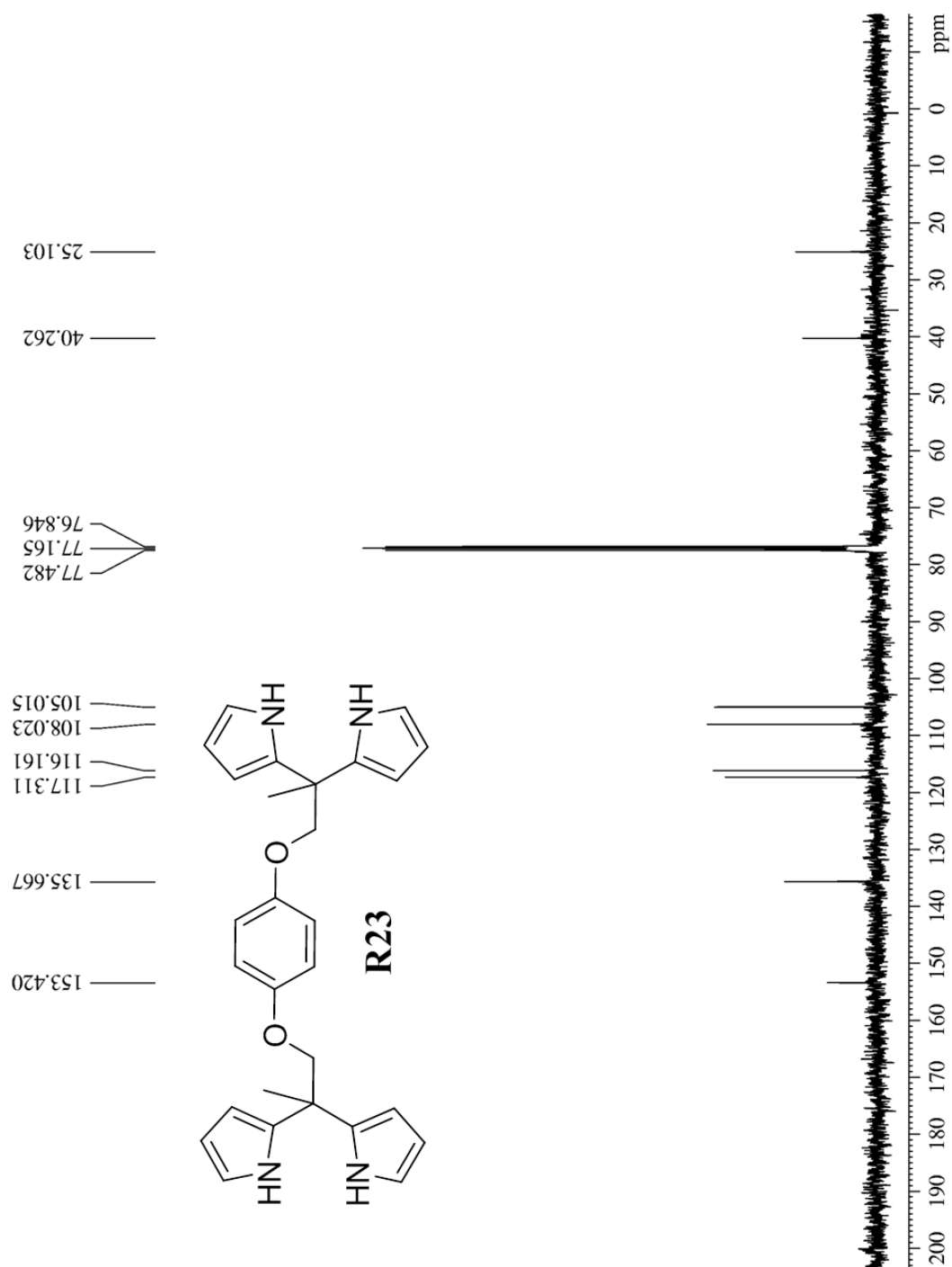


Figure A46: ¹³C NMR spectrum of **R23**

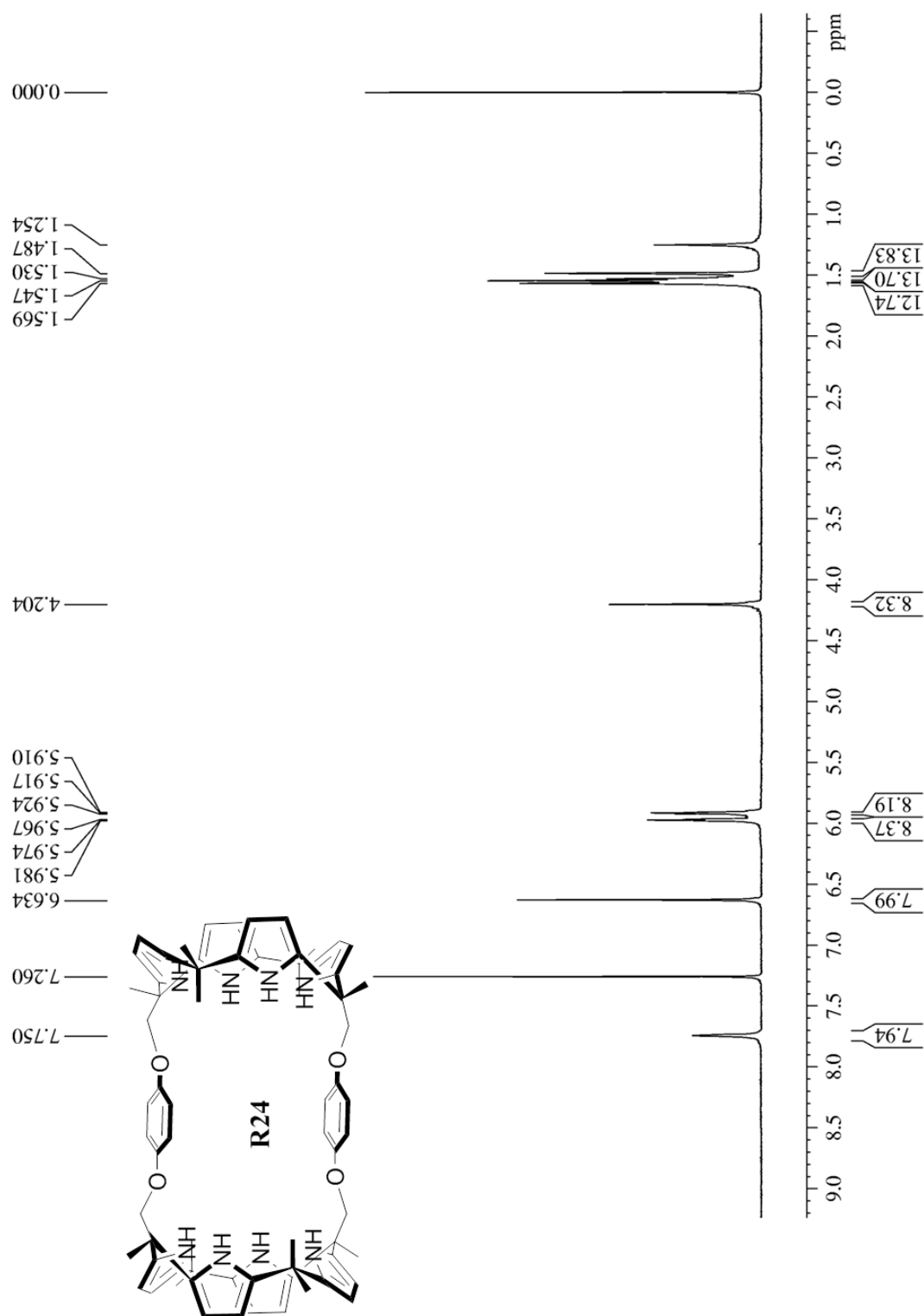


Figure A33: ^1H NMR spectrum of **R24**

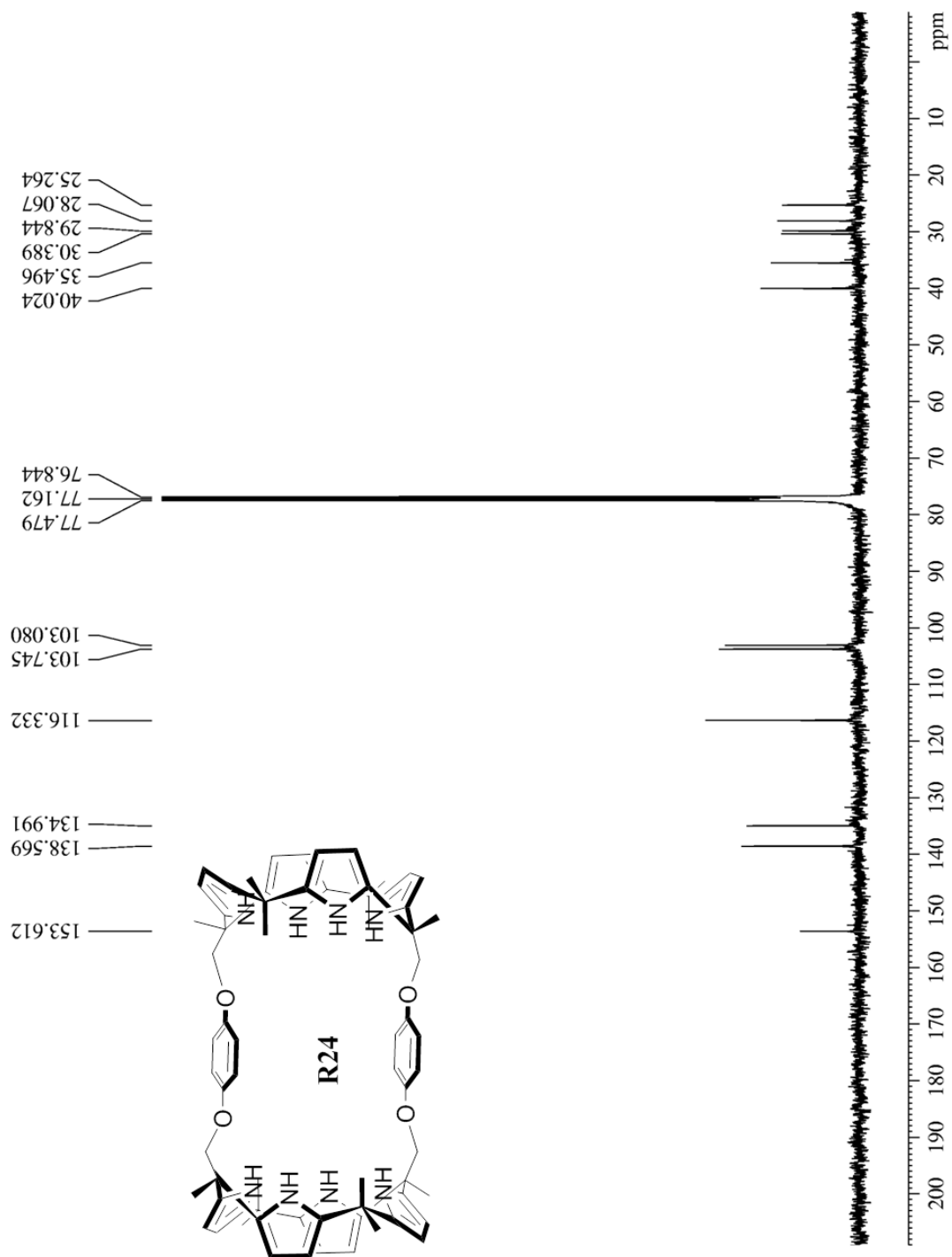


Figure A34: ^{13}C NMR spectrum of R24

Publications

1. New strapped calix[4]pyrrole based receptors for anions, **Samanta, R.**; Mahanta, S. P.; Chaudhari, S.; Panda, P.; Narahari, A. *Inorg. Chim. Acta* **2011**, 372, 281-285.
2. Naphthalene strapped fluorescent calix[4]pyrrole isomers: halide ion selectivity based on strap topography, **Samanta, R.**; Mahanta, S. P.; Ghanta, S.; Panda, P. K. *RSC Adv.* **2012**, 2, 7974-7977.
3. **Samanta, R.**; Panda, P. K. (Manuscript under preparation).

Conference Presentations

1. Poster presented on “*Synthesis of a new Fluorescent Strapped Calix[4]pyrrole and its Anion Binding Studies*”, National Conference on Frontiers in Chemical Sciences, December 4-5, **2010**, IIT Guwahati, Guwahati, India.
2. Poster presented on “*Synthesis of a new Fluorescent Strapped Calix[4]pyrrole and its Anion Binding Studies*”, 8th Annual in-house symposium CHEMFEST, February 25-26, **2011**, School of Chemistry, University of Hyderabad, Hyderabad, India.
3. Poster presented on “*Effect of Shortest Possible Strap on the Anion Binding Properties of Calix[4]pyrrole and their Bromo derivatives*”, New Directions in Chemical Sciences(NDCS) December 7-9, **2012** at IIT Delhi, Delhi, India.
4. Oral presentation on “*Effect of Shortest Possible Strap on the Anion Binding Properties of Calix[4]pyrrole and their Bromo derivative*” 11th Annual in-house symposium CHEMFEST, February 21-22, **2014**, School of Chemistry, University of Hyderabad, Hyderabad, India.